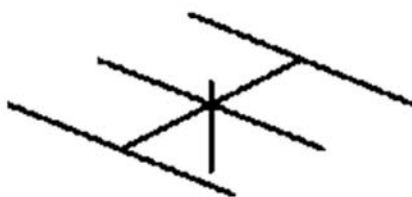
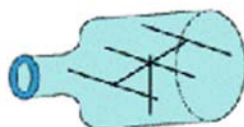


Antenna Modeling Notes



Volume 5



L. B. Cebik, W4RNL

Antenna Modeling Notes

Volume 5

L. B. Cebik, W4RNL

***Published by
antenneX Online Magazine***

<http://www.antennex.com/>

POB 271229

Corpus Christi, Texas 78427-1229 USA

Copyright 2009 by ***antenneX Online Magazine***. All rights reserved. No part of this book may be reproduced or transmitted in any form, by any means (electronic, photocopying, recording, or otherwise) without the prior written permission of the publisher.

ISBN: 1-877992-55-0

Table of Contents

Preface.....	5
101. Modeling the Un-Modelable.....	7
102. True Azimuth Models – NSI Software.....	22
103. True Azimuth Models – EZNEC Software.....	36
104. PS: I Change.....	50
105. Models, Symmetry and Loads: A Couple of Reminders.....	62
106. Refining Our Notions of Azimuth Patterns.....	79
107. Scaling Models.....	91
108. Dipoles: Variety & Modeling Hazards Linear, V & Folded Dipoles in NEC.....	104
109. Dipoles: Variety & Modeling Hazards Linear, V & Folded Dipoles in MININEC.....	117
110. Dipoles: Variety & Modeling Hazards Tapered-Diameter, Bent and Hatted Dipoles.....	132
111. Dipoles: Variety & Modeling Hazards Zigzag, Fold-Back and Fan Dipoles.....	148
112. Wires Meeting Ground: 2 Cases.....	165
113. When Simple Geometries Become Complex: A Rhombic Study.....	182
114. Modeling Folded Monopoles.....	201
115. Single, Bifilar and Quadrifilar Helices.....	221
116. Insulation Revisited.....	240
117. Modeling and the Logic of Question Resolution.....	252
Other Publications.....	264

Preface

This collection of antenna modeling notes continues the compilation of the series that I began in 1998 in *antenneX*. It contains numbers 101 through 117 of the long-running series that continues even today. The time came to collect these columns into a more convenient form for the reader. There is just too much material for a single volume, so the collection is broken into numerous units. I have reviewed the text and graphics for each column to ensure as much accuracy as I can muster. I have also reviewed the sample models used in each column. That process permitted me to add something to these volumes that is not available in *antenneX* or at my own web site. Some models require elements of the command set not included in entry-level programs such as EZNEC. Others require NEC-4

At the time of writing some of the columns, reference was made to the use of NEC-Win Plus for some of the models presented. However, since then, software maker Nittany-Scientific appears to have drifted into a state of instability and with an unknown future and the reader should not rely on the use of that software. The software was written for MS Win95, but appeared to work okay through MS Win2k. MS operating systems later than Win2k are known to have issues with NSI software. It is not compatible with VISTA at all as of this writing.

Along the way, we shall explore some basic NEC calculations, including electric fields at a distance. We shall also learn how to supplement NEC calculations by using its output data to arrive at circular gain. Finally, we shall explore the relationship between the EX command and the PT command for special receiving-mode models. The NEC-2 and NEC-4 manuals provide fundamental collections of sample models designed to illustrate in the most compact way possible as many NEC features as possible. These models appear only in print form. In this volume, we shall examine the models, and the model collection will include them in .NEC format.

The adequacy of our models is, as it should be, a continuing challenge. Therefore, we shall revisit the convergence test with particular reference to its use with NEC. In addition, we shall take a look at some of the correctives that we use to work around some of the core's limitations. However, finding limitations and faults is not our goal. Rather, the goal is to make effective use of the program. Toward that end, we shall look at a techniques that will let us in NEC-2 handle insulated wires in a way that is comparable to the IS command in NEC-4. We shall

also examine the various ground calculation systems that appear in NEC (and MININEC) software.

Although the list of topics seems to grow more advanced and complete, the appearance is an illusion. The command set is far too large for full coverage even in 4 volumes. As well, good antenna simulations depend as much on the ingenuity of modelers as they do on simply knowing how to apply various commands. Hence, the list of techniques by which to improve our models may well be endless. Mastering antenna modeling software has a further benefit: the use of the software to educate ourselves on the capabilities of various types of antennas. If we add this dimension of the use of NEC and MININEC to further mastery of the command structures and additional modeling techniques, then we may fairly predict that the series is far from its final episode.

101. Modeling the Un-Modelable

An alternative title for this episode might be **"The Intimate Connection Between Modeling and Measuring--Both Before and After Modeling."** With appropriate measurements before modeling, we can sometimes model structures that are technically outside the range of what NEC models best: bare round wires. We cannot model everything successfully, but by making some pre-modeling calibration measurements, we can model a good bit more than we might initially think. Let's see if we can approach the subject in a roughly systematic manner.

NEC Limitations

NEC (both -2 and -4) employs algorithms that presume thin round wires. When we model antenna structures that make use only of round wires, we tend to assume that the program is accurate. Often, we assume too much, forgetting that NEC has limitations. Tapered diameter elements plague NEC-2, and extreme tapers can lead to some errors even in NEC-4. Angular junctions of dissimilar diameter wires also lead to errors, and the Leeson corrections that apply to linear tapered diameter elements will not work. As well, the correctives will not work with mid-element loads or transmission lines that disrupt the current stepping from one segment to the next. Some angular junctions of wires with dissimilar diameters can also create a few problems. For example, a fat monopole with a set of thin radials at right angles to the main element tends to model accurately. However, sloping the radials tends to create errors.

For these common cases, we have tests internal to NEC for evaluating and sometimes correcting errors created by at least mild cases of surpassing the round-wire limitations. The Average Gain Test, described in at least 2 past episodes, provides a model-adequacy figure of merit. For a lossless version of the model in free space, a value of 1.00 is ideal (2.00 if tested using a perfect ground). Anything less than 1.00 or greater than 1.00 indicates a level of inadequacy. The greater the departure from the ideal value, the less adequate the model. For some purposes, we can convert the Average Gain Test value into a correction for the reported gain value and for the reported feedpoint resistance value. For structures that include anything more than linear elements, the

Average Gain Test is required. However, the Average Gain Test is a necessary and not a sufficient condition of model adequacy.

NEC also comes with considerable advice on obtaining accurate results. For a given linear element, all segments should be the same length. This good-modeling practice is especially important in the region of the source. The source segment should be the same length as the adjacent segments. If wires are closely spaced, the segment junctions should align as closely as feasible for highest accuracy. The segment length should be several times the wire radius. As we create ever-narrower angles, we run risks of adjacent wire surface penetrations that may adversely affect accuracy. This quick scan of some of the normal round-wire modeling guidelines is just a reminder of the total list of good modeling practices.

Even following all of the guidelines, we can still run into situations that defy the precision we tend to assume for models of dipoles and simple Yagis. Consider a right triangle with three sides having different lengths. Now feed the antenna at the most acute angle. Even with perfect proportions--that is, with identical segment lengths throughout--the model may not converge. The chief indicator of the fact that something is amiss is the fact that if we alternatively provide the model with a standard voltage source and then an indirect current source, we may obtain different feedpoint impedance values. This model prevents the source segment--or even the source-segment pair--from obtaining equal current levels in the segments immediately adjacent to each end of the source segment or segments.

This brief review of some--but by no means all--NEC limitations is not designed to cast aspersions on either of the most-used NEC cores. Rather, the catalog does no more than record that NEC has something in common with all software that makes highly complex calculations: the software has limits and ways to determine in large measure how close to those limits a given model might be.

Types of Models

Over the years, I have developed some general categories of modeling efforts to flag what models may be good for. The borders between categories are judgment calls that perhaps only experience can certify. Nevertheless, they may be useful to illustrate the levels at which modeling may be useful.

1. *Design Models*: the "design-model" category is reserved for antenna models with an existing track record of construction and testing to the model specification. The correlation between model and physical reality is sufficient to build directly from the dimensions specified in the model. Such models, of course, have passed all internal adequacy tests. In addition, they carry with them a set of physical correlation instructions or limitation notations. For example, a model may specify that it is for a non-conductive or well insulated/isolated support boom.

The design category has very high standards, but is not at all unusual. From some Moxon rectangle and monoband quad designs that have been modeled by equation, many implementations have successfully emerged without the need for more than routine initial set-up procedures. The model of a 50-Ohm Moxon rectangle with uniform-diameter elements can be set up for design by entering only the element diameter and frequency. See **Fig. 1**. Numerous Yagi designs guide commercial production in several countries. Going beyond the limits of NEC, hybrid programs are yielding wireless antenna designs of all sorts.

Frequency (MHz)
Start: 146
End: 146
Step Size: 1

Ground
No Ground

Radiation Patterns
1°<Az<360°,El=1°,Step=1°
0°<E<180°,Az=0°,Step=1°
Zo = 50 Ohm

Geometry
Stepped
inches

Equations

	A	B	C	D	E	F	G	H
1	Var.	Value	Comment	Scratch Pad				
2	F =	146	Primary Frequency (MHz)	-0.000857143	aa	Moxon Rectangle Set Up in Equation Format For Automated Design by Entering Frequency and Element Diameter		
3	W =	=299.8/B2/Model P	= "Wavelength(" & Model Params!\$B\$5"	-0.009571429	ab			
4	A =	=(D2*(1^2))+(D3*I)	Side-to-side Dimension	0.339857143	ac			
5	B =	=(D5*(1^2))+(D6*I)	Driver Tail Length	-0.002142857	ba			
6	C =	=(D8*(1^2))+(D9*I)	Tail-to-tail Gap	-0.020357143	bb			
7	D =	=(D11*I)+D12*W	Reflector Tail Length	0.008285714	bc			
8	E =	=B+C+D	Front-to-Back Dimension	0.001809524	ca			
9	G =	=F	Design Frequency	0.017809524	cb			
10	H =	=0.0808	Wire Diameter (units)	0.051642857	cc			
11	I =	=LOG(H/W)	Log of dia. in wvl	0.001	da			
12	J =			0.071785714	db			

Fig. 1

The design category also includes the other side of the modeling coin--analysis. Recently, I examined data on an interesting small antenna and was able to replicate the design and the test results. Some matters, difficult to measure in the test set-up, move from presumption to confirmed analysis status by virtue of the reliable model produced. One need not begin with a model: instead, modeling often serves as a supplementary analytical tool, not to mention as an educational tool when rightly used.

2. *General Guidance Models*: models provide general guidance when they are reliable as models, but not necessarily models of an antenna that either exists or will be built exactly as modeled. The models meet all rigorous standards of adequacy, but do not have a direct correlation to any particular existing or anticipated set of construction processes.

General guidance models require further design effort to move to the design-model category. The model would have to take into account significant appurtenances that may affect RF performance in the physical implementation. These added factors may range anywhere from a simple change of materials to lumpy brackets and other hardware within the mutual coupling range of the elements.

Nonetheless, since the models are known to be reliable, they often serve as the basis for systematic modeling studies. Since one may create a sequence of models more efficiently than a sequence of test antennas, the relationship between the model and a test situation is normally not a 1:1 affair. Instead, models may identify key test points to confirm or disconfirm modeling trends that emerge from the study. As well--and as more than a mere incidental--general guidance models often save prototype and test efforts from any unproductive byways. As well, they often turn up unexplored directions in antenna work and provide a first-order quantification of information that has hitherto been only anecdotal. Such was the case, judging by the feedback, from some notes I produced on the loss "knee" frequency and the patterns of a typical terminated wide-band "folded dipole." See **Fig. 2** for a sample pattern.

Sample Pattern
Comparison
Between a
90' Doublet
and a 90'
Wide-Band
"Folded-Dipole"

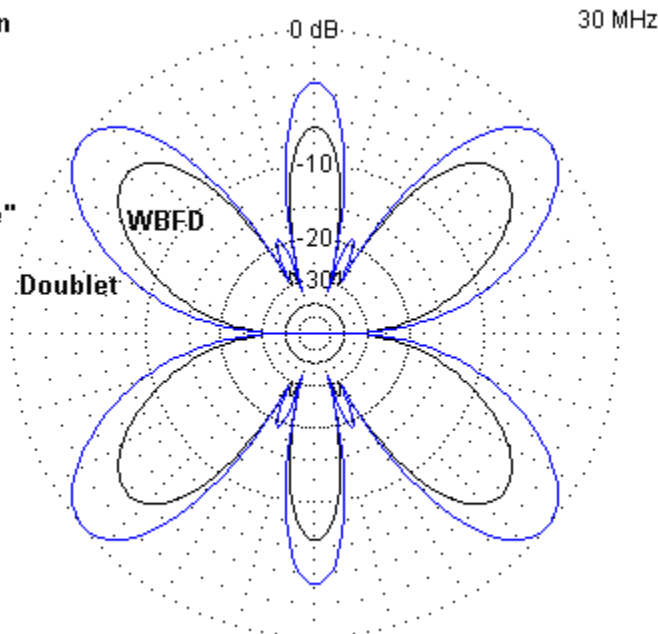
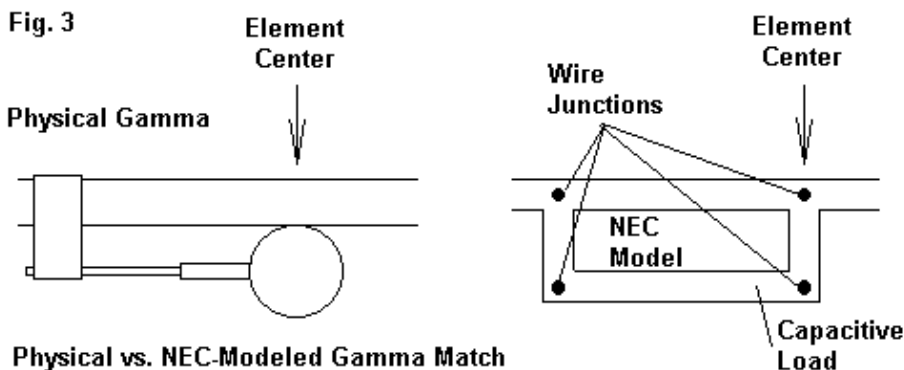


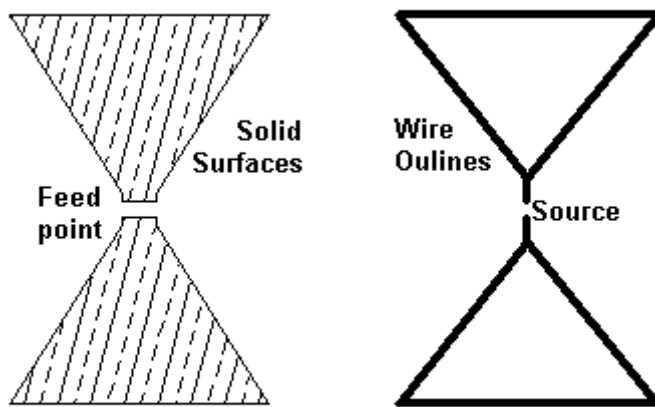
Fig. 2

3. *Proof-of-Principle Models*: This special category of model may be difficult to place properly with an example or two. Consider the gamma match (or the Tee match) used extensively in Yagi design and elsewhere. Ordinary procedures for building such a match employ gamma match tubing or rod that is much smaller in diameter than the elements to which it is attached. NEC does not handle well very closely spaced wires of different diameters and lengths, even when one carefully aligns the segment junctions. As well, there will be angular junctions of wires having dissimilar diameters. To model a gamma match and remain within the boundaries of what NEC does well, one must use gamma rod, connecting rod, and element diameters that are equal. The proportions required for this model do not correspond to normal Yagi construction, but do fall well within gamma match calculations. See **Fig. 3** for a rough outline of the differences. Hence, one may not be able to model a given gamma match in NEC, but one can model a gamma match to prove the principle of the matching system as a physical construct and to examine certain properties, such as the currents along

the gamma rod. (For a better correlation between models and physical implementations of gamma-matched antenna elements, a well-calibrated version of MININEC is often superior.)



Consider next a solid-sheet fan dipole that might be used at UHF frequencies. The antenna may be too small for effective wire-grid construction, and even a wire-grid may prove problematical in terms of reflecting accurately the current distribution on a fan. One may approximate such a fan as a wire outline, as suggested in **Fig. 4**. The outline fan may not have the full frequency range of the solid-surface fan, but it will exhibit a good part of the broadband effects. Hence, in comparisons with other types of elements that might be used in an array, it can provide a proof of principle of those effects in a complex array, but is not quite satisfactory for full general guidance or design-level work.



UHF Fan Dipole and Its Model

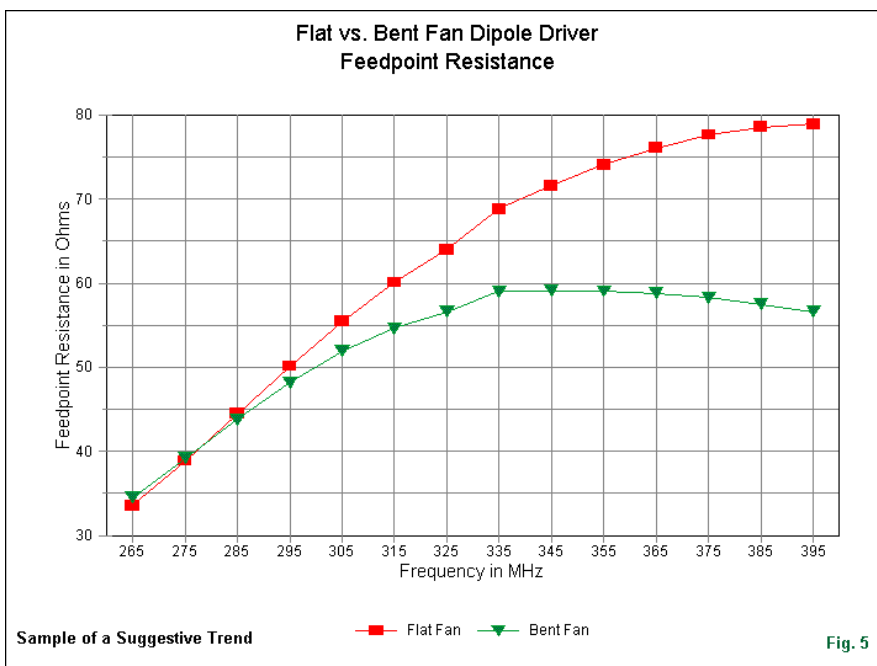
Fig. 4

Proof-of-principle models do not have relaxed standards as models. Indeed, to serve as a proof of a principle, they need to be fully adequate as models within the software system being used. As well, the modeler must have enough knowledge of the system being modeled in principle to be able to specify both the correlations to and departures from reality, plus enough understanding of the principles themselves to be able to show that the model falls within the limits of those principles. Proof-of-principle modeling is not simply a matter of approximating an antenna system or getting into a ballpark estimate of what is happening. There must be a reasonably well-understood relationship between the models and physical antennas to be able to confirm that both fall under the same principles of operation. Theoretically, every proof-of-principle model should be susceptible to physical replication and testing, even if no one actually conducts the test.

4. *Suggestive Models*: Sometimes it is not possible to construct a model that rigorously meets all internal standards of adequacy, but it may come close. In such borderline cases, the model may give every indication that over some part of the of the reported output data, there are reliable trends, even if the specific numerical data for any single item fail to meet reliability standards. Such models--

when accompanied by a carefully wrought justification and set of limitations--may be used as suggestive of directions for further study.

I recently approximated a Brown-Woodward bent fan dipole within a corner reflector array. The AGT value for the construct was too far from perfect for high confidence in it as a model of the actual driver. However, the relationship between the planes of the modeled version and of the corner reflector surface yielded some interesting impedance curves, especially when compared to standard fan and linear dipoles. See **Fig. 5** for a sample of these curves. At most, these curves are suggestive of how the driver manages to widen the bandwidth of the corner array, but they are not adequate yet as proof-of-principle models.



Categorizing modeling results requires a level of judgment that comes from long experience and solid familiarity with the foundations, procedures, and limitations of antenna modeling within a given software system. The process also requires

solid familiarity with antenna theory and practice, as well as construction and testing techniques and practices.

Physical Post-Modeling Testing

I have briefly and incompletely reviewed some of NEC's limitations for two reasons. First, for a large number of modeling enterprises that fall well within the well-known limits of the core, we approach the exercise without thought to the limits. As a result, we tend to assume that the results are accurate to the realities of a physical implementation of an antenna design. That assumption is, of course, a dangerous temptation if we carry it outside the region of well-verified results. Second, even when we do not make assumptions about the correctness of NEC reports relative to corresponding physical antenna structures, most modelers reserve testing and measurement activities to post-modeling exercises. That is, they create a modeled design and then build a prototype to match the model and test its performance.

Post-modeling physical testing is extremely important, and I have no intent to reduce that importance in these notes. However, we do tend to encounter two distinct groups of individuals whenever the measured results for a physical antenna do not agree closely with the reported results for the model. One group tends to almost automatically presume that there is something wrong with either the model or the software. The other group tends to presume that there is something wrong with the physical prototype.

In principle, either possibility may be correct, but never as a presumption. In most cases, those who conduct the physical construction and testing of an antenna are not the same individuals who do the modeling. In sundry consulting activities, I have discovered that one of the chief causes of disparity between test measurements and modeling results is a failure of communication. When communications are clear, concise, and complete, virtually all dissimilarities between test measurements and model reports tend to dissolve.

Dissolution of disparities tends to come in two forms. The first is a refinement of both the testing and the modeling structures and environments so that one can say that the modeled antenna is a very close analog of the physical antenna--and vice versa. The second form of removing conflicts between a model and a physical antenna is a comprehensive understanding of differences between the

two. A physical Yagi may connect the elements to a conductive boom, with resultant changes in the required element lengths relative to a model. A model may involve geometric structures that require reference to and correction by the Average Gain Test value for gain and source resistance values. In many cases, apparent differences between a model and a physical antenna may disappear under appropriate calculation to adjust for those differences.

The logic of this situation makes measurement a post-modeling activity, regardless of the temporal order of the modeling and the field testing. Equally, we might call the situation one of post-construction testing against a model. Consider **Table 1**.

Table 1. Modeled and tested resonant lengths of round-element 146 MHz dipoles.

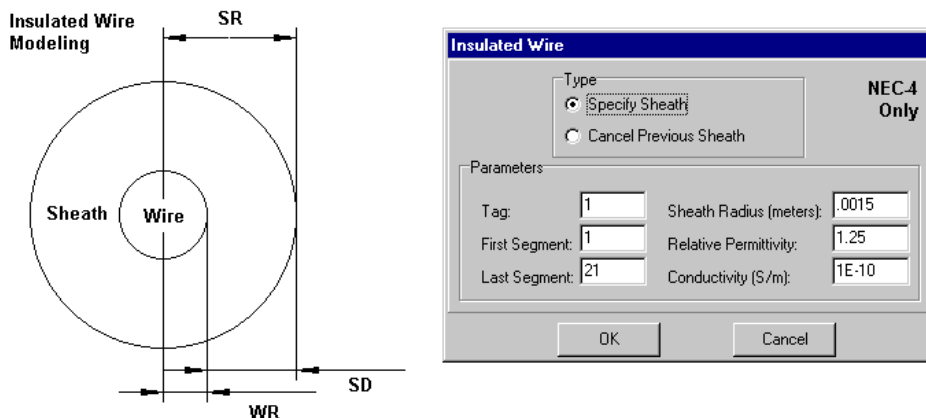
El. Diameter (inches)	Modeled Length (inches)	Tested Length (inches)
0.125	38.42	38.31
0.1875	38.28	38.25
0.25	38.10	38.06
0.375	37.80	37.81
0.5	37.60	37.44
0.75	37.30	36.94

The table provides parallel columns of values for the length of a dipole resonant at 146 MHz. One column lists the measured value of the length of round elements trimmed to resonance. The other column lists the length of modeled dipoles trimmed to resonance within the software. It makes no difference which activity comes first in time. We simply cannot make a comparison until we have both columns filled in.

Pre-Modeling Physical Testing

There are a number of situations that NEC cannot directly model, many of which involve the proximity of the conductor with a non-conductive material. Of course, NEC-4 is able to model wires having an insulated sheath. **Fig. 6** illustrates the dimensions involved and shows the parameters involved, as listed on a GNEC assistance screen. NEC-2 lacks this facility, but there is a work-around that is

applicable in many situations. See episodes 50 and 83 for further details of modeling insulated wires with NEC.

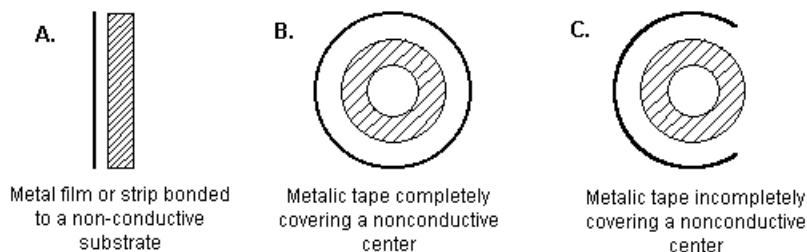


Wire Radius (WR) + Sheath Depth (SD) = Sheath Radius (SR)

Fig. 6

The questions of NEC's ability to model a structure emerge from situations other than the simple insulated wire. **Fig. 7** shows some typical cases that have often occasioned e-mail questions.

Some Potentially Problematical Structures for NEC Modeling



Note: Shaded area represent a non-conductive material.
Dark line represents a metallic surface.

Fig. 7

The situation that invites the most inquiries involves the left-most sketch, where a relatively thin and flat conductor is bonded to a non-conductive substrate. In fact, NEC has no direct means of dealing with this "PC-board" style of structure, although the use of such materials is common in the UHF region. First, the conductor is not round, and there is no standard list correlating flat strip surface areas to the surface areas of round conductors, at least not in any reliable way. Second, the substrate represents an insulator having a thickness, a relative permittivity, and a conductivity, but bonded to only one side of the conductor. Hence, we can assume that some sort of electrical lengthening occurs, but we cannot say in advance what the velocity factor will be. When we combine the two problems, we usually end up in a quandary about effectively modeling subject antennas without investing in very expensive hybrid software.

The problem set may increase for many antenna designs adapted to printed circuit board materials. For example, a Yagi or a log-periodic dipole array may etch the elements on a single plane so that the adjacent elements expose their thin edges to each other. In addition, the substrate may fill part of the region between the elements, at least on one side of the plane of the element strips. Consequently, the substrate material plays a role not only in determining the electrical length of the elements, but as well in their mutual coupling.

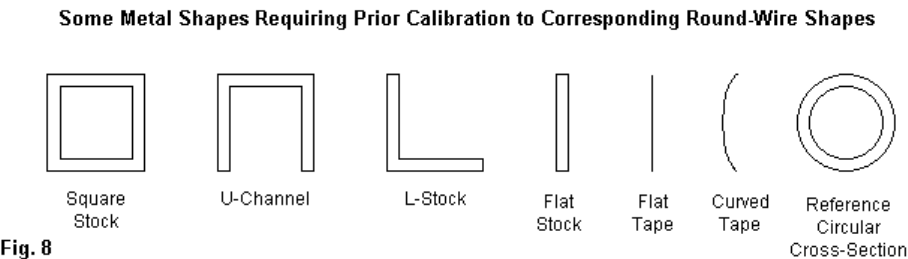
The situation of the center sketch in **Fig. 7** often occasions questions, but is in fact quite simple. A number of antenna builders--mostly to use local materials--apply conductive tapes around non-conductive round structures and thereby form antenna elements. The sketch shows one typical case in which the tape completely circles the support and forms a closed cylinder. In this case, we may treat the element as a wire having the outer diameter of the tape surface. Of course, this assumes that the tape forms a fully complete and closed circle around the central support. The result is not dissimilar to the copper-clad steel wire known as copperweld. That steel has some conductivity and the central support for the tape has little or none matters not at all, since the RF currents will be near the surface in both cases.

The right-most portion of **Fig. 7** changes matters considerably. We still have a central support and an overlay of conductive tape. However, the conductive surface does not form a complete circle around the center material. If the circle is almost closed, then the element may act as if it were closed. However, if the gap is wide enough, then the semi-circle of tape may act more like the left-most

figure. To the best of my knowledge, there are no handy guidelines for converting various forms of the right-most figure into equivalent round-wire values for modeling.

There are methods for creating a conversion table between the structures on the left and right in **Fig. 7** and round-wires values that we may model. They involve preliminary test antennas to determine the round wire-equivalent values for a given physical structure. One technique is simplicity in itself: create a dipole at the frequency of interest for the material and then find its corresponding round-wire equivalent diameter for resonance at the same element length.

Fig. 8 shows a variety of shapes of alternative materials used for antennas in the amateur 2-meter band. Most of the materials come from hardware outlets. Builders use some of them because they are locally available. In some cases, builders find stock with flat surfaces easier to work. A few materials, such as measuring tape or rabbit ears, may have special features useful in transporting the antenna or using it in rough terrain.



Prior to modeling, we may calibrate any of these materials to a selected round-wire diameter by using the dipole-resonance technique. **Table 2** lists some results of measurements made locally at 146 MHz with some typical materials. Each material lists the resonant length and the round wire diameter with the most similar length from **Table 1**.

Table 2. Tested 146-MHz resonant lengths of alternative element materials.

Material	Tested Length (inches)	Nearest Round Element
Aluminum Flat Stock		
1/2" by 1/16"	37.31	0.5
1/2" by 1/8"	37.19	0.5
3/4" by 1/16"	37.06	0.75
Aluminum L-Stock		
1/2" by 1/2" by 1/16"	37.44	0.5
3/4" by 3/4" by 1/16"	37.00	0.75
Collapsible Whips		
1. 5-section TV "rabbit ear," maximum extension 48.5" with "button" tip. Approximate diameters: 0.25", 0.219", 0.1875", 0.125", 0.0625"		
a. With largest sections fully extended	37.88	0.375
b. With smallest section fully extended	40.00	<0.125
2. Radio Shack 5-section cordless telephone replacement (#270-1405A); maximum extension 23" with button tip. Approximate diameters: 5-mm, 4.125-mm, 3.25-mm, 2.375-mm, 1.5-mm		
Roughly equal section extension	38.88	<0.125
Metal Measuring Tapes		
1" (15/16" with curve)	37.38	0.5
3/4" (11/16" with curve)	37.63	0.375-0.5
5/8" (9/16" with curve)	37.88	0.375
1/2" (15/32" with curve)	38.25	0.1875

The sample tables are for 146 MHz. It is not known how far from the listed frequency that the equivalencies would apply. For example, stock that is 1/16" thick is about $7.7\text{e-}4$ wavelength at 146 MHz but only about $7.4\text{e-}5$ wavelength at 14 MHz. Whether that change in relative thickness brings the 1/16" stock down to measuring tape thickness requires a re-run of the tests for the frequency of interest.

Although the pre-modeling test runs are useful for independent elements, the tests have additional limitations besides their potential frequency restrictions. For arrays in which mutual coupling between elements is critical, very flat and wide stock may show some differences depending upon whether the elements are edge-to-edge or flat-to-flat. As well, without specific pre-modeling tests, one

cannot know the effects of a continuous substrate on the mutual coupling between elements. However, with proper equipment, such tests are possible and may lead to round-wire, open-space equivalents.

Despite the limitations, the exercise does demonstrate that all is not lost with respect to modeling if we use materials other than the round wires upon which NEC's algorithms are based. One question is whether all of that work is worth the effort. In most cases, of course, pre-testing or calibration of materials will be confined to only a few selected candidates. As well, once a material has found its round-wire equivalent diameter, then we may construct relatively diverse and complex arrays within the models and reserve prototype testing until we are satisfied with the modeling results. Hence, when we view the design of an antenna as a full-scale activity set, the modeling saves enough time to make the pre-testing phase well worth the effort involved.

Conclusion

We began with the idea that there is an intimate connection between modeling and measurement that extends from pre-modeling calibrations through post-modeling prototype testing. Modeling does not exist in a vacuum, since its results are either a physical antenna or an understanding of the performance of a physical antenna. These columns have tended to focus on modeling's internal working. However, we should never lose sight of the fact that modeling has an integral place within a larger set of activities that may involve measurement both before and after the modeling itself. As well, with appropriate pre-modeling calibration measurements, we may effectively model many (but not all) materials that would otherwise violate the NEC round-wire premises. Without those pre-modeling measurements, trying to model such materials would amount to mere speculation.

102. True Azimuth Models - NSI Software

After a short time in modeling with NEC, the core conventions become almost second nature. You model the antenna geometry using Cartesian conventions for each wire-end coordinate set. The core data produces phi and theta patterns. A phi pattern counts degrees counterclockwise. A theta pattern counts angles from the zenith downward toward the horizon. The pattern conventions are just the opposite of everyday and field engineering conventions. The latter use azimuth angles, generally counted from 0 at North clockwise. Elevation angles count from the horizon upward toward the zenith. The 2 systems appear in **Fig. 1**. Phi and theta angles are inside the circles, while azimuth and elevation angles are outside.

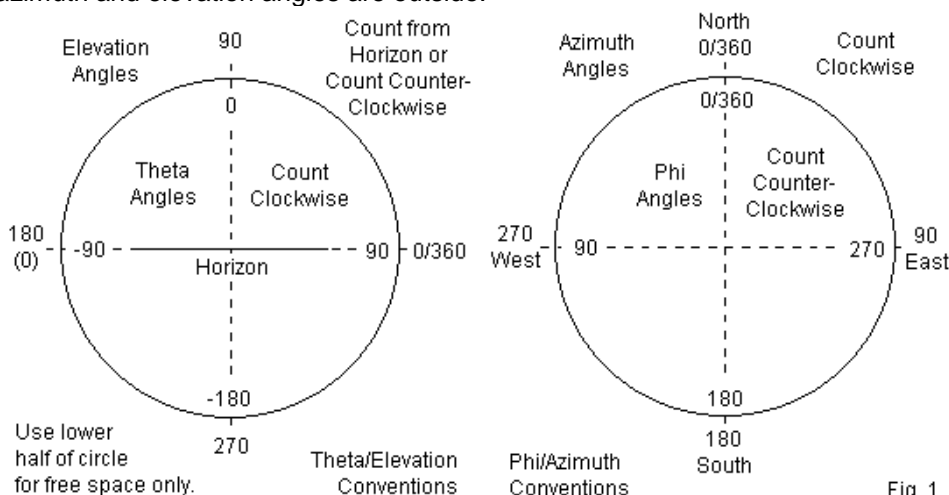


Fig. 1

Software implementations of NEC use various means of presenting polar plots. Virtually all commercial implementations of NEC do an easy conversion of theta plots into elevation plots. They simply subtract the theta angle from 90 to obtain an elevation angle. Azimuth patterns are a bit more difficult to handle. For example, EZNEC simply uses the phi conventions, but calls its plots "azimuth." There is a compass plot that we shall work with in a subsequent episode.

Simple Rotational Models in NEC-Win Plus

NSI products (NEC-Win Plus, NEC-Win Pro, and GNEC) handle the polar-plot situation in a different manner. They offer the user the option of pairing phi and

theta plots or of selecting azimuth and elevation plots. Elevation plots convert theta plots by the usual method. Phi and azimuth plots use the outer-ring angle markings appropriate to each pattern, as shown in **Fig. 2**.

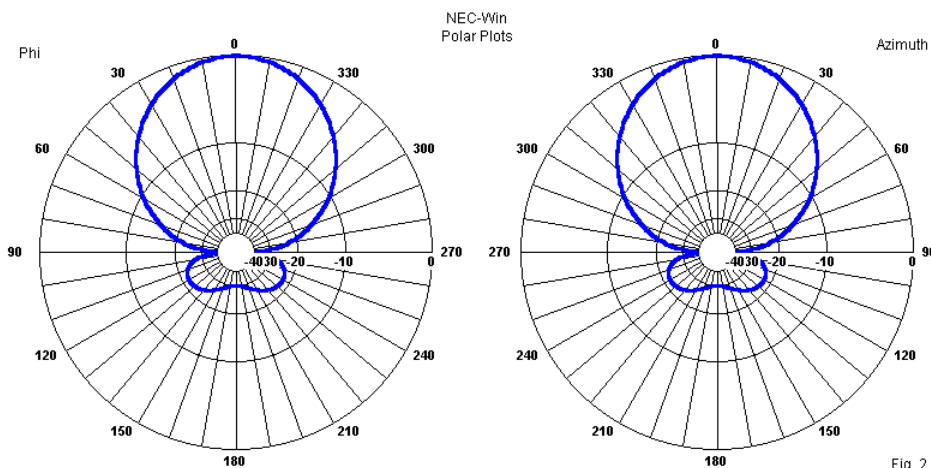


Fig. 2

By placing 0 degrees at the top of the plot, NSI polar plots can use the very same data, angle-by-angle, for both plots. Whether the plot on the right is a true azimuth pattern depends in part on the symmetry of the pattern. For antennas that produce symmetrical patterns, we cannot tell a true azimuth model from one that is casually modeled in the Cartesian coordinate system.

There are some modeling tasks that require not just patterns that bear azimuth labels, but as well, true azimuth models. The NSI VOACAP output depends on using compass or azimuth bearings. Broadcast antennas make FCC submissions using azimuth concepts both to describe the antenna and to provide sample patterns. These submissions may include MW BC towers and antennas, or they may involve one or more antennas on a tower--and each such antenna may point in a different direction on the compass. No less complex are some of the fields of antennas used by government, military, and even advanced amateur installations. Hence, it may pay to learn how easy it is to create true azimuth models to make use of the polar plot labels to yield true azimuth patterns. We shall move from that point to creating true azimuth models.

The process begins by attending to the correlation within NEC of the Cartesian coordinate system to the phi angles (and as a direct consequence, to azimuth angles). Consider **Fig. 3**.

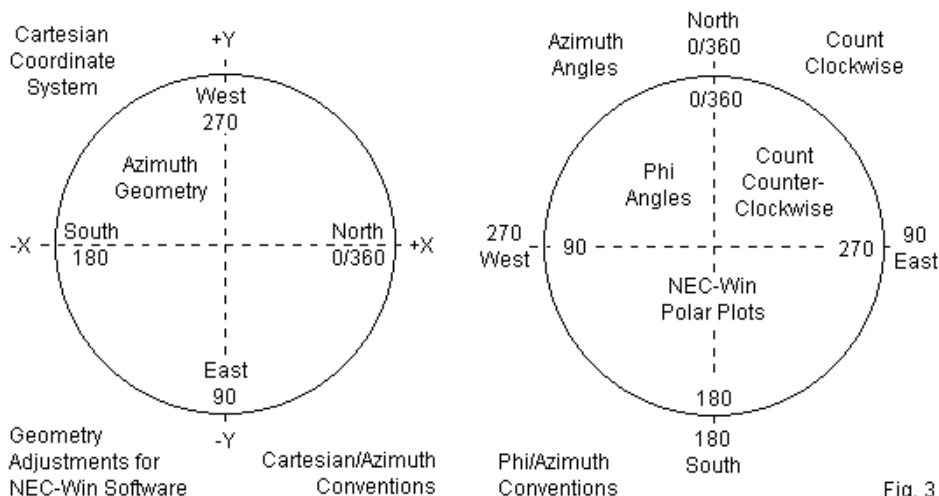


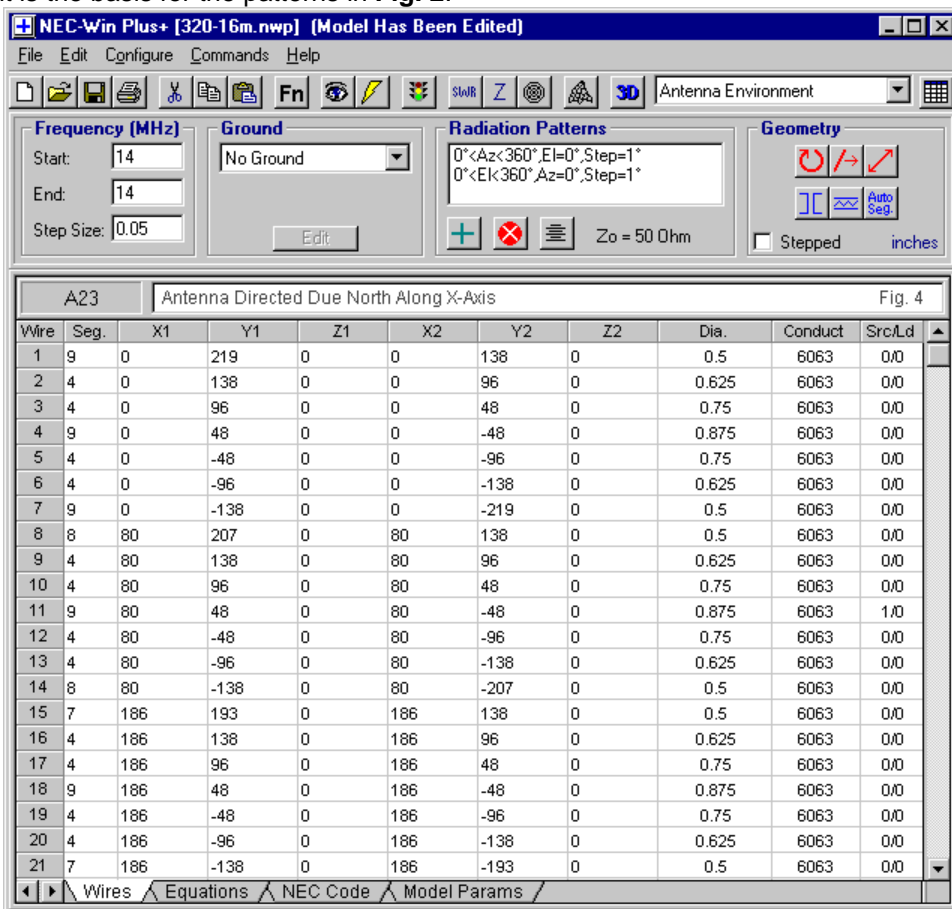
Fig. 3

The circle on the right is identical to its right-side counterpart in **Fig. 1**. The circle on the left provides the connection between the coordinates used to set up the model and the polar plots. Zero degrees always corresponds to values extended along the +X axis of the coordinate system. If we select a phi pattern, then the pattern angles count counterclockwise toward 90-degrees phi or toward the +Y axis. The values proceed around through 180 and 270 degrees phi before return home to zero degrees.

However, if we wish a true azimuth pattern, then we must proceed clockwise in the polar plot, with zero degrees representing North. Moving in a clockwise position toward East or 90-degrees azimuth, we end up at values extended along the -Y axis. From that point, we proceed to South or the -X axis, and further to West or the +Y axis. Finally, we return home to North and zero degrees once more.

The trick to obtaining a true azimuth model is to set up the geometry adhering to the directions that will eventually yield a true azimuth pattern for the result. For antennas that have symmetrical patterns, such as the pair shown in **Fig. 2**, the process is simple: extend the boom or direction of radiation from the -X toward the +X direction. That will align the model and pattern toward North, with identical pattern features on both side of the North-South line. **Fig. 4** shows a NEC-Win

Plus version of a model designed precisely in accord with this instruction. In fact, it is the basis for the patterns in **Fig. 2**.



The values in the X1 and X2 columns show that the antenna structure proceeds from a reflector at X=0 toward a director at X=186 (inches, in the case of this 14-MHz Yagi). The elements are linear and extend equally toward +Y and toward -Y. The result is a true azimuth model, and so the azimuth pattern is also true. Suppose that we need the antenna pointed Northeast, that is, at 45 degrees azimuth or compass bearing. The procedure is simple and may use more than one means. Programs like NEC-Win Pro and GNEC give access to the GM

command. By specifying a 45-degree rotation around the Z-axis, we can effect the change of heading, so long as we remember to rotate clockwise. Since GM rotation would follow the phi conventions, we would specify the rotation angle as -45 degrees.

NEC-Win Plus (which is also an "insert" within both Pro and GNEC) uses a different method. There is a main screen rotation control labeled with a circular arrow. To use this control, we first block the entire antenna geometry, that is, the entire set of wire entries on the main screen. Then, we click on the rotation button to open a screen that is similar to the help screen in Pro and GNEC for the GM command. One option is to rotate the blocked wires around the Z-axis by a specified amount. For the antenna to point Northeast, we select a rotation angle of +45 degrees. *Note: the NEC-Win Plus rotation control around the Z-axis operates in accord with azimuth conventions, not in accord with phi conventions..*

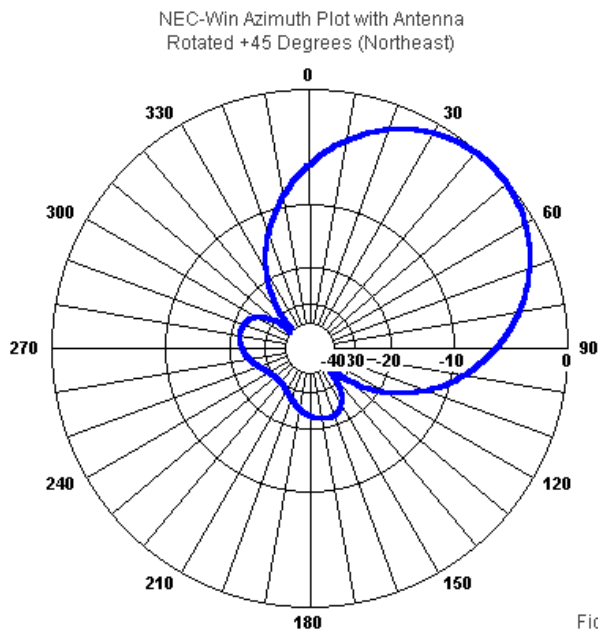
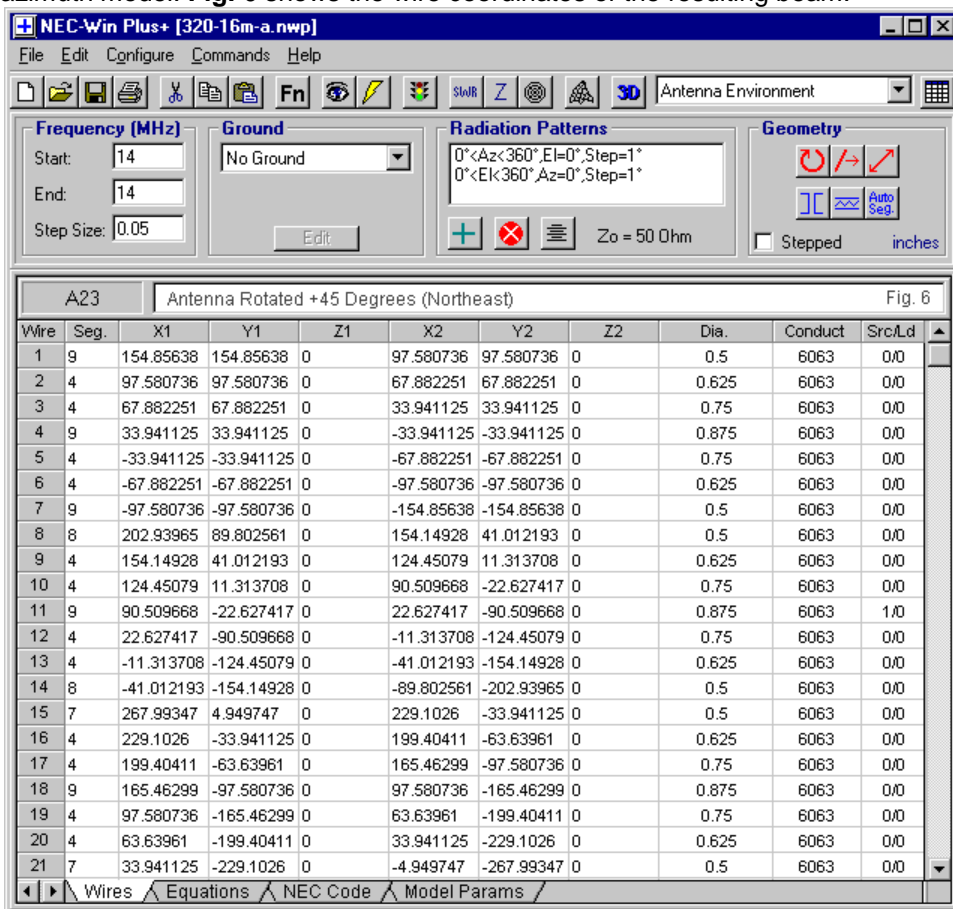


Fig. 5

Fig. 5 shows the resulting true azimuth pattern for the rotated beam. By comparing the original and new patterns, we can easily see the success of our maneuver. The result is not only a correct or true azimuth pattern for the

antenna, one that includes the correct angular labels. As well, we have a true azimuth model. **Fig. 6** shows the wire coordinates of the resulting beam.



Although inspection may initially make the numbers seem to be a jumble of coordinate values, you may do a little mental math on the center wires for each complete element (wires 4, 19, and 18) to see that the beam's boom extends along a line that is 45 degrees from either axis and that the elements extend at right angles to the boom. On one side of the boom, the end-1 coordinates extend toward +X and +Y, and on the other side, the end-2 coordinates extend toward -

X and -Y. Remember that these are directions and hence relative. End-1 coordinates are simply more positive and less negative than end-2 coordinates. Suppose that we had 2 identical beams in a stack, one above the other. In such a case, we might wish to see the outcome of rotating one or both beams until there is some desired angular separation in the boom directions. Normally, a stack of Yagis will have each antenna mounted so that the center of mass equalizes the boom-forward and boom-rearward moments. The mounting center will be very close to, but usually not precisely at the center of the boom, as measured from the rear-most element to the forward-most element. For most purposes we may model the mast position as the boom center.

To reposition each antenna with a boom-center at coordinates 0,0, we can use one of several procedures. The most straightforward would be to subtract one-half of the boom length (0.5×186 or 93 inches) from each X dimension while the boom is still aligned North and South. A second alternative is the use the NEC-Win Plus translation control and effect a block movement of the same amount on all wires in the model. A third way to the same goal is to use the GM command (if available) to effect a translation along the X-axis by the same amount. If we wish to move the antenna along the boom-line and to rotate it 45 degrees by using the GM command, we must use 2 separate GM commands. The GM command rotates before it translates, but our goal is to translate before we rotate. Hence, we cannot combine the two movements into a single command.

To create a stack of 2 Yagis from our original model (**Fig. 4**), we shall illustrate the process by block copying the first antenna and pasting the result below the first 21 wire lines. To effect a vertical separation (arbitrarily 800" for the example), we set the Z-value for 21 wires to that number--or we may use the translation facility to make that move. Next, as shown by the left side of **Fig. 7**, we shall block all of the wires and move or translate both antennas -93 inches so that each is centered on its boom along the X-axis. The final step, shown on the right in **Fig. 7**, is to rotate one of the antennas. We block the wire lines for the antenna or 21-wire set of choice and enter the rotation as 45 degrees, remembering that in NEC-Win Plus, the rotation control system operates clockwise.

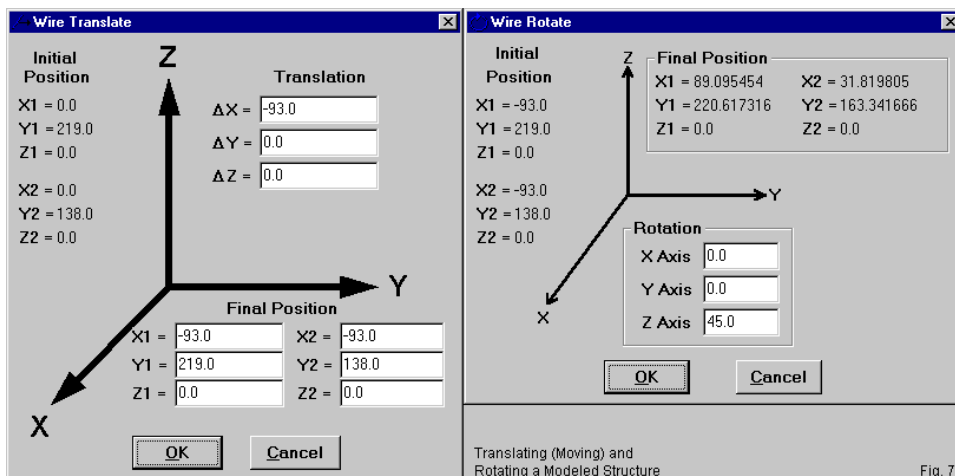


Fig. 7

The result of the work appears on the right side of **Fig. 8**. Note that the boom center is close to but not on the coordinate system center (0,0). Had we gotten the order of operations reversed and rotated before translating, we might have stacked the antennas as shown on the left in **Fig. 8**. The result might not have produced serious errors in this case, but in other cases it might yield vary wrong results.

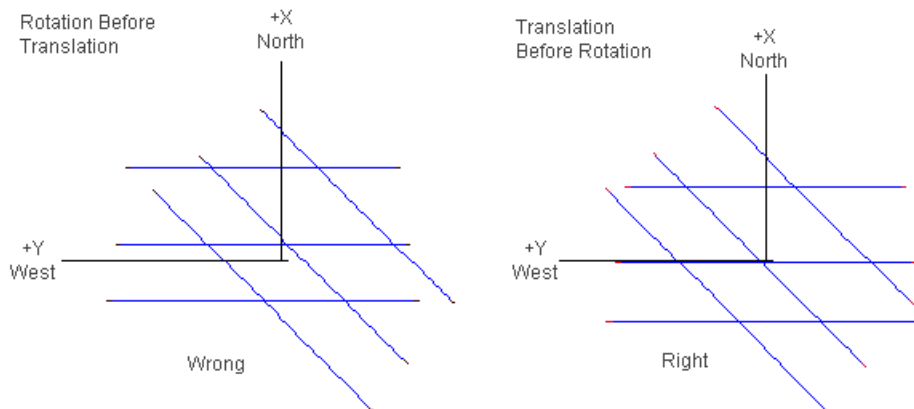


Fig. 8

True Azimuth Models in NEC-Win Plus

Not all efforts to create a true azimuth model and plot combination are quite so simple as rotating an antenna having a symmetrical pattern. There are many modeling problems in which we begin the process with one or another form of azimuth data describing the geometry of the antennas. We shall explore a couple of simpler cases in order to maintain clarity on the principles involved. Suppose that we had a set of 3 monopoles that are 1/4-wavelength at 1 MHz. Since a wavelength at 1 MHz is 300 m, the monopoles are each 75-m long. Although a real-world exercise might include a buried radial system for each monopole, we shall use a perfect ground for our exercise. As well, the individual antennas have an arbitrary diameter of 0.1 m and use a conductivity appropriate to steel. Also for simplicity, we shall feed the individual antennas in phase.

In many situations, one monopole may serve as a key against which we determine the positions of the others. We might receive a data list such as the following.

Tower Number	Distance Meters	Azimuth Bearing Degrees
1	---	---
2	150	060
3	300	060

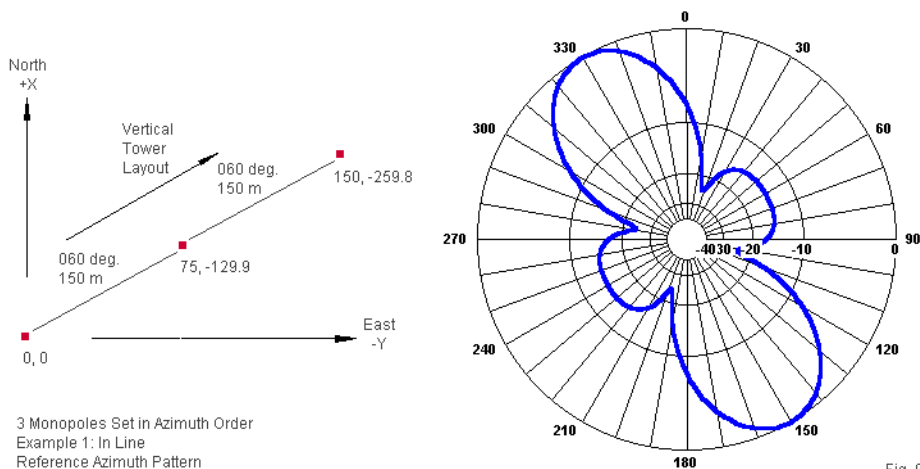
We shall read this data by using tower 1 as the key, with the subsequent distances and bearings referenced to it. Without much difficulty, we recognize that this system forms a set of 3 monopoles fed in phase, with each monopole spaced by 1/2 wavelength from an adjacent monopole.

NEC, and most commercial NEC input systems, do not allow inputs using distances and headings derived from azimuth or compass data. We still need to translate this data into X and Y coordinates that create a true azimuth model. (Of course, we also need to handle the Z-coordinates, but they will each be 0 at end 1 and 75 at end 2 with meters as the unit of measure.) 60 degrees lies in the first azimuth quadrant. Hence, the towers will form a line between North and East, that is, between the +X and the -Y axes.

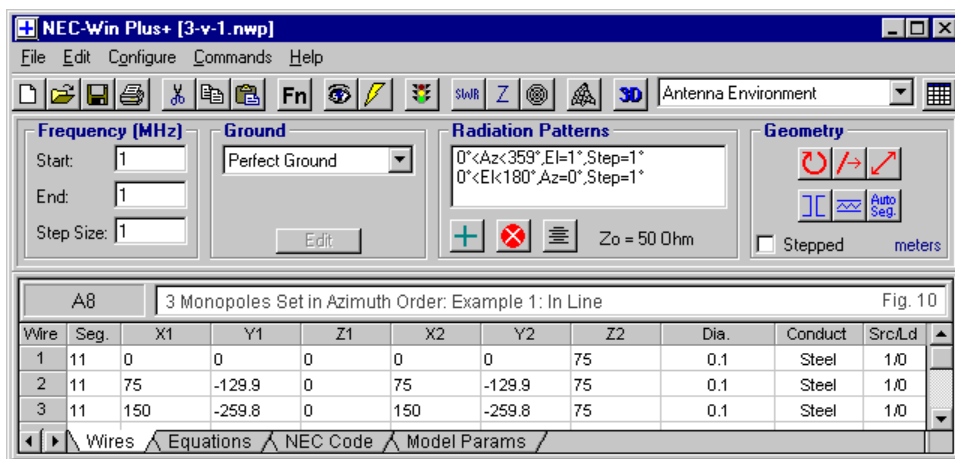
We define the extension along the +X axis by the cosine of 60 degrees (0.5) and the extension along the -Y axis by the sine of 60 degrees (0.866). These two simple trig operations allow us to translate the original table so as to yield corresponding coordinates for each data entry.

Tower Number	Distance Meters	Azimuth Bearing Degrees	+X coord	-Y coord
1	---	---	0	0
2	150	060	75	-129.9
3	300	060	150	-259.8

Fig. 9 visually portrays the layout in terms of both the original and the derived data. The figure uses the distance between the towers rather than the cumulative distance from the origin. On the right is an azimuth pattern that confirms the accuracy of our set-up work.



Since the pattern is symmetrical across the line formed by the towers, strict adherence to the conventions of correspondence between azimuth headings and coordinates may seem excessively finicky. However, many FCC and other filings require a pattern that accurately reflects the gain (and often the field strength) in all map directions. Hence, a precision model is more than a desire; it is a necessity. **Fig. 10** provides a screen view of the resulting model.

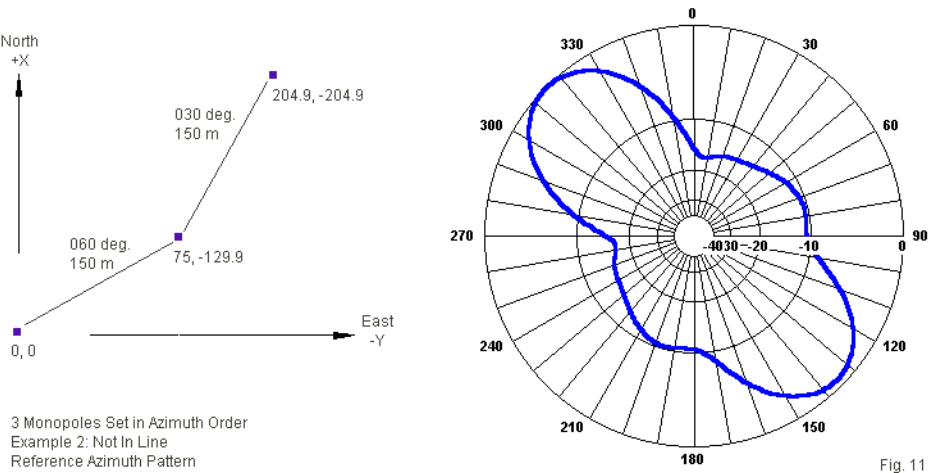


An alternative form of initial data would use each succeeding monopole as a reference for the next. Let's examine such a case, again keeping the background elements simple. We shall retain the steel 0.1-m diameter monopoles and feed them in phase, although they will not form a straight line in this case. In fact, the initial data might take the form of the following table.

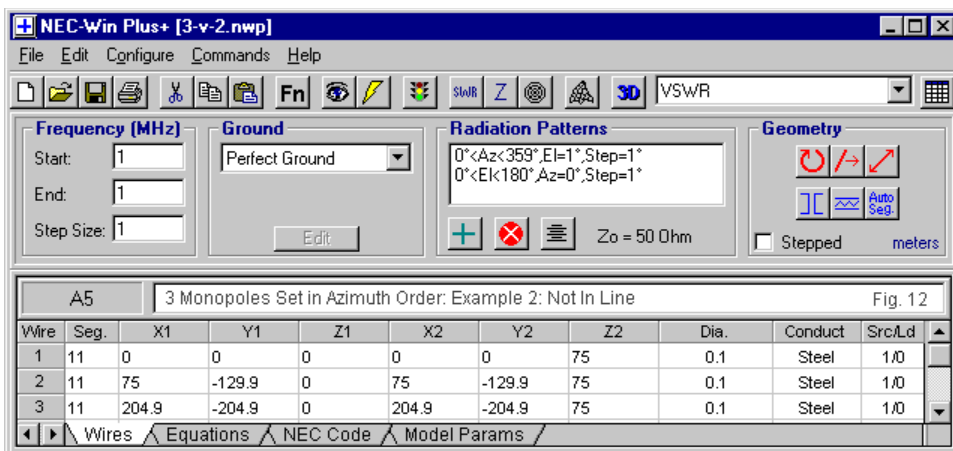
Tower Number	Reference Tower	Distance Meters	Azimuth Bearing Degrees
1	---	---	---
2	1	150	060
3	2	150	030

We can proceed in a cumulative manner, as in the first problem. However, that route would require us to calculate the end position in terms of a distance and angle from the origin. For the present case, that task is simple, but many other cases might involve solutions to irregular triangles. For now, it is easier to solve the two positions successively. For the second case, we shall initially assume a start at the origin and then simply add the +X and -Y values to the new +X and -Y values to arrive at the final coordinates. To keep the math simple, I selected the 30-degree azimuth heading for the 3rd monopole since the values of sine and cosine are simply flipped relative to the values for the 60-degree heading. The final data table prior to creating the model itself resembles the following one. Remember that the X values are positive and the Y values are negative.

Tower Number	Reference Tower	Distance Meters	Azimuth Bearing Degrees	+X coord	-Y coord
1	---	---	---	0	0
2	1	150	060	75	-129.9
3	2	150	030	204.9	-204.9



As **Fig. 11** shows, we have a bent line of monopoles, each a half-wavelength from an adjacent monopole. The line formed from monopole 1 to monopole 3 has an azimuth bearing of 045 degrees. When fed in phase, the array produces the pattern shown to the right (over a perfect ground). Note that, relative to the line of towers if overlaid on the polar plot, the pattern is no longer symmetrical. We might easily contrive any number of non-symmetrical patterns by altering the feedpoint current magnitude and phase angle for each monopole. **Fig. 12** provides the NEC-Win Plus model that produces this pattern and arrangement of monopoles.



It is not necessary to use the first monopole as the key. In fact, in any array, we may set any point as the coordinate center and calculate from that point. For example, consider a system of 6 towers with a virtual center in a 2-by-3 arrangement. If we have the field dimensions and the bearing along the rectangle formed by the monopoles, we can easily calculate the azimuth bearing and distance to each monopole from the field center. With that data, simple sine and cosine operations will yield the required coordinates to produce a true azimuth model.

Alternatively, we might have a field of rotatable directional beams. We would use the same techniques to locate the coordinates of the center of each beam antenna in the field relative to the point selected as the coordinate center. Since NEC-Win and NEC rotational commands use one of the coordinate axes as the center of rotation, we might have to use a multi-step process to place each antenna in its correct position pointing along the correct bearing. Create the antenna --centered along its boom--at the coordinate center and rotate it to the correct heading. Then move (translate) the antenna to the final position of the boom center at its field location.

In any complex modeling exercise, it pays to pre-plan each maneuver and set up an order of operations--*on paper*. Although the exercises just suggested only count as moderately complex, it is still easy to lose track of what move occurs next in the progression. Hence, developing a detailed checklist that includes not just the order of operations, but also the quantities involved in each move, can go

a long way toward making the process second nature, smooth, and (most important of all) accurate.

The key to the effort lies in understanding the relationship between the polar plot in its azimuth form and the Cartesian coordinates that result in a true azimuth model. +X is always North or zero-degrees azimuth. Clockwise, East or 90-degrees azimuth corresponds to the -Y direction on the coordinate system. Note also that these directions apply to the NSI implementations of NEC. They only apply to other software if that software follows the same conventions for translating a phi pattern into an azimuth pattern. One limitation in some software is to place zero-degrees phi on the far right, allowing 90-degrees phi to occur at the top of the polar plot. This system is at odds with standard azimuth conventions in which zero degrees or North is always at the top of a plot. Such systems do not permit us to use the same set of rules for forming a true azimuth model.

One of the implementations of NEC using the alternative polar-plot set up is EZNEC. Still, the program does have a compass plot facility. In the next episode, we shall explore how to create true azimuth models within the program.

103. True Azimuth Models - EZNEC Software

In the first of our 2 episodes on creating true azimuth patterns, we explored NSI software to see how to develop both true azimuth patterns and the models that yield those patterns. Because the NEC-Win polar plot places zero degrees at the top of the plot, the apparent difference between a phi plot (the inherent NEC plot from the radiation pattern tables) and an azimuth or compass plot is simple. The phi plot counts degrees in a counterclockwise direct, while a compass plot counts degrees in a clockwise direction.

The creation of true azimuth models, however, requires something more from us as modelers. North equates with the +X-axis in the Cartesian coordinate system. Hence, East or 90-degrees azimuth corresponds to the -Y axis. For irregular sets of positions in the X-Y plane, we need to do some careful planning to obtain a model whose geometry produces a correct azimuth plot. Each step in the process is simple enough, even when we receive initial data in the form of distances and bearings. However, we can easily develop a model of moderate complexity and lose track of what comes next. Hence, I recommend a detailed pencil-and-paper procedure for setting up such models.

Nevertheless, in NSI software, we can in a straightforward way create true azimuth or compass-oriented models that are useful for VOACAP, BC, and large antenna field analyses. In fact, we may do the same using EZNEC software. However, the procedures will not be identical, simply because the polar plot display conventions in EZNEC differ from those used by NSI software. Once we master the conventions applicable to EZNEC, we shall discover that every step possible in one software package is available in the other. They will simply differ in accord with convention differences. One result is that a true azimuth model created for one software set will not be readable as a true azimuth pattern by the other without significant revision of the model geometry.

Simple Rotational Models in EZNEC

EZNEC (Version 4) comes in 3 sizes: standard, plus, and pro. The last version is available with either the NEC-2 or NEC-4 core. However, all required functions to

create true azimuth models are available on even the most basic version of the program.

The process of creating true azimuth models begins with an understanding of the EZNEC azimuth plot. In its raw form, without the supplemental data shown, the plot is somewhat opaque, as suggested by **Fig. 1**. The plot shows the pattern of the same 3-element Yagi used to start the NSI notes, with the boom aligned along the X-axis. Thus, we discover the first difference between NSI software and corresponding EZNEC software. EZNEC places the standard plot zero-degree position on the far right. This procedure allows a pattern that coincides roughly with the normal way of presenting the Cartesian X and Y axes on a flat surface: The X-axis receives a horizontal line and the Y-axis receives a vertical line. In the plot shown, +Y corresponds to the top position of the plot circle.

*** Total Field**

EZNEC

Standard EZNEC Azimuth
(Phi) Pattern with Boom
Aligned Along X-Axis

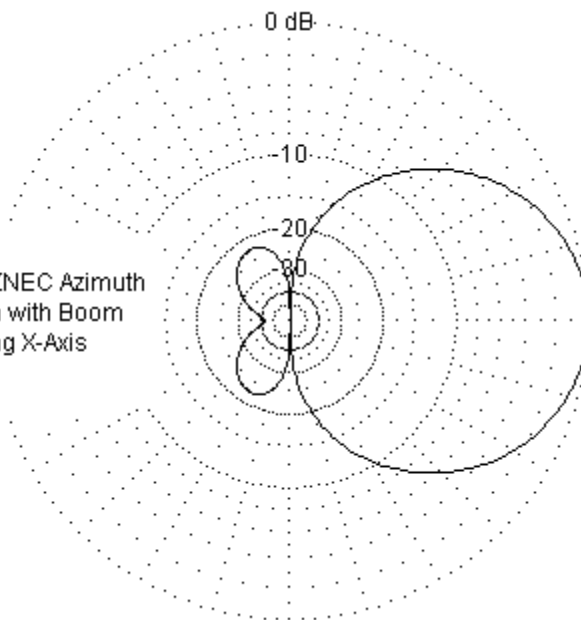


Fig. 1

Because the plot does not show the degrees on the outer ring of the plot circle, the nature of the plot may not be immediately apparent. There is a data set attached to each plot to record various headings of interest in plot analysis. However, in this plot transfer, the only way to obtain degree markings is to add them with a paint program. Although EZNEC refers to the plot as an azimuth plot, it is actually a phi plot and counts degrees counterclockwise. (The EZNEC elevation plots do count degrees from the horizon upward.) For a myriad of antennas with symmetrical patterns on each side of the virtual boom line, the difference does not make a difference relative to understanding the antenna's operation.

Among its options, EZNEC does offer a "Compass" plot. The compass plot counts degrees clockwise, with zero degrees positioned at the top of the plot circle. Note that there is a 90-degree difference between the zero-points of the standard plot and the compass plot. If we wish to create a model of an antenna pointed North, we must adopt a new set of convention. **Fig. 2** shows the relationship of the plot conventions to the Cartesian geometry conventions.

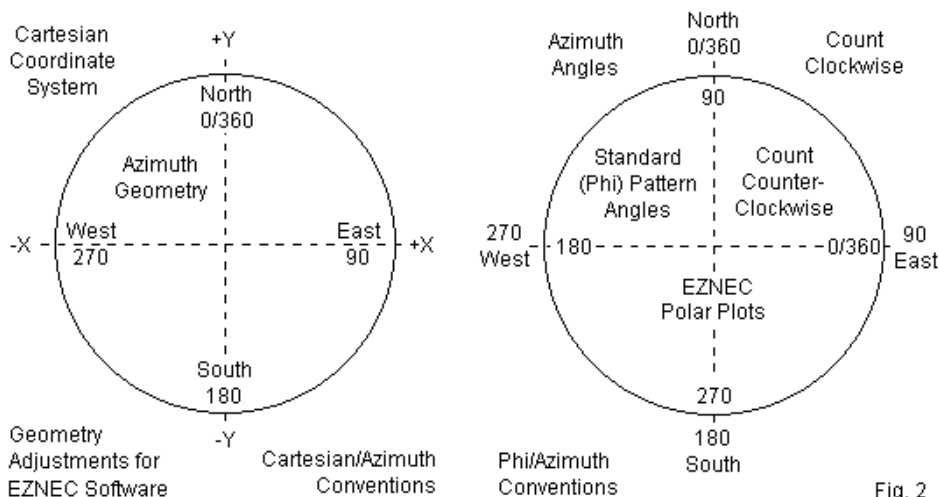
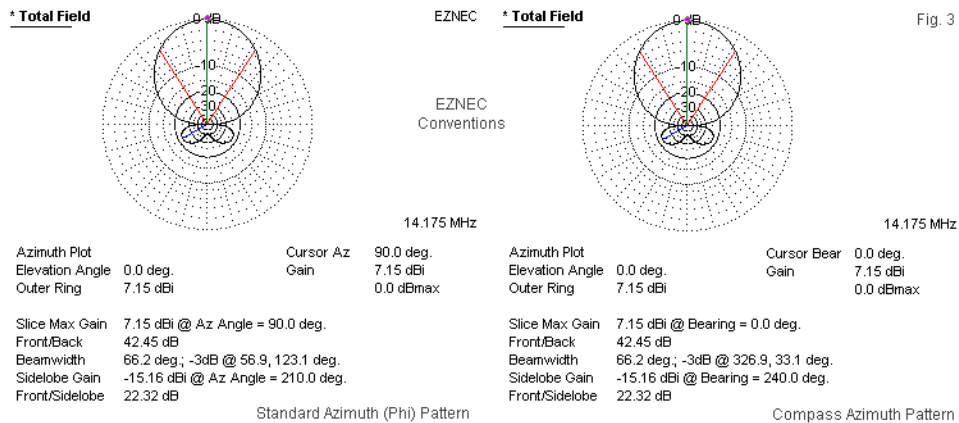


Fig. 2

Since North corresponds to the Cartesian Y-axis, to point an antenna North requires that we form the model with the boom pointed toward +Y. The revised model will then have its elements extended (for a symmetrical model with linear

elements) along the -Y to +Y axis with East corresponding to the +X direction. If we revise our 3-element Yagi model accordingly, we can obtain both a standard and a compass pattern, as shown in **Fig. 3**.



Note that there is no difference between the graphical portions of each plot. The differences appear in the data beneath the plot. The standard plot shows the cursor and the maximum gain heading to be 90 degrees, which we would expect of the phi pattern for a plot oriented 90 degrees counterclockwise to the plot in **Fig. 1**. In contrast, the compass plot shows the cursor and maximum gain at zero degrees, corresponding to the model's boom pointing North along the +Y axis.

Fig. 4 provides us with the wire table for the model. If you compare it with the wire table from NEC-Win Plus in the preceding episode, you will find that all X-column Values are now in the Y column and vice versa.

Wires

Wire Create Edit Other

Wire Table

Antenna Pointing North

Show Wire Insulation

Fig. 4

Coord Entry Mode

Preserve Connections

Wires

No.	End 1				End 2				Diameter	Segs
	X (in)	Y (in)	Z (in)	Conn	X (in)	Y (in)	Z (in)	Conn	(in)	
1	-219	0	0		-138	0	0	W2E1	0.5	9
2	-138	0	0	W1E2	-96	0	0	W3E1	0.625	4
3	-96	0	0	W2E2	-48	0	0	W4E1	0.75	4
4	-48	0	0	W3E2	48	0	0	W5E1	0.875	9
5	48	0	0	W4E2	96	0	0	W6E1	0.75	4
6	96	0	0	W5E2	138	0	0	W7E1	0.625	4
7	138	0	0	W6E2	219	0	0		0.5	9
8	-207	80	0		-138	80	0	W9E1	0.5	8
9	-138	80	0	W8E2	-96	80	0	W10E1	0.625	4
10	-96	80	0	W9E2	-48	80	0	W11E1	0.75	4
11	-48	80	0	W10E2	48	80	0	W12E1	0.875	9
12	48	80	0	W11E2	96	80	0	W13E1	0.75	4
13	96	80	0	W12E2	138	80	0	W14E1	0.625	4
14	138	80	0	W13E2	207	80	0		0.5	8
15	-193	186	0		-138	186	0	W16E1	0.5	7
16	-138	186	0	W15E2	-96	186	0	W17E1	0.625	4
17	-96	186	0	W16E2	-48	186	0	W18E1	0.75	4
18	-48	186	0	W17E2	48	186	0	W19E1	0.875	9
19	48	186	0	W18E2	96	186	0	W20E1	0.75	4
20	96	186	0	W19E2	138	186	0	W21E1	0.625	4
21	138	186	0	W20E2	193	186	0		0.5	7
*										

Let's rotate the antenna 45 degrees toward the Northeast (compass bearing 045 degrees) to parallel the same operation in the last episode. To set up the antenna for rotation, we should first move the wires by 93" so that the rotation point (coordinates 0,0) is at the center of the boom. EZNEC has move and rotate functions comparable to those in NSI software. They appear as options within the wire table array of possible modifications. Just like using the GM command, we must move the wires first and then rotate them. **Fig. 5** shows the relevant maneuvers in terms of the assistance screens that appear. To center the antenna along its boom for a compass pattern, we move the wires -93" along the Y-axis or boom line. Then we rotate the antenna 45 degrees clockwise around the Z-axis to move the boom direction from North to Northeast.

Move Wires XYZ

First wire to move: 1
Last wire to move: 21

Move X by: 0 (in)
Move Y by: -93 (in)
Move Z by: 0 (in)

Buttons: **Ok**, **Cancel**

Rotate Wires

First wire to rotate: 1
Last wire to rotate: 21

Rotation Amount: 45 Deg
☒ CW
☐ CCW

Rotation Axis:
☐ X
☐ Y
☒ Z

Rotation Center:
☒ Axis
☐ Wire
 Number: 1
 ☒ End 1
 ☐ End 2
 ☐ Center
☐ Coordinate
 X: 0
 Y: 0

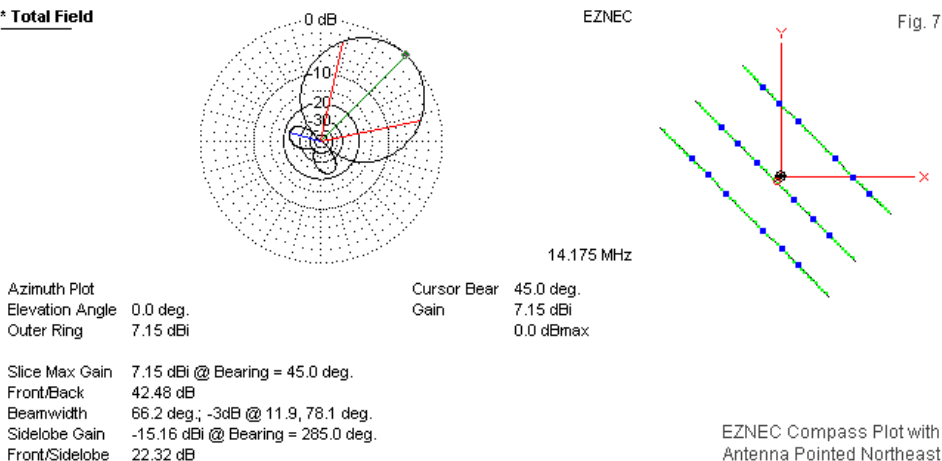
Buttons: **Ok**, **Cancel**

Fig. 5

For reference, **Fig. 6** shows a composite wire table after each maneuver. The table shows only the end-1 values, with the post-move set on the left and the post-rotation set on the right. If we had wished to place the antenna after rotation at some other position within a field of antennas, we would next perform another

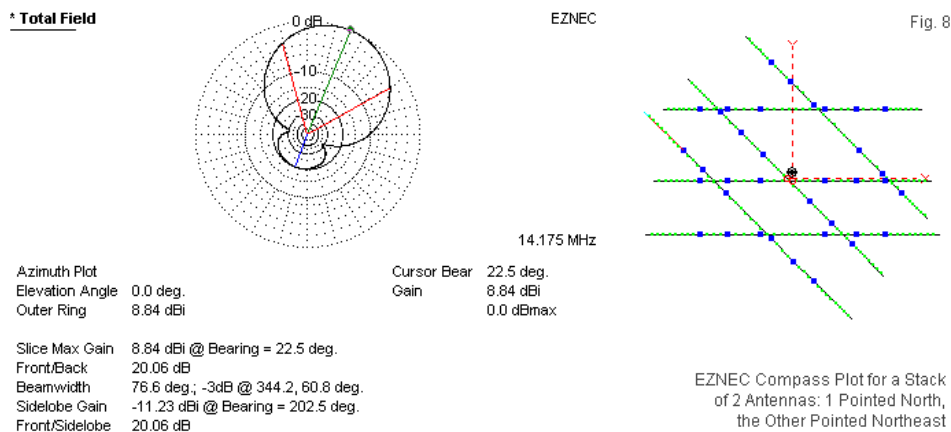
that the virtual boom center is offset by a small amount from the center or driver element. The feedpoint circle and the axis center circle do not coincide.

* Total Field



Since we have turned the antenna after moving it, let's create a stack of 2 Yagis. We shall want the 2 antennas in the stack to point in different directions, perhaps one headed Northeast and the other North. EZNEC provides a variety of ways to create the stack. One way to proceed is to copy the existing wires to create a new set. The next step is to use either the height function or the move function to create a spacing between the 2 sets of wires. For this small exercise, I have selected 800" as the arbitrary separation. We may then rotate the new wires 45 degrees counterclockwise to point them North along the boom. If we wish to test other angles of separation between the antennas in the stack or other separation distances, we can use the move and rotate functions appropriately. Since we already have a beam pointing North, we can also import the file description from that model. For identical antennas in a stack, this procedure might be more cumbersome, since we would need to separate the antennas and ensure that each rotated on its boom center. However, there are many exercises in which we may have different antennas in the modeled stack. In that case, importing the added antenna model may prove to be the most practical maneuver.

The operations to create stacks are available also in NSI software. The spreadsheet main face of NEC-Win Plus allows block copying of the first Yagi into a second version. The translation (move) function then allows us to set the separation. To create a stack of different antennas, we may block copy a set of wires and appended sources and loads from one model file to another. In advanced software that makes the full NEC command set available, we can accomplish the copy and move functions with the GM command. The results of our EZNEC stacking operations appear in **Fig. 8**. Although the wire table is too long to reproduce, the plot, the data, and the antenna model outline should suffice to establish that we have a successful true azimuth model and plot of the stack. I set the radiation pattern increment to 0.5 degrees so that the heading for maximum gain would read correctly (rather than showing the nearest integer value). Since the model is in free space, the maximum gain occurs rather exactly between the headings of the identical beams. Placing the stack over ground might amend the heading of maximum gain due to slightly different ground effects on the two antennas in the stack.



There are many good reasons for studying the patterns of a stack with the individual beams pointing in different directions--assuming that this condition is among the planned modes of operation. Forward gain of the composite pattern is only 1 of several interesting facets of the stack. You may also wish to compare the beamwidth for a single antenna (66 degrees) with the beamwidth for the

stack (77 degrees). Note also the change in the rearward lobes. Then mentally overlay two sets of individual-antenna rear lobes at 45 degrees to each other. Although the two antennas have some interaction with each other, the overlay process goes a long way toward showing the revised shape of the rearward radiation pattern in the stack.

True Azimuth Models in EZNEC

To complete our tour of setting up true azimuth models in EZNEC software, we must also tackle the types of situations that we examined for NSI software. There are many modeling problems in which we begin the process with one or another form of azimuth data describing the geometry of the antennas. We shall explore a couple of simpler cases in order to maintain clarity on the principles involved. Suppose that we had a set of 3 monopoles that are 1/4-wavelength at 1 MHz. Since a wavelength at 1 MHz is 300 m, the monopoles are each 75-m long. Although a real-world exercise might include a buried radial system for each monopole, we shall use a perfect ground for our exercise. As well, the individual antennas have an arbitrary diameter of 0.1 m (100 mm) and use a relatively low conductivity. Also for simplicity, we shall feed the individual antennas in phase. As we did with the NSI exercises, we may begin with data provides in the form of bearings and distances, perhaps against a map or site plat.

Tower Number	Distance Meters	Azimuth Degrees	Bearing
1	---	---	
2	150	060	
3	300	060	

The system once more consists of the monopole in a line, with 1/2-wavelength spacing between the individual antennas. For the exercise, we shall feed each monopole at its base in phase with the other two monopoles. Because the heading is 060 degrees, the line extends from Southwest to Northeast. If we let the first monopole be the key and place it at coordinates 0,0, then the remaining monopoles will fall somewhere between North and East. Once more, we can make use of the sine and cosine functions of 60 degrees to form multipliers for the distances and derive the proper coordinates. Because the second and third monopoles fall in the first quadrant, both X and Y will be positive. Since the Y-axis is North or zero degrees and the X-axis is 90 degrees, the X coordinate will be the sine of the angle times the distance or $0.866 * 150 = 129.9$ m. The Y coordinate will be the cosine of the angle times the distance or $0.5 * 150 = 75$ m. The monopoles form a single line, so the second coordinate set can simply

use the cumulative distance for $X = 259.8$ m and $Y = 150$ m. The completed table is below.

Tower Number	Distance Meters	Azimuth Bearing Degrees	X coord	Y coord
1	---	---	0	0
2	150	060	129.9	75
3	300	060	259.8	150

Fig. 9 provides a visual presentation of the monopole layout against the Y and X axes that form the South-to-North lines and the West-to-East line. The annotated antenna view has been turned so that the axes assume their proper positions relative to an azimuth map. The compass plot confirms that the main lobes of the radiation pattern are broadside to the line of monopoles, with maximum gain at 135 and 315 degrees azimuth.

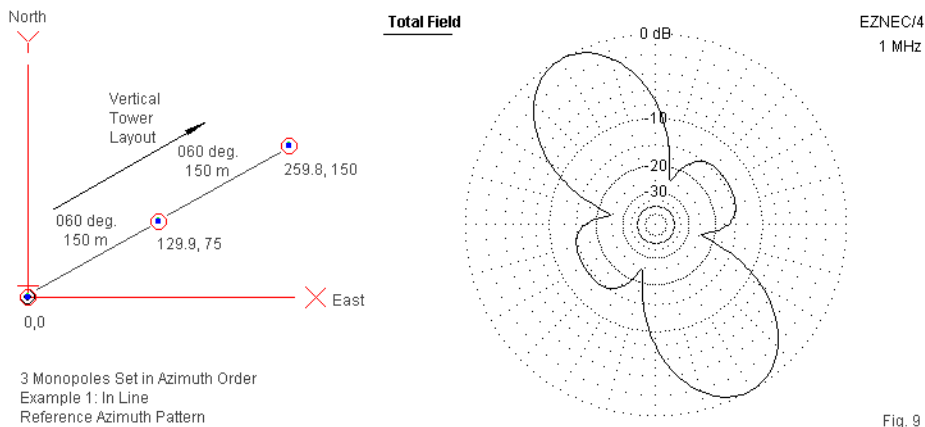
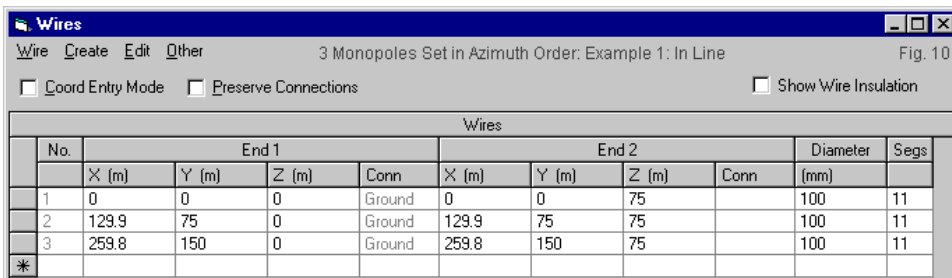


Fig. 10 shows the wire table for the model to confirm the use of the coordinates in the tables. As noted in the preceding episode, there are many applications in which precision azimuth pattern are required. Hence, the small bit of pre-modeling calculation that it takes to set up the true azimuth model is minuscule compared to having a pattern rejected by a licensing agency.



The second exercise involves 3 towers that do not form a single line. Instead, the third tower moves off from the second at a different angle. We shall retain the in-phase feeding system over perfect ground to preserve the model's simplicity, since our goal is to get a handle on how to organize the coordinates within EZNEC to obtain a true azimuth model.

Tower Number	Reference Tower	Distance Meters	Azimuth Bearing Degrees
1	---	---	---
2	1	150	060
3	2	150	030

We may easily calculate the coordinates for the second monopole using the techniques employed for the first monopole system. Next, we can assume that the second monopole is at the coordinate center and calculate its coordinates. To the values for X and Y, we simply add the values for each coordinate derived for the position of monopole 2. The result of the small trig exercise appears in the following completed table.

Tower Number	Reference Tower	Distance Meters	Azimuth Bearing Degrees	X coord	Y coord
1	---	---	---	0	0
2	1	150	060	129.9	75
3	2	150	030	204.9	204.9

The results appear more graphically in **Fig. 11**, where the annotated antenna outline shows the final positions along with the original data and the calculated coordinates. The compass plot is identical to the one produced using NEC-Win Plus and the pattern is broadside to the virtual line from the first to the last of the

monopoles. The lack of perfect symmetry on each side of that lines reveals the effects of the irregular line formed by the 3 antennas.

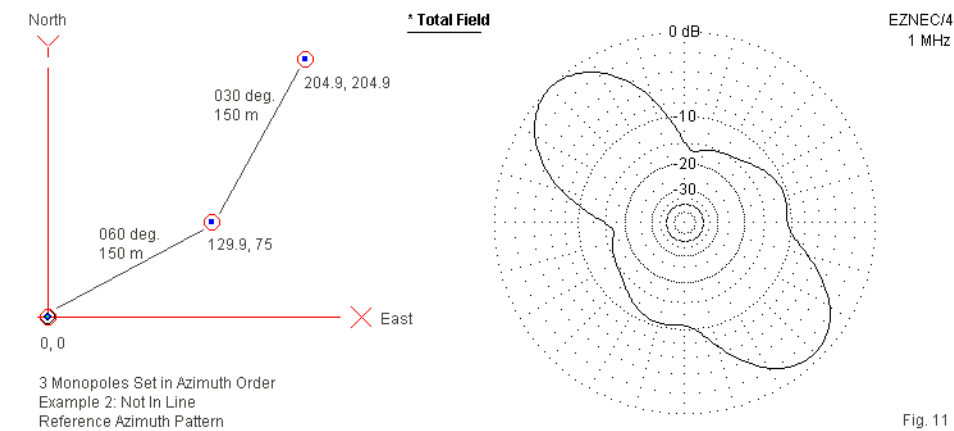


Fig. 11

As a confirmation of the model's use of the calculated coordinates, **Fig. 12** shows the model's wire table.

Wires										
3 Monopoles Set in Azimuth Order: Example 2: Not In Line										
Fig. 12										
<input type="checkbox"/> Coord Entry Mode <input type="checkbox"/> Preserve Connections <input type="checkbox"/> Show Wire Insulation										
Wires										
	No.	End 1				End 2				Segs
		X (m)	Y (m)	Z (m)	Conn	X (m)	Y (m)	Z (m)	Conn	
	1	0	0	0	Ground	0	0	75		11
	2	129.9	75	0	Ground	129.9	75	75		11
	3	204.9	204.9	0	Ground	204.9	204.9	75		11
	*									

Producing true azimuth patterns in EZNEC turns out to be as straightforward as it did using NSI software. Once we located North (the +Y axis) and East (the +X axis), the remain steps became a matter of calculating coordinates from any data that might be supplied in terms of distance and azimuth bearing. Of course, we can always begin with coordinate data, so long as we remember to place the antenna or its parts against a paper version of the X-Y system with North set

along the correct axis line. Figuring the antenna coordinates then becomes a matter of arranging the coordinates. If an antenna has an area as defined in the X-Y plane, then it may be easiest to arrange the antenna along one or another axis and then to move and/or rotate the antenna to the desired orientation. EZNEC and NEC-Win Plus both use proprietary file formats, neither of which is the standard ASCII NEC-input file format. However, NEC-Win Plus will save files in the standard format, and EZNEC Pro will do so as well. Hence, my own work often involves moving from one piece of software to the other by way of an intervening NEC model file. There is a relationship between the systems needed to produce true azimuth models in each type of software. When moving from NEC-Win Plus to EZNEC, rotate the antenna or antenna field 90 degrees counterclockwise in EZNEC. When moving from EZNEC to NEC-Win Plus (or other NSI software), rotate the antenna or antenna field 90 degrees clockwise in the NSI program. The results will yield true a azimuth model if the initial model was truly an azimuth model within its software.

Producing true azimuth models is certainly not necessary for a large part of the modeling enterprise. However, for applications demanding true azimuth models and patterns, the two bodies of software that we have sampled provide guides to almost any other software implementing NEC. The software must have an azimuth pattern that counts degrees clockwise. With that available, the rest of the task has only 2 steps. The first is to determine how the azimuth pattern relates to the software's standard phi pattern. The second is to calculate the necessary coordinates for the antenna to produce a true azimuth model and a true azimuth pattern.

104. PS: I Change

Suppose that we create a model of a ground-plane monopole with 4 radials. Let's use 7.15 MHz as the test frequency. The monopole will be 10.071 m long and 0.0125 m in radius. The radials will be 11.57 m long and 0.002 m in radius. We shall equip the model with a GM line so that we can readily change the height of the antenna assembly over ground, using the radials as the base height.

```
CM monopole 7.15 MHz 25-mm dia.
CM over ave gnd
CM 90-deg radials
CE
GW 1 11 0 0 0 0 0 10.071 .0125
GW 2 11 11.57 0 0 0 0 0 .002
GM 1 3 0 0 90 0 0 0 2 1 2 11
GM 0 0 0 0 0 0 0 83.858
GE -1 -1 0
GN 2 0 0 0 13.0000 0.0050
EX 0 1 1 0 1 0
FR 0 1 0 0 7.15 1
RP 0 181 1 1000 -90 0 1.00000 1.00000
EN
```

The model might begin as high as 2 wavelengths over ground (using the constants for average ground in this case). However, we shall be interested in lower heights, down to and including placing the radials below ground. We shall have to change the model design just slightly to accommodate NEC-4 guidelines that require a wire or segment junction at $Z=0$. One easy way to achieve this is to run the monopole down to the ground. Then let the innermost segment of each radial slope from $Z=0$ down to the radial level. The remaining radial segments form a flat plane. The radials are 0.001 wavelength below ground, about 0.042 m or 1.65".

```

CM monopole 7.15 MHz 25-mm dia.
CM buried radials .001 wl
CM 90-deg radials
CE
GW 1 11 0 0 0 0 0 10.071 .0125
GW 2 1 1.05 0 -.042 0 0 0 .002
GW 2 10 11.57 0 -.042 1.05 0 -.042 .002
GM 1 3 0 0 90 0 0 0 2 1 2 11
GE -1 -1 0
GN 2 0 0 0 13.0000 0.0050
EX 0 1 1 0 1 0
FR 0 1 0 0 7.15 1
RP 0 361 1 1000 -90 0 1.00000 1.00000
EN

```

If we plot the data for models as they approach and then penetrate ground, we obtain an interesting set of discontinuities. All data use the usual units of measure.

4-Radial 90-Degree Ground-Plane Monopole From 2-WL Up to Below Ground: Performance with Various Ground Types

Free-Space Reference Performance Monopole:

Len 10.071 m, Radius 0.0125 m Freq.: 7.15 MHz

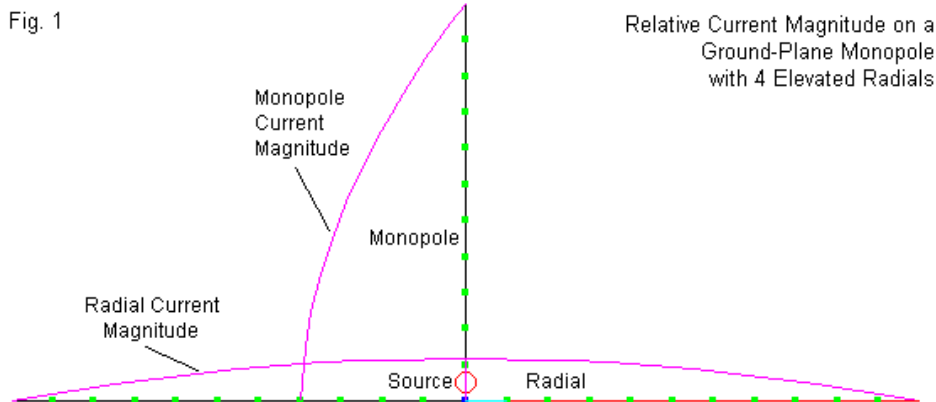
Rad-L m	Rad-R m	Gain dBi	Bmwidth	Resist	React
11.57	0.002	1.35	102	21.34	0.06

Ground Type Average: C 0.005, P 13

Height wl	Height m	Gain dBi	TO Angle	Resist	React
0.1	4.193	0.24	70	24.35	-4.84
0.05	2.096	0.10	67	28.64	-3.48
0.025	1.048	-0.04	65	31.75	0.22
0.01	0.419	-0.22	64	34.64	7.85
0.005	0.210	-0.38	64	36.52	16.53
0.001	0.042	-1.37	64	47.26	52.34
-0.001	-0.042	-2.37	64	64.75	7.98
-0.005	-0.21-	-2.49	64	66.25	10.30

Note that as we enter the ground, the gain drops rapidly. More significantly, the feedpoint impedance changes considerably. If we add more radials, the transition will be less extreme, but the 4-radial model makes a useful tool, if for no other reason than to arouse a bit of curiosity.

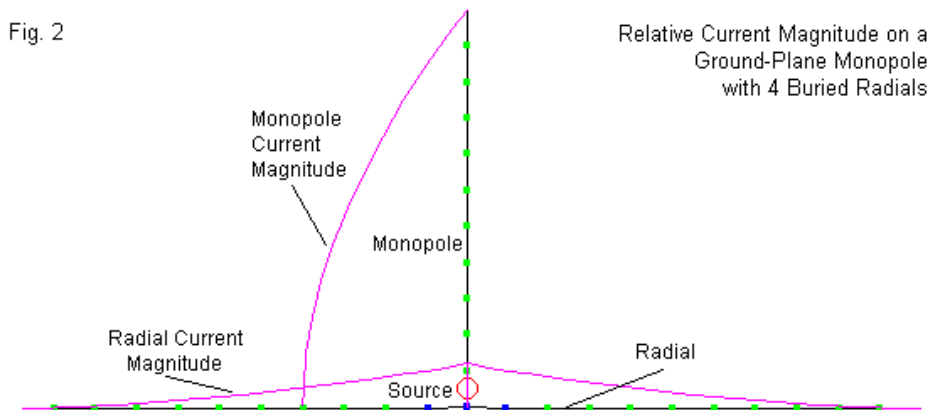
Fig. 1 shows the relative current magnitude along the vertical monopole and along 2 of the 4 radials forming the ground plane. The model shows the current distribution is in free space, but any model having all of its wires above ground would show the same set of characteristics. I have set the maximum monopole current on the 4th segment of the radial as a marker. Note that the maximum radial current is just above the first monopole segment, indicating that we have very close to equal currents on the radials and on the monopole. Of course, each radial carries 1/4 of the total current below the feedpoint.



Both current curves have very similar shapes. However, current magnitude does not tell us the complete story. The following list shows both the relative current magnitude and the current phase angle based on a source current of 1.0 at 0°. If we count upward on the monopole to the 5th entry, we find a magnitude of 0.81245. The corresponding entry for the radial, counting downward, is 0.21420, very close to 1/4 the monopole value. As well, note the similarity of current-phase value at the monopole top and the radial end. Remember that the radial has a much smaller radius than the monopole.

Monopole		Radial	
Magnitude (A.)	Phase (Deg.)	Magnitude (A.)	Phase (Deg.)
.09260	-2.93	.25147	-0.08
.24609	-2.71	.24966	-0.27
.38339	-2.49	.24298	-0.43
.50941	-2.26	.23114	-0.56
.62371	-2.01	.21420	-0.67
.72512	-1.75	.19237	-0.78
.81245	-1.47	.16600	-0.89
.88456	-1.17	.13553	-0.99
.94034	-0.82	.10146	-1.09
.97902	-0.42	.06417	-1.19
1.0000	0.00	.02318	-1.29

If we lower the antenna so that the radials are below ground, we shall have to modify the model slightly. The monopole will just touch the ground. The radial wires will have 2 sections. The innermost segment will slope from ground level at the monopole base down to 0.001 wavelengths below ground (about 0.042 m or 1.65"). The remaining segments will extend to 11.57 m to produce the same total length as the radials in the above-ground model. **Fig 2** shows the model and the relative current magnitudes, followed by a tabular listing of magnitudes and phase angles.



Monopole		Radial	
Magnitude (A.)	Phase (Deg.)	Magnitude (A.)	Phase (Deg.)
.09286	-6.00	.24242	-7.83
.24693	-5.66	.21041	-28.95
.38486	-5.30	.17479	-51.49
.51154	-4.90	.14094	-73.58
.62647	-4.47	.11038	-95.00
.72839	-3.99	.08337	-115.4
.81606	-3.44	.05966	-134.6
.88806	-2.81	.03914	-152.5
.94333	-2.06	.02223	-170.1
.98087	-1.10	.00972	170.08
1.0000	0.00	.00222	139.95

Since the models differ very slightly in construction due to the need to develop subsurface radials, the monopole current magnitudes are very close, but not identical, to the values for the preceding model. However, we do find a difference in the current phase angle range. For identical source values (1.0 A. at 0°), the preceding model tip current phase angle was only -2.93°, whereas the model with buried radials has a tip-segment phase angle of -6.0°. The above-ground model is a free-space version of the antenna with a source impedance of $21.35 + j0.07$ Ohms. The model with buried radials uses average ground (C 0.005 S/m, P 13) and reports a source impedance of $64.69 - j 7.84$ Ohms.

The differences between the radial currents for the above-ground and the buried radial models are far more dramatic. Visually, the radial curve differs by rapidly decreasing in current magnitude as we move from the hub outward. The table confirms the curve. At the 5th entry upward, the monopole shows a value of 0.81606, while the corresponding radial entry shows a value of 0.11038, only half the magnitude for that position on the above-ground radial. The current phase changes along the buried radial are far more radical than those along the above-ground radial. One NEC convention is to maintain all phase reports in the 0°-180° range. The outer-most value is equivalent to a value of -220.05°, about 214° out of phase with the tip of the monopole. Note that these values are not true tip values, but the values at a position roughly comparable to the center of the relevant wire segments in the models.

The comparison makes clear that the common above-ground portions of the two antennas yield essentially the same current distribution. However, the parts that

move from above ground to below ground change their current distribution. Most modelers seem to be wholly unaware of this phenomenon. So it bears some exploration. Let's begin by reviewing some fundamentals about NEC's treatment of ground.

For any given ground quality, we measure (or find in some table) values for conductivity (sigma) and relative permittivity (epsilon-r). Relative permittivity rests on the permittivity in free space (epsilon-0). Essentially, the program combines the listed values for conductivity and permittivity into a complex relative permittivity (epsilon-g):

$$\epsilon_g = \epsilon_r - j\sigma / (2\pi f\epsilon_0)$$

The term f is the frequency in Hz. As f changes, so too does the value of epsilon-g. Therefore, the effects of ground on buried-radial ground-plane antenna performance vary with conductivity, permittivity, and frequency.

NEC also calculates another value called k_s , the wave number in the sinusoidal current expansion in NEC. This value applies to any wire within a medium other than free-space (or a vacuum). Hence, it applies to all insulated wires and to any wires below ground level (assuming that a real ground is operative in the model). The value of k_s modifies the length of a wave for the calculation of current along a wire. Hence,

$$\lambda_s = 2\pi / k_s$$

The current-propagation wave number has the effect of lengthen every applicable segment with respect to current calculations. The exact amount of lengthening depends upon the frequency and ground constants that the modeler selects.

We can easily determine the effect of the wave number on segment length by employing the PS command in NEC-4. The command requires only the command letters, with no following numerical entries. In fact, we can perform segment-length adjustment calculations without further model execution by following the PS command with EN, as in the following sample model. The model contains all of the GW, GN, FR, and EX elements to form a complete model,

except that it lacks an output request other than the PS command. Hence, calculations stop after the PS command has done its work.

```

GW 1 11 0 0 0 0 0 10.067 .0125
GW 2 10 10.4823 0 -.04193 .953 0 -.04193 .002
GW 2 1 .953 0 -.04193 0 0 0 .002
GM 1 3 0 0 90 0 0 0 2 1 2 11
GE -1 -1 0
GN 2 0 0 0 13 .005
EX 0 1 1 0 1 0
FR 0 1 0 0 7.15 1
PS
EN

```

Although the report in the NEC output file shows the value of k_s , we may confine our attention to the effects on segment lengths. I ran models of 160-m and 40-m ground-plane monopoles with 4 buried radials through the PS command, using 3 diverse ground-quality values, those for very good (C 0.0303 S/m, P 20), for average (C 0.005 S/m, P 13), and for very poor (C 0.001 S/m, P 5) soil. I also ran the same model in free space to illustrate how much wire values change as we bury the radials. Note that in the following lists, all values are normalized to fractions of a wavelength. As well, I converted the entries from engineering to decimal notation. In both cases, the monopole physical segment length is 0.02183 wavelength with a physical radius of 0.000298 wavelength.

Radial Segment Length and Radius			
Frequency	Soil Quality	Segment Length	Segment Radius
1.85 MHz	None	0.02273 WL	0.0000477 WL
	Very Good	0.3904	0.0008194
	Average	0.1612	0.0003383
	Very Poor	0.0713	0.0001577
7.15 MHz	None	0.02273 WL	0.0000477 WL
	Very Good	0.2017	0.0004233
	Average	0.09664	0.0002028
	Very Poor	0.05376	0.0001128

To extract a simple example from the listing, the 7.15-MHz average-ground segment length is about 4.3 times the physical length, that is, the length in free-space when normalized to a fraction of a wavelength. With respect to current expansion, the radial point corresponding to the 5th monopole entry in the earlier model (**Fig. 4-2**) actually lies just inside the second segment, where we find a current magnitude of about 0.21. However, notice that the radius increases to the

same degree, resulting in what appears to be a more rapid change of current phase angle. Since the current does not go to zero until we reach the radial tip, most of the table entries for the buried radial show very low values compared to the free-space model.

The NEC-4 manual recommends that we use λ -s as the basis for calculating segment lengths for any wire within a medium other than free space, where free space includes any region above a real ground. Examining the PS command report shows that the calculated segment length for current expansion along a buried radial no longer agrees with the segment length for the monopole that is above ground. The segment-length difference appears at one end of the source segment, suggesting a possible error source in the model. The AGT cannot show this potential error, since the test uses free space as its venue. So the next question is what degree of error we might expect from not adjusting the segment length in accord with the value of λ -s.

To obtain a sense of what error might be possible, I used the 40-m monopole and ran it in two forms, using very good, average, and very poor soil. The first run used the standard segmentation of the sloping-radial construction with a total of 11 segments per radial. The following lines sample the model over average ground.

```
GW 1 11 0 0 0 0 0 10.067 .0125
GW 2 10 10.4823 0 -.04193 .953 0 -.04193 .002
GW 2 1 .953 0 -.04193 0 0 0 .002
GM 1 3 0 0 90 0 0 0 2 1 2 11
GE -1 -1 0
GN 2 0 0 0 13.0000 0.0050
EX 0 1 1 0 1 0
FR 0 1 0 0 7.15 1
RP 0 181 1 1000 -90 0 1.00000 1.00000
EN
```

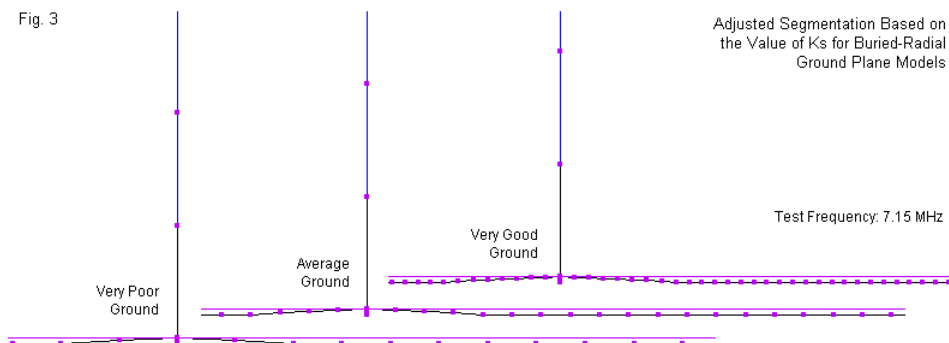
Next, I adjusted the number of segments in the radial entries (GW2) so that the calculated segment length for current expansion would more evenly match the monopole segment length. Again, here is a sample over average ground. Note the use of the PS command to allow confirmation of the segmentation.

```

GW 1 11 0 0 0 0 0 10.067 .0125
GW 2 40 10.4823 0 -.04193 .953 0 -.04193 .002
GW 2 4 .953 0 -.04193 0 0 0 .002
GM 1 3 0 0 90 0 0 0 2 1 2 44
GE -1 -1 0
GN 2 0 0 0 13 .005
EX 0 1 1 0 1 0
FR 0 1 0 0 7.15 1
PS
RP 0 181 1 1000 -90 0 1.00000 1.00000
EN

```

For the adjusted models, the outlines in **Fig. 3** show the distribution of segments between the sloping and the straight portion of the radials. The monopole, of course, remains unchanged. The look of the model outline represents the physical dimensions and not the electrical length of segments as calculated by NEC for use in the current expansion.



From the total of 6 models, I obtained the following results. The entries showing 11 segments per radial represent the unaltered models. The alternate model segment numbers represent values that yield calculated segment lengths about equal to those in the monopole.

7.15-MHz Ground-Plane Monopole with 4 Buried Radials

Soil Quality	Segments/Radial	Gain dBi	Source Impedance
Very Poor	11	-4.24	88.94 + 29.22 O
	26	-4.13	86.63 + j26.22
Average	11	-2.36	64.60 + j7.29 O
	46	-2.35	64.44 + j4.28
Very Good	11	0.46	50.91 + j8.19
	98	0.24	53.53 + j5.75

None of the possible error differences are either fatal or unambiguous. For example, the amount of difference is greatest for the antenna over very good soil, but so too is the increase in the radial wire radius. The calculated radius is greater than the monopole radius. In some instances, using the calculated values of segment length and radius as a basis for adjustment may lead to an impossible conflict among NEC guidelines. For precision work, the problem would require considerable thought before finalizing a model. However, for general guidance in determining trends and rough properties, using unaltered models with 11 segments per radial will largely suffice. Remember that NEC ground systems have other limitations. For example, they presume a homogenous ground from horizon to horizon and from the surface downward. In many cases, the actual ground will be stratified, and the exact values of conductivity may not be measurable to the depth of RF penetration.

Within the context of NEC models using buried radials, the exercise does provide a foundation for understanding the different current distributions that we find in those radials, relative to above-ground models.

A Note on IS and PS

Because the IS or insulated sheath command also places a non-free-space medium around a specified wire, NEC-4 will adjust the segment lengths and radii for implementing the current expansion. Out of curiosity, you may invoke the PS command in trial models to see what happens. Let's begin with a simple dipole for 7.15 MHz using a 0.001-m radius wire.

```

CM 7.15-MHz dipole in free space
CM Radius 0.001 m
CE
GW 1 21 0 -10.2 0 0 10.2 0 .001
GE
FR 0 1 0 0 7.15 1
EX 0 1 11 0 1 0
PS
RP 0 1 361 1000 90 0 1.00000 1.00000
EN

```

With a length of 20.4 m, the dipole is resonant, showing a source impedance of $70.11 - j0.08$ Ohms. The free-space gain of this lossless wire is 2.14 dBi. Next, let's add an IS command to place an insulating sheath around the wire. We shall use a high-quality plastic with a relative permittivity of 3 and a conductivity of $1\text{E-}10$. The insulation will be 2-mm thick, resulting in a sheath radius of 0.003 m (around the 0.001-m radius wire). An insulation thickness that equals the wire diameter might fall into the relatively heavy insulation category, although thicker insulations certainly exist.

```

CM 7.15-MHz dipole in free space
CM Radius 0.001 m
CM insulated
CE
GW 1 21 0 -9.726 0 0 9.726 0 .001
GE
IS 0 1 1 21 3 1e-10 .003
FR 0 1 0 0 7.15 1
EX 0 1 11 0 1 0
PS
RP 0 1 361 1000 90 0 1.00000 1.00000
EN

```

To obtain resonance we must shorten the antenna to 95.4% of its bare-wire form. The source impedance reports $66.34 - 0.04$ Ohms and a free-space gain of 2.11 dBi.

Note that both models implement the PS command, since it takes so little run time and report space. However, only the report for the insulated wire model is relevant to satisfy our curiosity. If we explore the PS portion of the report, we encounter some entries in normalized form, that is, expressed as fractions of a

wavelength. These values are for the adjusted segment length and adjusted wire radius. We must calculate the normalized physical dimensions by dividing the physical segment length and radius by 41.92902 m, a wavelength at 7.15 MHz. Now we can compare the results within the limits expressed by the report entries.

Insulated 7.15-MHz Dipole		
	Segment Length	Segment Radius
Normalized Physical Dimensions	2.209E-2	2.385E-5
Adjusted Dimensions for Current Expansion	2.209E-2	2.385E-5

Within reporting limits, there is no difference in the values, although the effects of the insulation show up in the performance reports. However, the extent of the medium change is so small, that for all practical purposes, the modeler can ignore any segment length changes and use the same segmentation as he or she used for a bare wire model.

If the modeler specifies an upper medium (UM), usable only with the RCA ground system, the situation would be similar to specifying a ground, but apply to the region formerly treated as a vacuum or free-space. Under those conditions, application of the PS command in order to evaluate overall model segmentation is certainly in order.

105. Models, Symmetry, and Loads: A Couple of Reminders

While diagnosing an ailing model, I encountered a couple of areas in which a bit of clarification might be useful to other modelers. Since the points that we shall cover may be second nature to some modelers and temptations to error for others, let's just call these notes reminders.

The Destruction of Symmetry

The NEC manuals provide a list of conditions that "automatically reset the symmetry condition." The first item on the list--which is all that we need for this exercise--read this way: "Addition of a wire or patch (GW, GH, CW, SP, etc.) will destroy all symmetry." The conditions apply equally to the GX and the GR symmetry commands.

The most common interpretation that newer modelers seem to apply to the statement is that the core will fail to produce the symmetric structure specified in either the GX or GR command. This interpretation is incorrect. Rather, the core produces the desired structure, but does not use the shorter form of calculation to arrive at the matrix values. Instead, the model is reset for the entire structure to a non-symmetry mode of calculation.

Consider the following models, all of which have the properties shown in **Fig. 1**.

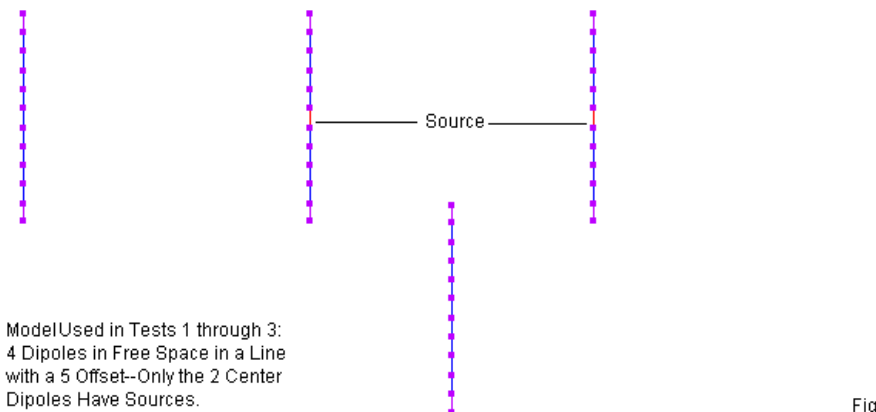


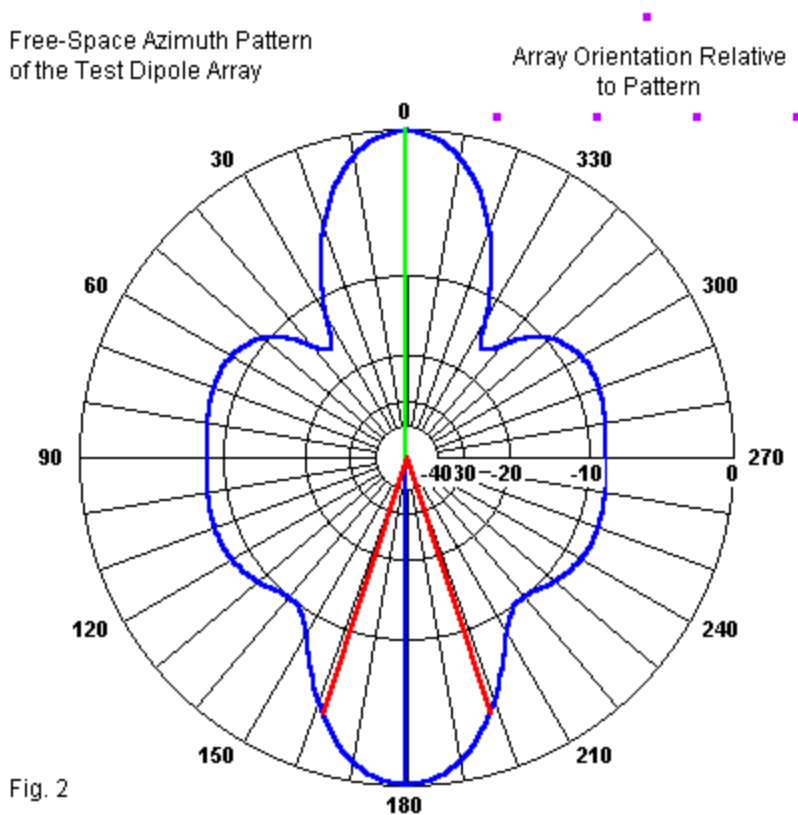
Fig. 1

The most direct form for this model would create all 5 wires in separate GW commands, using the following lines.

```
CM Test model: 4 vertical dipoles, inner 2 fed
CM 5th passive vertical dipole at a distance
CM Full version
CE
GW 1 11 0 -.75 -.245 0 -.75 .245 .001
GW 2 11 0 -.25 -.245 0 -.25 .245 .001
GW 3 11 0 .25 -.245 0 .25 .245 .001
GW 4 11 0 .75 -.245 0 .75 .245 .001
GW 5 11 .5 0 -.245 .5 0 .245 .001
GE 0 -1 0
FR 0 1 0 0 299.7925 1
EX 0 2 6 0 1 0
EX 0 3 6 0 1 0
RP 0 1 361 1000 90 0 1.00000 1.00000
EN
```

The relevant performance data for the model is a maximum gain of 6.04 dBi, with a 36-degree beamwidth in the main or maximum-gain lobe. The reported source impedance is 49.383 -j21.986 Ohms. Both of the variations on this model will

yield the same results to the last decimal place. The free-space azimuth pattern has the shape shown in **Fig. 2**. Note that the main lobe (by a tiny fraction of a dB) is away from the 5th vertical dipole.



An alternative to listing GW 3 and GW 4 is to use the GX commands to replicate the first 2 wires symmetrically across the Y-axis. This alternate form would take this appearance.


```
CM Test model: 4 vertical dipoles, inner 2 fed
CM 5th passive vertical dipole at a distance
CM GX, symmetry defeated
CE
GW 1 11 0 -.75 -.245 0 -.75 .245 .001
GW 2 11 0 -.25 -.245 0 -.25 .245 .001
GX 1 010
GW 5 11 .5 0 -.245 .5 0 .245 .001
GE 0 -1 0
FR 0 1 0 0 299.7925 1
EX 0 2 6 0 1 0
EX 0 3 6 0 1 0
RP 0 1 361 1000 90 0 1.00000 1.00000
EN
```

Since a GW entry (GW 5) follows the GX command, the common misconception is that wires 3 and 4 will not appear. Instead, the correct interpretation is that the GX command produces the required 2 wires, but does not invoke symmetry in its calculations. The following extract from the NEC output report gives us the telltale line.

```
TOTAL SEGMENTS USED= 55 NO. SEG. IN A SYMMETRIC CELL= 55 SYMMETRY FLAG= 0
```

If symmetry had been invoked, the number of segments in the symmetric cell would have been 22, the number of segments in the first 2 wire entries. As well, the symmetry flag would equal 1 rather than zero. The total number of segments in the model is 55, indicating that the core has created the requisite new wires or tags. The performance reports and the segment and current tables also show the existence of the created wires, but without the symmetry calculation shortcuts. In fact, the run times for this test model and for the first one were identical.

On some occasions, it may be necessary to successfully invoke symmetry due to model size or other factors. That route is irrelevant to the present array, but the model may be useful in its simplicity for illustrating one way to go about the process. The technique involves the use of a Numerical Green's File (NGF). We have examined NGFs in past episodes, but always in the context of saving the file for use with multiple new models that call up the results. We need not use separate NGF formation and use files. Instead, we can create and use the NGF results within the same model or .NEC file. We only need to use the NX or next

structure command between the saving of the NGF and the call-up of its contents. Note that NEC-2 requires that the first command following NX must be a comment (CM or CE). However, NEC-4 permits a geometry command to directly follow the NX command. We may use the following model as a guide.

```
CM Test model: 4 vertical dipoles, inner 2 fed
CM 5th passive vertical dipole at a distance
CM GX, symmetry via NGF
CE
GW 1 11 0 -.75 -.245 0 -.75 .245 .001
GW 2 11 0 -.25 -.245 0 -.25 .245 .001
GX 1 010
GE 0 -1 0
FR 0 1 0 0 299.7925 1
WG test3.ngf
NX
CE
GF test3.ngf
GW 5 11 .5 0 -.245 .5 0 .245 .001
GE 0 -1 0
EX 0 2 6 0 1 0
EX 0 3 6 0 1 0
RP 0 1 361 1000 90 0 1.00000 1.00000
EN
```

The first half of the model, prior to the NX command, creates the first 2 vertical dipoles and requests their replication via symmetry across the Y-axis. As in all NGF operations, we include ground, loading, and frequency information for the affected wires within this file. The WG command saves the results. The program used for these exercises allows the user to specify a file name and extension for the data storage. However, raw NEC-2 has limitations of the NGF filename, and different implementations of NEC-2 may use different specifications for this entry. Finally, note that we do not use the EN command before the NX command, because EN would terminate calculations.

Following the NX command, I have inserted a CE line so that the model will run on NEC-2 or NEC-4. The GW entry established the 5th dipole, while the EX lines provide the two sources. The results of this model are identical to those of the preceding tests, although we want to examine one special line-set of the NEC output report.

TOTAL SEGMENTS USED= 44 NO. SEG. IN A SYMMETRIC CELL= 22 SYMMETRY FLAG= 1
STRUCTURE HAS 1 PLANES OF SYMMETRY

In the first set of core calculations, the GX command creates 22 new segments, for a total of 44. The symmetry cell has the initial 22 segments and the flag is set to 1, indicating that symmetry is invoked for 1 plane. Because the model is so small and contains both parts of the process, the run time is no different than for the first 2 tests. However, for this demonstration, run time was not in question. For very large models, it may well become a key reason for using this technique. Our goal was to show how we can invoke symmetry and complete our modeling all within the same .NEC file.

If we wish to consider matters of file size and run times, we can turn to a different sort of model and simultaneously illustrate the same points for the GR or rotational symmetry command.

Fig. 3

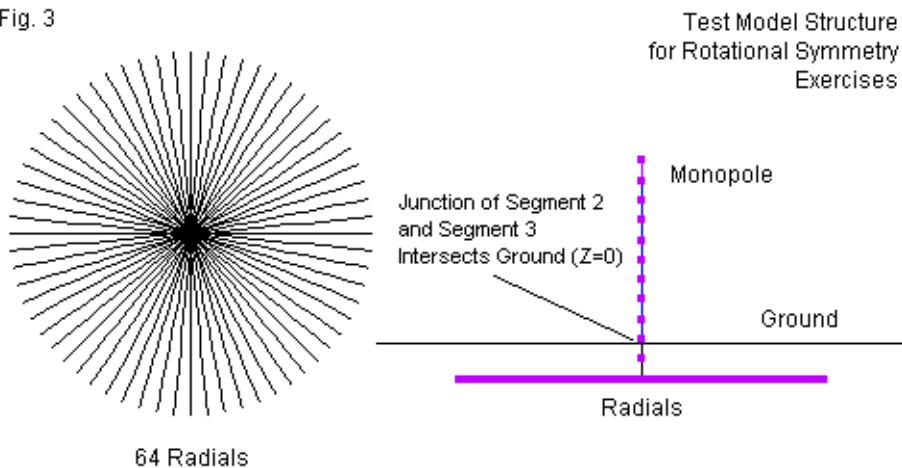
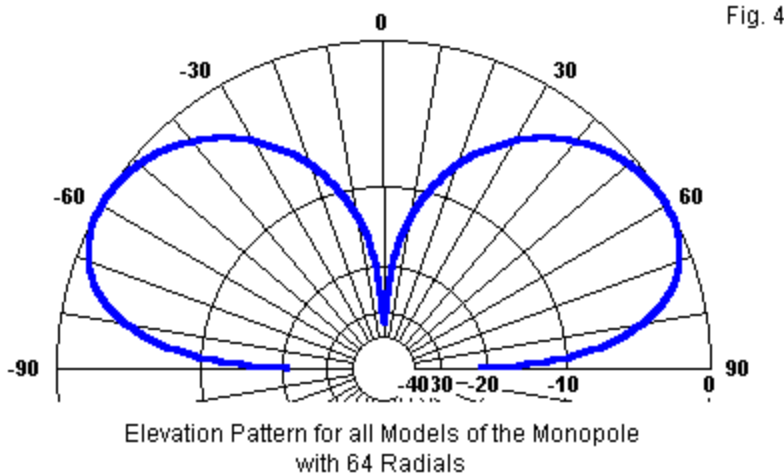


Fig. 3 shows the general properties of the models that we shall construct for this exercise. At the usual test frequency (299.2975 MHz, where 1 wavelength = 1 meter), we shall place 64 1/4-wavelength radials 0.05 m below ground. At the

center, we shall construct a single monopole wire that meets the radials below ground and extends 0.25-wavelength above ground. By assigning 11 segments to the monopole wire, the junction of the second and third segments will intersect $Z = 0$, the ground level. The following model illustrates the simple set-up, using the GM command to replicate the radials 63 times beyond the original GW 1 specifications.

```
CM 64 buried radials with monopole
CM GM
CE
GW 1 11 0 0 -.05 .25 0 -.05 .001
GM 1 63 0 0 5.625 0 0 0
GW 65 11 0 0 -.05 0 0 .25 .001
GE -1 -1 0
FR 0 1 0 0 299.7925 1
EX 0 65 3 0 1 0
GN 2 0 0 0 5 .001
RP 0 181 1 1000 -90 90 1.00000 1.00000
EN
```

The model yields a maximum gain of -0.42 dBi at a TO angle of 59 degrees (theta). **Fig. 4** shows the elevation/theta pattern for the model. The model made no attempt to achieve resonance, but used instead easily remembered dimension values. Hence, the reported source impedance is $46.125 - j730.025$ Ohms. All versions of the model report identical results.



To shorten run times and further simplify model formation, many modelers replace the GM command with a GR command. The GR command allows rotational symmetry and calculates the angle between each radials, so the modeler does not have to remember that a 64-radial system has a 5.625-degree angular separation between radial wires. The replacement model appears in the following lines.

```
CM 64 buried radials with monopole
CM GR
CE
GW 1 11 0 0 -.05 .25 0 -.05 .001
GR 1 64
GW 65 11 0 0 -.05 0 0 .25 .001
GE -1 -1 0
FR 0 1 0 0 299.7925 1
EX 0 65 3 0 1 0
GN 2 0 0 0 5 .001
RP 0 181 1 1000 -90 90 1.00000 1.00000
EN
```

Note that the GR entry is followed by the monopole GW entry. We could not place the monopole ahead of the GR command. That move would have resulted

in the creation of 64 monopoles in the same position. By placing the monopole wire after the GR command, we obtain only one monopole, we create only a single monopole, but we defeat the invocation of symmetry. However, we do not defeat the creation of the radials themselves. The critical line from the NEC output report for the model confirms these notes.

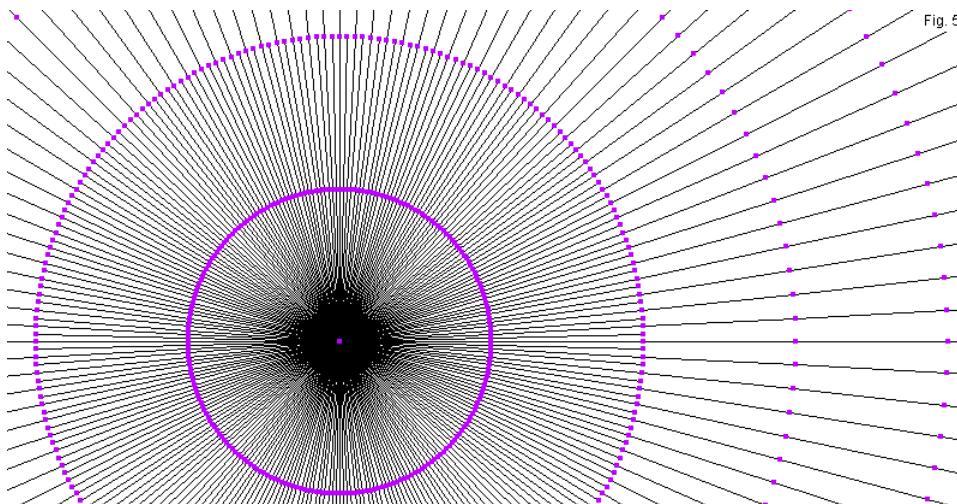
TOTAL SEGMENTS USED=715 NO. SEG. IN A SYMMETRIC CELL=715 SYMMETRY FLAG=0
The entire model--all 715 segments--form one symmetric cell, and the symmetry flag = 0; hence, the radials exist in the model, but it does not use symmetry in the calculations. The run time for this version of the model is identical to the run time required by the version using the GM command.
To invoke symmetry, we may employ the model style used for the final version of the vertical dipole array. We may create and run the radials alone and save the results in an NGF file. Within the same model, we may use the NX command to begin a second run that calls up the stored results and applies them to the enlarged model that now contains the monopole. The final model in this series appears in the following lines.

```
CM 64 buried radials with monopole
CM GR + NGF
CE
GW 1 11 0 0 -.05 .25 0 -.05 .001
GR 1 64
GE -1 -1 0
FR 0 1 0 0 299.7925 1
GN 2 0 0 0 5 .001
WG radials.ngf
NX
GF radials.ngf
GW 65 11 0 0 -.05 0 0 .25 .001
GE -1 -1 0
EX 0 65 3 0 1 0
RP 0 181 1 1000 -90 90 1.00000 1.00000
EN
```

If you run this model on NEC-2, insert at least a CE command prior to the GF entry that follows NX. The key NEC output report lines tell us that the first portion of the multi-run model has invoked symmetry.

```
TOTAL SEGMENTS USED= 704 NO. SEG. IN A SYMMETRIC CELL=11 SYMMETRY FLAG= -1
STRUCTURE HAS 64 FOLD ROTATIONAL SYMMETRY
```

To create the NGF data, the first run uses only the total number of segments in the radials. The remaining 11 segments in the monopole do not appear until the second run. The symmetric cell shows only the number of segment in the initial radial, and the symmetry flag = -1, indicating rotational symmetry. The total file begins to show the run-time advantage of using the GR command. The total run time for this latest version of the model is about 1/3 the time for the other two versions. Neither time is truly long for the current generation of PCs. However, the savings are indicative of what may accrue for larger models. To illustrate that point, I enlarged the radial system to 120 1/4-wavelength radials. To replicate a common BC industry practice, I also inserted a set of 120 shorter radials between the longer radials. The total system-- or at least a portion of it--appears in **Fig. 5**.



Only the short radials appear fully, with all segments shown to give an idea of the model construction. However, the model-file appearance does not change much compared to the 64-radial models that we just viewed. Indeed, the only difference is a second GW line (which uses the same tag number as the first wire).

```
CM 240 buried radials with monopole
CM GR + NGF
CE
GW 1 11 0 0 -.05 .25 0 -.05 .0001
GW 1 2 0 0 -.05 .04546 .0012 -.05 .0001
GR 1 120
GE -1 -1 0
FR 0 1 0 0 299.7925 1
GN 2 0 0 0 5 .001
WG radials.ngf
NX
GF radials.ngf
GW 65 11 0 0 -.05 0 0 .25 .0001
GE -1 -1 0
EX 0 65 3 0 1 0
RP 0 181 1 1000 -90 90 1.00000 1.00000
EN
```

The symmetry-cell size and the flag setting both tell us that the model invoked symmetry. Even so, the increased model size required about 21 times longer to run than the 64-radial model using the same technique. As we increase the number of segments, run times increase exponentially. Without symmetry, we would need to add a further multiplier to the run time.

```
TOTAL SEGMENTS USED=1560 NO. SEG. IN A SYMMETRIC CELL=13 SYMMETRY FLAG= -1
STRUCTURE HAS 120 FOLD ROTATIONAL SYMMETRY
```

The model style shown has one drawback. We are likely to forget that the file called `radials.ngf` remains in the directory (or folder) where we store models. Using symmetry, the file is not very large, only 314 KB. But it does take up space. Directory cleaning is an important adjunct function for almost all modeling. (Some implementations of NEC do not save any files except the model file unless the modeler makes a specific request to save something else.) Indeed, if we had created the radial system using the `GM` command and stored the results for possible future use, the `.NGF` file might have reached 10 MB of storage space, depending upon the number of segments in each radial. So the `GR` function has a second benefit besides run time: it produces smaller `NGF` files.

A Loaded Reminder

In the NEC manual, there is a chart of control commands that collects them into 3 groups. The following list is from the NEC-4 manual

Group I: FR, GN, IS, JN, LD, UM, VC

Group II: EX, NT, TL

Group III: CP, EN, GD, LE, LH, NE, NH, NX, PL, PQ, PS, PT, RP, WG, XQ

The 3 groups correspond roughly to the 3 steps of solution generation. First comes the interaction matrix: calculation and factoring in preparation for solving for currents. The next step is to solve for currents with a given excitation. Finally comes the calculation of near and/or far fields. The first step depends only upon geometry commands and control commands in Group I. The current solutions depend upon commands in both Group I and II. Following a Group II entry by a Group I entry may result in a repetition of the current solution, since the Group I entry would result in a change of the conditions necessary for that solution. The re-calculation would depend upon the placement in the control command sequence of commands that execute, such as XQ and RP.

In the course of examining our first 3 test cases, involving the collection of vertical dipoles, the importance became apparent of arranging to the extent possible all control commands in the sequence of the groups. **Fig. 6** shows the set up for this modified version of the dipole array in free space. The loads will all be LD4 types with zero reactance and resistance values as shown in the diagram (in Ohms).

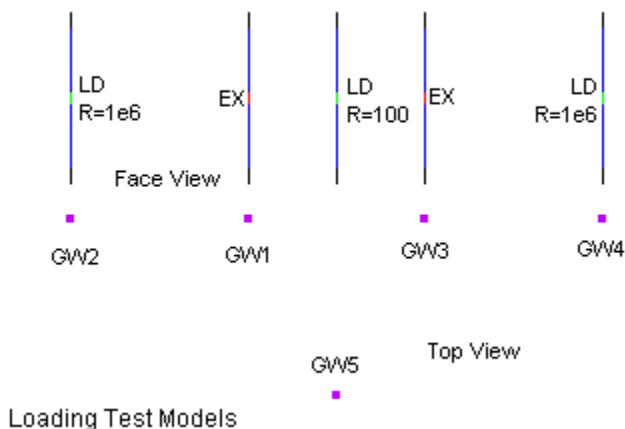


Fig. 6

The first of the models uses a straightforward separate specification for each vertical dipole. It follows the simple geometry entries with the Group I entries of FR and LD, with all 3 LDs placed sequentially. Next come the 2 Group II EX commands. A pattern request completes the model.

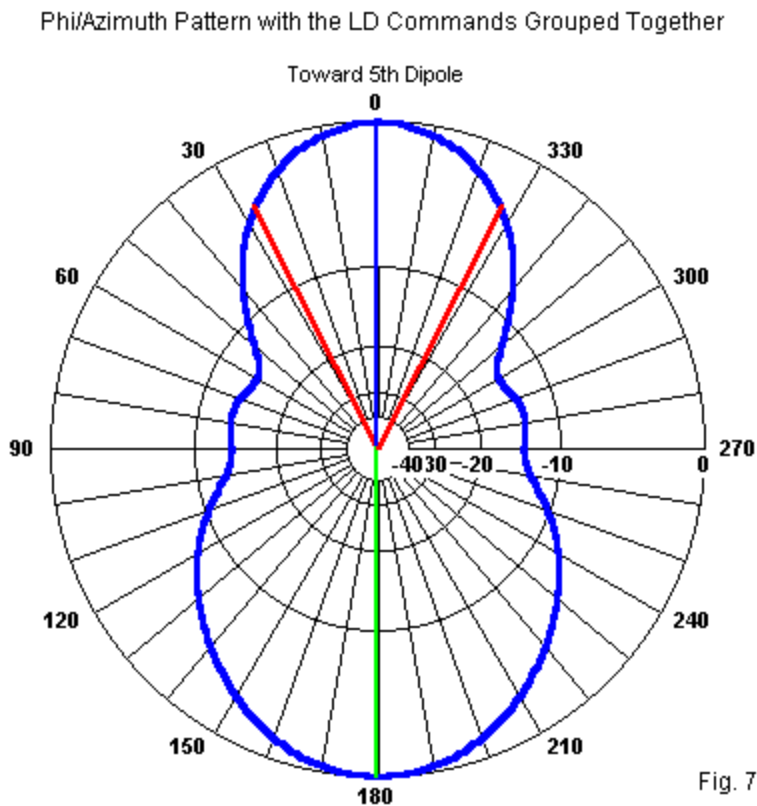
```

CM Test model: 4 vertical dipoles, inner 2 fed
CM 5th passive vertical dipole at a distance
CM Full version-LD4s all before EX
CE
GW 1 11 0 -.75 -.245 0 -.75 .245 .001
GW 2 11 0 -.25 -.245 0 -.25 .245 .001
GW 3 11 0 .25 -.245 0 .25 .245 .001
GW 4 11 0 .75 -.245 0 .75 .245 .001
GW 5 11 .5 0 -.245 .5 0 .245 .001
GE 0 -1 0
FR 0 1 0 0 299.7925 1
LD 4 1 6 6 1e6 0
LD 4 4 6 6 1e6 0
LD 4 5 6 6 100 0

```

```
EX 0 2 6 0 1 0
EX 0 3 6 0 1 0
RP 0 1 361 1000 90 0 1.00000 1.00000
EN
```

The model reports a maximum gain of 4.73 dBi with a 54-degree beamwidth. The reported source impedance is $61.157 - j12.362$ Ohms. **Fig. 7** shows the phi/azimuth pattern for the model.



Now let's revise the model to reflect a tendency among some modelers. Suppose that we had only specified the 1-MOhm loads for GW 1 and GW4, followed by the 2 EX commands. Then we went back to add a load of 100 Ohms resistance to the 5th dipole. We might inattentively insert the new LD4 command just before the request for pattern (RP) command. The following lines show the basic model file.

```
CM Test model: 4 vertical dipoles, inner 2 fed
CM 5th inert vertical dipole at a distance
CM Full version-LD4 on GW5 separated from other LD4s by EX
CE
GW 1 11 0 -.75 -.245 0 -.75 .245 .001
GW 2 11 0 -.25 -.245 0 -.25 .245 .001
GW 3 11 0 .25 -.245 0 .25 .245 .001
GW 4 11 0 .75 -.245 0 .75 .245 .001
GW 5 11 .5 0 -.245 .5 0 .245 .001
GE 0 -1 0
FR 0 1 0 0 299.7925 1
LD 4 1 6 6 1e6 0
LD 4 4 6 6 1e6 0
EX 0 2 6 0 1 0
EX 0 3 6 0 1 0
LD 4 5 6 6 100 0
RP 0 1 361 1000 90 0 1.00000 1.00000
EN
```

Interestingly, the model shows a maximum gain of 6.74 dBi with a beamwidth of 36 degrees. **Fig. 8** shows the phi/azimuth pattern. The model reports a source impedance of 58.156 - j14.714 Ohms.

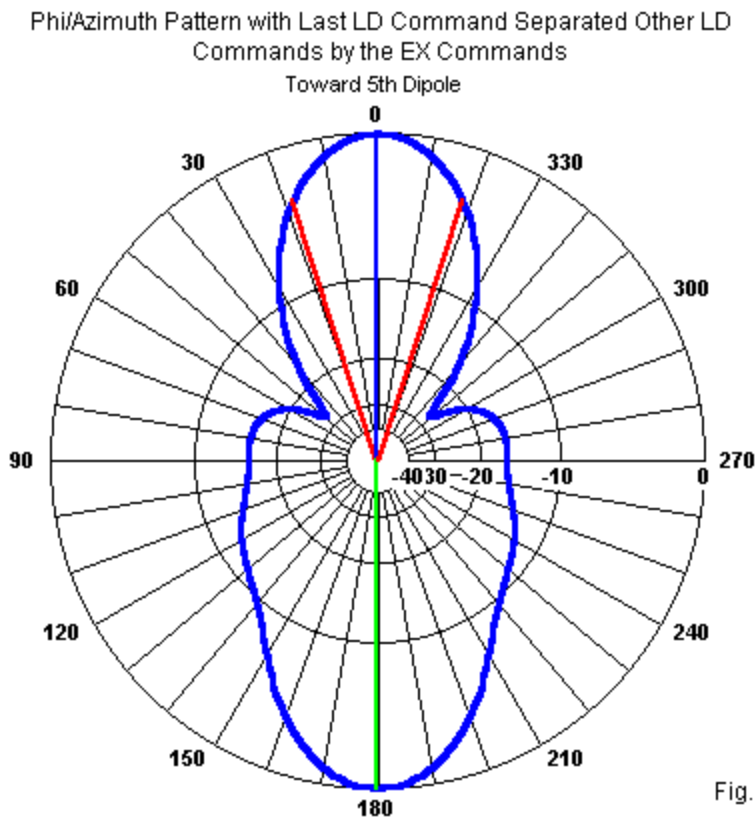


Fig. 8

The revised pattern alone is enough to show that something has gone astray in at least one of the 2 models. Just what went amiss becomes clear from the following revised model. It simply removes the high-resistance loads on GW1 and GW4 from the model.

```
CM Test model: 4 vertical dipoles, inner 2 fed
CM 5th inert vertical dipole at a distance
CM Full version-LD4 on GW5 only
CE
GW 1 11 0 -.75 -.245 0 -.75 .245 .001
```

```
GW 2 11 0 -.25 -.245 0 -.25 .245 .001
GW 3 11 0 .25 -.245 0 .25 .245 .001
GW 4 11 0 .75 -.245 0 .75 .245 .001
GW 5 11 .5 0 -.245 .5 0 .245 .001
GE 0 -1 0
FR 0 1 0 0 299.7925 1
EX 0 2 6 0 1 0
EX 0 3 6 0 1 0
LD 4 5 6 6 100 0
RP 0 1 361 1000 90 0 1.00000 1.00000
EN
```

The new model with no loads on the outer passive vertical dipoles returns the identical results that we obtained from the version with the load on the 5th dipole following the EX commands and separated from the other LD4 loads. **Fig. 8** is the correct phi/azimuth pattern for this model. In the earlier model, separating the load entries by the EX commands resulted in a re-calculation that in effect omitted the earlier loads. If we want to include the loads on the outer dipoles in the model results, we have to use a modeling format similar to the first model in the final sequence of tests.

The lesson of these models is that it pays to group commands first by group level and second by type. The payback involves more important factors than mere run time. It also pays in terms of the accuracy of the output data.

Conclusion

Occasionally, we encounter interesting models that require diagnosis, and in the process, we either learn something new about the operation of NEC or we are reminded of some fine points about model construction that we might have let slip over months and years of modeling. This month's reminders are examples of that process. In fact, I might not have thought to mention either of the main ideas without the presence of a set of models to diagnose. While not every modeler might need these reminders, I thought I would pass them along while a. they were on my mind and b. I had a reasonable set of simple models by which to illustrate them.

106. Refining Our Notions of Azimuth Patterns

Many of these columns evolve from e-mail correspondence that I receive relative to antenna modeling. Sometimes, I receive over a short period of time multiple notes on a single subject. At other times, I receive seemingly diverse inquiries that turn out to have a common thread. The latter situation provides the basis for these notes in pursuit of a better understanding of so-called azimuth patterns.

The generic term in NEC for patterns taken along or parallel to the X-Y plane is a phi pattern. Starting with the X-axis, we count counterclockwise in degrees around the circle created by any phi pattern. When we speak of azimuth, we are resorting to the language of seamen, airmen, surveyors, and field engineers. That language presumes that there is a ground level at zero degrees elevation. (We shall, like NEC, presume a flat earth.) We count degrees from the North in a clockwise compass rose. In free-space, NEC may still have its phi pattern, since free space has a Cartesian X-Y plane. However, the idea of azimuth becomes problematical, because we lack a ground. So we often speak in terms of E-plane and H-plane patterns, but these patterns designations depend on how we have oriented the antenna, assuming a relative linear polarization. Software makers--for simplicity--tend to label all X-Y plane patterns as azimuth patterns. However, in many cases, the pattern produced is really a phi pattern that counts counterclockwise.

As daunting as the mere labeling of phi/azimuth patterns can be, the problem is small compared to others that may occur if we are not careful. In these notes, we shall deal with only 2. One is the continuing subterranean discussion about the use of log vs. linear polar plots. The other involves azimuth patterns over ground when the pattern's elevation angle is more than a few degrees above the horizon.

Log vs. Linear Polar Plots

Although 3-dimensional plotting capabilities come with much modeling software, the most telling data usually derives from 2 dimensional patterns. We have already described the phi/azimuth pattern. Corresponding to it, but with a vertical dimension, is the theta/elevation plot. Most often, we set the phi/azimuth angle for a theta/elevation plot by reference either to the centerline of an antenna array or with respect to the direction of the strongest forward lobe. We can use other angles as the need arises. Theta/elevation patterns seem to present no major

problems to newer antenna modelers. Even the translation between theta and elevation conventions is simple. An elevation angle is 90 - a theta angle (degrees) and vice versa. Perhaps the only difficulty involves setting up an elevation pattern's range of angles to be sure that we obtain a full circle in free space.

Over ground, the phi/azimuth pattern causes the most discussion. The discussion tends to extend itself into free space because the plots with and without a ground beneath have such similar shapes. The discussion hinges around whether we ought to be using a logarithmic or a linear scale for the rings in the pattern. Some modelers, especially radio amateurs, may have never seen a linear plot, since most publications in the field use one or another form of log plot. Many developmental and field engineers are most experienced with linear plots, sometimes because the regulatory submissions that they make set requirements of plots--and they are almost always on linear scales.

Over the years, the discussion has acquired some spurious reasoning. For example, a few linear plot proponents claim that we receive unrealistic plots using a log scale, since power gains are already in decibels, a log concept. More interesting is the claim that a log scale makes the main forward lobe of an antenna more dominant, giving a more favorable impression of the antenna performance than it deserves. Since most proponents of a log scale prefer it by habituation, there have been few replies, although log plots tend to dominate the presentations in most publications.

So our question is simple: what difference does it make whether I use a linear or a log scale when making a polar plot? We can settle some of the issues by pursuing a simple exercise. Let's set up a model in free space and plot its phi/azimuth/E-plane pattern. My model is the following simple NEC listing.

CM 12-element Yagi, 223.5 MHz

CE

```
GW 1 19 0. .3225463 0. 0. -.3225463 0. .003175
GW 2 19 .2628857 .3125082 0. .2628857 -.3125082 0. .003175
GW 3 19 .3613731 .2856135 0. .3613731 -.2856135 0. .003175
GW 4 19 .5981218 .2833407 0. .5981218 -.2833407 0. .003175
GW 5 19 .8807049 .2799316 0. .8807049 -.2799316 0. .003175
GW 6 19 1.209123 .2767118 0. 1.209123 -.2767118 0. .003175
GW 7 19 1.577314 .2738708 0. 1.577314 -.2738708 0. .003175
```

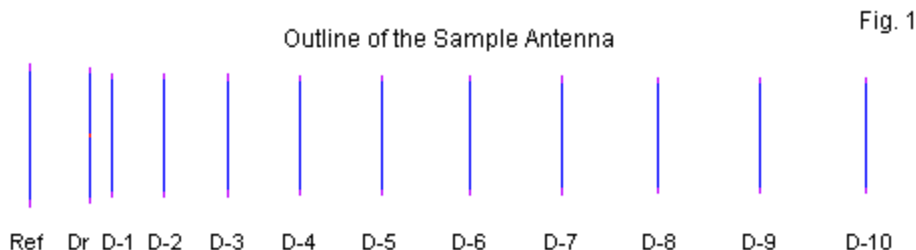


```

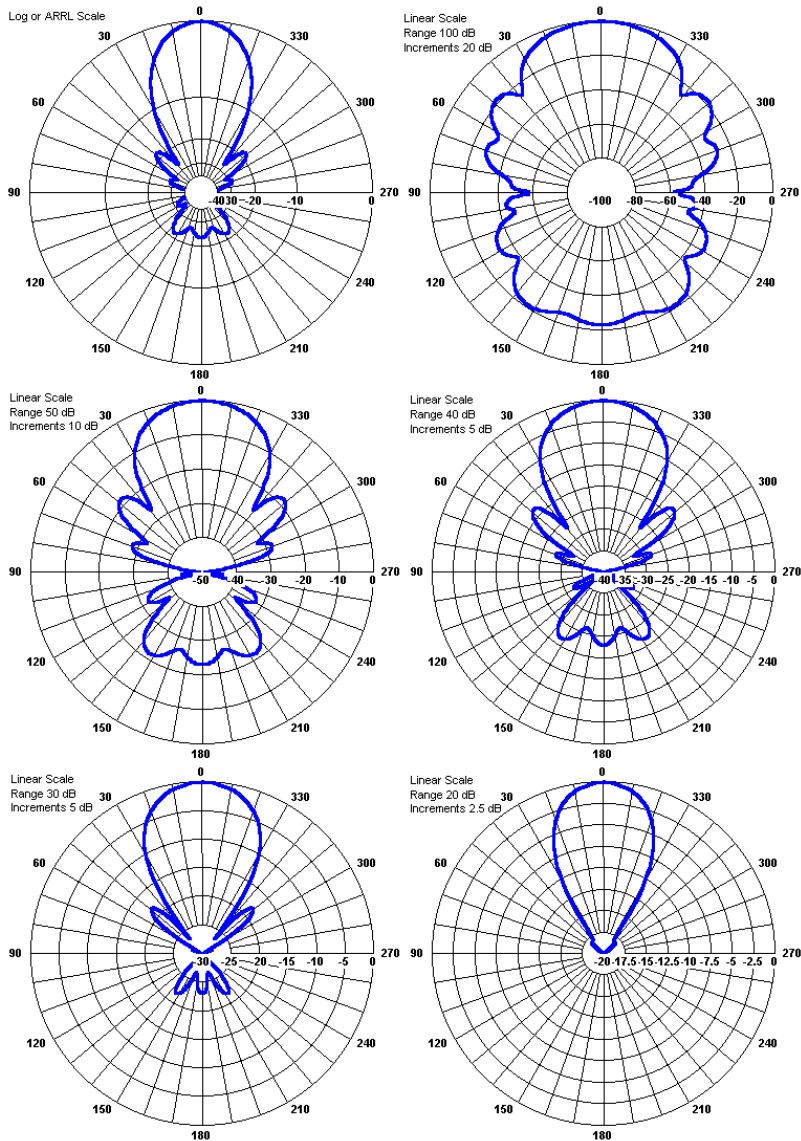
GW 8 19 1.971453 .2712192 0. 1.971453 -.2712192 0. .003175
GW 9 19 2.385479 .2691358 0. 2.385479 -.2691358 0. .003175
GW 10 19 2.819392 .2672419 0. 2.819392 -.2672419 0. .003175
GW 11 19 3.272813 .2655372 0. 3.272813 -.2655372 0. .003175
GW 12 19 3.745931 .2640221 0. 3.745931 -.2640221 0. .003175
GE 0 0 0
LD 5 0 0 0 2.5E+07 1.
FR 0 1 0 0 223.5 1
GN -1
EX 0 2 10 0 1.00000 0.00000
RP 0 1 361 1000 90 0. 1.00000 1.00000 0.
EN

```

The dimensions of the 12-element Yagi are in meters. The LD5 entry casts the antenna in aluminum. The operating frequency is in the middle of the U.S. 220-MHz band. As shown in the outline sketch in **Fig. 1**, the second element is the driver, fed at its center.



The antenna design rests on the work of DL6WU, Guenter Hoch. I am less interested at the moment in the overall performance of the antenna than in the fact that DL6WU designs tend to have significant forward sidelobes that are down from the main forward lobe by between 15 and 18 dB. That will give our polar phi/azimuth/E-plane plot a certain look. In fact, the look will not change if we use a log scale and move from one software package to another, assuming that we normalize the plot, that is, set the plotting software so that the outer ring and the maximum forward lobe just meet. Therefore, GNEC and EZNEC Pro/4 patterns will appear identical. A plot produced by an ARRL publication may initially look different, but will be essentially the same. ARRL likes to place lines in 3 or 6 dB intervals, while most software uses 10 dB as a major circle in the plot. In short, the plot will look like the one at the upper left of **Fig. 2**.



One Antenna, Six Free-Space E-Plane Patterns

Fig. 2

Perhaps the most significant reason for using a log-based polar plot of phi/azimuth/E-plane patterns is the fact that for any antenna, if we do not change the antenna placement or environment, the plot will be the same no matter which software we use for the plotting. We cannot make the same claim for linear polar plots.

The plots shown comes from NSI software for a reason. EZNEC allows only one form of linear plot, but NSI software lets the user specify the inner limits and the ring increment for linear plots. As we change the inner limit and the increment, our polar plots may change their shape. Precisely here lies one of the problems with linear plotting of antenna patterns. If we do not have an external standard to direct our plotting, we can make the antenna look as sorry or as distinguished as we please. There are numerous applications in which we find external standards and some in which we find corporate standards that rest on long experience. In either case, we may directly compare plots and conduct fair evaluations.

In the absence of such standards, the field is wide open. For example, the upper right pattern of **Fig. 2** uses an inner limit of -100 dB with a 20-dB increment in the plotting circles. Using these scale factors, we can tell almost nothing about the antenna except perhaps that its front-to-back ratio is about 20 dB. The middle pair of linear scales use -50 and -40 dB inner limits. At this level, some of the antenna pattern details become much clearer. In fact, the -40-dB version of the plot is essentially the linear scale provided by EZNEC software. Where the scale rings have good labeling, we would have no trouble gleaning essentially the same information from both linear patterns. In fact, newer modelers may wish to track both patterns against the log pattern at the upper left in order to gain a more intuitive grasp of the differences between where on the plot various pattern levels occur.

Just as the upper right pattern seems to obscure important data by virtue of its bulbous shape, the two patterns at the bottom of **Fig. 2** may obscure important data by using an inner limit and increment level that are too small. In both cases--one somewhat more extreme than the other--the plot tends to enhance the pattern and to give it a purity that simply does not exist. I have seen plots of this order used in older articles, most recently in a review of professional literature on rhombic antennas. The plots could give the impression to the unwary reader that a rhombic antenna has no sidelobes worth mentioning, when in fact, the antenna sprays sidelobes everywhere, with the strongest ones only 8 to 12 dB below the strength of the main lobe.

The linear pattern has plenty of uses and is not inherently simply a means to yield false impressions of an antenna. Field strength readings in volts/meter lend themselves to linear plotting. However, even in this enterprise, one needs a set of plotting standards to facilitate comparisons among plots. The one sure way to make such plots yield misimpressions is to allow scaling decisions to be idiosyncratic. The log plot of power gains obviates the danger by using a relatively constant scale, with only ring values as a plotting option. Having the scale prescribed and in unison with patterns produced by others is a good assurance to less experienced modelers that their results will in fact be comparable with other work. (This positive fact does not eliminate the many other ways in which one can mess up a model or the polar plot that we take of it. One common problem for azimuth plots over ground is the switching of the values for ground conductivity and relative permittivity. I have also seen plots that have intentionally used high values of conductivity and permittivity solely to enhance an antenna pattern. However, the connecting thread of these notes is not the ways in which we can give false impressions of an antenna's performance.) In the end, the use of plots--whether based on log or linear scales--requires good sense and standards if we are to derive from them all of the information available. If a linear plot is necessary for a power gain or other antenna property pattern, then in all cases the plotter needs to annotate the plot so that the user knows exactly how to interpret the data it encases. As well, the text should provide a rationale for the selected inner limit or a reference to an external standard, if it is applicable to the plot.

Azimuth Plots Over Ground

Phi/azimuth patterns taken over ground hold another potential problem--a lack of reader appreciation of what such patterns really are. Even those who make such plots using standard plotting techniques (for example, the usual log plot) may not fully appreciate what the data from the patterns may be telling us. The most common far-field plots shown on phi/azimuth patterns use relatively shallow elevation angles--somewhere between 1 and 25 degrees. At higher angles, we very often have an interest only in the general pattern shape and the maximum gain, so a lack of full understanding of the terms of an azimuth pattern holds no especial dangers. However, when we begin to look at the fuller data attached to such patterns, we often encounter hurdles for which we are not prepared.

Once more, let's use a specific example. In this case, I shall select a very long-boom Yagi for 432 MHz. The antenna design specifically aims for high performance in as many categories as possible. The gain level is normal for the

boom length. The good front-to-back values are overshadowed by the very high level of sidelobe attenuation. In addition, the antenna provides a direct 50-Ohm match and a passband wide enough to cover the entire 70-cm amateur band.

Fig. 3 provides the free-space patterns and data, as well as a scale outline of the array. In this case, the patterns are log scale and from EZNEC Pro/4.

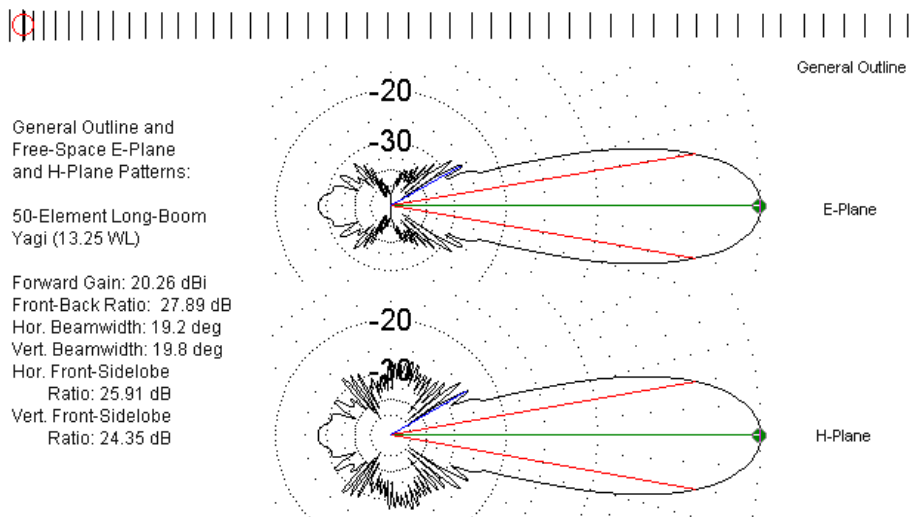


Fig. 3

One application for an antenna of this size is earth-moon-earth (EME) communications, using the moon as a passive and low-efficiency reflector. EME service requires that we be able to control the azimuth and elevation angles of the antenna. Therefore, one interest we may have in the antenna is its performance at various elevation angles. The antenna requires a minimum boom-center height of about 7.5 wavelengths to keep the reflector at least 1 wavelength above ground when pointed straight upward. I sampled the antenna performance at elevation angles from zero degrees through 90 degrees in 15-degree increments. The results appear in the series of elevation and azimuth plots shown in **Fig. 4**. The following table (**Table 1**) shows the values that correlate with the patterns.

50-Element Long-Boom
Yagi (13.25 WL)

Centered 7.5 WL above
Average Ground

H-Plane (Elevation)
and E-Plane (Azimuth)
Patterns

Angle designations refer
to aiming angle along
the boom. See text for
resulting elevation angle
of the resulting pattern.

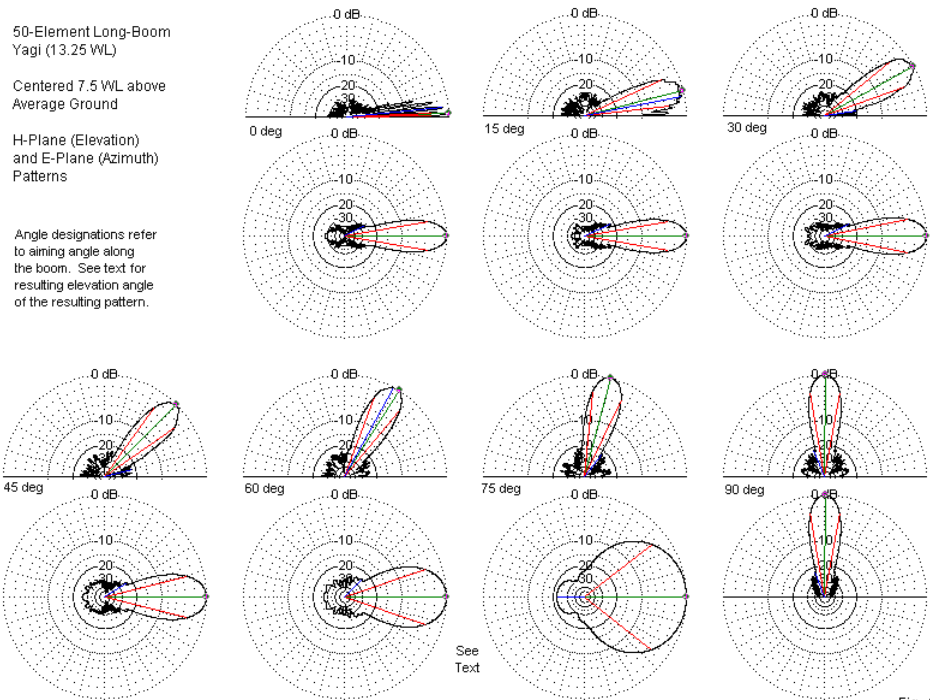


Fig. 4

Table 1. Performance of a 50-Element, 13.25- λ Long Yagi at 7.5 λ Center Height above Ground Using Stepped Tilt Angles

Tilt Angle (deg)	EI Angle (degrees)	Gain (dBi)	Front-Back Ratio (dB)	Hor BW (degrees)	Ver BW (degrees)	Hor FSL Ratio (dB)	Ver FSL Ratio (dB)
0	1.9	26.11	27.91	19.2	1.4	25.82	0.95
15	14.5	20.69	34.67	20.2	17.9	21.70	0.49
30	29.1	20.47	30.69	22.4	19.5	22.76	19.48
45	45.4	20.48	25.66	27.8	19.1	23.18	21.86
60	57.8	20.31	26.75	37.4	19.3	24.09	0.06
75	75.0	20.20	22.07	75.9	19.9	22.07	21.64
90	90	20.20	---	20.0	20.0	22.51	21.65

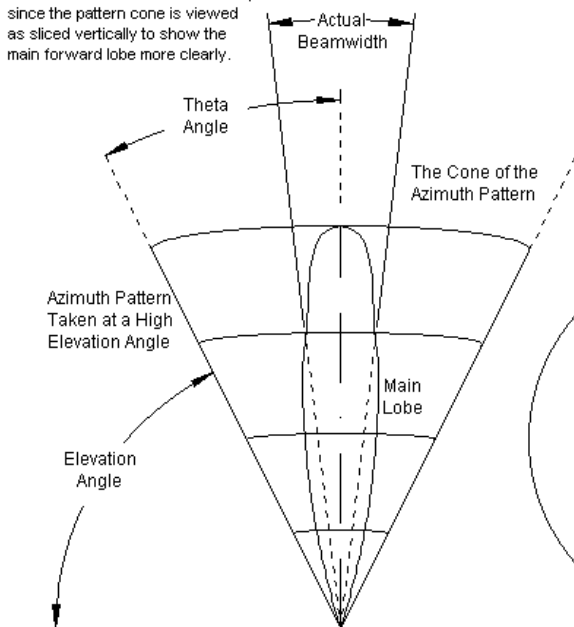
If we first examine only the elevation plots, we can observe an interesting pattern. As we elevate the antenna above an angle where the free-space vertical beamwidth interacts with the surface of the ground, the vertical beamwidth

stabilizes at or very near to the free-space vertical beamwidth. We essentially achieve that situation by an elevation angle of 30 degrees.

If we next examine the azimuth patterns, we find an oddity (at least, at first sight). The horizontal beamwidth increases steadily until we pass the 75-degree elevation level. Indeed, the azimuth pattern forward and rearward elements appear to broaden with each increase in elevation angle. However, the patterns for an elevation angle of 90 degrees return essentially to free-space values, with the exception that there are no longer any rearward lobes. Of course, we have changed the procedure at a 90-degree elevation angle and substituted H-plane and E-plane elevation patterns for the expected elevation and azimuth patterns. Below 90 degrees elevation, we do not have this option. Our task is to understand why the horizontal beamwidth and other aspects of the azimuth pattern broaden with an increasing elevation angle.

The answer lies in simple but often overlooked aspects of the conical geometry that is a function of taking phi/azimuth patterns over ground. In every case, we use an elevation angle that is greater than zero. (Over perfect ground, we may take a phi/azimuth pattern at zero-degrees elevation, but over real ground, the results are either a negligible set of power gain values or a message informing us that we have requested an illicit phi/azimuth pattern. If we need far-field values very near to ground level, we may specify a very small elevation angle, such as 0.1 degree and also set a finite distance for the pattern's field strength readings.) The result of our phi/azimuth pattern request is a pattern that involves something other than a flat circle. Instead, the field strength and power gain values occur on the surface of a cone. Many directional antenna patterns do not show the same elevation angle for the strongest forward lobe as for the strongest rearward lobe. When we examine the 180-degree front-to-back ratio calculated from pattern data by NEC software implementations, we discover that the ratio rests on the strength of the rearward lobe at the same elevation angle that we set for the forward lobe. At very low angles, the polar plot pattern does not show any significant distortion that results from the transfer of the conical surface data to a flat circular or polar plot. However, as we increase the angle, foreshortening distortions occur. **Fig. 5** shows a sample of the situation, although the sketch is itself imperfect.

Note: Rearward lobes not shown, since the pattern cone is viewed as sliced vertically to show the main forward lobe more clearly.



Understanding Azimuth Patterns

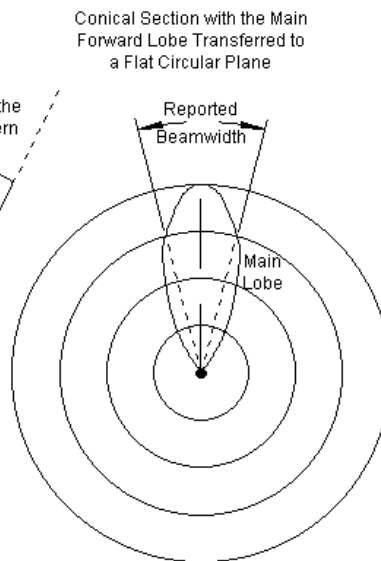


Fig. 5

The conical section on the left shows an elevation angle of 60 degrees (or a theta angle of 30 degrees). Let us suppose that we have sliced the cone vertically at page or screen level so that we see only half of the cone's surface. The visible section shows us the forward lobe of a hypothetical beam. The angle marked at the top of the sketch shows the beamwidth of the visible lobe. However, even this angle is slightly off the mark, since it transfers a curved surface that slopes away (or toward) the page or screen directly onto the flat page or screen. Nevertheless, the angle is close enough to the actual value to demonstrate what happens when we create a phi/azimuth pattern from this information.

On the right is a polar plot of the pattern. The circles represent rings around the cone. For simplicity, the polar plot uses a linear set of ring scales so that the distance between rings is the same for both the conical section and for the polar plot. When we plot the points of contact between the rings and the pattern width onto the polar plot, we obtain the pattern in the flat polar plot. The plot produced by any graphic addition to NEC uses the data in its radiation pattern report, and

this data results in the plot shown, assuming that we have specified the phi/azimuth pattern situation shown on the left.

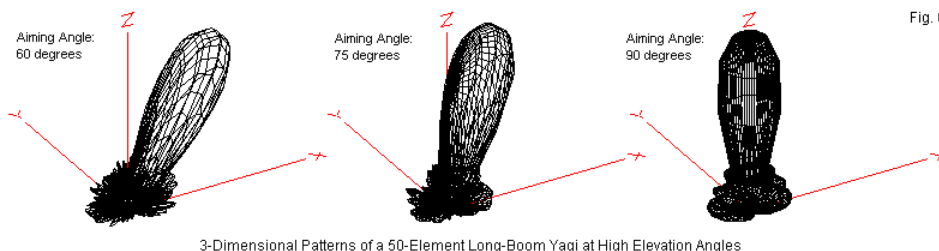
The conical section assumes that the half-power points of the pattern happen to coincide with the intersection of the pattern line with the next-to-outermost ring. Each point will show a gain value that is 3 dB lower than the maximum power gain for the antenna. Those points will yield the same gain values when transferred to the flat polar plot. If we create the angle included between those points on the polar plot, we obtain an angle that is a bit over twice as wide as the angle included by the corresponding points on the surface of the cone. In fact, the proper relationship for the 60-degree elevation angle is 2:1, but remember that the representation of the cone surface is distorted by its representation on a flat surface.

For most cases where the antenna is considerably above ground, we may determine (or approximate) the actual horizontal beamwidth from the reported value that results from the foreshortening effect of transferring a conical section to a flat circle.

$BW_a = BW_r * \cos(\text{elevation})$ or $BW_a = BW_r * \sin(\text{theta})$

BW_a is the actual horizontal beamwidth, BW_r is the NEC report of the beamwidth, and the indicated angles are the elevation or theta angle at which we take the phi/azimuth pattern. For example, at an elevation angle of 45.4 degrees (the take-off angle that results from pointing the antenna at an angle of 45 degrees upward), we have a reported horizontal beamwidth of 27.8 degrees. The cosine of 45.4 degrees is 0.702. Multiplied times the reported horizontal beamwidth, we obtain 19.5 degrees actual beamwidth, a value that falls between the listed free-space value and the E-plane value that occurs with an elevation angle of 90 degrees.

To confirm that the horizontal beamwidth has not actually undergone any significant change as we elevate the antenna, let's examine a few 3-dimensional patterns. **Fig. 6** shows the subject antenna's patterns at aiming angles of 60, 75, and 90 degrees relative to ground. The pattern resolution is only 5 degrees, so considerable detail is missing from the graphics. The alternative would be to use a very small pattern increment and end up with patterns that appear only as black blobs.



Despite the missing detail, we can observe that the main lobe of the beam retains its essential shape throughout the changes in elevation angle.

Conclusion

These notes represent an attempt to improve our understanding of oft-overlooked aspects of phi/azimuth patterns. The first exercise explored the differences between logarithmic and linear plots. The log plot emerged essentially to lend to phi/azimuth patterns a uniformity that had been lacking in commonly used linear plots. Since we may select the inner limit and the increment for a linear polar plot, these patterns may vary widely for applications that are not subject to external standards. Any user-developed linear polar plot of power gain values should plainly show the inner limit used. As well, the text should explain the rationale for the inner limit selection, even if the explanation is no more than a reference to an external or corporate standard.

Phi/azimuth patterns over ground represent patterns taken on a conical surface. At small elevation angles, polar plots do not severely distort the conical section by transferring the data to a flat circle. However, as we increase the elevation angle for the phi/azimuth plot, the transfer does introduce appreciable foreshortening or broadening of the actual pattern. One result is a misreport of the horizontal beamwidth of an antenna, although we may use a simple calculation to produce a reasonable approximation of the correct value.

These are but two of many aspects of NEC modeling results that we tend to overlook in the process of trying to produce usable data from a carefully constructed model geometry. However, even the best model is subject to misinterpretation of the output data unless we are very careful in how we present it and how we read the presentation.

107. Scaling Models

Scaling antennas from one frequency to another is common practice. In general, we wish to capture certain performance characteristics that we find at one frequency and transfer them to another. The most straightforward way to achieve this goal is to scale the antenna that has the desired characteristics.

We often need or desire to scale antenna models from one frequency to another. The techniques of model scaling are identical to those of direct antenna scaling, although the way in which we go about the task may differ with the implementation of NEC or MININEC that we are using. Many implementations of modeling cores have a pre-core-run facility for either full or partial model scaling. As well, we may use one of the commands within the full NEC command set to arrive at the same result--a sort of unadvertised special.

Basic Scaling

To scale a model from one frequency to another requires us to change the element length, the element spacing, and the element diameter (or radius) everywhere in a model or antenna. Let's call the general idea of something to change when scaling the "dimension." We shall have an old or starting set of dimensions and a new or final set of dimensions. The amount of change depends on the old frequency or wavelength and the new frequency or wavelength. The basic formula is simple:

$$\frac{\text{new wavelength}}{\text{old wavelength}} = \frac{\text{old frequency}}{\text{new frequency}} = \frac{\text{new dimension}}{\text{old dimension}}$$

Note that the dimension changes are directly proportional to the ratio of ratio of wavelengths and inversely proportional to the ratio of frequencies. Since we generally work with frequency in most initial thinking, we simply take the ratio of the old to the new frequency and multiply every old dimension by the value. The easy way to check on whether we are using the correct ratio is to remember that elements get shorter and thinner as we scale up in frequency and longer and fatter as we scale down in frequency.

Some implementations of NEC and MININEC allow you to enter the wire diameter as an AWG value. In many instances, we forget to scale the wire diameter along with the element length and spacing. The cure is to remember to look at the wire gauge or diameter before declaring that the scaling is complete. In some cases, very thin wire antenna elements will show only small performance changes if we forget to change the wire size and if we are only scaling over a limited frequency range--for example, converting a 14-MHz antenna design to 18 MHz. However, the fatter the element or the greater the scaling ratio, the more significant it becomes to make certain that we scale the element diameter or radius along with the other dimensions.

In NEC and MININEC, precise scaling will yield identical performance at both the old and the new frequencies only if certain model conditions exist. First, the antenna material should be "perfect" or "lossless." Even high conductivity materials such as copper show different working values of conductivity as we change frequency. The skin effect changes slowly as we change frequency--enough to show up in results that only make a relatively small frequency change during scaling. Second, the antenna environment should be free space or a perfect ground. Ground effects from any lossy ground change with frequency, again enough to show up in models that we scale over a relatively small range if the antenna is within a few wavelengths of the earth's surface.

In most cases, it is useful to remove material losses and a lossy ground from an antenna model prior to scaling. Then proceed with the scaling calculations and test the model using the new values--remembering to a. change the test frequency for the revised model and b. save the model under a revised file name. Once you are satisfied that the scaling operation is correct, you can add in the material loss factor (LD5) and the lossy or real ground constants (GN).

Sample Program Scaling Facilities

Many implementations of NEC and MININEC contain facilities to assist in the scaling process. Let's sample a full scaling facility and a partial scaling facility. For a subject antenna, we shall begin in all cases with a 2-element Yagi designed for 28.5 MHz. To further focus on the scaling activity, I have placed it in free space and used lossless elements. So our only project will be to scale the antenna to 14.25 MHz. The ratio of the old frequency to the new frequency is 2:1 to keep the arithmetic obvious.

We also have the option of manually calculating the new dimensions and manually entering them into the wire or GW entries. However, in some programs, such as EZNEC, we need not go through this process. Consider the 2 screens in **Fig. 1** taken from the initial 10-meter antenna model. The upper screen shows the wire entries with all dimensions in meters. The lower screen shows our design frequency.

The screenshot shows the EZNEC software interface. The top window is titled 'Wires' and contains a table of wire entries. Below the table is a 'Frequency' dialog box. The 'Wires' table has columns for No., End 1 (X, Y, Z, Conn), End 2 (X, Y, Z, Conn), Diameter (mm), and Segs. The 'Frequency' dialog box has a text input for frequency in MHz, a 'Rescale' checkbox, and 'Ok' and 'Cancel' buttons.

No.	End 1				End 2				Diameter (mm)	Segs
	X (m)	Y (m)	Z (m)	Conn	X (m)	Y (m)	Z (m)	Conn		
1	0	2.643	0		0	-2.643	0		25.4	21
2	1.295	2.408	0		1.295	-2.408	0		25.4	21
*										

Frequency

Enter frequency in MHz, or 0 for 1m wavelength.
Check the 'Rescale' box to rescale antenna to the new frequency.

Frequency (MHz)

☐ Rescale

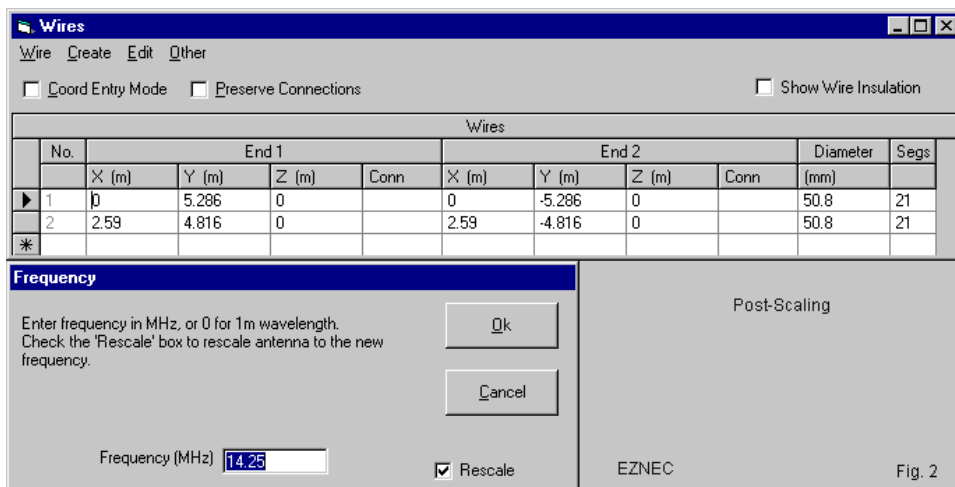
Ok Cancel

Pre-Scaling

EZNEC

Fig. 1

EZNEC implements scaling through the frequency selection screen. Note the box marked "Rescale." Let's revise the frequency to 14.25 MHz and also click on the rescale box. The result will be the set of wire entries shown in **Fig. 2**. The user made none of the changes in the wire tables. Rather, the program made the necessary changes after the user entered the new frequency and checked the rescale box.



Element length values appear in the Y-columns, with the spacing values in the X-columns. The program uses wire diameter as the entry dimension, and it has its own column. A quick comparison of **Fig. 1** and **Fig. 2** shows that EZNEC's scaling facility has doubled the element length, the element spacing, and the element diameter for the entire model geometry. The version of EZNEC on which I ran these models used NEC-4. For both models--the 10-meter and the 20-meter versions--the free-space gain reported as 6.28 dBi, with a 180-degree front-to-back ratio of 11.25 dB. In both cases, the feedpoint or source impedance was 32.59 - j0.30 Ohms.

Not all programs that provide scaling facilities scale everything. Consider the same model in its NEC-Win Plus form, as shown by the upper portion of **Fig. 3**. The 10-meter antenna has the same dimensions as the EZNEC model. Because NEC-Win Plus uses NEC-2, we expect very small changes in the output report values. The free-space gain is 6.28 with a front-to-back value of 11.25. The source impedance is 32.58 - j0.55 Ohms. The differences from the NEC-4 report are wholly insignificant.

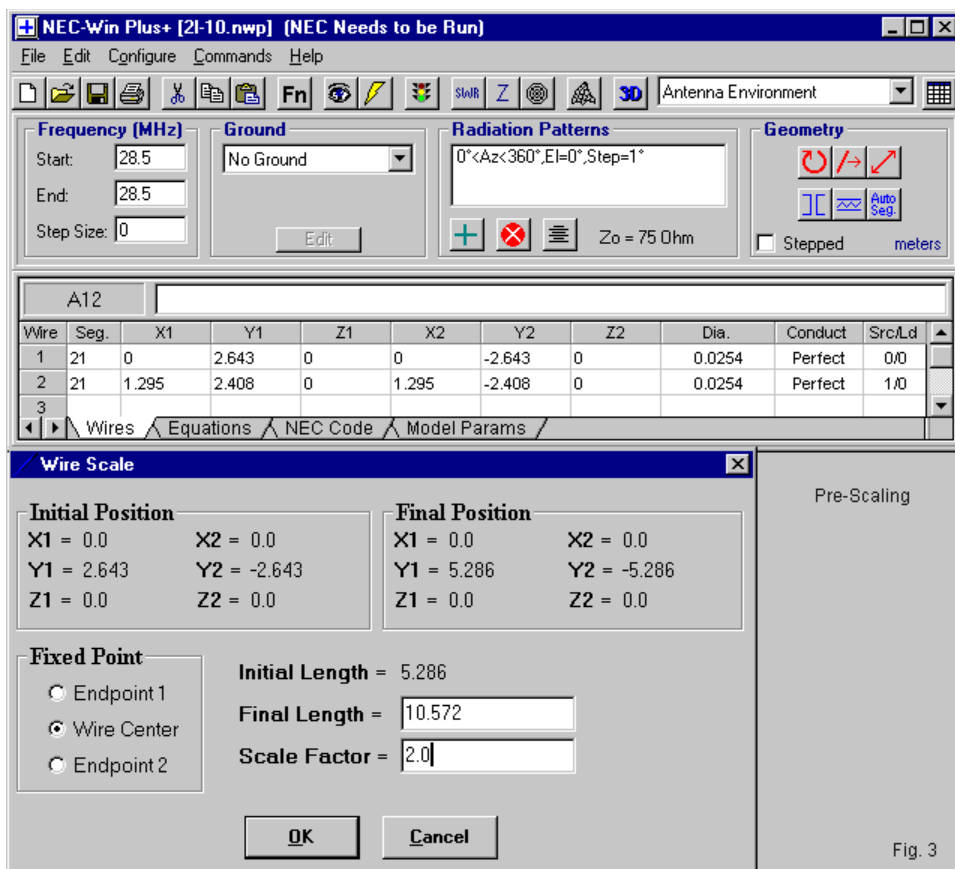


Fig. 3

The lower portion of the figure shows the scaling screen that the user accesses by clicking on a special button near the top of the NEC-Win Plus screen. The screen contains a wealth of information on the scaling maneuver, showing both initial and final values before the user locks the changes into place. To use this screen effectively, I blocked the full wire lines for the model from the left to the right extremes. The blocking encompassed everything, including segmentation, coordinates, wire diameter, and wire material.

The scaling operation requires the user to enter the scaling factor, in this instance, 2.0. As well, the user must remember to change the model frequency before running the revised model. After making these changes and locking in the re-scaling, I ran the model. It returned a gain of 6.18 dBi, a front-to-back ratio of 11.72, and a source impedance of 33.57 - j70.01 Ohms. Something has gone astray, and in this case, it was carrying over operational expectations from one program to another.

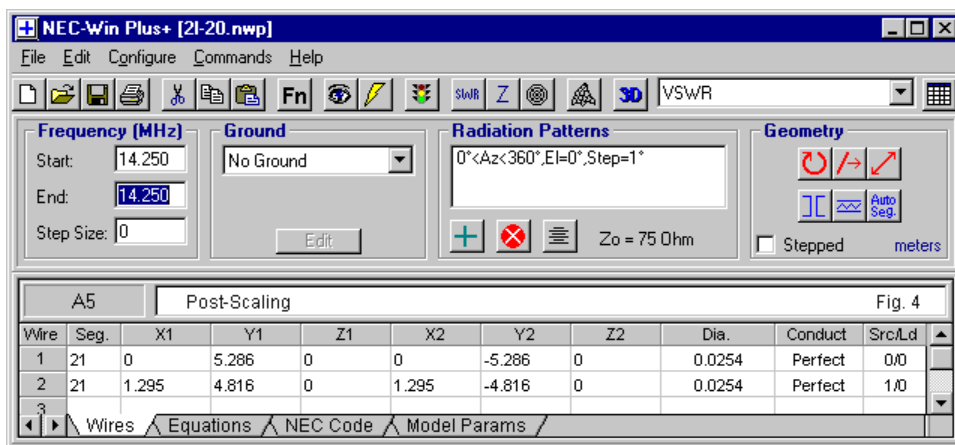


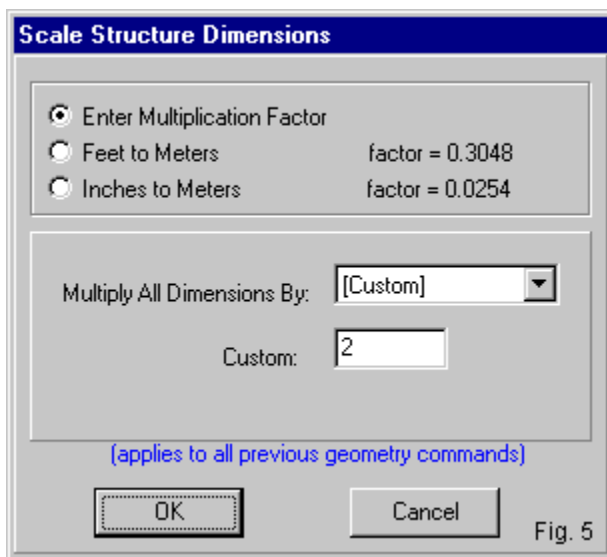
Fig. 4 shows us what went wrong by not reading the instructions appropriate to this implementation of NEC-2. The NEC-Win Plus scaling facility changes only the element lengths. However, as the X-column shows, it does not automatically change the spacing. As well, the diameter column shows that the program does not automate the diameter scaling. Hence, the model that gave us the aberrant results is not a true scaling of the original antenna. If we double both the element spacing and wire diameter, the corrected 20-meter scaling of the 10-meter Yagi produces the same output reports.

Different implementations of NEC and MININEC will handle re-scaling a model in ways that range from a totally manual operation to complete automation. Since scaling is such a simple arithmetic operation, it usually makes little difference how we make the required changes. The key is to make all of them.

The NEC GS Command The GS command in the NEC set is so easy to use that most instruction sets tend to overlook it. Even the NEC manuals give it only brief treatment. The command structure has only 3 entries, two integers and one floating decimal.

CMD	I1	I1	F1 (FSCALE)
GS	0	0	0.3048

The command's common use is to convert the units of measure in preceding geometry commands (such as GW) into meters, if they are not already in meters. The command must appear after all of the geometry commands that use an alternative unit of measure and before the GE or geometry section end command. NSI software provides a help screen for entering the scaling values, as shown in **Fig. 5**.



For manual entry of the conversion unit, the integer entries are zero. Some manuals say they are not used. However, some core versions have automated conversion entries. If I1 = 1, then the conversion is from feet to meters (0.3048). If I1 = 2, then the conversion is from inches to meters. In these cases, I2 and F1 might not appear, or I2 might be zero. However, if both I1 and I1 are zero, then

F1 must have a conversion factor value. The user can insert any appropriate value. For example, if the geometry entries are in millimeters, then the value of F1 is 0.001.

```
CM 2el Yagi 7.9/8.67/4.25 fs
CE
GW 1 21 0. 8.67 0. 0. -8.67 0. .04167
GW 2 21 4.25 7.9 0. 4.25 -7.9 0. .04167
GS 0 0 0.304800
GE 0
FR 0 1 0 0 28.5 0
GN -1
EX 0 2 11 0 1.00000 0.00000
RP 0 1 361 1000 90. 0. 1.00000 1.00000 0.
EN
```

The sample model is essentially the same 2-element 10-meter Yagi, but with the 2 elements entered in feet. Hence, the conversion factor in the GS line is 0.3048. Since the dimensions are rounded, we shall find a very slight variance in the output reports, but at levels that are wholly insignificant. For example, the reported source impedance for the Yagi is 32.54 - j0.36 Ohms using the NEC-4 core.

Suppose that we enter our coordinates and wire radius in meters. Since we do not need to convert the units to meters, we might overlook the GS card. The top portion of **Fig. 6** shows the 10-meter Yagi entered in meters. However, the GS card is still useful to us in scaling the antenna to 14.25 MHz from its original frequency, 28.5 MHz. Note the "custom" conversion factor shown in **Fig. 5**. The lower portion of **Fig. 6** shows the revised and scaled Yagi model with the GS card used to do the scaling--along with the required revision of the FR entry.

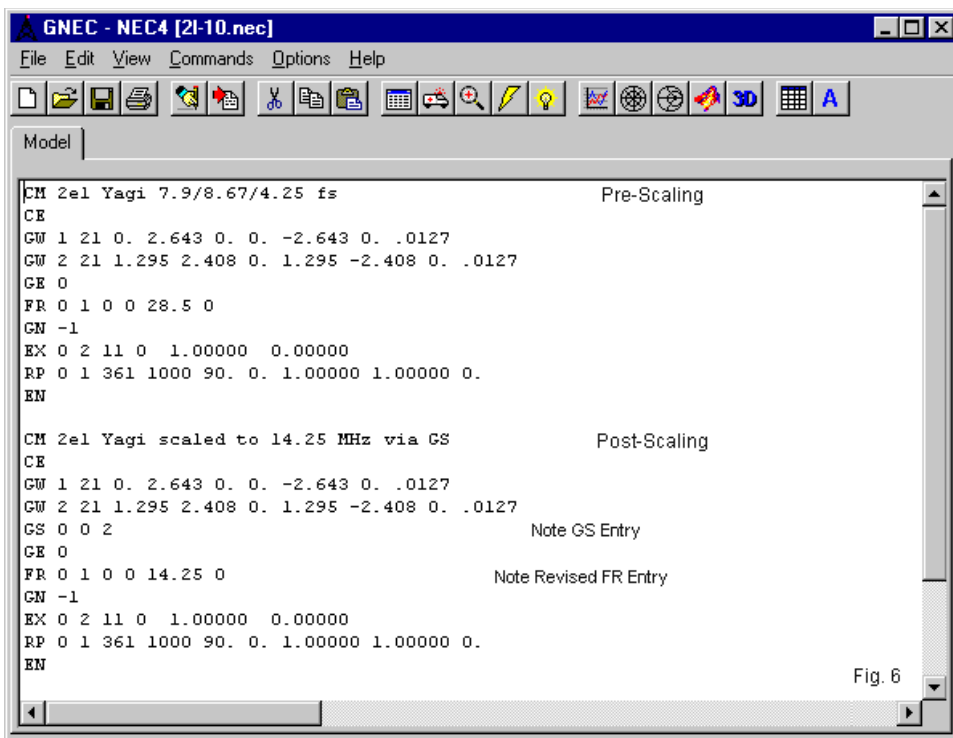


Fig. 6

To confirm the correct functioning of the GS command, we may examine a 1-line extract from the NEC output report's "Segmentation Data" section that lists the coordinates of all segments in the model. The first line for one end of the GW1 command appears for both the pre-scaled and the post-scaled models. The Y-coordinate, the segments lengths, and the wire radius entries show the scaling accomplished by the GS command. Both models in NEC-4 report a gain of 6.28 dBi, a front-to-back ratio of 11.25 dB, and a source impedance of 32.58 - j0.33 Ohms.

28.5-MHz Yagi Model

SEG.	COORD OF			SEG.	CTR	SEG.	ORIENT	ANGLES	WIRE	CONNECT	DATA	TAG	
NO.	X	Y	Z			LGTH	ALPHA	BETA	RADIUS	I-	I	I+	NO.
1	0.00	2.52	0.00			0.252	0.00	-90.00	0.012	0	1	2	1

14.25-MHz Yagi Model

SEG.	COORD OF			SEG.	CTR	SEG.	ORIENT	ANGLES	WIRE	CONNECT	DATA	TAG	
NO.	X	Y	Z			LGTH	ALPHA	BETA	RADIUS	I-	I	I+	NO.
1	0.00	5.03	0.00			0.503	0.00	-90.00	0.025	0	1	2	1

Other GS Potentials

The GS command scaling potential is not limited to simple one-shot frequency conversions. The following practice is one sample of what we may do with the command in a more systematic way. We shall initially enter all geometry commands in meters. We shall also change the subject antenna to a 6-element Yagi. However, our basic design will use a frequency of 299.7925 MHz. At this frequency, 1 meter = 1 wavelength. Our basic model might resemble the following lines.

```
CM 6-el 300 Yagi
CE
GW 1 21 0. .251 0. 0. -.251 0. .001
GW 2 21 .1251 .2484 0. .1251 -.2484 0. .001
GW 3 21 .1705 .2312 0. .1705 -.2312 0. .001
GW 4 21 .321 .225 0. .321 -.225 0. .001
GW 5 21 .4617 .225 0. .4617 -.225 0. .001
GW 6 21 .6713 .2167 0. .6713 -.2167 0. .001
GE 0
FR 0 11 0 0 295 1
GN -1
EX 0 2 11 0 1.00000 0.00000
RP 0 1 361 1000 90. 0. 1.00000 1.00000 0.
EN
```

We may scale this Yagi to any frequency whatever using the GS command and one easy calculator step. The required GS custom conversion entry adheres to a simple equation where CF is the conversion factor.

CF = 299.7925 / new frequency

Suppose that we wish to scale the Yagi to 15 MHz. The value of CF is 19.986167 (or any usable rounding of that value). The revised model would have the following appearance.

```
CM 6-el 300 Yagi
CM Scaled to 15 MHz via GS
CE
GW 1 21 0. .251 0. 0. -.251 0. .001
GW 2 21 .1251 .2484 0. .1251 -.2484 0. .001
GW 3 21 .1705 .2312 0. .1705 -.2312 0. .001
GW 4 21 .321 .225 0. .321 -.225 0. .001
GW 5 21 .4617 .225 0. .4617 -.225 0. .001
GW 6 21 .6713 .2167 0. .6713 -.2167 0. .001
GS 0 0 19.986167
GE 0
FR 0 1 0 0 15 1
GN -1
EX 0 2 11 0 1.00000 0.00000
RP 0 1 361 1000 90. 0. 1.00000 1.00000 0.
EN
```

Both models return a free-space gain of 10.28 dBi, a 180-degree front-to-back ratio of 31.12 dB, and a source impedance of $58.77 + j10.09$ Ohms at 299.7925 MHz and at 15 MHz. The purpose of using the 6-element Yagi lies in the original model's frequency sweep specification. For a center frequency of about 300 MHz, the usable operating passband is about 10 MHz. Within that passband, the design has a free-space gain of at least 10.1 dBi, a 180-degree front-to-back ratio of 19.5 dB or higher, and a 50-Ohm SWR of under 1.3:1. When we apply the scaling conversion factor, we must also apply it to the operating passband. Hence, at 15 MHz, the equivalent passband is only about 0.5 MHz wide.

The scaling technique is perfectly general and may be useful in a variety of modeling activities. However, it also has limitations. Perhaps the most notable limit is the wire radius, which is just under 20 mm at 15 MHz. Unless we are very judicious in constructing our master models, we may still have to optimize them at other frequencies for changes in wire radius, as well as for tapered element diameter schedules in HF antennas. However, any method of scaling an antenna design will result in these same supplementary tasks.

One tendency among modelers is to freeze the potential for the GS command into an unbreakable habit. For example, some modelers believe that the GS command must precede the GE command and follow all other geometry commands. However, the command is more flexible than this over-simplified view. The GS command must simply follow the set of geometry commands that use a unit of measure other than meters. The following artificial sample mixes measures. GW1, the reflector, has its units in feet, while GW2, the driver, uses meters. We may as an exercise retain the mixed measures by inserting the GS card immediately after GW1 to convert its dimensions to meters. The following GW2 entry is unaffected by the action of the GS command.

```
CM 2el Yagi 7.9/8.67/4.25 fs
CE
GW 1 21 0. 8.67 0. 0. -8.67 0. .04167
GS 0 0 0.304800
GW 2 21 1.295 2.408 0. 1.295 -2.408 0. .0127
GE 0
FR 0 1 0 0 28.5 0
GN -1
EX 0 2 11 0 1.00000 0.00000
RP 0 1 361 1000 90. 0. 1.00000 1.00000 0.
EN
```

The technique just described has very limited application. Using a uniform set of coordinate measures throughout the geometry section of a model is always good practice. Nevertheless, the technique does illustrate that the GS command is a bit more flexible than we might have previously thought.

A more common situation might be to develop an initial model in a preferred set of units that are not meters. Then we might wish to scale the antenna. Although we shall use our simple 2-element Yagi as an illustration, the time factor required for manual revision of all geometry entries will increase very sharply for highly complex models. However, we might ease the task by using multiple GS cards. Consider the 28.5-MHz Yagi with its dimensions in feet. Next, we wish to scale the antenna to 14.25 MHz. The resulting model might have the following appearance.

```
CM 2el Yagi 7.9/8.67/4.25 fs
CM Scaled to 14.25 MHz via GS
CE
GW 1 21 0. 8.67 0. 0. -8.67 0. .04167
GW 2 21 4.25 7.9 0. 4.25 -7.9 0. .04167
GS 0 0 0.304800
GS 0 0 2
GE 0
FR 0 1 0 0 14.25 0
GN -1
EX 0 2 11 0 1.00000 0.00000
RP 0 1 361 1000 90. 0. 1.00000 1.00000 0.
EN
```

The example shows that we may use strings of GS entries to accomplish different tasks. We might also have combined the two conversion factors externally. However, Murphy's Law tells us that in 3 months, we will no longer be able to remember what the GS value of 0.6096 means. Sometimes, separate entries (each with an appropriate side notation) are more useful. The small time it takes to enter 2 GS commands can save much head-scratching time later on.

Conclusion

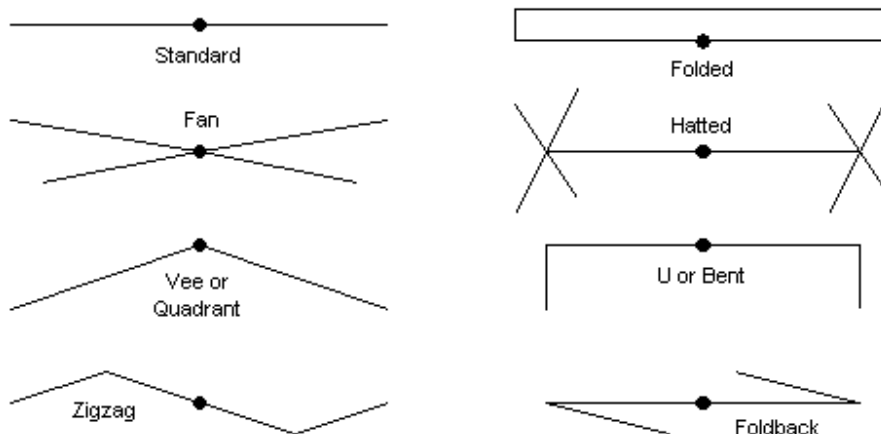
Frequency scaling of antenna designs has a wide range of uses. They encompass practical design work as well as systematic explorations of antenna properties at various frequencies. As noted early on, scaling best occurs using a free-space or perfect-ground environment, with other model variables introduced after verification of successful scaling.

The methods available to us for scaling designs also cover a considerable territory. We may manually calculate and enter scaled geometry values. We may use the facilities provided by the interface programming of the particular NEC or MININEC implementation that we are using. If we have access to the complete NEC command set, then we may achieve the same ends via the GS or geometry scaling command. The command is useful for more activities than just converting units of measure to meters. To confirm correct command use or to record the resulting coordinate and radius values, we must consult the NEC output report, using the segmentation-data section as our primary resource. I do not anticipate widespread use of the GS command for frequency scaling exercises in NEC. Nevertheless, it is useful to be aware of the command's potential and versatility.

108. Dipoles: Variety and Modeling Hazards Linear, V, and Folded Dipoles in NEC

A dipole is in basic texts any antenna that exhibits a single current maximum to minimum transition from the center feedpoint to the wire end, and conversely, transitions from minimum to maximum voltage as we move from the center to the outer end of the wire. Basic antenna theory rests to some degree on the performance or the behavior of very short dipoles. In practical antenna circles, the term "dipole" is generally shorthand for a specific subset of these antenna. A practical dipole is a center-fed, resonant or near resonant 1/2-wavelength antenna usually using linear (wire or tubing) construction. When the antenna grows too long, we no longer have the current and voltage transitions that define the dipole, and so the antenna becomes a doublet--a center-fed wire with otherwise relatively undefined characteristics.

In these notes for relative newcomers to antenna modeling, I shall use the practical-dipole definition. Practical dipoles include the idea of resonance, that is, a center feedpoint impedance that is entirely resistive (or nearly so), with no (or very little) remnant reactance. These antennas are very practical for many applications. At this point, we begin to encounter physical variations on the usual linear dipole construction. The key parameter shifts from the pattern of current and voltage along the wire to resonance, and we use resonance to determine that an antenna is an electrical half-wavelength long and hence a dipole. Under this revised view of a practical dipole, we encounter many configurations, all of which count as dipoles if we use resonance and an electrical half-wavelength as the key determining factors. **Fig. 1** shows a number of these configurations, but by no means all of them.



Some Dipoles That I Have Known

Fig. 1

The standard linear dipole and its impedance-transforming partner, the folded dipole, are most familiar to virtually all antenna users. The fan dipole is actually 2 dipoles for separate frequencies with a common feedpoint. The V dipole occurs most commonly as an inverted V, although we may set the V angle at any value. At 90 degrees, with the legs parallel to the ground, we obtain a quadrant antenna. We may also form Ls and inverted-Ls with corner feedpoints as variations on the Vee. The zigzag dipole is simply any set of relative small departures from a truly linear arrangement, usually done to fit a dipole within a restricted space. The hatted dipole uses symmetrical structures at each end of the main element to obtain resonance with a shorter overall length than a full-length dipole requires. The bent or inverted-U form achieves element shortening with single extensions. However, these extensions radiate with vertical polarization, whereas the hat structures usually have self-canceling fields. The final example of a shortened dipole uses fold-back structures. The sketch shows only one of many possible forms, sometimes called the lazy N.

These notes are not designed to evaluate the relative merits of the various configurations. Instead, we want to examine the modeling challenges that some of them might present. Some of the practical dipoles can easily result in unreliable models if we do not attend to software limitations, especially of NEC. So we shall examine the dipoles using both NEC-2 and NEC-4. One of our tools

will be the Average Gain Test (AGT), which assesses the reliability of a model by sampling a lossless model in free space (or over perfect ground, which is not relevant here) over a full sphere of points and comparing the average gain to an isotropic source. Hence, an AGT value of 1.000 is excellent, but values above and below that value indicate potential degrees of unreliability. For source impedances close to resonance, we can derive corrected values by multiplying the AGT value times the reported source resistance. We can also convert the AGT value to a value in decibels. If the derived AGT-dB value is positive, we subtract it from the reported gain to obtain a correct gain value. (This note applies at any vector from the antenna, not just to maximum gain.) If the derived AGT-dB value is negative, we add its absolute value to the reported gain, since it tells us by how much (approximately) the gain report is low. We must always remember that the AGT is a necessary but not a sufficient condition of model adequacy. A good AGT score does not guarantee model adequacy.

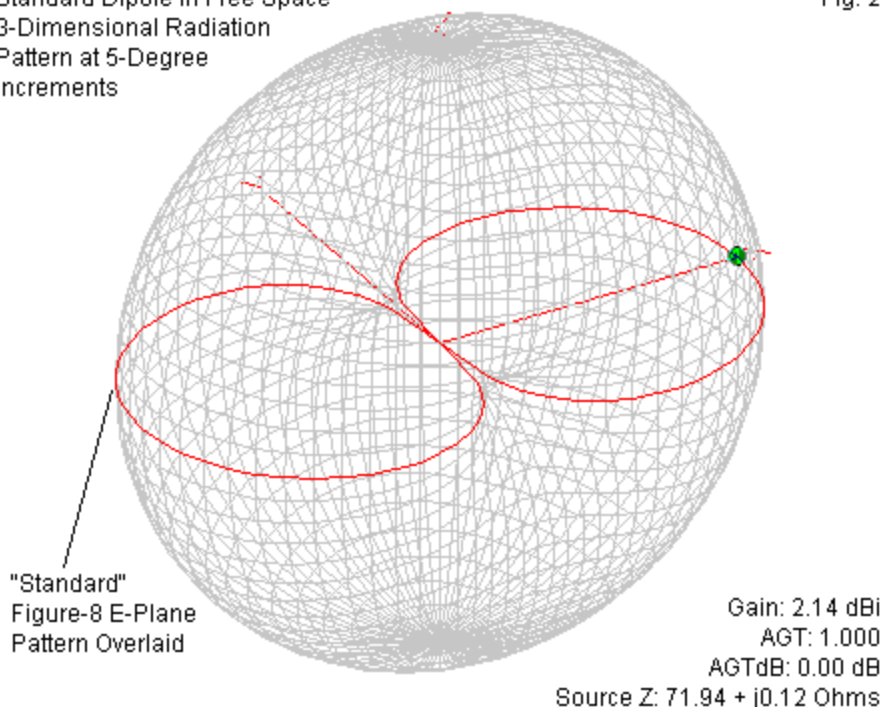
This first portion of our journey will deal only with modeling some of the dipoles in NEC (both -2 and -4). In the next episode, we shall compare our results with modeling the same antennas in at least two versions of MININEC. Once we have the basic terms and limits of each program under our belts, we can take up the remaining versions of the dipole using both general types of antenna modeling programs.

The Standard Linear Dipole

We may begin with the linear dipole. For our tests, we shall use a frequency of 28 MHz, with a 1" diameter lossless element. The only challenge is not skimping on the segments. Although the minimum segmentation per wavelength is 10, the recommended minimum is 20. Of course, in NEC, we use an odd number of segments to obtain a center source position. However, we need not always strive for the minimum recommended number of segments. The test model uses 41 segments. Our only opposing danger would be to use so many segments that we press the segment-length to wire-diameter (or radius) ratio. 41 segments with a 1" diameter comes nowhere close to such pressure. **Fig. 2** shows the 3-dimensions free-space pattern and overlays the typical E-plane (azimuth) figure-8 pattern with which we are familiar. The listed gain figure sometimes surprises newer modelers who hear that a lossless dipole in free space has a gain of 2.15 dBi. That value applies to dipoles using vanishingly thin elements, which would be significantly longer than our 1" element. Shortening a linear dipole, even if only enough to restore resonance due to using a fat element, results in a gradual gain reduction.

Standard Dipole in Free Space
3-Dimensional Radiation
Pattern at 5-Degree
Increments

Fig. 2



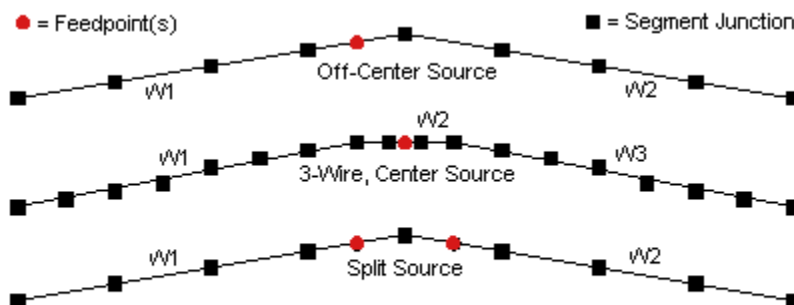
The impedance figure is from NEC-4. NEC-2 yields $71.95 + j 0.17$ Ohms. Both values are from the EZNEC cores through version 4.0.20. Different implementations of NEC-2 and NEC-4 may use different Fortran compilers and result in values that differ even from these. In fact, different CPUs in various computer types can also result in variations, although all will be harmlessly small. Both NEC-2 and NEC-4 agree on the AGT score: 1.000, which requires no corrective on the gain or source resistance report.

The total antenna length for our sample model is 199.4", although it will be more convenient for us to speak in half-lengths: ± 99.7 ". For many of our "deviant" dipoles, the half-length will be a useful catalog number. Although the antenna is an electrical half-wavelength, as indicated by the resonant source impedance, the physical wire is only 0.473-wavelength.

The V Dipole

V dipoles occur using almost any included angle between the wires. Let's restrict ourselves to a single angle of 90 degrees between wires. That is equivalent to bending each leg 45 degrees from the linear configuration. In terms of modeling, the action will necessarily result in a model with at least 2 wires. MININEC models will place the source on the junction of the two wires at the apex. However, uncorrected MININEC 3.13 will provide two kinds of errors if we are not careful. First, there is a frequency offset that increases with rising frequency. Second, MININEC creates errors in current calculations at sharp angular wire junctions. We can largely overcome the second error condition by using a very large number of segments, since the amount of error varies with the segment lengths. However, many later implementations of MININEC 3.13 provide corrections for both error sources within the code and yield very reliable results. However, unless you possess more than one version of MININEC 3.13, you may not be able to assess the level of correction available within the program you use. I have provided some performance comparisons over a number of MININEC potential trouble spots in a past column.

NEC users face a slightly different challenge. Since the apex of the V will be a junction of 2 wires and since NEC sources lie within segments, we must figure out where to place the source. **Fig. 3** shows 3 of our options. The black squares are segment junctions, while the red dots are potential source locations. For all of our tests here, we shall stay at 28 MHz and retain the 1" diameter lossless element.



Source Placement on a V Dipole

Fig. 3

The top version of the V model uses a simple procedure of placing the source on one of the segments adjacent to the apex of the V. The justification lies in the fact

that at high current regions of most antennas, the current changes very slowly as we move away from the precise antenna center. Hence, the potential error is very small, especially since these models use the same total number of segments as the linear dipole (actually 42). The bottom model uses a split or dual source, with a source placed on each side of the apex. EZNEC will internally total the sum of the two source impedance values, but manual addition is simple enough. Otherwise, the model is identical to the top offset-source model.

The middle model uses a different technique. It creates a level wire at the center. The wire uses 3 segments so that the segments adjacent to the center source segment are of equal length with the source segment. That model design maneuver tends to yield maximum accuracy in the current calculations. Each wire extends +/- 7.5" from the center point. The sloping legs each have 19 segments, for a total of 41 segments in the model, and the leg segment lengths are close to the length of the segments in the source wire.

Fig. 4

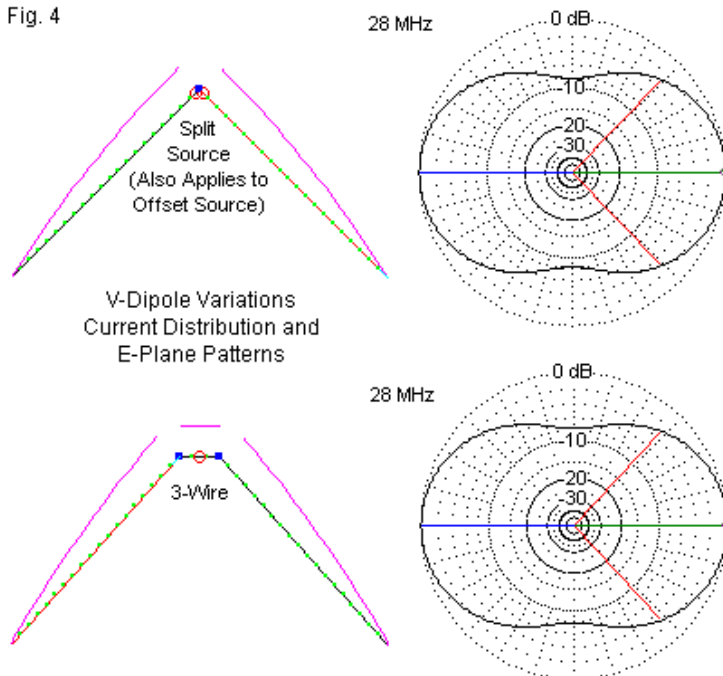


Fig. 4 shows two relevant facts about the models. The wire layouts have superimposed current magnitude curves that verify the current distribution as appropriate to a dipole as defined earlier. The E-plane patterns broadside to the plane of the V structures are virtually identical. To a casual viewer, the models might seem indistinguishable. However, the following table shows that there are indeed a few important distinctions among them.

Comparison of V-Dipole Models in NEC-2 and NEC-4
All models use 1" diameter lossless elements in free space.

Source Method	Core	Wire Length Inches	Gain dBi	Source R	Impedance +/- j X Ohms	AGT	AGT-dB	Corrected Gain dBi
Offset	NEC-2	+/-103.3	1.52	44.75	+ j0.02	0.949	-0.23	1.75
	NEC-4	+/-103.3	1.50	45.00	- j0.22	0.943	-0.25	1.75
Split	NEC-2	+/-103.3	1.52	44.75	+ j0.22	0.949	-0.23	1.75
	NEC-4	+/-103.3	1.50	45.01	+ j0.02	0.943	-0.25	1.75
3-Wire	NEC-2	+/-102.3	1.72	41.31	+ j0.25	1.004	0.02	1.70
	NEC-4	+/-102.3	1.73	41.26	+ j0.00	1.005	0.02	1.71

Note: Wire Length is the total half-element length from the apex to the tip in offset and split-source versions and from the source point to the wire tips in the 3-wire version.

Between the offset-source and the split-source models we find only tiny differences. For each core, the difference falls mostly in a 0.2 consistent differential in the source reactance. We might assign the gain difference between NEC-2 and NEC-4 versions to differences in the core. This assignment would be correct, but not merely due to random compiler or CPU operations. If we move to the AGT and AGT-dB columns, we find values that are far less than perfect. The differences in the AGT values relative to the 2 cores are small but significant. If the initial gain report seemed low, it was. A corrected gain report brings the value more within expectations for a full-size antenna, even if we allow for some broadside gain loss to compensate for the shallower side nulls in the E-plane patterns.

The less than perfect AGT values result from the use of relatively fat elements. Each segment is about 5" long, and the wire diameter is 1". At the apex of the V, the wire segments that join inter-penetrate a considerable, but not fatal distance relative to any use to which one might apply the model. If we had used thin wires, the small wire diameter would have resulted in much less penetration toward the junction segment centers, and the AGT values would have been closer to ideal

values. Obviously, I have constructed the sample model to reveal the effect, rather than hiding it by the use of thin wires.

The 3-wire version of the model achieves a set of AGT values much closer to ideal. Whether the very small difference in correct gain values is a function of the core or of the slightly different structure is indeterminate from the available data, but we do note that the total amount of element from the source point to the element tip differs by an inch from the 2-wire models. As well, we may note that the 3-wire models result in lower source resistance values. However, you may wish to compare the values after multiply each reported resistance by the basic AGT value.

Even if we discount this sequence of models as unlikely candidates for implementation, they do reveal the importance of making constant reference to the AGT values of a model. Had we used the raw reports from the 2-wire models as a comparator to the linear dipole, we would have drawn very wrong conclusions about the degree of gain deficit. As well, we should not be too hasty in discounting the models, since the design, turned 90 degrees so that all elements parallel the ground surface, forms a common structure of some antennas with forward-sweep elements.

Folded Dipoles

Folded dipoles are actually hybrid constructions. They are indeed dipoles, but the folded structure adds an extra set of currents. These transmission-line currents are a function of the folded dipole's impedance transformation relative to a linear dipole. The upper left portion of **Fig. 5** shows the result of combining the 2 sets of currents. The transmission line currents are relatively constant in magnitude. Hence, the radiation currents overlay them. The resulting curve rises above and falls below the average current magnitude, but does not go to zero at the ends of the wires, as we would find for a linear dipole.

The Folded Dipole

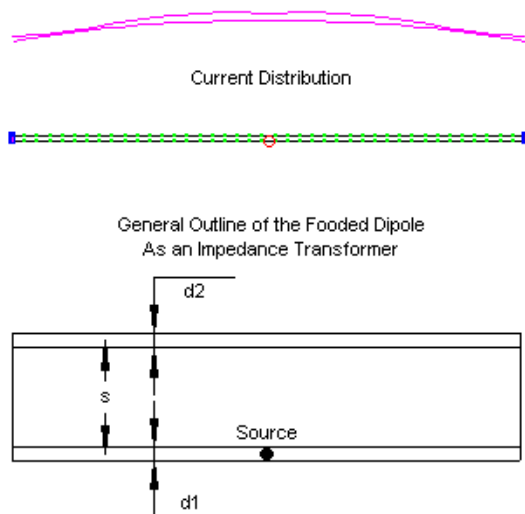
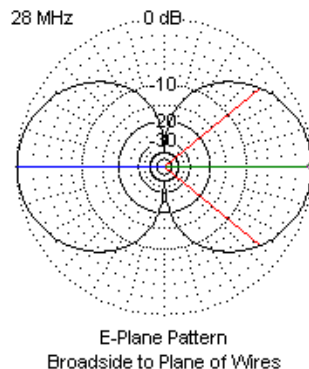


Fig. 5

Once we separate the two currents, the radiation currents are virtually identical to those that we find in a linear dipole. Hence, the radiation pattern on the upper right is indistinguishable from the patterns of standard dipole. The resonant folded dipole will be shorter than a line dipole, since the effective diameter of the two parallel wires, each the same diameter as the single wire in a linear dipole, is considerable greater. The 28-MHz model of a folded dipole with 1" diameter elements is 4.5" shorter at resonance than the linear dipole that we reviewed earlier. The modeled folded dipole uses a wire separation of 2" center-to-center, with 41 segments in each long element section.

With both elements having an equal diameter, the resonant impedance is between 281 and 282 Ohms, or about 4 times the impedance of a single element dipole (70 Ohms). However, the exact ratio of impedance transformation is only 4:1 if both elements have the same diameter. The lower half of **Fig. 5** shows the key elements in calculating the transformation ratio, R. The equation involves the spacing (s) between elements and the relative diameters of the two element sections, where d1 is the section with the feedpoint and d2 is the section parallel



$$R = \left(1 + \frac{\log \frac{2s}{d_1}}{\log \frac{2s}{d_2}} \right)^2$$

Impedance Transformation
Calculation

to the driven section. Note that s, d1, and d2 must use the same units of measure for the equation to produce usable results. If both elements have the same diameter, then the ratio of logs reduces to 1, and the ratio turns out to be 4. If the driven section is smaller, then the ratio is greater than 4:1. If the undriven section is smaller, then the ratio is less than 4:1 but always greater than 1:1.

We may reduce the undriven section to any diameter. Let's use 0.1". The equation yields 1.89:1 as the transformation ratio. If we assume a linear dipole impedance of 70 Ohms, then the folded dipole with a larger driven section and a smaller undriven section should show impedance close to 132.5 Ohms. Slight variations will occur because the equation does not take the end connecting wires into account. We shall use the same segmentation level (41 segments per section) that we used on the folded dipole with equal-diameter sections. Since the transformation involves only the transmission-line currents, the gain and pattern of the folded dipole with unequal-diameter elements should be the same (within close tolerances) as the corresponding results from the equal-diameter folded dipole. The following table summarizes the results for both kinds of folded dipole using both NEC-2 and NEC-4.

Comparison of Folded-Dipole Models in NEC-2 and NEC-4: Equal and Unequal Diameter Elements

All models use 1" diameter lossless driven elements in free space.
Second elements are 1" or 0.1" diameter lossless wires.

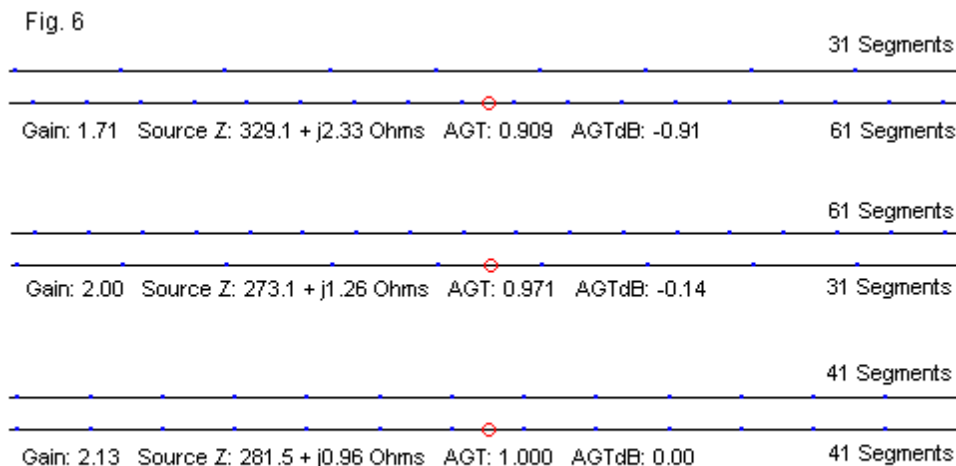
Diameters	Core	Wire Length	Gain	Source Impedance	AGT	AGT-dB	Corrected
Driv/other		Inches	dBi	R +/- j X Ohms			Gain dBi
1"/1"	NEC-2	+/-97.45	2.13	281.6 - j0.54	1.000	0.00	2.13
	NEC-4	+/-97.45	2.13	281.5 - j0.96	1.000	0.00	2.13
1"/0.1"	NEC-2	+/-99.2	4.34	230.2 - j10.59	1.662	2.21	2.13
	NEC-4	+/-99.2	2.96	164.5 + j0.60	1.209	0.82	2.14
Calculated Impedance			132.5				

Note: Wire Length is the total half-element length from the center to the tip.

The equal-diameter version of the folded dipole shows good results from both NEC-2 and NEC-4, since both cores produce an AGT of 1.000. The gain values are identical, and the reported impedance values are almost identical. However, the reported values for the folded dipole with unequal diameter sections fall way off the mark. NEC-2 is considerably worse than NEC-4 with respect to anticipated values of gain and impedance. In fact, both NEC-2 and NEC-4 become error prone with angular junctions of wires having dissimilar diameters. NEC-4 improves upon the performance of NEC-2 in this regard, but falls

seriously into error as the change of diameter increases. In this model, the ratio is 10:1, so that even NEC-4 yields an unacceptable AGT value. Note that the AGT-dB values bring the gain report close to the anticipated value. However, at a certain level, the AGT value itself becomes useless in correcting the reported source resistance. MININEC does not share the NEC limitation relating to changes in element diameter at wire junctions. Hence, it is generally able to handle models like the folded dipole with unequal-diameter element sections with no problems. If the version of MININEC 3.13 has had other limitations corrected, then it should yield quite accurate results for our test case.

Both models that we have just examined used 41 segments on each long wire. The results are a set of well-aligned segment junctions in the closely spaced parallel wires. Although providing each wire with the same number of segments seems quite natural, we sometimes encounter cases of somewhat careless segmentation. **Fig. 6** shows the center portions of equal-diameter folded dipoles that differ only in the assignment of segments per wire. (All end connection wires use 1 segment.) In one case, we have 61 segments on the driven wire and 31 on the other wire. The second case reverses the assignment. At the bottom, the figure shows the segmentation of the preferred model.



Some Consequences of Careless Segmentation: Folded Dipole

The upper two models clearly do not show a pattern of well-aligned segment junction. The following table shows the results of the misalignment, with all other factors being the same for all three models.

Comparison of Folded-Dipole Models in NEC-2 and NEC-4: Careless vs. Careful Segmentation
All models use 1" diameter lossless elements in free space.

Segments	Core	Wire Length	Gain	Source	Impedance	AGT	AGT-dB	Corrected
Driv/other		Inches	dBi	R +/- j	X Ohms			Gain dBi
61/31	NEC-2	+/-97.45	1.88	342.5 +	j2.31	0.946	-0.24	2.12
	NEC-4	+/-97.45	1.71	329.1 -	j2.33	0.909	-0.41	2.12
31/61	NEC-2	+/-97.45	1.84	263.6 +	j2.23	0.937	-0.28	2.13
	NEC-4	+/-97.45	2.00	273.1 +	j1.26	0.971	-0.13	2.12
41/41	NEC-2	+/-97.45	2.13	281.6 -	j0.54	1.000	0.00	2.13
	NEC-4	+/-97.45	2.13	281.5 -	j0.96	1.000	0.00	2.13

Note: Wire Length is the total half-element length from the center to the tip.

Fig. 6 provides the NEC-4 reported data for each model. The degree to which the unevenly segmented models depart from correct values depends on both the core used (NEC-2 or NEC-4) and the ratio of segments in the 2 wires, where the ratio shows the misalignment. Admittedly, the sample models provide cases of extreme misalignment. However, even small misalignments can draw the results away from the ideal AGT values attained by the model with well aligned segments. Alignment becomes ever more critical as we close the spacing between wires. Once more, it pays dividends to check the AGT values for any model. Checking those values becomes even more important when we need or wish to compare the reports of one model with another, whether we are using similar or dissimilar geometries.

Conclusion to Part 1

We have not gone very far in our exploration of resonant half-wavelength dipoles, and already we have seen some modeling snares. Some of those traps are modeling practices that we can easily avoid. Others involve limits to the NEC cores that we cannot avoid except by deferring the model construction. Folded dipoles with unequal elements form one of those NEC limitations and require the use of antenna modeling software that lacks the particular limitation involved. MININEC is one of those usable cores.

In addition to running into potential pitfalls, we have also run out of room in this column. Therefore, we shall have to resume our journey in the next episode. We shall discover whether or not MININEC can handle those odd folded dipoles--and more.

109. Dipoles: Variety and Modeling Hazards Linear, V, and Folded Dipoles in MININEC

In the last episode, we explored modeling dipoles in NEC (-2 and -4). Along the way, we discovered (or re-discovered) some NEC limitations. Although we noted the use of MININEC along the way, we did not pause long enough to see clearly the degree to which MININEC (3.13) is subject to the same limitations, is subject to more severe limitations, or is able to overcome the noted limitations in NEC. Since many newer modelers (and a good number of quite experienced modelers) use MININEC, we should re-trace our steps, highlighting the alternative modeling program along the way.

Our focus is on the many forms of the dipole, understood in practical rather than textbook terms. For our purposes, a dipole is a center-fed resonant or near resonant antenna that is about 1/2-wavelength electrically. In fact, resonance defines what an electrical half wavelength is, since the forms in which we encounter dipoles are many. Among the types listed at the beginning of the last episode are the standard or linear dipole, the V or quadrant, the folded dipole, the fan dipole (usually a dual-band pair of dipoles with a common feedpoint), the bent or inverted-U, the hatted dipole, and the dipole with element fold-backs. In the course of looking at just the standard, V, and folded dipoles, we encountered enough potential modeling hazards to give us pause. We shall continue the NEC journey in the next episode, but for now, let's examine our initial dipoles with MININEC.

NEC calculating cores tend to show only small variations among them. Most result from developments at the LLNL source. Since NEC-2 is public domain, we find most variants in commands within its iterations. NEC-4 has undergone fewer post-release developments and shows much greater uniformity. In fact, there are only two commercial implementations of NEC-4. Public domain MININEC (version 3.13) has undergone far greater modification from a larger number of programmers. Originally written in Basic, the program is almost always found in one of the Windows languages these days. As well, raw MININEC had a considerable number of limitations that recent programming has overcome. However, not all programmers have attended to all limitations. For example, the MININEC ground calculation system has two major problems. First, when using a lossy ground, MININEC calculates the source impedance as if over perfect ground. Second, for any antenna with a horizontal component to the total far field

pattern, the MININEC ground calculations become ever more inaccurate relative to antenna gain and impedance as the antenna drops below about 0.2 wavelength. Because MININEC uses a simplified reflection coefficient, little is possible to correct it. However, a few programs have successfully grafted the NEC Sommerfeld-Norton ground calculation system onto MININEC.

Less obvious but equally significant are certain errors that infect some MININEC calculations. First, MININEC begins to show an offset relative to both NEC-2 and NEC-4 calculations. Some, but not all, implementations of MININEC have introduced corrections for this offset. Second, MININEC uses a system of current "pulses," which are at segment junctions (in contrast to NEC's current placement at segment center regions). Hence, without correction or the use of a very large number of segments, MININEC models of angular antenna geometries can show significant error. In fact, the more acute the angle, the larger the error. Raw MININEC also shows some error for very close spaced wires, and this difficulty has undergone correction in many MININEC implementations. Finally, MININEC lacks the extensive command structure that we find in NEC. Hence, it is limited in the manipulations that we can perform on both the geometry and on the output. For example, it does not permit the use of elliptical plane waves and segment current analysis useful in receiving and radar reflection analysis. As well, we find no near-field analysis, inter-segment coupling analysis, transmission lines, or networks. To overcome these voids, a number of programmers have introduced adjunct programs to allow the modeler to perform calculations involving some of these elements while using the implementation of MININEC. Given that virtually no two implementations of MININEC resolve the same set of limitations in the same way, the program has well earned the distinction between "raw" and "cooked" versions. There is, of course, a revised "Expert MININEC" set of programs, but these proprietary efforts do not use the same algorithms as MININEC 3.13.

Since we cannot hope to treat every version of MININEC and still attend to the variety of dipoles and their limitations for modelers, I have chosen 2 from my small stock: Antenna Model (the most corrected version of MININEC commercially available) and MMANA (one of the least-revised versions with the virtue of being free). Because MININEC cores undergo such regular modification, it is significant to give the versions involved: V1.77 for MMANA and 2.0.0.595 for Antenna model. At the same time, I shall adhere to the basic structure of all antennas that we examined in the preceding episode. The test frequency is 28.0

MHz. The antenna elements--unless re-specified for a special test--will be 1" in diameter and be lossless. The environment will be free space.

For most NEC models, I used 41 segment per half-wavelength. The fairly large number ensures convergence within NEC. The odd number of segments in a linear element places a centered source directly at the element center, since NEC places sources on segments and not on segment junctions. In MININEC, current pulses and therefore sources occur at segment junctions. Hence, to precisely center a source requires an even number of segments on the element. We shall normally use 40 segment.

With these preliminaries, we are ready to examine the baseline antenna for all other work, the linear or standard dipole.

The Standard Linear Dipole

The linear or standard dipole is the root antenna for all of these exercises. As in NEC, a MININEC model must adhere to certain limits on the ratio of the wire diameter or radius to the length of a segment. However, there appears to be no full agreement on the absolute limiting ratio. Antenna Model (AM) provides warnings if the segment falls below 1.25 the wire diameter. However, the program also provides an Average Gain Test (AGT) value as a second check on the model. AGT is not a standard MININEC feature, but an added provision of the AM programmers.

Linear (Standard) Dipole Outline

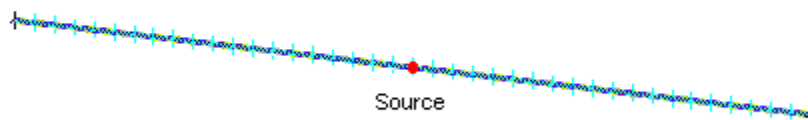


Fig. 1

Fig. 1 shows the model geometry of the MININEC dipole. The markers indicate segment junctions. The NEC models used 41 segments, so the basic MININEC model will use 40 segments. The feedpoint appears on pulse 20, a fact that is informative: a pulse does not occur on the segment-1/end-1 point of the antenna. For initial comparisons, I used the same element length that yielded resonant antennas in NEC: 199.4" or 5.065 m. (My version of MMANA counts in meters.)

The following table compares the results of NEC-2, NEC-4, AM, and MMANA models of the dipole at 28 MHz.

Comparison of Linear Dipole Models in NEC-2, NEC-4 and MININEC
All models use 1" diameter lossless driven elements in free space. AGT data not available in MMANA.

Core	Wire Length Inches	Gain dBi	Source Impedance R +/- j X Ohms	AGT	AGT-dB	Corrected Gain dBi
NEC						
NEC-2	+/-99.7	2.14	71.94 + j0.12	1.000	0.00	2.14
NEC-4	+/-99.7	2.14	71.95 + j0.17	1.000	0.00	2.14
MININEC						
A-M	+/-99.7	2.13	71.79 - j0.54	1.000	0.00	2.13
MMANA	+/-99.7	2.12	70.48 - j5.46			

Note: Wire Length is the total half-element length from the center to the tip.

Between the 2 NEC cores and AM, there is no difference. However, MMANA, a relatively uncorrected version of MININEC 3.13, reports a source impedance that indicates a slightly short length for the dipole. MMANA reports a resonant length of about 200.4" (5.10 m) with an impedance of 71.14 + j0.40 Ohms. The length differential is a bit over 0.5%: not a fatal difference, but an indicator of an offset that continues to grow more important with rising frequency.

The AGT is only one test of model adequacy. Equally important--especially in MININEC--is the convergence test. Basically, the convergence test provides information on the level of segmentation necessary for a given model's geometry. At some level of segmentation, successive increases in the number of segments per wire should not yield any significant changes in the reported gain or source impedance. There is no fixed level of adequate convergence, since the required level is normally a function of the use to which one puts a modeling task. However, there are some models that never converge, and convergence is a necessary condition of model adequacy. As well, some models arrive at good convergence with a low number of segments, while others require a higher segment density.

As a second mode of comparison, I altered the segment count in both the AM and MMANA dipoles, beginning with 10 and doubling that number in successive steps. The last step yields segment lengths that trigger the AM warning about the

ratio of wire diameter to segment length. In all cases, the dipole remained at its initial 199.4" length. The following table compares results.

A Comparison of Convergence Tests for a Linear Dipole in 2 Versions of MININEC. AGT data not available for MMANA.

Program	No. of Segments	Gain dBi	Source Impedance R +/- j X Ohms	Change in Resistance	AGT
AM	10	2.10	70.08 - j1.31	---	0.9981
	20	2.12	71.34 - j0.96	1.26	0.9991
	40	2.13	71.79 - j0.54	0.45	0.9996
	80	2.13	71.92 - j0.53	0.13	0.9998
	160	2.13	72.06 - j0.36	0.14	0.9999
MMANA	10	2.10	67.95 - j9.73	---	
	20	2.12	69.55 - j7.33	1.60	
	40	2.12	70.47 - j5.46	0.92	
	80	2.13	71.02 - j4.03	0.55	
	160	2.13	71.16 - j4.21	0.14	

For many purposes, both models might be considered to be adequately converged at the lowest segment density. However, it is clear that AM shows a higher level of convergence at lower levels of segmentation than does MMANA. We may note in passing that AM reports a more nearly ideal AGT value with increasing segmentation, although all 3 of the reported values round to 1.000. In the end, the point of the exercise is a. to stress the importance of running convergence tests, even on models using a simple geometry, and b. to note that different implementations of MININEC may shows differentials in the rate of convergence.

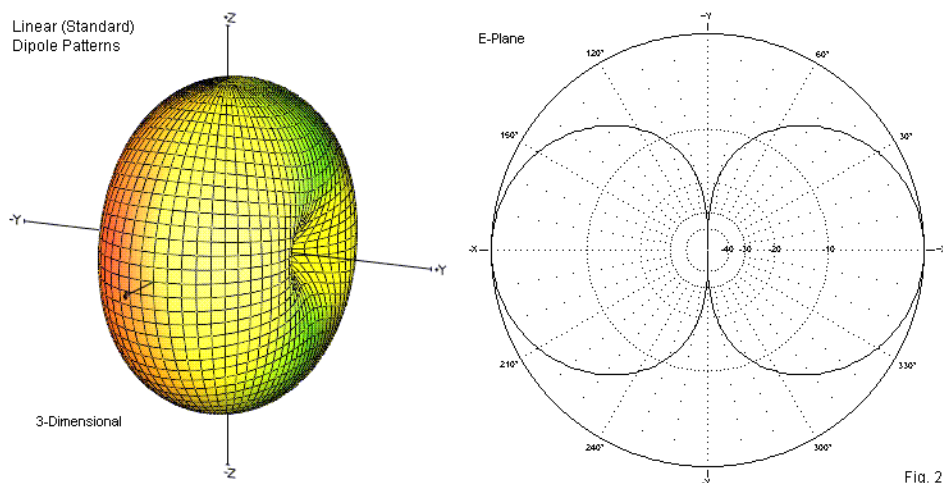


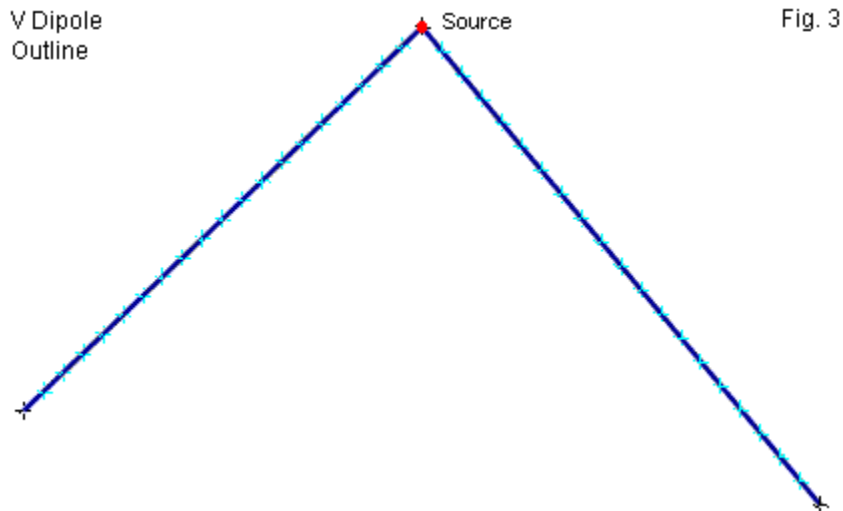
Fig. 2 provides both 3-dimensional and E-plane patterns for the dipole. Although these plots come from AM, the E-plane pattern does not differ in MMANA. Note that the side nulls are exceptionally deep for the linear dipole, yielding a nearly indefinitely large front-to-side ratio. Do not expect such deep nulls if you place the model over ground. At very low heights, the E-plane pattern will be at best an oval. At height of about 1 wavelength or more, the pattern will resemble a peanut.

The V Dipole

The V dipole includes in principle any electrical half-wavelength, near-resonant antenna with legs that do not form a 180-degree angle. Although Vs come in many angles and orientations, the test models use a 90-degree angle (also called a quadrant antenna when both legs are parallel to the ground).

In NEC, the construction of a V dipole model required attention to the placement of the source. The actual feedpoint of a physical V antenna will be at the apex of the angle formed by the 2 wires. In NEC, we might use an offset source on the first segment of one of the wires meeting at the apex. Alternatively, we might use a split source, which yields two offset sources. We sum the impedance reported by both. The third alternative is to use a short level 3-segment wire and to place the source on the center segment. The angled wires then connect to the ends of the level wire. Although any of the three methods may be adequate for general purpose modeling, only the 3-wire model produced near-ideal AGT values.

Again, the antenna used relatively fat (1" or 25.4 mm) elements to reveal any latent limitations that thin wire models might not detect.



In MININEC, modeling V dipoles is simpler, as shown in **Fig. 3**. Since the source appears at a pulse or a junction of 2 segments, we may place it directly at the apex of the V. The test models used 20 segments in each of the two wires. The following table compares the results for the NEC (-2 and -4) 3-wire model with the results for the AM and MMANA models. The AM model has priority in terms of setting the leg lengths. The MMANA model uses the AM dimensions to determine to what degree its reports may be at variance with the AM model reports.

Comparison of V-Dipole Models in NEC-2, NEC-4, and MININEC
All models use 1" diameter lossless elements in free space.

Program	Core	Wire Length Inches	Gain dBi	Source R +/- j	Impedance X Ohms	AGT	AGT-dB	Corrected Gain dBi
3-Wire	NEC-2	+/-102.3	1.72	41.31	+ j0.25	1.004	0.02	1.70
	NEC-4	+/-102.3	1.73	41.26	+ j0.00	1.005	0.02	1.71
AM	MININEC	+/-104.65	1.76	44.32	- j0.68	1.002	0.01	1.75
MMANA	MININEC	+/-104.65	1.75	43.54	+ j2.67			

Note: Wire Length is the total half-element length from the apex to the tip in MININEC models and from the source point to the wire tips in the 3-wire NEC version.

We cannot draw any immediate conclusions from the difference in wire length from the antenna center to the tip because the MININEC and NEC models have slightly different geometries. However, the MININEC model achieves an excellent AGT rating in AM with the single centered source and only 2 leg wires.

The MMANA V-dipole model seems to be more coincident with the AM model than was the MMANA linear dipole model. However, MININEC has two potential error sources at work. One is the frequency offset. The other is the corner effect. If both are uncorrected, then they may in some cases be additive and in other cases be partially canceling. These error sources do not self-identify. However, we may again perform a convergence test on the two MININEC models of the V in order to compare changes in the performance. In the following table, the segment entry indicates the total number of segments. Half appear in each leg of the V.

A Comparison of Convergence Tests for a V Dipole in 2 Versions of MININEC.
AGT data not available for MMANA.

Program	No. of Segments	Gain dBi	Source Impedance R +/- j X Ohms	Change in Resistance	AGT
AM	10	1.79	42.59 - j47.98	---	1.0081
	20	1.77	43.80 - j15.69	1.21	1.0046
	40	1.76	44.32 - j0.68	0.52	1.0025
	80	1.76	44.55 + j6.03	0.23	1.0013
	160	1.76	44.65 + j8.09	0.10	1.0009
MMANA	10	1.76	41.56 - j23.24	---	
	20	1.75	42.82 - j5.82	1.26	
	40	1.75	43.54 + j2.67	0.72	
	80	1.75	43.99 + j6.64	0.45	
	160	1.75	44.14 + j7.56	0.15	

Although the models show only small overall convergence test changes, the AM model is slightly more converged at lower segmentation levels than the MMANA model. AGT data are not available for the MMANA model. However, the AM models shows improving AGT values as the segmentation level increases, just as did the linear dipole model in AM. We may also note that the MMANA spread of reactance values is smaller than for AM. In this instance, the addition of segments to the model wires reduces the effect of the corner error tendency. Since most available versions of MININEC no longer have the very restricted total segment allowance that bothered DOS versions of the program, the use of many segments is no longer a hindrance to model construction or calculation speed, and accuracy improves in most cases. Although we must keep in mind that the MMANA model may be a product of two error tendencies that appear to partially cancel with the particular geometry of the present antenna, there is no reason not to use either MININEC model as the basis for building a V antenna (at least in free space).

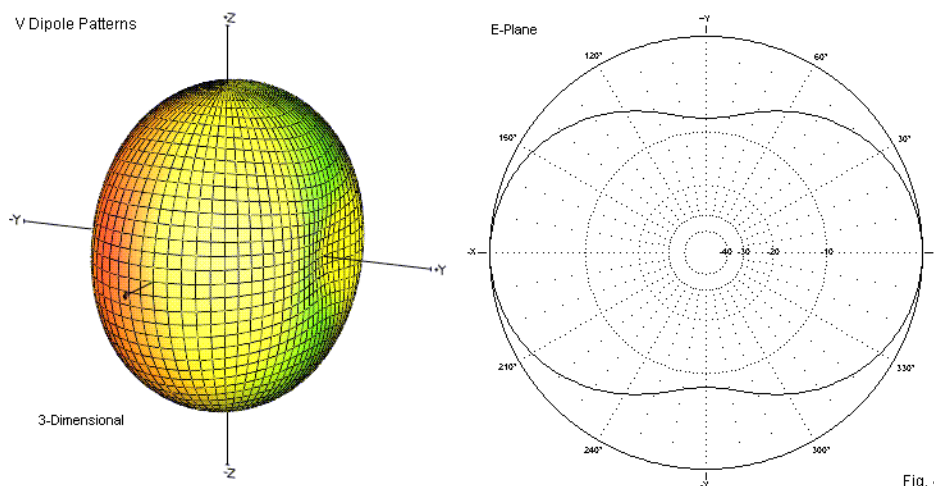


Fig. 4

The models used for the V dipole extend their legs in the $-Z$ direction (downward, in earth terms). Hence, they radiate side-to-side as well as broadside. Both the 3-dimensional and E-plane patterns in **Fig. 4** show the reduced depth of the side nulls. Since the patterns are normalized to the maximum gain of the antenna, we must consult the data tables to find the loss in maximum gain relative to a linear dipole that makes up the energy that fills in the side nulls.

Folded Dipoles

Both NEC-2 and NEC-4 handled the standard folded dipole well. The standard folded dipole employs driven and undriven long element sections that use wires having the same wire diameter. However, if we attempt to transform the feedpoint impedance by ratios other than 4:1, NEC models begin to fail. The degree of failure depended on the ratio of the two wire diameters, because NEC becomes error prone with angular junctions of wires with dissimilar diameters.

Modeling folded dipoles (and related structures, such as T matches and gamma matches) is an arena in which MININEC is superior to NEC. MININEC generally lacks any tendency toward error when we change the element diameters either along a linear section or at corners. To set up a MININEC folded dipole, we use an even number of segments in the long element sections, since on one of those sections, we shall center a source. **Fig. 5** shows the general layout, along with the impedance transformation equation for reference.

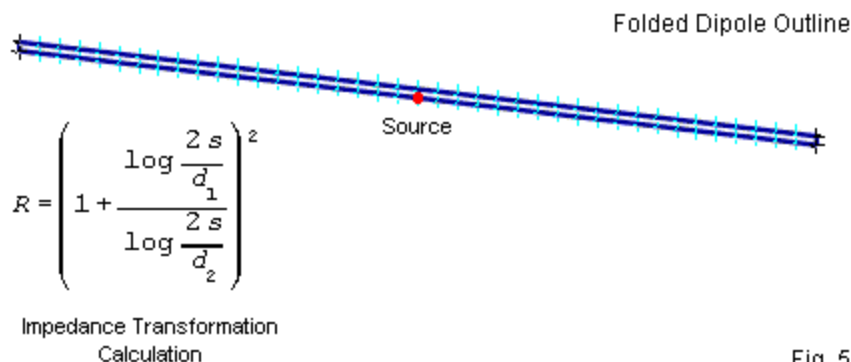


Fig. 5

In the standard or 4:1-ratio folded dipole, all 4 wires will use 1" diameter lossless material, and the wires will be 2" apart. The alternative folded dipole uses 0.1" diameter elements for all wires except the 1" wire with the source segment. The MININEC long wires will use 40 segments, with 1-segment end wires. As we calculated in the last episode, the folded dipole should show a source impedance close to 132.5 Ohms. Let's run the MININEC models in both AM and MMANA and compare the results with those obtained from NEC-2 and NEC-4.

Comparison of Folded-Dipole Models in NEC-2, NEC-4, and MININEC: Equal and Unequal Diameter Elements.

All models use 1" diameter lossless driven elements in free space.

Second elements are 1" or 0.1" diameter lossless wires.

Diameters	Core	Wire Length	Gain	Source Impedance	AGT	AGT-dB	Corrected
Driv/Other	Inches	dBi	R +/- j X Ohms				Gain dBi
1"/1"	NEC-2	+/-97.45	2.13	281.6 - j0.54	1.000	0.00	2.13
	NEC-4	+/-97.45	2.13	281.5 - j0.96	1.000	0.00	2.13
	AM	+/-97.70	2.13	281.9 + j0.35	1.000	0.00	2.13
	MMANA	+/-97.70	2.11	278.6 + j37.92			
1"/0.1"	NEC-2	+/-99.2	4.34	230.2 - j10.59	1.662	2.21	2.13
	NEC-4	+/-99.2	2.96	164.5 + j0.60	1.209	0.82	2.14
	AM	+/-99.5	2.17	137.5 + j2.96	1.008	0.04	2.13
	MMANA	+/-99.5	2.17	133.3 + j4.89			
Calculated Impedance			132.5 (if a linear dipole = 70 Ohms)				

Note: Wire Length is the total half-element length from the center to the tip.

The data are very interesting and in more ways than establishing that both versions of MININEC are superior to NEC in handling folded dipoles with unequal elements. Note that when we use unequal element sizes (1" and 0.1" or 25.4 mm and 2.54 mm), the two versions of MININEC produce results that are very similar to each other, differing by no more than the linear dipoles differed. In contrast, the folded dipole with equal-diameter elements shows resonance in AM but has a considerable reactive component in MMANA. One possible source of the reactive component is the fact that uncorrected MININEC has a sensitivity to very closely spaced wires. With a pair of 1" diameter elements, the surfaces of the wires are 1" apart. When we use the unequal elements, the separation increases to 1.55".

In any model, it is always good practice to align to the degree feasible the segment junctions in parallel wires, especially when they are closely spaced. In NEC, we saw significant differences in the reported results when we radically misaligned the segments, using combinations of 31 segments in one wire and 61 segments in the other for the standard equal-diameter folded dipole. MININEC shows considerably less sensitivity to misaligned segments than either NEC-2 or NEC-4. To demonstrate the lesser sensitivity, I assigned 30 segments to one wire and 60 to the other for both AM and MMANA models. The following table shows the results, along with the NEC data for reference.

Comparison of Folded-Dipole Models in NEC-2 and NEC-4: Careless vs.
Careful Segmentation

All models use 1" diameter lossless elements in free space.

Segments Driv/Other	Core	Wire Length Inches	Gain dBi	Source Impedance R +/- j X Ohms	AGT	AGT-dB	Corrected Gain dBi
61/31	NEC-2	+/-97.45	1.88	342.5 + j2.31	0.946	-0.24	2.12
31/61		+/-97.45	1.84	263.6 + j2.23	0.937	-0.28	2.13
41/41		+/-97.45	2.13	281.6 - j0.54	1.000	0.00	2.13
61/31	NEC-4	+/-97.45	1.71	329.1 - j2.33	0.909	-0.41	2.12
31/61		+/-97.45	2.00	273.1 + j1.26	0.971	-0.13	2.12
41/41		+/-97.45	2.13	281.5 - j0.96	1.000	0.00	2.13
60/30	AM	+/-97.70	2.13	285.8 - j1.77	1.002	0.01	2.12
30/60		+/-97.70	2.12	278.0 + j1.17	0.999	-0.01	2.13
40/40		+/-97.70	2.13	281.9 + j0.35	1.000	0.00	2.13
60/30	MMANA	+/-97.70	2.12	282.3 + j38.95			
30/60		+/-97.70	2.10	274.5 + j39.19			
40/40		+/-97.70	2.11	278.6 + j37.92			

Note: Wire Length is the total half-element length from the center to the tip.

The AM model shows only very small differences among its reported results, with gain deviations of no more than 0.01 dB relative to the well-aligned case.

Although AGT correctives are not available for MMANA, its range of values are nearly as tightly clustered as the AM values. Since one example cannot certify the relative lack of sensitivity for all model geometries, good segment alignment remains good modeling practice, whatever core you may be using.

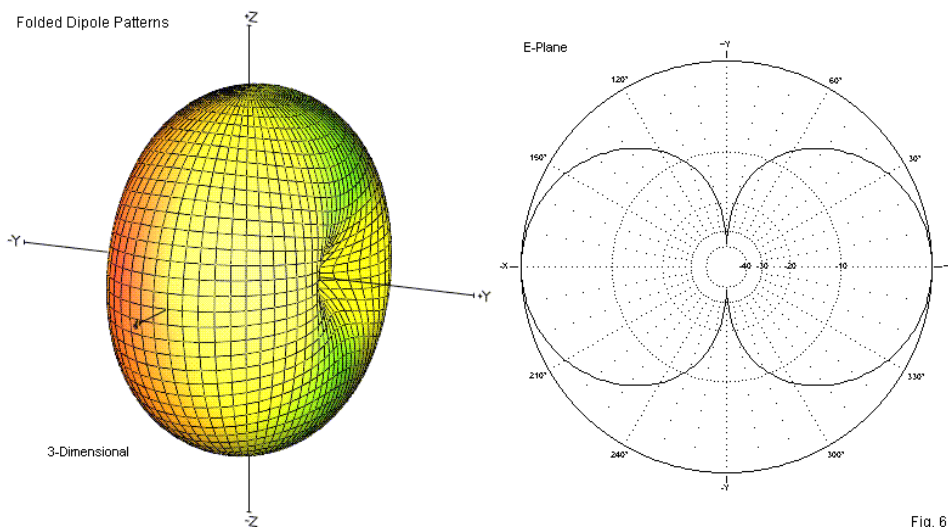


Fig. 6

Fig. 6 shows 3-dimensional and E-plane patterns in free space for the equal-diameter folded dipole, as modeled in AM. The MMANA E-plane pattern would be identical, as would be the patterns for the unequal-diameter versions of the antenna. Note that the side nulls are almost but not quite as deep as the side nulls for the simple linear dipole. Do not forget that even the short end-connection wires do radiate, even if only a little.

Conclusion to Part 2

We have caught up to the NEC dipoles with our MININEC models. By framing the MININEC models in an episode of their own, we have been able to see a bit of the difference between corrected and uncorrected versions of MININEC, although in the HF region, the differences are small. Some of the differences become very significant at VHF and UHF frequencies, such as the frequency offset. As well, we have been able to see some modeling applications for which MININEC is superior to NEC, especially for geometries similar to the unequal-diameter folded dipole. Those applications are more numerous than one might initially believe. For that reason, I keep versions of both NEC and MININEC at hand, using the most accurate tool for any given job. Of course, we have also seen that for a number of cases, it makes no differences whether we use NEC or MININEC.

Still, we have fallen behind in our journey through the variety of dipoles. We have yet to work with inverted Us and hatted dipoles. Farther down the trail, the zigzag and fold-back versions await us. And at the end of this trip--but certainly not the end of all dipole varieties--stands the fan dipole for multi-band use. From this point forward, we shall be able to deal with our dipole types using NEC and MININEC together. From the standpoint of identifying modeling pitfalls and work-arounds, the sojourn should prove interesting.

110. Dipoles: Variety and Modeling Hazards Tapered-Diameter, Bent, and Hatted Dipoles

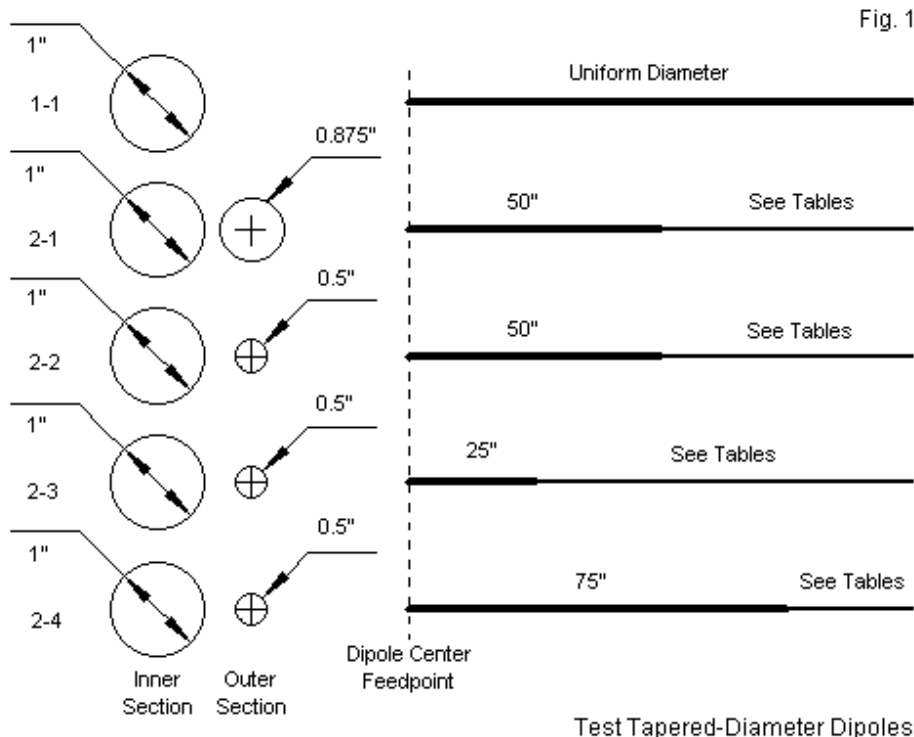
We have so far examined dipoles that are straight and uniform in diameter, as well as those that are center-bent to form a V. We also tackled folded dipoles. Our goal is not to give a lesson in dipoles, but to demonstrate modeling techniques and limitations that may even affect such a simple antenna. Throughout the first 2 parts of the sequence of episodes, we have treated dipoles as center-fed near-resonant half-wavelength antennas, setting aside the textbook "short" dipole concept as outside our needs.

We devoted an entire episode to modeling dipoles in NEC and a second session covered modeling those same dipoles in MININEC. As we proceed through the remaining collection of dipoles, we shall handle both programs together, since we no longer need to provide any introductory orientation to them. However, we shall continue to group the programs, covering NEC-4 and NEC-2 together and likewise collecting the Antenna Model (AM) and MMANA versions of MININEC 3.13--as very refined and relatively raw forms of the basic core.

Tapered-Diameter Dipoles

When we looked at linear or standard dipoles, we gave them a uniform diameter throughout the element. However, in the HF region, we commonly encounter tubular dipoles (and similar elements in more complex arrays) that use a tapered-diameter (or a stepped-diameter) element. In general, a tapered-diameter element is one that--counting from the center or feedpoint--uses gradually smaller diameter portions of the element. We shall presume that the taper is symmetrical relative to the element center.

Fig. 1 shows the general set-up for a series of test models that we shall examine. For simplicity, we shall use only 2 different diameters in creating the dipoles, a fatter inner section, where inner means closer to the feedpoint, and a thinner outer section that extends to the element tip. Hence, the outer or larger diameter applies to the inner element section, and the inner or smaller diameter applies to the outer element section. For 2 of our tests, the inner 1" section of the dipole will be +/-50" (total 100"), while the last 2 tests will change that length, using +/-25" (total 50") in one case and +/-75" (total 150") in the other. In all cases, I shall vary the segment assignment so that the total number of segments in the NEC models is 41 and in the MININEC models is 40.



For reference, the original uniform-diameter 1" dipoles are $\pm 99.7"$ (total 199.4") at the 28.0 MHz test frequency, using lossless wires in free space. One feature that we cannot fail to notice about the tapered-diameter elements is that every one of them is longer. The increased length is a function of the fact that the effective diameter of the total element is well under 1", requiring a longer element. We shall examine what counts as the effective diameter shortly. However, let's first tell a short story about NEC.

NEC-2 used current algorithms that created an inherent problem using tapered-diameter elements. In brief, NEC-2 could not yield reliable results for elements using tapered-diameter linear elements. NEC-4 revised the current algorithms to overcome the limitation. In fact, NEC-4 considerably improves the performance of the system for tapered-diameter elements, but it is not perfect. How imperfect

it might be depends on several different factors. NEC-4 tends to be more perfect when the step between diameters is relatively small. Hence, we have the first case that uses a diameter step from 1.0" down to 0.875". If we use a larger step, say, from 1" to 0.5" as in the second case, then NEC-4 is less perfect. The perfection of NEC-4 results also rests on where along the dipole that the step occurs. In general, the higher the current in the region where the step occurs, the more imperfect the result will be. Hence, we have cases 3 and 4 that use the 1"-0.5" combination, but with different lengths of 1" tubing.

NEC-2 shows the same general pattern as NEC-4, but more extremely so. The first two sections of the following table create resonant directly modeled NEC-4 dipoles and then re-runs each of them with NEC-2. For the NEC-2 and NEC-4 directly modeled dipoles, the performance of the uniform-diameter dipole appears as a point of reference. In all cases, NEC-2 shows significant deviation from NEC-4. The higher the ratio of the two diameters, the greater the deviation. As well, the shorter the inner-fatter dipole section, the greater the deviation. Note that the NEC-2 AGT value is always higher than the NEC-4 value (except for the uniform-diameter reference dipole). In NEC-4, case 3 (with the short inner dipole section), we find an AGT value that deviates more than a little from the ideal. However, the NEC-2 value for the same case is much higher yet. Our justified conclusion is that raw NEC-2 is unreliable with tapered-diameter linear elements. While NEC-4 is superior, it has limitations.

NEC Performance with Various Tapered-Diameter Elements

Model	Method	Out/In Dia	In/Out Length	Segment Order	Gain dBi	Source Imped R +/- jX Ohms	AGT	AGTdB
NEC-4								
1-1	Direct	1	99.7	41	2.14	71.94 + j0.12	1.000	0.00
2-1		1/0.875	50/50.6	10-21-10	2.15	72.37 + j0.06	1.002	0.01
2-2		1/0.5	50/54.5	10-21-10	2.20	74.10 - j0.12	1.010	0.04
2-3		1/0.5	25/77.9	15-11-15	2.26	73.52 - j0.04	1.023	0.10
2-4		1/0.5	75/28.3	5-31-5	2.16	72.85 - j0.01	1.003	0.01
NEC-2								
1-1	Direct	1	99.7	41	2.14	71.95 + j0.17	1.000	0.00
2-1		1/0.875	50/50.6	10-21-10	2.17	72.80 + j4.30	1.007	0.03
2-2		1/0.5	50/54.5	10-21-10	2.30	76.10 + j19.43	1.033	0.14
2-3		1/0.5	25/77.9	15-11-15	2.47	71.49 + j13.12	1.074	0.31
2-4		1/0.5	75/28.3	5-31-5	2.20	76.15 + j15.71	1.009	0.04
Leeson corrections (Apply to NEC-2 and to NEC-4 Models)								
2-1	Leeson	1/0.875	50/50.6	10-21-10	2.13	71.72 - j0.68	1.000	0.00
2-2	Subs	1/0.5	50/54.5	10-21-10	2.13	70.28 - j6.40	1.000	0.00
2-3	Elem	1/0.5	25/77.9	15-11-15	2.13	70.58 - j5.51	1.000	0.00

2-4		1/0.5	75/28.3	5-31-5	2.13	71.56 - j1.27	1.000	0.00
Leeson Revised for Resonance								
2-1	Leeson	1/0.875	50/50.6	10-21-10	2.13	71.72 - j0.68	1.000	0.00
2-2	Subs	1/0.5	50/54.8	10-21-10	2.14	71.93 + j0.17	1.000	0.00
2-3	Elem	1/0.5	25/78.45	15-11-15	2.14	71.90 + j0.02	1.000	0.00
2-4		1/0.5	75/28.45	5-31-5	2.14	71.87 + j0.11	1.000	0.00

Notes: Outer and inner diameters in inches. Inner and outer lengths are for each half of the element, with dimensions in inches. Segmentation order is for the full elements for the left outer section, the middle section, and the right outer section. All element wires are lossless, and the environment is free space.

The standard method of providing more accurate results for linear tapered-diameter elements in both NEC-2 and NEC-4 is to use substitute uniform-diameter elements having the same impedance at the test frequency as the tapered-diameter elements. The equations used were developed by David Leeson, based on original work by Schelkunoff. (See Chapter 8 of *Physical Design of Yagi Antennas*.) When using the Leeson corrections, the program does not calculate with the originally modeled elements. Instead, it uses substitute elements having the calculated equivalent uniform diameter and length. **Fig. 2** shows case 3 in final form. The equivalent uniform diameter is about 0.56", just a little fatter than the smaller of the two materials used in the dipole with the short inner section. Note also that the tip length limit is shorter than the tapered element in the upper section. The modeler does not vary the uniform-diameter substitute element. Instead, he changes the dimensions of the physical tapered-diameter element parts to achieve the desired goal--in this case, resonance.

Wires

Wire

Create

Edit

Other

NEC Corrections for Tapered-Diameter Wires

Fig. 2

☐ Coord Entry Mode
 ☐ Preserve Connections

Physical Wires

☐ Show Wire Insulation

Wires											
	No.	End 1				End 2				Diameter (in)	Segs
		X (in)	Y (in)	Z (in)	Conn	X (in)	Y (in)	Z (in)	Conn		
▶	1	0	-103.45	0		0	-25	0	W2E1	0.5	20
	2	0	-25	0	W1E2	0	25	0	W3E1	1	11
	3	0	25	0	W2E2	0	103.45	0		0.5	20
*											

Stepped Diameter Correction

Edit

Other

Equivalent Uniform-Diameter Wires

Model 2-3

Wires											
	No.	End 1				End 2				Diameter (in)	Segs
		X (in)	Y (in)	Z (in)	Conn	X (in)	Y (in)	Z (in)	Conn		
▶	1	0	-100.406	0		0	-24.2644	0	W2E1	0.563412	20
	2	0	-24.2644	0	W1E2	0	24.2644	0	W3E1	0.563412	11
	3	0	24.2644	0	W2E2	0	100.406	0		0.563412	20

The tapered- or stepped-diameter element corrections do have restrictions. There must be at least two wires in the group. At least two of the wires must have different diameters. All wires in the group must be collinear (in a straight line). All wires must be connected to each other. Both ends of the group must be open, or one end open and one connected to ground (a case that we shall not examine in these dipole notes). The group must be nearly resonant (within about 15% of half-wave resonance if both ends are open). Only one source is permitted in the group, and it must be at the center if the ends are open. If the ends are open and the center of the group is a wire or segment junction, the source must be a split source. The rules for loads are the same as for sources, except that two equal loads must be used wherever a split source would be used. A single transmission line can be connected to the group. If the ends of the group are open, the center of the group must be a segment center--not a segment or wire junction--and the transmission line can be connected only to this segment.

The third section of the table shows the corrections applied to the physical dimensions generated in the original NEC-4 models. With only a small diameter step, the model called 2-1 shows very similar results in NEC-4 with or without the corrections. Likewise, the model called 2-4--which uses a long inner section and a shorter tip--also displays similar impedance values for the uncorrected NEC-4 and the corrected versions. (Note that the table shows corrections using NEC-4

only. Corrected NEC-2 values are too close to the corrected NEC-4 values to require repetition. In fact, the 2 cores yield corrected values that are about as close together as the NEC-2 and NEC-4 values for model 1-1, the uniform-diameter dipole.)

The difficult cases are the second and third, both of which use a large diameter change between the two dipole sections, along with a shorter inner section. Although the gain report is not a problem, the source impedance is off the mark relative to establishing resonant lengths. Therefore, the final part of the table revises the physical tip length to yield corrected elements that are resonant. Comparing the outer-section lengths between the third and fourth parts of the table will give you an idea of what sort of adjustment these cases require--about 3/4" per dipole leg or about 1.5" overall.

One fair question that we might pose about the corrections is the method used to substantiate the essential correctness and adequacy of the equations. Part of the confirmation process involved comparing the corrected results with MININEC dipoles that we may directly model (without any correction) using the same stepped-diameter structure. Since MININEC uses current pulses located at segment junctions, it does not undergo the same errors with stepped-diameter elements experienced by NEC.

As a demonstration of MININEC's ability to handle tapered-diameter elements without need for correction. I took the final corrected structure lengths and created models in AM. The top portion of the following table shows the results. Only case 2-4 shows a significant deviation between the corrected NEC models and the MININEC model. However, for each case in which the source reactance report exceed $\pm j1$ Ohm, I revised the AM model to bring it within our working definition of resonance. In one case (model 2-3), I needed no revision. In two other cases, the tip-length revision was 0.2" or less.

MININEC Performance with Various Tapered-Diameter Elements

Model	Out/In Diameters	In/Out Length	Segment Order	Gain dBi	Source Impedance R +/- jX Ohms	AGT	AGTdB
AM							
1-1	1	99.7	40	2.13	71.79 - j0.54	1.000	0.00
2-1	1/0.875	50/50.6	10-20-10	2.13	72.12 - j2.14	1.000	0.00
2-1A	1/0.875	50/50.8	10-20-10	2.13	72.62 - j0.33	1.000	0.00
2-2	1/0.5	50/54.8	10-20-10	2.16	75.30 - j1.38	1.000	0.00
2-2A	1/0.5	50/54.9	10-20-10	2.16	75.56 - j0.51	1.000	0.00
2-3	1/0.5	25/78.45	15-10-15	2.15	75.97 - j0.47	1.000	0.00
2-4	1/0.5	75/28.45	5-30-5	2.14	72.09 - j4.33	1.000	0.00
2-4A	1/0.5	75/29.0	5-30-5	2.17	73.35 - j0.06	1.000	0.00
MMANA							
1-1	1	99.7	40	2.12	70.47 - j5.48		
2-1A	1/0.875	50/50.8	10-20-10	2.13	71.29 - j5.27		
2-2A	1/0.5	50/54.9	10-20-10	2.15	74.20 - j5.59		
2-3	1/0.5	25/78.45	15-10-15	2.15	74.76 - j5.22		
2-4A	1/0.5	75/29.0	5-30-5	2.14	71.97 - j5.20		

Notes: Outer and inner diameters in inches. Inner and outer lengths are for each half of the element, with dimensions in inches. Segmentation order is for the full elements for the left outer section, the middle section, and the right outer section. All element wires are lossless, and the environment is free space. All models are direct.

I re-created the revised MININEC models using MMANA. The lower part of the table shows the MMANA results. Note that there is a consistent -j5-Ohm reactance on all of the sources, the same value that applies to the MMANA version of the uniform-diameter dipole. In the last episode, we attributed this reactance--relative to resonance in the AM models--to an uncorrected frequency offset in raw MININEC 3.13. In all other respects, the results are consistent with those of AM.

Inverted-U Dipoles

The NEC element taper corrections apply only to straight or collinear elements. However, not all dipoles are straight. In fact, one very old design--with many contemporary applications--is the inverted U, a dipole using a straight or horizontal section with the outer parts of the element pointed vertically downward (or, in free space, in the -Z direction). Although the bent section may have the same diameter as the horizontal section, when we use a tubular inner or horizontal element, the verticals often use either smaller tubing or wire. Therefore, to see the effects of changing vertical leg sizes, I set up the variations shown in **Fig. 3**.

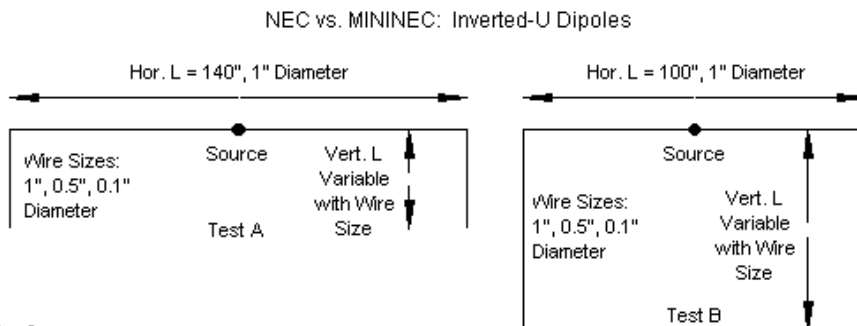


Fig. 3

The first option uses a horizontal length of $\pm 70"$ (total 140"), with the vertical legs long enough to achieve resonance. The second option shortens the horizontal dimension to $\pm 50"$ (total 100"), again with vertical legs long enough to resonate the dipole. For each option, I used 1", 0.5", and 0.1" diameter vertical end wires.

In the first table, we find the results for NEC-4 and NEC-2. Since the element corrections do not work with angular junctions in the elements, we only find the results for direct modeling. I resonated each models in NEC-4 and then re-ran it in NEC-2 to see the amount or variance created by the older core's lesser ability to handle junctions of wire with different diameters.

NEC Performance with Various Inverted-U Dipoles

Core	Horizontal Length	Vertical Diameter	Vertical Length/End	Gain dBi	Source Impedance R +/- jX Ohms	AGT	AGTdB
NEC-4	± 70	1"	34.0	1.96	58.19 - j0.52	1.002	0.01
NEC-2				1.96	58.35 + j0.43	1.002	0.01
NEC-4	± 70	0.5"	37.8	1.95	58.28 - j0.30	1.002	0.01
NEC-2				1.94	60.91 + j16.55	1.001	0.01
NEC-4	± 70	0.1"	45.4	1.91	58.53 + j0.43	1.002	0.01
NEC-2				1.90	65.69 + j45.32	1.002	0.01
NEC-4	± 50	1"	55.3	1.60	38.97 + j0.19	1.004	0.02
NEC-2				1.60	39.06 + j1.16	1.004	0.02
NEC-4	± 50	0.5"	59.1	1.57	39.11 - j0.62	1.005	0.02
NEC-2				1.56	40.48 + j17.46	1.006	0.03
NEC-4	± 50	0.1"	66.5	1.49	39.64 + j0.11	1.007	0.03
NEC-2				1.49	43.32 + j48.20	1.015	0.06

Notes: All horizontal sections use 1" diameter wire. Vertical legs use 1", 0.5", or 0.1" wire. All element wires are lossless, and the environment is free space. All dimensions in inches.

In both the long and short horizontal options, NEC-2 handles the 1" vertical end wires quite well, and the variance from NEC-4 values is minimal. The NEC-4 and NEC-2 AGT values are the same, and the source impedances vary by only about $j1$ -Ohm reactance. However, as we reduce the diameter of the vertical end wires and create a higher ratio between the diameters of the horizontal and vertical wires, the variance increases dramatically. The variance level is almost independent of the horizontal length.

When we turn to MININEC, we once more find that we may use the program directly without concern for the difference in the element diameter. However, this statement presumes that we are using a version of MININEC with the angular problem and the frequency offset corrected. In the present case, the use of 40 segments in the half-wavelength dipole overall is sufficient to overcome the corner problem by minimizing the corner shortening effect.

The following table presents the MININEC results, starting with models in AM that use the NEC-4 resonant dimensions. In every case, we find that MININEC produces slightly different results, even when both the horizontal and the vertical element sections have the same diameter. Therefore, the table includes revised AM models to bring the MININEC models to resonance. As we decrease the diameter of the vertical wires, the NEC-4 dimensions work less and less well. In addition, shortening the horizontal section of the inverted U produces an increase in the amount by which the AM MININEC results deviate from the NEC-4 results. Since even NEC-4 has difficulty with wire junctions with different diameter wires, the MININEC results are the more reliable.

Before we complete our examination of the data in the new table, compare the AGT values for the MININEC models in AM with the values for the NEC-4 models. The AGT values for the NEC models appear to be very good or better for all models. However, the MININEC results suggest otherwise. The Average Gain Test is a necessary but not a sufficient condition of model adequacy. In this case, the AGT fails to reveal the inadequacies of the NEC-4 models when the horizontal and the vertical wires have very different diameters.

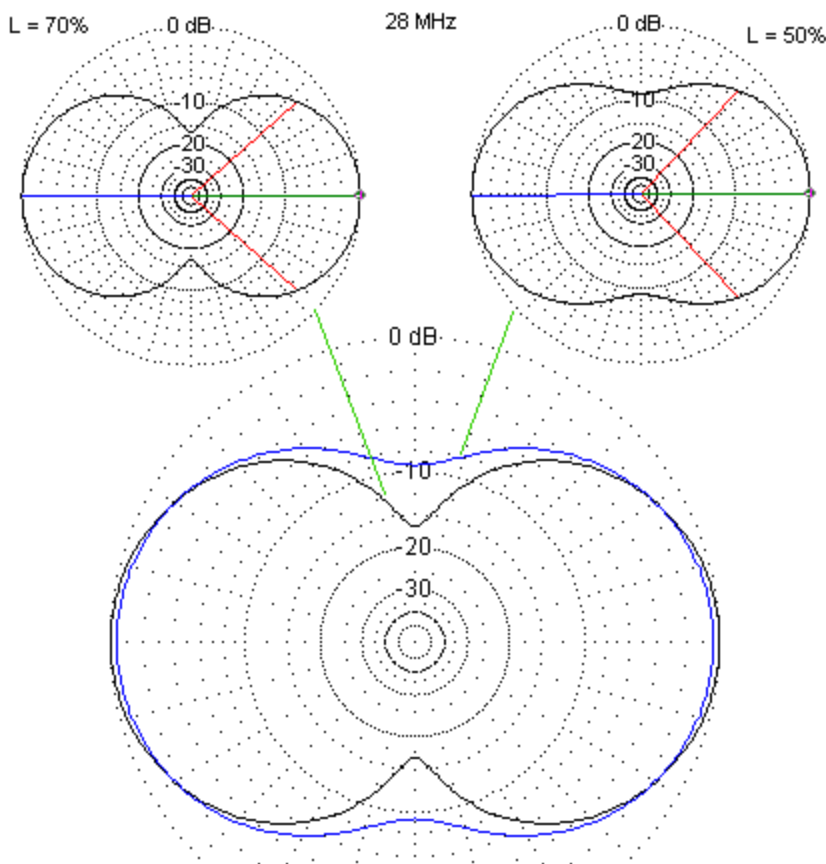
MININEC Performance with Various Inverted-U Dipoles

Core	Horizontal Length	Vertical Diameter	Vertical Length/End	Gain dBi	Source Impedance R +/- jX Ohms	AGT
AM	+/-70	1"	34.0	1.95	58.42 - j1.78	0.9989
AM-Revised			34.2	1.95	58.67 - j0.23	0.9989
MMANA			34.2	1.95	57.59 - j5.19	
AM	+/-70	0.5"	37.8	1.93	57.16 - j9.70	0.9989
AM-Revised			39.1	1.93	58.72 - j0.20	0.9989
MMANA			39.1	1.93	57.61 - j5.41	
AM	+/-70	0.1"	45.4	1.91	55.18 - j18.90	0.9989
AM-Revised			48.1	1.89	58.87 - j0.50	0.9989
MMANA			48.1	1.89	57.56 - j6.93	
AM	+/-50	1"	55.3	1.58	39.10 - j3.04	0.9989
AM-Revised			55.6	1.58	39.32 - j0.64	0.9989
MMANA			55.6	1.58	38.64 - j5.46	
AM	+/-50	0.5"	59.1	1.56	38.42 - j13.82	0.9989
AM-Revised			60.8	1.53	39.74 + j0.10	0.9989
MMANA			60.8	1.53	39.04 - j4.92	
AM	+/-50	0.1"	66.5	1.48	37.90 - j26.17	0.9989
AM-Revised			69.5	1.41	40.51 + j0.53	0.9989
MMANA			69.5	1.42	39.70 - j5.71	

Notes: All horizontal sections use 1" diameter wire. Vertical legs use 1", 0.5", or 0.1" wire. All element wires are lossless, and the environment is free space. All dimensions in inches.

The MMANA models all use the same dimensions as the revised AM models. As a result, they all show the same trend in the capacitive reactance at the feedpoint. As well, within about +/-j1 Ohms, the values are consistent with those for the linear dipoles using both uniform and tapered-diameter elements.

The gain differences between the inverted Us with longer and shorter horizontal sections seem numerically noticeable. However, operationally, the maximum gain difference is not as great as it might seem. **Fig. 4** compares the patterns for the two types of inverted Us in a free-space environment. The overlaid patterns show only a very small difference in maximum gain.



Comparative Inverted-U Free-Space E-Plane Patterns
Horizontal Length: 70% and 50% of a Linear Dipole

Fig. 4

Where the two types of inverted Us differ most noticeably from an operational perspective is in the depth of the side nulls. As the horizontal section grows shorter and the vertical legs become longer, we obtain more radiation off the dipole "ends," that is, in line with the horizontal wire. With a horizontal section that is about 70% of the overall dipole length, the side nulls are almost 20 dB weaker than the maximum broadside lobes. In contrast, as we shorten the horizontal section to about 50% of the total length and extend the vertical legs to compensate, the side nulls are down by under 10 dB (or about 1.5 S-units)

relative to maximum gain. You may wish to compare these patterns to the patterns for the V dipole with its legs forming a 90-degree angle, that is, with each leg dropped 45 degrees from the presumed horizontal line of a linear dipole.

Hatted Dipoles

One type of shortened dipole tends to show less variance than the inverted-U: the hatted dipole. The inverted U uses a simple extension of the main wire, but in a different direction. All parts of the wire contribute to the antenna's radiation pattern. However, the hatted dipole uses a shortened main element along with symmetrical structures at each end to bring the entire structure to resonance.

Fig. 5 shows the outline of one type of hatted dipole. In this case, the end structures consist of 4 equal-length and equal-diameter spokes. We might also have used shorter spokes with a perimeter connecting the tips. We may increase the number of spokes for either assembly. Each increase in the number of spokes results in a decrease in spoke length (assuming that we make no changes in the horizontal element). Ultimately, we might use a circular solid surface as the end piece.

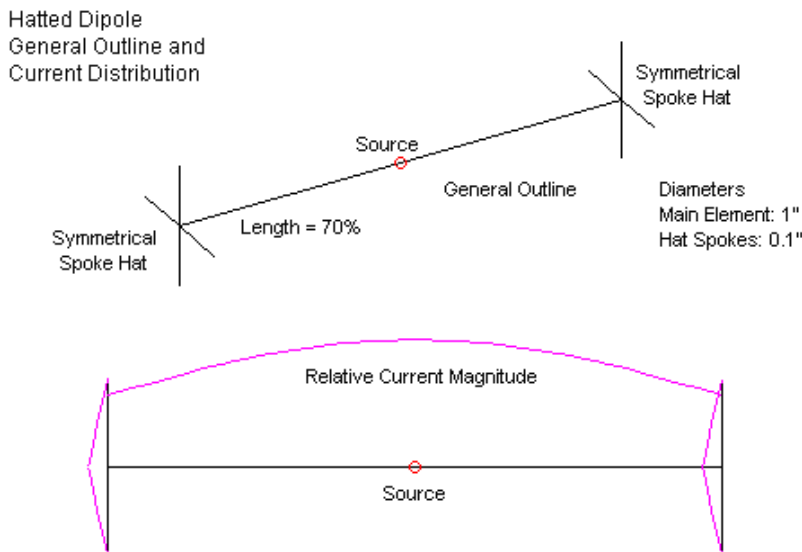


Fig. 5

One key to the hatted dipole is the fact that each spoke provides a current distribution path for the antenna. The current in each spoke at the junction with the horizontal element is $I \cdot 1/n$, where n is the number of spoke and I is the current magnitude in the main element at the junction. The lower portion of **Fig. 5** displays the current division graphically, but shows only 2 of the 4 spokes at each end of the dipole. The other key to the hat is its symmetrical structure. Since each spoke has the same current magnitude as every other spoke, the fields created tend to cancel out. Hence, the hatted dipole exhibits virtually no far-field radiation from the hat. The result is that, among all methods of loading dipoles in order to achieve resonance with a shorter length, the hatted dipole exhibits the highest gain and the highest resonant source resistance for any given horizontal section length.

Because the hat radiation is self-canceling, hatted dipoles tend to show considerably less variation between NEC-2 and NEC-4 models, and between NEC and MININEC models, than the inverted U and similar shortened dipoles with asymmetrical extensions of the horizontal element. To test this tendency, I created NEC and MININEC models of the hatted dipole with a horizontal length of $\pm 70''$ (total $140''$) for the $1''$ diameter material. The 4 spokes at each end use $0.1''$ diameter wires. Due to the shorter length of each spoke, they use 4 segments each so that their segment lengths are about the same as their segment lengths in the horizontal portion of the element. The following table summarizes the results of the tests.

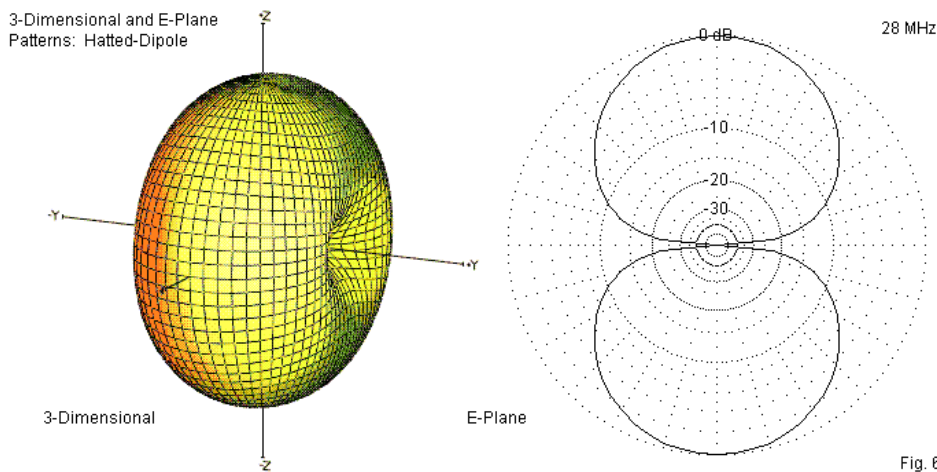
NEC and MININEC Performance with Hatted Dipoles					
Core	Spoke Length	Gain dBi	Source Impedance R +/- jX Ohms	AGT	AGTdB
NEC-4	18.8	2.02	58.17 - j0.12	1.001	0.00
NEC-2	18.8	2.02	59.59 + j8.81	1.000	0.00
AM	18.8	2.01	56.78 - j11.26	0.999	0.00
MMANA	18.8	2.01	55.72 - j16.33		
AM-Revised	19.6	2.01	58.48 - j0.37	0.9988	-0.01
MMANA-Revised	19.6	2.07	57.37 - j5.62		

Notes: All horizontal sections use $1''$ diameter wire and are $\pm 70''$. Hat spokes use $0.1''$ wire. Each end hat uses 4 spokes (with other designs possible). All element wires are lossless, and the environment is free space. All dimensions in inches.

The NEC-4 initial models called for 18.8" spokes to arrive at resonance. Note the nearly ideal values of AGT, despite the difference between the NEC-4 and NEC-2 source impedance values. The MININEC models showed some deviation from the NEC-4 models, so I created a revised resonant version of the AM MININEC model using 19.6" spokes. In both the original and the revised MININEC models, the MMANA version shows a $-j5$ -Ohm offset in source impedance from the AM models, a value that has been consistent for all of the models reviewed in this episode.

Perhaps the most notable aspect of the NEC-MININEC comparison is the reduction in the differences between NEC-4 and MININEC for the hatted dipole. With a 70% horizontal 1" element, the MININEC model of the inverted-U showed an 18-Ohm differential in reactance. The hatted dipole, using the same horizontal element and the same diameter (0.1") end wires, shows a difference of only 10 Ohms reactance. Since MININEC does not react adversely to junctions of wires with different diameters, we might then conclude that NEC is less sensitive to such changes when we create symmetrical structures at the main element ends.

I noted that the hatted dipole is the most successful among all shortened dipoles in retaining the characteristics of a full-size linear dipole. We can confirm part of that claim in the reported gain values for the hatted dipole. Despite shortening the main element by about 30%, we lose only about 0.13-dB of gain. **Fig. 6** tells something of the rest of the story by showing 3-dimensional and E-plane patterns.



Unlike the V dipole and the inverted U, the hatted dipole pattern shows deep side nulls that are very comparable to the side nulls of a full-size linear dipole in the same free-space environment. The depth of these side nulls is also confirmation that the hat structures on the ends of the dipole have virtually no far-field radiation. (If they had even small but noticeable radiation, the side nulls would have been much shallower.) Despite the improved performance of the hatted dipole, we rarely find them in use. Offsetting the improvements is the fact that placing hats at the outer ends of a dipole creates weight and wind resistance at a position that we least want it to appear.

Conclusion

In our survey of tapered-diameter, bent, and hatted dipoles, well-corrected MININEC has proven to provide the most reliable results. In many cases, the differences between NEC and MININEC are too small to matter. Even some numerically noticeable differences wash out in the variables of construction methods that we do not model in detail. Modeling is rarely a substitute for field testing and adjustment. Instead, modeling simply puts us much closer to the final adjustment values.

MININEC's superiority with some forms of dipole structures is not a sufficient reason to throw out NEC and buy new software. At the start of this sequence of episodes, I noted a number of features that even well-corrected versions of

MININEC lack. As well, NEC has some performance advantages over MININEC in with some geometries. To explore these matters, we shall require one more leg on our journey. Next time, we shall explore zigzag, fold-back, and fan dipoles.

111. Dipoles: Variety and Modeling Hazards Zigzag, Fold-Back, and Fan Dipoles

We have been examining the behavior of NEC and MININEC calculations for various kinds of dipoles, where the dipole is a center-fed near-resonant 1/2-wavelength antenna. In this final episode of the sequence, we shall be paying close attention to angles. All of the antennas that we shall discuss will use 1" diameter lossless wire at all points, and the environment will once more be free space at 28 MHz. By holding down the number of variables, we can once more focus on how each antenna modeling package treats the antenna's geometry.

So far, we have looked at linear, V'd, and folded dipoles, as well as at dipoles with tapered-diameter, bent, and hatted elements. In our final collection, we find zigzag, fold-back, and fan dipoles. The last sample is not a simple dipole, but actually a combination of dipoles for separate frequencies that share the same feedpoint.

Zigzag Dipoles

Zigzag dipoles are most common in the lower HF region. Very often, antenna builders have too little space for a full-size dipole. One way to squeeze the antenna into the available space is to create as symmetrically as possible a zigzag shape. Our sample zigzag shape will depart from the norm a bit. Most zigzag dipoles have a relative constant height above ground and change direction in the X-Y plane. Our samples will zigzag vertically. As well, we conventionally measure a zigzag dipole by drawing a virtual line from one tip to the other through the feedpoint. In this exercise, we shall hold the central part of the element at a constant value of Z--comparable to a constant height above ground--and run the zigzag ends in the Z-axis.

In fact, we shall look at two designs of the zigzag dipole. One version, shown on the left in **Fig. 1**, uses a 90-degree angle at the zigzag points. The other version, on the right, bends the zigzag farther so that the end wires form a 45-degree angle with the inner section of the dipole. In both cases, the center section will occupy about 50% of the dipole length (if it had been a linear dipole, that is, +/- 50" (total 100"). The end sections will use whatever length we need to approach resonance at the source.

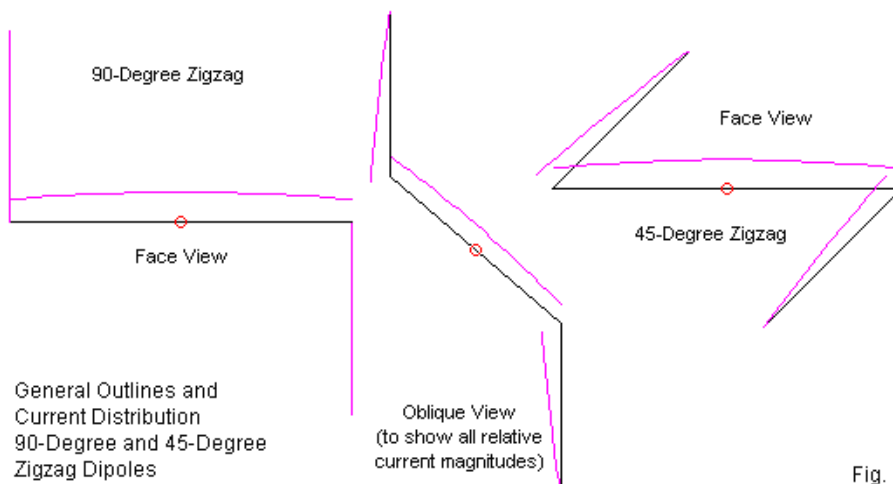


Fig. 1

As **Fig. 2** shows, both versions of the zigzag antenna qualify as dipoles by effecting a single transition between maximum and minimum current on each side of the centered source. As in past models, the center section of the model will use 21 segment in NEC and 20 segments in MININEC. The number of segments used in the end wires will depend on their length, but each segment will be approximately the same length as the segments in the center section.

In past exercises, I have started with a NEC-4 model and then tried to see by how much the NEC-2 results deviated from the reports of the NEC-4 model. I then transferred those dimensions to a MININEC model in AM. Often, I created a revised AM model at resonance in order to compare the results with the version of MININEC in MMANA. The latter versions has few, if any, corrections, while the AM version is highly corrected. In this exercise, we can abbreviate the procedure somewhat. I shall still begin with a NEC-4 model, if only because that starting point is consistent with past starting points. However, the amount of deviation among the cores will be too small to call for the creation of additional models. One contributing factor to this situation is the fact that for our angular models, all wires have the same diameter. The following table shows the results for both the 90-degree and the 45-degree zigzag dipoles.

Zigzag Dipoles in NEC and MININEC

All elements 1" diameter and lossless in free space.

90-Degree Zigzag: Central Length: +/- 50", End Length: 56"

Segmentation: NEC: 12-21-12, MININEC 12-20-12

Program	Gain dBi	Source Impedance R +/- jX Ohms	AGT	AGTdB	Corrected Gain dBi
NEC-4	2.03	45.27 + j0.86	1.005	0.02	2.01
NEC-2	2.03	45.33 + j1.19	1.004	0.02	2.01
AM	2.01	45.29 - j2.15	0.9986	-0.01	2.02
MMANA	2.00	44.50 - j6.71			

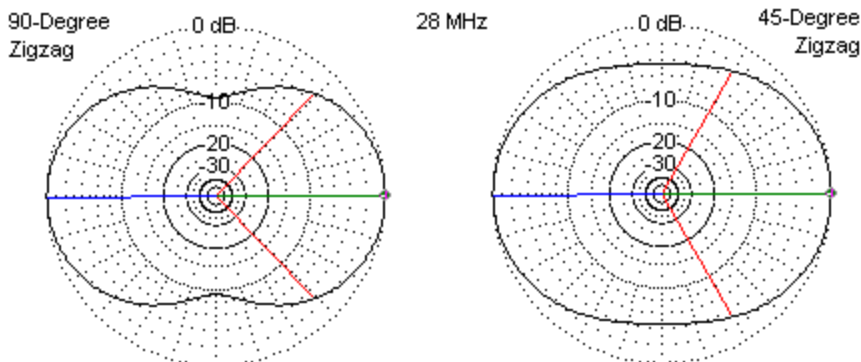
45-Degree Zigzag: Central Length: +/- 50", End Length: 67.85"

Segmentation: NEC: 14-21-14, MININEC 14-20-14

Program	Gain dBi	Source Impedance R +/- jX Ohms	AGT	AGTdB	Corrected Gain dBi
NEC-4	2.00	18.49 + j0.06	1.010	0.04	1.96
NEC-2	1.99	18.57 + j1.17	1.008	0.03	1.96
AM	1.94	18.79 - j2.27	0.9989	0.00	1.94
MMANA	1.94	18.50 - j6.30			

The 90-degree zigzag dipoles form a tight cluster of results. Only the MMANA source impedance shows more than a +/-j2-Ohm reactance shift, and it is about -j4.5 Ohms relative to the AM model--close to the amount that we have come to expect in dipoles from the uncorrected frequency offset at 28 MHz. The NEC cores actually show slightly less ideal values of AGT than the AM MININEC value. Although the MMANA core does not return an AGT value, we would expect it to approximate the AM value, since the frequency offset would not affect the AGT computation. As well, the use of a high number of segments is sufficient to minimize any further offset from corner foreshortening.

The 1" diameter elements, although well within NEC segment-length to diameter (or radius) limits, is fat enough to create a degree of inter-penetration at the junctions of the 45-degree zigzag dipole. Hence, both the NEC-4 and the NEC-2 departures from the ideal (1.000) are about double the departures with 90-degree corners. In contrast, the AM version of MININEC is highly corrected for raw-MININEC corner aberrations. Hence, it yields an AGT value very close to ideal. The MMANA data is interesting because the source reactance is only about j4 Ohms off the AM value. In earlier episodes we noted the possibility that the frequency offset and the corner error potential might work in opposite directions. The difference in source reactance between AM and MMANA was between j5 and j5.5 Ohms for a linear dipole. The 90-degree zigzag reduced that value to about j4.5 Ohms, and the more acute angle of the 45-degree zigzag reduces the difference still further. We have at least partial confirmation of our earlier hypothesis.



Free-Space E-Plane Patterns for the Sample Zigzag Dipoles

Fig. 2

Fig. 2 provides E-plane patterns for the two zigzag dipole models. Due to our method of model construction, the modeling cores define the E-plane as aligned with the center section of the antenna, even though the wire extensions take off in opposite directions. Note the relatively low side-null values for these two antennas. The 90-degree version has side nulls that are down about 10 dB, while the 45-degree model sidelobes are down only about 5 dB, giving the pattern an oval appearance.

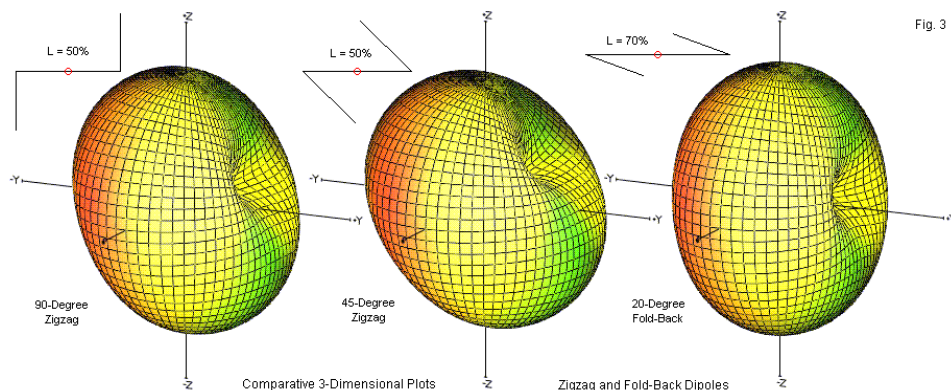


Fig. 3

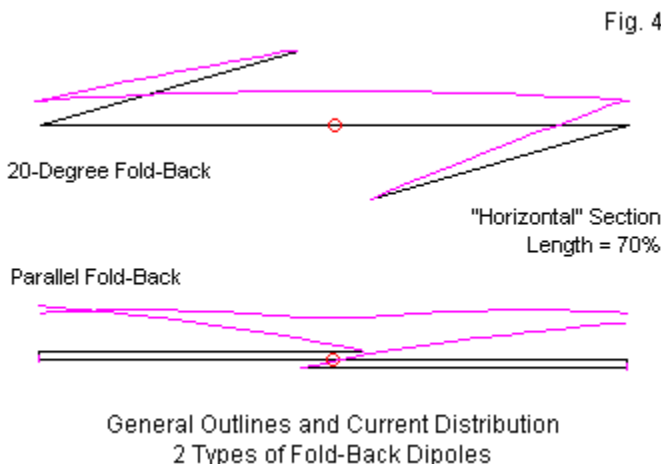
In fact, the radiation fields from the zigzag dipoles broadside to the plane of the wires are not linear. The terms E-plane and H-plane generally apply to antennas with linear polarization, such that the E-plane is aligned with the polarization, and the H-plane is at right angles to the polarization. Because so much of the element resides in the extensions that are angular to the center section, a considerable portion of the radiation is in a plane other than the plane of the center section. The net result is elliptical polarization with the major axis at an angle to the center section of the antenna. The left two 3-dimensional plots in **Fig. 3** show to what degree the zigzag dipole tilt the radiation field. The key indicator is the location of the true side nulls. Those nulls are both quite deep. The Y-axis line shows how angularly far from the true nulls that we find the E-plane patterns in **Fig. 2**.

Fold-Back Dipoles

The pattern on the far right in **Fig. 3** represents a dipole with a different name, although it may initially seem like just another zigzag dipole with a tighter angle between the center section and the tip wires. First, we likely noticed from the tabular data that as we increased the zigzag angle, the end wires grew longer. As well, the source impedance dropped from a highly usable value with the 90-degree version to an impractically low value with the 45-degree version. To avoid having end wires that are longer than the entire center section and to restore--at least partially--the resistive component of the source impedance, we normally use a longer center section when we apply relatively extreme angles to the end wires. The longer center section combines with the fact that the end wires are more in line with the center section to produce a field that is almost oriented like the field for a linear dipole. Note that the Y-axis line almost (but not quite) coincides with the deepest part of the side null in the right-most 3-dimensional patten in **Fig. 3**.

The resulting antenna uses a center section that is about 70% the length of a linear dipole, that is, about +/-70" (total 140"). Although the antenna is in the same family as the zigzag dipoles, it usually bears the name "fold-back" dipole. The name arises from the origins of the antenna, in which the builder could not fit elements into a given space and therefore folded them back at some convenient angle not too far from the orientation of the center section. The angle for the sample is 20 degrees, which requires end wires that are about 59.2" each for resonance with all-1" element construction. If you reverse the antenna image, you will find another name for the antenna--the lazy N. We occasionally find the antenna used vertically with an off-center feedpoint at one end of the center

section as a convenience. However, for consistency with our other models, I have left the antenna horizontal and center-fed. **Fig. 4** at the top shows the antenna outline, along with the relative current magnitude distribution along its total length.



As suggested by the lower portion of **Fig. 4**, we have multiple ways to effect element fold-back. I once developed a B antenna (which one may also view as a sigma from the reverse side). For this exercise, I have modeled another fold-back antenna, again using the $\pm 70^\circ$ center section of 1" lossless wire. The fold-backs are squared and parallel to the center wire section at a 2" distance. Note that the end sections for this antenna are longer than $1/2$ the center section. One effect is to require that we place the end wires on opposite sides of the central wire, although this position has been optional with the earlier examples. Perhaps more significantly, note the relative current magnitude curve in **Fig. 4**. The feedpoint or source position does not mark the current peak. Rather, we have twin peaks that are somewhat separated from the source position. You might rightly ask whether this antenna qualifies as a true dipole under the definition that we imposed at the beginning. However, the only way to bring this antenna to resonance is to allow the deviant current curve. As well, the curve emerges as a natural evolution of such curves as we start with a linear dipole and gradually shorten the end section and add fold-back end wires. There are no discontinuities in the evolution of the current distribution. Therefore, we shall keep the model and save any disputation over the application of names for another day.

With the longer center section, we expect to find that NEC-4 and NEC-2 will yield better AGT values than they did for the 45-degree zigzag dipole with its shorter center section. The following table confirms our expectation. In fact, the 2 NEC cores and the AM version of MININEC yield a very tight grouping of values across the span of data columns. Only the MMANA source data are out of line, with the MMANA MININEC core showing a large difference from the AM MININEC core. In terms of source reactance, we see a difference of $j14.8$ Ohms. To account for this larger deviation, we may note that the corner error in uncorrected MININEC increases as we move toward more acute angles. At 20 degrees, even the relatively high segmentation of the model is not sufficient to overcome this problem in MMANA.

Fold-Back Dipoles in NEC and MININEC

All elements 1" diameter and lossless in free space.

20-Degree Angled Fold-Back: Central Length: +/- 70", End Length: 59.2"

Segmentation: NEC: 13-31-13, MININEC 13-30-13

Program	Gain dBi	Source Impedance R +/- jX Ohms	AGT	AGTdB	Corrected Gain dBi
NEC-4	1.94	29.95 - j0.09	1.003	0.01	1.93
NEC-2	1.93	30.33 + j3.49	1.001	0.00	1.93
AM	1.92	30.90 + j2.98	0.9986	-0.01	1.93
MMANA	1.91	29.84 - j11.82			

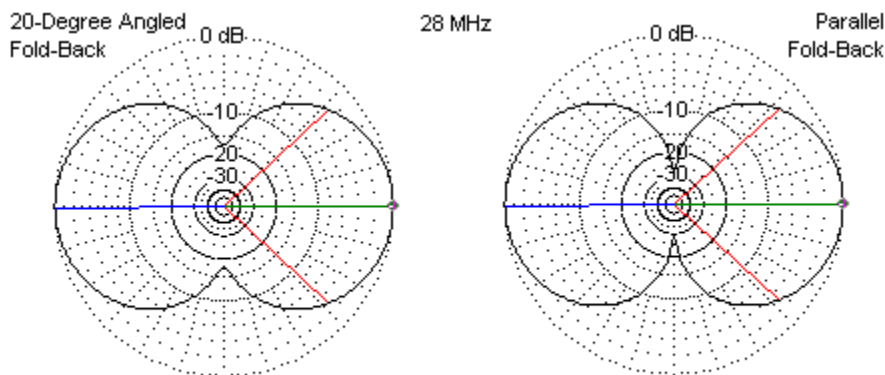
Parallel Fold-Back: Central Length: +/- 70", Spacing 2", End Length: 78.2"

Segmentation: NEC: 17-31-17, MININEC 17-30-17

Program	Gain dBi	Source Impedance R +/- jX Ohms	AGT	AGTdB	Corrected Gain dBi
NEC-4	1.59	15.33 - j0.13	0.921	-0.36	1.95
NEC-2	1.61	15.28 + j2.27	0.926	-0.34	1.95
AM	1.94	15.24 + j8.67	0.9983	-0.01	1.95
MMANA	1.94	15.10 - j1.54			

The squared and parallel fold-back of the alternative model reveals a different problem in uncorrected MININEC. AM corrects for the error potential in very close wires. With a 2" center-to-center separation between the middle section and the fold-back sections of the antenna, the wire surfaces are only 1" apart. Under these conditions, the uncorrected version of MININEC in MMANA (at least in the version used for these exercises) shows a $j10.2$ -Ohm difference in reactance relative to the AM model. The reactance shown in the source data for the AM model is a function of having begun with the NEC-4 modeled dimensions.

Both NEC-4 and NEC-2 show deficiencies in modeling the parallel fold-back geometry. Although the dimensions are likely off the mark (at least relative to the AM model indications), the most dramatic evidence lies in the AGT values for both NEC cores. The gain report is more than 1/3-dB off its proper value. The corrected value tallies very well with the AM gain value. In fact, NEC makes the fold-back dipole look far worse than it really is in terms of dipole performance. The most likely source of the error that yields the AGT values reveals is the proximity of the wires. We did not encounter such an error when we examined folded dipoles that used the same spacing, wire diameter, and segmentation level. However, the folded dipole used wires that had the same length, end to end. The fold-back dipoles use wires with different lengths, even though the segmentation produces segment junctions that are as well aligned as the required lengths permit. The situation is simply one of the documented weaknesses within NEC. In this case, note that the level of the problem is virtually the same for both NEC-2 and NEC-4.



Free-Space E-Plane Patterns for the Sample Fold-Back Dipoles

Fig. 5

Fig. 5 provides E-plane patterns for both versions of the fold-back dipole. The angled fold-back model shows deeper side nulls than either of the zigzag dipoles, but as we saw in **Fig. 3**, the conventional E-plane does not quite coincide with the angle of the deepest nulls. The parallel fold-back model shows very deep nulls that are limited only by the need for end connecting wires between the center and the fold-back wires.

The fold-back dipoles show a pattern similar to the one that we encountered with zigzag dipoles. As we change construction in ways that require longer end wires, the source resistance decreases. Although the value for the 20-degree fold-back model falls within the usable range, the source resistance for the parallel fold-back model is impractically low. Such antenna performance features do not affect modeling adequacy and accuracy, but they may heavily influence the designs for antennas that we actually plan to build.

Fan Dipoles

The last of our exercise dipoles is actually two dipoles in one. A common technique used in both amateur and commercial dipole construction is tying together dipoles for more than one frequency by using separate dipole legs, but with a common feedpoint. Let's simulate this situation with combined dipoles for 28 MHz and for 14 MHz. The structure, for simplicity, will use 1" lossless wire throughout. The dipoles will have about a 30-degree angle between the wires for each frequency. Our question is not whether such a structure makes good building sense. Rather, we want to examine the best way to model such an antenna in order to provide reliable data reports.

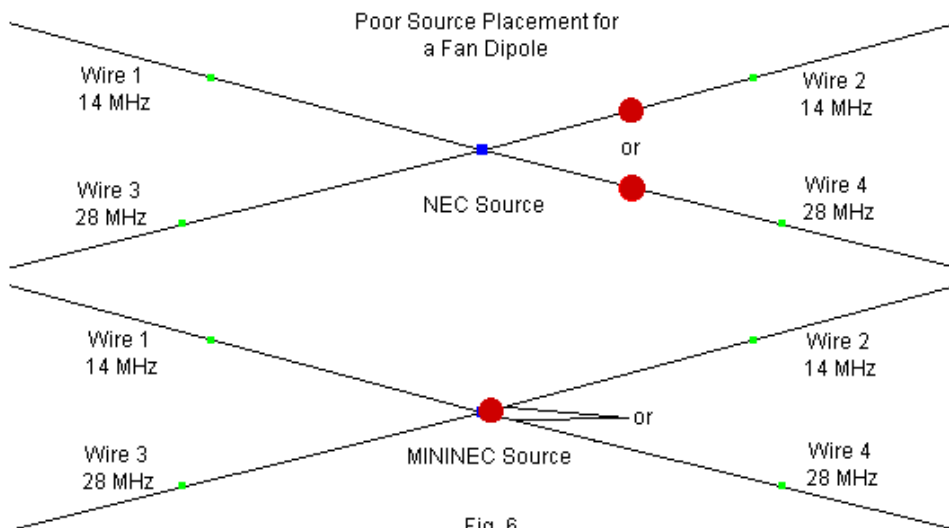


Fig. 6 shows a common way to model such antennas in both NEC and in MININEC. In NEC, we must place a source on a segment. With all wires joining at the center, we must choose which wire will receive the source. The source must be on either a 14-MHz wire or on a 28-MHz wire, but it cannot be on both. MININEC may give its users a false impression, since we normally say that pulses used for sources fall at segment junctions. Hence, it would appear that placing the source at one of the pulses at the junction of the wires would solve our problems. Conventional representations of the source position under these conditions will show it at the center of the junction. My representation in **Fig. 6** shows the source to be slightly offset and distinctly on either a 14-MHz wire or on a 28-MHz wire. The following table of source impedance values for the various options for the various cores confirms the situation.

Unreliable Fan Dipoles for 14 and 28 MHz in NEC and MININEC
All elements 1" diameter and lossless in free space.

Program	Source Element	28-MHz Source Z R +/- jX Ohms	14-MHz Source Z R +/- jX Ohms
NEC-4	28 MHz	33.02 + j26.58	32.53 - j323.2
	14 MHz	792.6 + j927.6	72.84 - j17.52
AM	28 MHz	30.14 + j21.23	9.72 - j261.9
	14 MHz	416.9 + j375.4	68.48 - j21.05

The NEC and the MININEC values both show that if we place the source on a 28-MHz wire, then the 28-MHz source impedance value is reasonable. (I did not bother to resonate the model, although that fact has nothing to do with the source impedance pattern.) With the source on the 28-MHz wire, both types of cores show very aberrant values for the source impedance on 14 MHz. Without changing antenna dimensions, if we move the source to a 14-MHz wire, then we obtain reasonable values of source impedance for 14 MHz. However, the 28-MHz source impedance values become wholly unusable. The small exercise shows that we must come up with an alternative procedure for modeling fan dipoles.

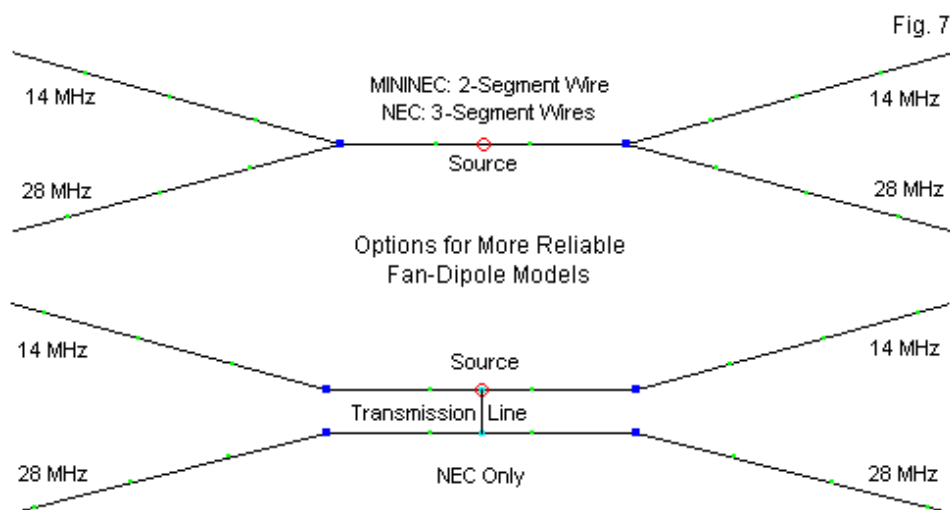


Fig. 7 shows a pair of alternative schemes. Let's first concentrate on the upper portion of the figure. We may create a source wire that is 3 segment long in NEC and 2 segments long in MININEC. In each case, the source position is exactly centered in this wire. As well, the wire has identical segment lengths on each side of the source and prior to any current division that will take place due to the use of dual dipoles. The dipole legs connect to the ends of the central source wire. The following tables shows the results for NEC-4, NEC-2, AM, and MMANA.

Fan Dipoles for 14 and 28 MHz in NEC and MININEC

All elements 1" diameter and lossless in free space. 30-degree angle between wires.

Program	Frequency MHz	Gain dBi	Source Impedance R +/- jX Ohms	AGT	AGTdB	Corrected Gain dBi
NEC-4:	3-Segment Source Wire					
	28	0.93	37.52 + j0.55	1.096	0.40	0.53
	14	2.53	55.27 + j0.32	1.110	0.45	2.08
NEC-2:	3-Segment Source Wire					
	28	1.24	35.10 + j3.87	1.185	0.74	0.50
	14	2.85	51.33 + j1.53	1.196	0.78	2.07
AM (MININEC):	2-Segment Source Wire					
	28	0.53	40.39 - j6.07	0.9951	-0.02	0.55
	14	2.07	61.18 - j3.00	0.9994	0.00	2.07
MMANA (MININEC):	2-Segment Source Wire					
	28	1.45	36.72 - j17.76			
	14	2.08	60.47 - j5.32			

Note: For 3-Segment Source-Wire models, the 14-MHz element is +/-199.3". The 28-MHz element is +/-106.7". Lengths include 1/2 the source wire.

With the same dimensions for each model, and using the NEC-4 model as our starting point, we find very reasonable results for the dipoles on both bands using a common feedpoint. The tabular data strongly suggest that in this case, AM would have been the proper starting point. It yields nearly ideal AGT values, while the NEC cores depart significantly from the ideal. The problematical AGT values would not occur had we used thin wire, which might be typical of a fan dipole installation. However, our goal is not to overlook potential problems, but to locate and identify them.

The less-than-ideal NEC AGT values are functions of the angle between the dipole legs at the points of junction with the source wire. One indication of this fact is the higher or less ideal AGT value produced by NEC-2 relative to NEC-4. NEC-4 improves on the ability of the core to handle smaller angles. (Note that the smallest angle that either core can handle depends upon a number of variables. In this case, the large wire diameter and the fact that the wires do not form a field whose radiation is self-canceling result in the difficulty.)

The lower portion of **Fig. 7** shows a very usable work-around that is applicable to both NEC-2 and NEC-4, but is not possible within MININEC. The starting point for this version of the fan dipole is the use of wholly separate wires for the two dipoles. The source wires parallel each other at a minimum spacing. In this

example, I used 2" center-to-center, although a slightly wider spacing would have been superior.

The key to having a single feedpoint is the placement of the source on one of the two source wires. Which wire makes no difference. Between the middle segment of each wire, we create a transmission line via the TL command. The line's characteristic impedance is inconsequential within broad limits. Given the approximate impedances from the first type of model, I used 50 Ohms. The key to achieving a true parallel connection is the length of the transmission line. Since NEC transmission lines are mathematical only, their length is not the spacing between the connection points unless we specify that value. Instead, the TL command allows us to make the line length any value whatsoever. Since in a near-zero-length line, the impedance will not transform by any detectable amount, we may use 1E-10 m as the length. In some implementations of NEC, a value this short may not be allowed; simply use the shortest line length that is allowed.

The resulting model is a more reliable NEC representation of the fan dipole. The dimensions may change relative to the common-wire source. In the following table, the 14-MHz legs are each 1.4" longer and the 28-MHz legs are each 2" shorter than in the previous model.

Fan Dipoles for 14 and 28 MHz in NEC

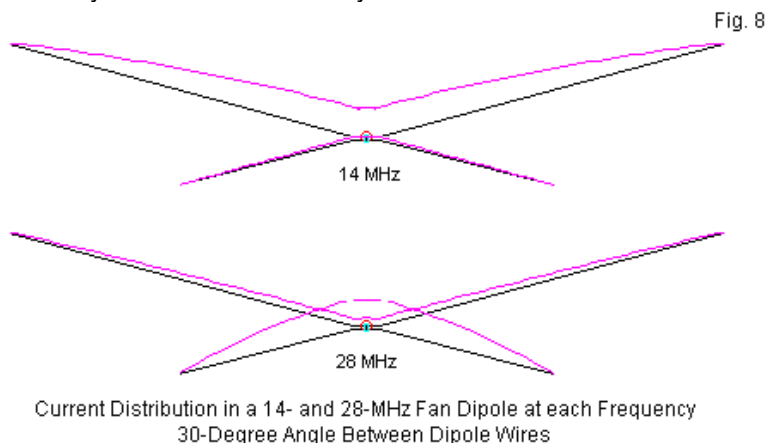
All elements 1" diameter and lossless in free space. 30-degree angle between wires.

Program	Frequency MHz	Gain dBi	Source Impedance R +/- jX Ohms	AGT	AGTdB	Corrected Gain dBi
NEC-4:	Transmission-Line Parallel Source					
	28	0.66	48.36 - j0.35	0.998	-0.01	0.67
	14	2.08	64.07 - j0.34	0.999	0.00	2.08
NEC-2:	Transmission-Line Parallel Source					
	28	0.65	48.96 + j0.25	0.992	-0.03	0.68
	14	2.05	64.47 - j0.32	0.993	-0.03	2.08

Note: For 3-Segment Source-Wire models, the 14-MHz element is +/-200.7". The 28-MHz element is +/-104.7". Lengths include 1/2 the source wire.

NEC-4 registers slightly superior AGT values, likely due to its small improvement in handling the closely spaced center wires relative to NEC-2. These wires, of course, are in the physical region of peak current. A small increase in the center-wire spacing would have yielded virtually ideal AGT scores. Noting all of this, a fan dipole constructed to approximate the model would still require considerable field adjustment of the leg lengths to account for construction variables. Fan dipoles are considerably more finicky or sensitive to minor changes than are almost any of the other models that we have examined, with the parallel fold-back model as a potential exception.

Throughout the progression of models, we have recorded values for the 14-MHz tests that are consistent with any full-size dipole. The slight V in the legs lowers the gain and source resistance by very small amounts that fall below the level of being operationally significant. However, the 28-MHz source resistance is considerably lower, and the 28MHz maximum gain is both very low and more variable among the models. **Fig. 8** shows part of the reason for the difference in performance. The upper sketch shows the current distribution at 14 MHz along all of the fan-dipole wires. The current magnitude on the 28-MHz dipole legs is very low and barely noticeable. However, when we operate the fan at 28 MHz, the relative current magnitude along the 14-MHz legs is appreciably higher. The consequence is that the 14-MHz elements exert partial control over the 28-MHz pattern. Most notable is an increase in the vertical component of the total field, which increases radiation to the sides of the array. At 14 MHz, the radiation had been almost totally broadside to the array.



The result of this complication is that the 14-MHz far field produces an almost ideal dipole pattern. The left side of **Fig. 9** shows 3-dimensional and E-plane plots at 14 MHz. With side nulls that are 20-dB down from maximum broadside gain, the pattern resembles the pattern for a V dipole, which is indeed what the antenna is at that frequency. The vertical component, which is at right angles to the main lobes, is very small, as shown by the small inner lobes of the pattern. Hence, the horizontal component and the total field form pattern lines that overlap for most of the E-plane circumference.

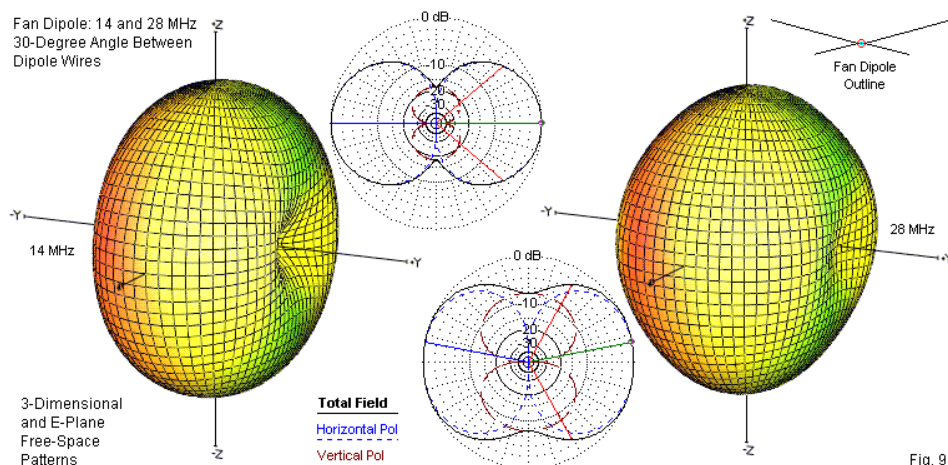


Fig. 9

At 28 MHz, the pattern has a much squarer appearance, as shown in the 3-dimensional and E-plane patterns to the right in **Fig. 9**. The side nulls are only about 8 dB below the maximum broadside gain, which does not occur on a perfect tangent to the antenna plane, but is offset slightly. The vertical component emerges from the combined radiation of the 14-MHz and the 28-MHz legs and rivals the horizontal component in strength--at least within about 8 dB. The total pattern, which is a combination of the 2 component patterns, takes on a much squarer shape. As well, it is sensitive to small changes in antenna shape--and in how the modeling software handles the calculations as one or more aspects of the antenna geometry press the limits of the modeling core. MMANA, for example, shows a higher maximum gain that is a function of calculating a larger vertical component. Hence, maximum gain occurs at a bearing well removed from the broadside tangent. In contrast, NEC and the AM version of

MININEC calculate somewhat lower vertical components, and the maximum gain occurs only a bit off the broadside tangent line.

Fan dipole users and builders tend to presume that the antenna operates "just like" a single dipole at each of the operating frequencies. Some combinations in fact approximate such performance. However, the sample that we have used illustrates a common case in which the performance of at least one of the two dipoles is unlike the performance of a standard or linear dipole. The examples have exacerbated the problems both in the antenna design and in the modeling of the design by using fat 1" diameter wires. Thin-wire versions of the fan dipole may well display the phenomena to a much lower degree.

Conclusion

We have not by any means exhausted the possibilities for variations on the 1/2-wavelength near-resonant dipole. However, it is likely that these notes have exhausted you. Except for the standard or linear dipole with a uniform diameter, the examples in the series of episodes have aimed to reveal various modeling pitfalls within a fairly unified context that has featured one of the most common antennas used in communications work at all frequencies. My goal has been to exhibit the pitfalls in a concrete setting rather than simply listing pitfalls and producing divergent examples to display the potential problems. Along the way, we have seen that the problems do not occur equally in all modeling cores. Each core has strengths and weaknesses when we press its limitations. Internally, MININEC exhibits the widest range of performance variability, since different implementations correct different numbers and types of raw MININEC difficulties. MMANA represents a virtually uncorrected core and AM represents a highly corrected and supplemented core. Versions of NEC-2 and of NEC-4 tend to yield very similar results to other versions of NEC-2 and NEC-4. However, the differences between the two NEC cores and the limitations that are common to both become the most significant features to observe when one is searching out modeling pitfalls.

Any summary judgment about the relative merit of a highly corrected MININEC and either version of NEC would be wholly out of place. We have examined the cores only as they model various forms of the dipole. We have not examined how each core handles spot loads. Nor have we examined the vast array of geometry and control commands within NEC that are not a part of MININEC. Not only is our database woefully shy of the level needed for a summary judgment, but as well, such a judgment might prove more harmful than useful. The goal is to use

each core where it is most reliable, effective, and efficient in generating and reporting on a desired model. In that regard, dipoles only begin the modeling work; they do not end it.

Nevertheless, I find it interesting to count the ways that we can get into trouble modeling simple dipoles if we are not careful and alert, and if we do not use all of the facilities of a program to detect problems as well as to produce modeling reports.

112. Wires Meeting Ground: 2 Cases

For various good reasons, programmers who implement either NEC-2 or NEC-4 provide warnings about vertical wires that meet the ground ($Z=0$) and end at that point. For example, EZNEC Pro warns that "If you connect a wire to ground when using the High Accuracy [Sommerfeld-Norton or S-N] real ground type, the program makes the connection with an unpredictable series resistance." EZNEC no longer makes the less-accurate reflection-coefficient approximation (RCA) ground calculation system available. It was designed for faster results in an era of much slower computer speeds. Today, there is no significant difference in model run times when using either ground calculation system, so EZNEC has omitted RCA. The system is widely available on other implementations of NEC-2 and NEC-4 (such as NEC-Win Pro, GNEC, 4NEC2, and NEC2GO). However, EZNEC does provide access to the MININEC ground calculation system from its implementations of NEC-2 and NEC-4. (4NEC2 also provides the MININEC ground system within a NEC package.) Nevertheless, for all general modeling purposes, the modeler should use the more accurate S-N ground calculation system. (Antenna Model, a version of MININEC, now includes the S-N ground system in its program.)

We have in past episodes explored the differences among the available ground calculation systems, listing the limits and the limitations of each one. In this episode, we shall focus on a slightly different way of looking at ground calculation systems by examining two different types of antennas that will test various ways of handling vertical wires that just reach the ground ($Z = 0$). The first case will extract data reports using a fairly standard test of wire-to-ground terminations. We shall look at differences among reports for a 1/4-wavelength monopole using the various ground systems when the monopole just reaches the ground and has no radials. We shall compare those reports with NEC-4 reports for the same monopole above ground, but with a buried radial system of 32 15' radials. We may call this the "normal" test situation for uncovering the problems that emerge when we fail to provide a proper termination for a wire that just touches the ground.

Then we shall look at a different type of antenna: a 10-wavelength terminated long wire. On common configuration for such antennas is to bring the ends of the wires vertically back to the ground. We place the source on one end and the terminating resistor on the other end, in both cases, right at ground level. (This is

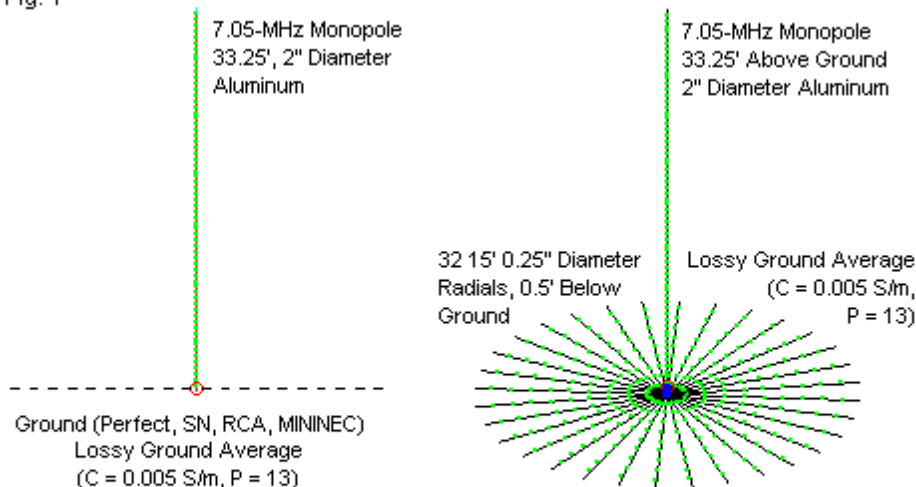
not the only possible configuration for a terminated long wire, but it is perhaps the most common configuration. Unlike some alternatives, it provides a very large operating bandwidth--several octaves--but with a changing pattern, since the antenna changes its length as we change the operating frequency.) We shall look at 4 different ways to model this antenna configuration, in each case placing the antenna's horizontal run 1 wavelength above ground.

As we shall discover, the matter of wires touching the ground with the S-N ground system (and others) are not quite so cut and dried as the simple modeling test might indicate.

The "Normal" Test Situation

Assessing the behavior of a vertical wire that just touches ground, with no other termination, when using the various ground systems in NEC-2 and NEC-4 usually involves setting up a 1/4-wavelength vertical monopole. So long as all models in the test sequence use the same monopole, frequency, and ground quality (wherever relevant), the selection of these parameters makes no significant difference to the test. Therefore, I shall begin with an aluminum monopole that is 33.25' tall with a 2" diameter. It will use 66 segments so that each segment is 0.5' long. This provision is not important for the tests that use the monopole alone. However, we shall also need a "properly" terminated monopole for comparison. For that set of runs, I shall extend the monopole 0.5' below ground and connect 32 aluminum radials, each 0.25" in diameter. Each radial will be 15' long. The length is short, but not so short as to invalidate the test comparisons. For adequate current distribution in a lossy medium, the radials are just about long enough, while allowing a very compact model. The ground quality--wherever relevant--will be average, that is, with a conductivity of 0.005 S/m and a relative permittivity of 13. **Fig. 1** shows the outlines of the two models required for the test sequence.

Fig. 1



The "Normal" Test Situation: Comparing A Monopole with Radials
to a Monopole without Radials over Various Ground Types

The model with buried radials requires NEC-4 because the radial wires are below ground. It also requires the S-N ground system for the same reason. However, the simpler model sets up a more complex situation. We shall run the model in both NEC-2 and NEC-4 for all tests. Every implementation of both cores provides access to a perfect ground, that is, one using the simple image-reflection calculation system built into NEC. Likewise, every implementation of both cores allows access to the S-N ground system. However, we must turn to programs like NEC-Win Pro and GNEC, if we wish to see the results of using the NEC reflection coefficient approximation system (RCA). To access the MININEC ground from within with NEC-2 or NEC-4, we must use EZNEC or 4NEC2. If we make all of the relevant model runs, we wind up with a table similar to **Table 1**.

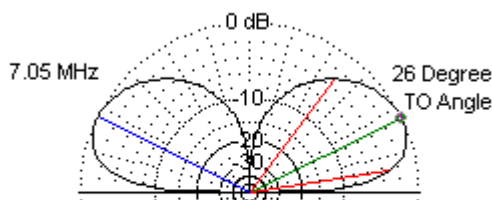
"Normal" Test of Variations for Antenna Ground Termination					
Monopole: 7.05 MHz, 33.25' Above Ground, 2" Diameter Aluminum					
Ground	Core	Program	Gain	TO Angle	Source Impedance
Perfect	NEC-2	EZNEC	5.14	0	35.99 + j0.01
		NWPro	5.14	0	35.99 - j0.01
S-N	NEC-2	EZNEC	-11.31	26	448.50 - j444.70
		NWPro	-11.31	26	448.49 - j444.73
RCA	NEC-2	NWPro	-14.25	26	681.22 - 2059.91
MININEC	NEC-2	EZNEC	-0.03	26	35.99 + j0.01
Perfect	NEC-4	EZNEC	5.14	0	35.98 - j0.04
		GNEC	5.14	0	35.98 - j0.05
S-N	NEC-4	EZNEC	-1.85	26	77.87 + j169.10
		GNEC	-1.12	26	46.13 + j2.85
RCA	NEC-4	GNEC	1.48	26	25.55 - j0.38
MININEC	NEC-4	EZNEC	-0.03	26	35.98 - j0.04
Monopole: 7.05 MHz, 33.25' Above Ground, 2" Diameter Aluminum					
32 15' Radials Buried 0.5' Below Average Ground (C = 0.005 S/m, P = 13)					
Ground	Core	Program	Gain	TO Angle	Source Impedance
S-N	NEC-4	EZNEC	-1.05	26	44.29 - j1.68
		GNEC	-1.06	26	44.36 - j1.83
Notes:	Gain: Maximum gain at TO angle in dBi				
	TO Angle: Elevation angle of maximum gain in degrees				
	Source Impedance: Feedpoint impedance in Ohms				
	Grounds:	Perfect: Image reflection ground, lossless			
		S-N: Sommerfeld-Norton system			
		RCA: NEC reflection coefficient system			
Table 1		MININEC: MININEC reflection coefficient system			

Let's read the table from the bottom up. Both implementations of NEC-4 (EZNEC and GNEC) return virtually identical results for the monopole with buried radials. The tiny numerical variations between the reports are largely functions of using different compilers for the cores. Indeed, different CPUs may show further variations, depending upon their architecture. We should note that the gain and impedance values will also change as we alter both the number and the length of

the radials beneath the monopole. Therefore, our reference buried-radial monopole array is simply one of many possible references that we might use.

The upper part of the table uses a single model with no permitted variation in its geometry (if we are to keep it consistent with the buried-radial antenna). Only the ground system changes among the model runs. Except for the use of a perfect lossless ground, we find one constant among all of the models: a take-off (TO) angle of 26 degrees. In fact, a single elevation plot, shown in **Fig. 2** is applicable to all of the models using a lossy ground.

Fig. 2



Elevation Plot Applicable to
All Monopoles in the "Normal" Test

Regardless of the core or the program, the results over perfect ground coincide as completely as we could expect from separate compilations of the NEC-2 and NEC-4 cores. EZNEC gives us access to the MININEC ground, and the NEC-2 and NEC-4 results also coincide. As well, the feedpoint impedance values remind us that the MININEC ground always returns the impedance for perfect ground, not for the lossy average ground on which the far-field report is based.

In NEC-2, the two programs (EZNEC and NECWin Pro) provide identical results for the S-N ground. Since only NECWin Pro (of the two programs) provides an RCA output in NEC-2, we can only note its values that appear to be even more divergent from reality than the S-N unusable results.

In NEC-4, we find an additional divergence both among cores and among programs. The EZNEC and the GNEC results for the S-N ground do not agree. The RCA result for GNEC differs from the S-N value for the same program by almost the same gain difference as in the NEC-Win Pro S-N and RCA reports, but this is not in itself a suggestion that the GNEC/NECWin Pro results are superior to those of the EZNEC cores.

In fact, we have no way to estimate--short of setting up a physical experiment--which set of reported values may be the more nearly correct for a monopole with no radials placed in contact with average soil. Internal consistency of results would be only one measure of reasonableness. As well, it would constitute a necessary but not a sufficient condition of reliability of the reports. However, we do not have internal consistency. In addition, we cannot use the reports for the antenna that uses 32 15' radials, because--at best--these results apply to only one of many possible arrangements. Other radial lengths and other numbers of radials would each yield different results for both the far-field gain and the feedpoint impedance.

Buried-radial monopole systems that we model by using the S-N ground in NEC-4 do have a very reasonable track record of reliability relative to physical antennas--within the bounds of construction variables and the potential in any area for stratified soil. For example, the results coincide very well with the experimental results published in the classic Brown-Lewis-Epstein work on the 1930s. Since we do not have a similar record for the monopole without radials, the entire set of results over lossy ground using either the RCA or the S-N ground fall into the category of being simply unreliable. (We have examined the shortcomings of the MININEC ground system in other episodes.)

Our sample model only illustrates the problem of trying to model a monopole without providing it with a radial system. Nevertheless, it shows why program manuals tend to recommend against simply bringing a vertical wire to ground and using no other termination for it.

The Terminated Long Wire

A single wire that is many wavelengths long, fed at one end and terminated by a correct impedance at the other end, creates a directional beam. It is one of the earliest directional antennas used in HF point-to-point communications. With the use of a proper termination, the antenna is capable of wideband operation over frequency spans of more than 4:1. However, the beamwidth and the sidelobes tend to vary as the antenna changes its length when measured in wavelengths as a function of the operating frequency.

The terminated long wire has a number of possible configurations, but we are interested only in the most common of these ways of setting up the antenna. Let's consider a long wire that horizontally is 10 wavelengths. We shall set the antenna 1 wavelength above average soil. The most common way to feed the

antenna is to bring a wire to ground and to place the source or feedpoint at the junction of the wire with the ground. Essentially, the ground forms the second terminal of the feedpoint. At the far end of the long wire, we shall also bring a wire from the end of the horizontal section down to ground. The ideal termination would be a complex impedance, the reactive part of which would vary with the operating frequency. However, for wideband use, we normally use a non-inductive resistor. Like the feedpoint, we place the resistor at the junction of the vertical wire and the ground. Ostensibly, the ground provides a return so that effectively the resistor and the feedpoint have a common terminal.

Ideally, we can find a load impedance that will provide the proper conditions for achieving full traveling-wave status for the terminated long wire. The calculation is based on treating the wire as a transmission line, and the load impedance must equal the characteristic impedance of the line. Balanis (*Antenna Theory: Analysis and Design*, p. 495) provides the following equation to approximate the proper value of the termination.

$$RL = 138 \log_{10} (4h/d)$$

RL is the value of the impedance load in Ohms, h is the height of the wire, and d is the wire diameter, when both are in the same units. Note that the impedance of the line and hence the approximate load value is independent of frequency and dependent only upon a set of physical measurements that use the same units of measurement. The approximate recommended value of RL is 776 Ohms. For many installations, terminating resistors tend to range between 600 and 800 Ohms. The wire diameter is 4.745e-6-wavelength (or 0.16" wire at 3.5 MHz).

Equally important to the model is the configuration that we employ for simulating the termination of the antenna ends at the ground. Essentially, we have 4 options (A though D) as sketched in **Fig. 3**.

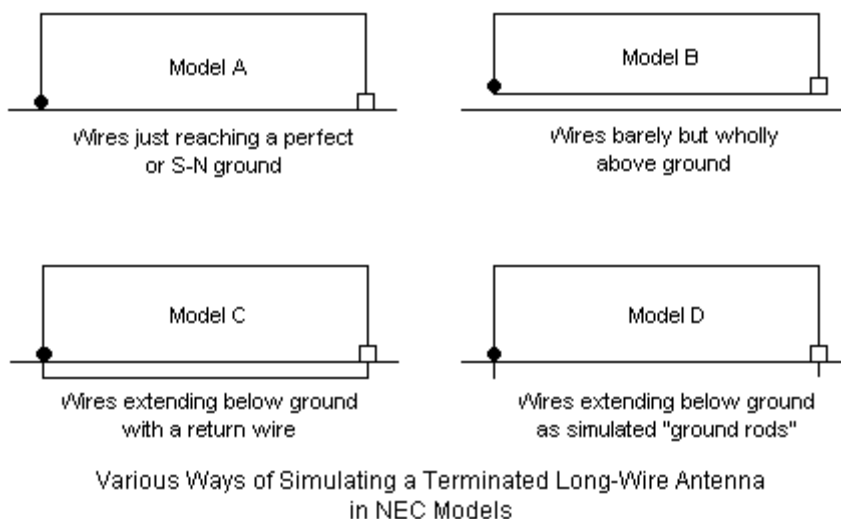
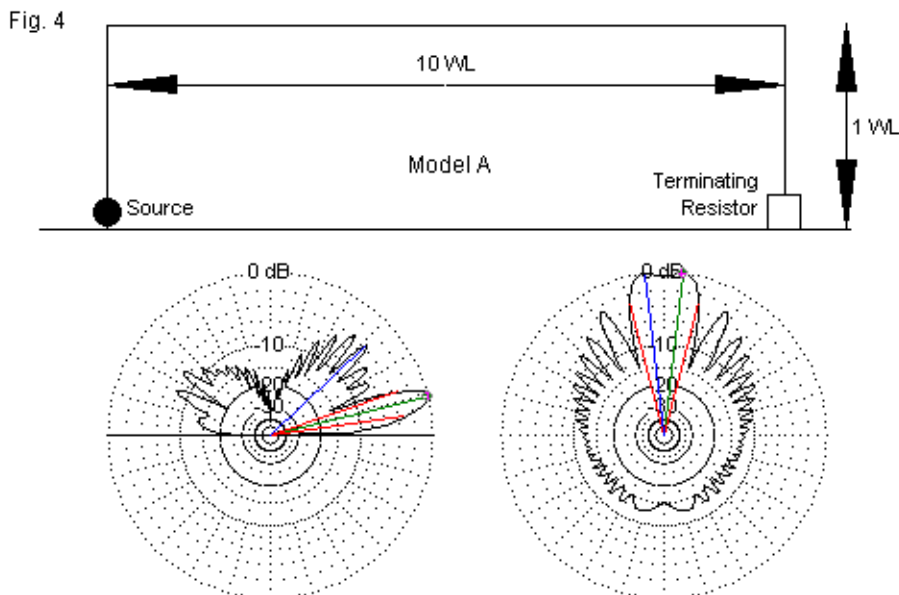


Fig. 3

Option A brings the vertical elements of the antenna down to ground. The source or feedpoint is the first segment above ground of the left wire, while the terminating load appears on the last segment above ground at the far end of the antenna. **Fig. 4** shows the general layout, along with elevation and azimuth patterns for the test model.



Model A: Wires Terminated at Ground ($Z = 0$); No Other Return Path

In the EZNEC Pro/4 implementation of NEC, we have at least 4 ways to model the structure: over perfect ground, with a Sommerfeld-Norton (S-N) average ground using NEC-4, with an S-N average ground using NEC-2, and with a MININEC ground. Use of a perfect ground provides a reference baseline for checking the sensibleness of other models. However, neither NEC-2 nor NEC-4 recommends simply bringing a source wire to ground, since at a minimum, the source impedance is likely to be off the mark. The MININEC ground does not provide accurate impedance reports for the ground quality selected, since it is restricted to using the impedance report for perfect ground.

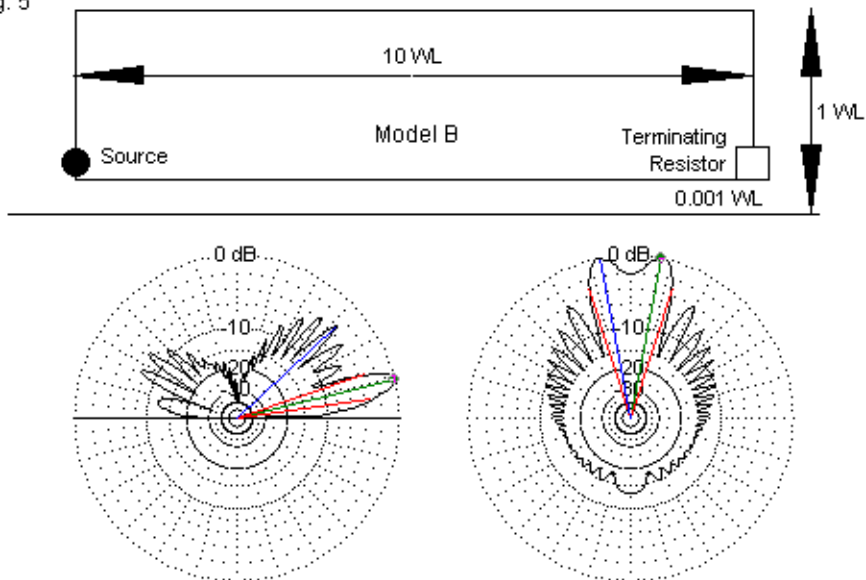
Despite the limitations, we can tabulate the results. As a test case, I used a 10-wavelength terminated antenna alternately using termination resistors of 600, 800, and 1000 Ohms. For each option, **Table 2** lists the maximum gain, the reported 180-degree front-to-back ratio, the elevation angle of maximum radiation, the beamwidth, the source impedance, and the 600-Ohm SWR at the test frequency.

Test Performance Values for Modeling Option A					10-WL Horizontal		
Load R	Gn dBi	FB dB	BW deg	EI Ang	Feed R	Feed X	SWR 600
Perfect Ground							
600	13.98	29.04	26.4	15	439	24	1.37
800	13.91	26.38	26.2	15	476	43	1.28
1000	13.87	19.57	26.2	15	504	59	1.23
Average S-N Ground, NEC-4							
600	11.54	11.57	35.2	11	460	593	3.01
800	11.49	12.63	35.2	11	495	588	2.85
1000	11.45	12.87	35.2	11	524	587	2.75
Average S-N Ground, NEC-2							
600	10.79	24.23	35.6	11	479	14	1.26
800	10.74	21.78	35.6	11	509	35	1.19
1000	10.72	18.11	35.6	11	532	52	1.16
Average MININEC Ground, NEC-4							
600	11.09	23.58	35.4	11	439	24	1.37
800	11.01	22.71	35.4	11	476	43	1.28
1000	10.98	18.55	35.4	11	504	59	1.23
Load R = Terminating resistance value in Ohms							
Gn dBi = Maximum gain in dBi							
FB dB = 180-degree frnt-to-back ratio in dB							
BW deg = Half-power beamwidth in degrees							
EI Ang = Elevation angle in degrees							
Feed R = Feedpoint resistance in Ohms							
Feed X = Feedpoint reactance in Ohms							
SWR 600 = 600-Ohm SWR							Table 2

Using the sequence over perfect ground as a background reference, the NEC-2 results for the S-N average ground and the MININEC average ground data appear to coincide fairly well. However, the NEC-4 runs for the S-N average ground appear to yield somewhat high gain values with more than anticipated inductive reactance in the source impedance. The gain values for NEC-4 and the S-N ground are only about 2.5-dB lower than the values over perfect ground.

Option B represents an adaptation of a NEC-2 technique for modeling vertical antennas with ground-plane radials. The return line between the load resistor and the source is 0.001-wavelength above ground, several times the diameter of the wire. See **Fig. 5** for the layout and the associated elevation and azimuth patterns.

Fig. 5



Model B: Return Wire 0.001-WL Above Ground

In principle, the model violates no constraints, but as **Table 3** for both NEC-2 and NEC-4 shows, it yields a poor model of the terminated long-wire antenna.

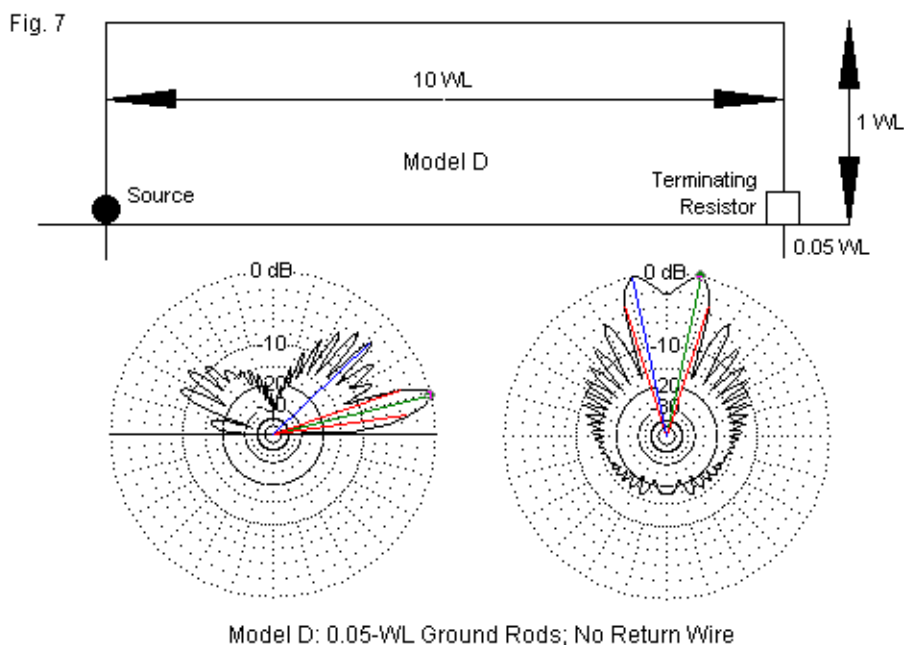
Test Performance Values for Modeling Option B					10-WL Horizontal		
Load R	Gn dBi	FB dB	BW deg	EI Ang	Feed R	Feed X	SWR 600
Average S-N Ground, NEC-4							
600	7.68	16.93	35.4	11	1170	-97	1.97
800	7.73	14.44	35.4	11	1182	-80	1.98
1000	7.77	13.36	35.4	11	1192	-67	2.00
Average S-N Ground, NEC-2							
600	7.68	16.10	35.4	11	1167	-99	1.96
800	7.72	14.59	35.4	11	1179	-82	1.98
1000	7.76	13.50	35.4	11	1188	-69	1.99
Load R = Terminating resistance value in Ohms							
Gn dBi = Maximum gain in dBi							
FB dB = 180-degree frnt-to-back ratio in dB							
BW deg = Half-power beamwidth in degrees							
EI Ang = Elevation angle in degrees							
Feed R = Feedpoint resistance in Ohms							
Feed X = Feedpoint reactance in Ohms							
SWR 600 = 600-Ohm SWR							Table 3

Although NEC-2 and NEC-4 show a very close coincidence of data, the low gain, low front-to-back ratio, and high feedpoint impedance reports combine to suggest that this model is highly inadequate. The antenna amounts to a corner-fed terminated loop in which the low wire is an active part of the antenna rather than just a return line. However, the beamwidth and elevation-angle reports are consistent with the other models.

NEC-4 does allow the use of a subterranean return wire, shown in *Option C* in **Fig. 6**. To test this option, I placed a return wire 0.01-wavelength below ground level, connecting it to the above ground vertical wires with short segments. Both the source and the load for the antenna remain above ground. The layout and patterns appear together in **Fig. 6**.

The results are modest, but coincide roughly with the NEC-2 results in Option A. The front-to-back reports are consistent with those for perfect ground. The difficulties with the model include the model size, since the return wire requires as many segments as its above-ground counterpart in Option B. As well, the return wire may actually yield slightly low gain reports by carrying more current than the ground itself. A real installation would not likely use a buried ground wire.

Therefore, I tried *Option D*, which replaces the below ground structure of option C with 2 simple ground rods. See **Fig. 7** for the layout details and the patterns.



Each rod is a 1-segment wire about 0.05 wavelength, which is the length of the segments in the vertical wires above ground. Therefore, the source has equal length segments on each side of the feedpoint segment. 0.05-wavelength is about 4.3 meters or 14'. This length may be longer than the average ground rod,

but substituting shorter segments did not change the reports by any significant amount. The results of the test appear in **Table 5**.

Test Performance Values for Modeling Option D					10-WL Horizontal		
Load R	Gn dBi	FB dB	BW deg	EI Ang	Feed R	Feed X	SWR 600
Average S-N Ground, NEC-4							
600	10.49	22.94	35.6	11	513	69	1.22
800	10.47	20.30	35.6	11	544	87	1.20
1000	10.46	17.29	35.6	11	567	102	1.20
Load R = Terminating resistance value in Ohms							
Gn dBi = Maximum gain in dBi							
FB dB = 180-degree frnt-to-back ratio in dB							
BW deg = Half-power beamwidth in degrees							
EI Ang = Elevation angle in degrees							
Feed R = Feedpoint resistance in Ohms							
Feed X = Feedpoint reactance in Ohms							
SWR 600 = 600-Ohm SWR							Table 5

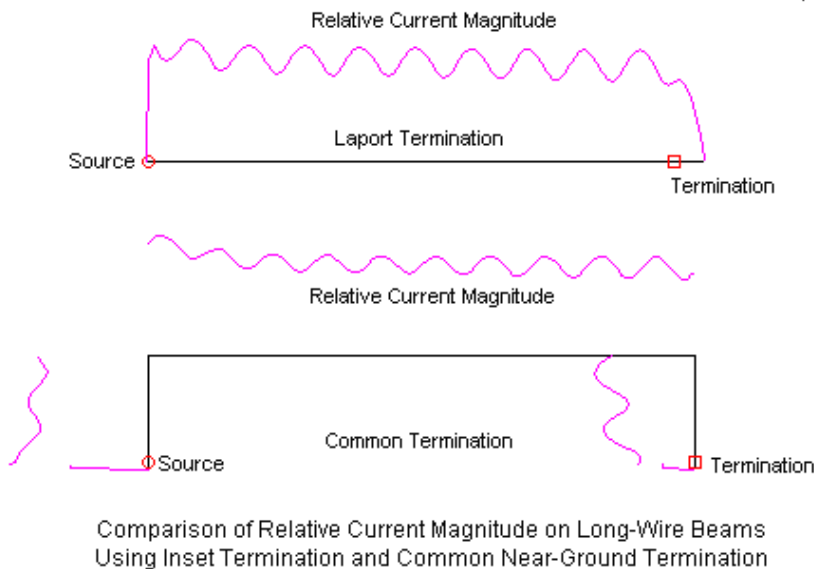
Except for the predicted very slight increase in maximum gain, all of the values correspond very well with those of the buried-return-wire model (option C), but with a 45% reduction in model size. For users of NEC-4, it is likely that this style of model is about as adequate as we may get for a terminated long-wire directional antenna. In fact, for users of NEC-2, the basic model (option A) coincides well enough for general guidance. In physical reality, there will be structural variables that will inevitably limit the precision attainable by any model. For example, the models presume a flat wire horizontal to the ground, which is not likely to appear with copper wire and real supports. Even if all supports provide the same height, catenary effects will vary the actual wire height above ground along the antenna pathway.

The net result of these preliminary tests suggest that option D is a very usable model capable of giving good guidance on the performance of the common-configuration single terminated long-wire antenna. We may largely dispense with the creation of complex radial systems under each end of the antenna, systems that would not likely be part of an amateur long-wire installation.

Almost incidentally, we may note two facts about these test long-wire antennas. First, we should expect some slight inductive reactance, since the wires are physically 10-wavelengths long. Hence, they are slightly long electrically,

Second, the use of vertical wires at the ends of the main horizontal section modifies the performance relative to a configuration that uses only a horizontal wire. **Fig. 8** compares the current distribution along two terminated long wires with equal-length horizontal sections. Since in long-wire technology, there is no perfect traveling-wave antenna, both versions show a standing wave superimposed on a certain constant traveling-wave current level. For the present context, the current distribution curves for the vertical sections of the lower sketch are most important. They limit both the gain and the front-to-back values for the antenna.

Fig. 8



In addition, the vertical wires also modify the transmission-line analogy that resulted in the choice of the terminating resistor. Virtually all of the tables show that as we increase values of the terminating resistor, the feedpoint impedance grows, but at a slower rate. Apart from the small inductive reactance, the feedpoint impedance would more closely match the terminating resistor value when both values are somewhat lower.

Conclusion

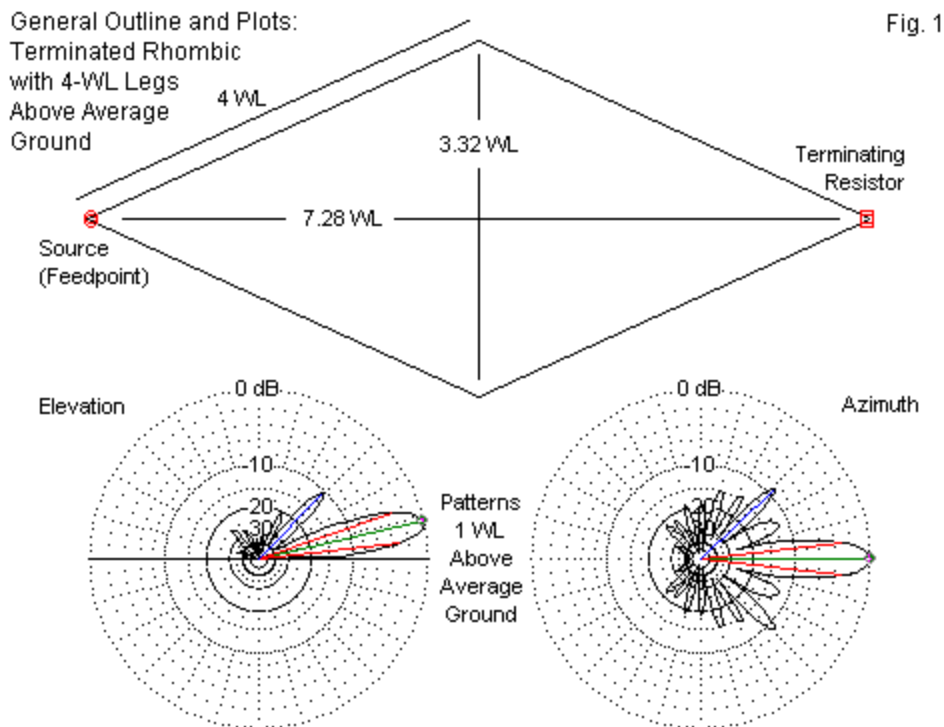
With a simple monopole and no radials, the NEC-2 model showed results that seemed most to diverge from our expectations of a physical antenna. The NEC-4 results appeared--however ultimately unreliable--to be considerably closer to reality--as indicated by the reference model using radials.

In contrast, options C and D of the long-wire model with at least some buried elements provide a reference against which to measure the models without ground penetration. In this case, The NEC-2 model of option A more closely approximated the reference values on options C and D than did the corresponding option-A version using NEC-4. Although we cannot expect high precision (but only general planning guidance) from any of the models, the exercise does illustrate that we cannot draw singular universal conclusions. When wires just touch the ground, a model is suspect in the reliability of its reports. However, the level of reliability and the reasons for any given measure of distrust may vary with the type of antenna that we are modeling.

113. When Simple Geometries Become Complex A Rhombic Case Study

The terminated rhombic beam holds the position of king among all long-wire arrays. It is an extension of basic long-wire technology, a small piece of which we sampled in the preceding episode. Initially developed by Edmond Bruce in the early 1930s, the antenna served point-to-point communications needs well into the 1960s. During the 4-decade heyday of the rhombic, amateurs dreamed of having one of these high-gain, narrow-beamwidth, broad-band antennas--and of the acreage necessary to hold it. One humorist reported that his ideal antenna would be a very large rhombic located on a rotatable island in the Caribbean.

These notes are not aimed at evaluating the relative merits of the terminated rhombic. Instead, the goal is to address some questions that may arise in the course of modeling rhombic antennas of various types. Perhaps the simplest rhombic model appears in **Fig. 1**. The legs are 4 wavelengths each, which results in the specified dimensions. I selected the angle (alpha) between the centerline and each leg to yield the maximum gain for this model, which happens to be at a 3.5-MHz test frequency. The lossless model wires are 0.16" in diameter.



The patterns below the model outline show the reported elevation and azimuth plots for the modest rhombic. One main reason for the commercial use of the rhombic was the very narrow beamwidth as well as the high gain. However, the relatively strong sidelobes remained a concern for rhombic designers into the 1960s. The last major rhombic development was the dual offset rhombic design of Edmund Laport.

The following abbreviated list of references will provide more information on rhombics for those intrigued by long-wire technology. For a systematic treatment from a modeling perspective, see *Long-Wire Notes*, available from *antenneX*.

Bruce E., "Developments in Short-Wave Directive Antennas," *Proceedings of the IRE*, August, 1931, Volume 19, Number 8: the introduction of the terminated inverted V and diamond (rhombic) antennas.

Bruce E., Beck A.C., and Lowry L.R., "Horizontal Rhombic Antennas," *Proceedings of the IRE*, January, 1935, Volume 23, Number 1: the classic treatment of rhombic design, repeated in many text books.

Graham, R. C., "Long-Wire Directive Antennas," *QST*, May, 1937: an excellent summary of long-wire technology to the date of publication.

Harper, A. E., *Rhombic Antenna Design* (1941): a fundamental text on rhombics, based on engineering experience, with tables and nomographs as design aids.

Johnson, R. C. (Ed.), *Antenna Engineering Handbook*, 3rd. Ed., Chapter 11, "Long-Wire Antennas" by Laport.

Laport E. A., and Veldhuis, A. C., "Improved Antennas of the Rhombic Class," *RCA Review*, March, 1960, Volume XXI, Number 1: the introduction of the off-set dual rhombic.

Multi-Modeling Potentials

The model that produced the sample plots in **Fig. 1** provides general guidance, but not refined analysis suitable for use as a final pre-building design. Besides lacking the environmental inputs relevant to a prospective building site, there are some fundamental modeling issues that preclude the use of this model as a precision replication of some particular rhombic or other long-wire array. First, the model uses one of several possible input configurations possible in NEC. Each configuration has its own strengths and weaknesses relative the NEC calculations. Second, the model uses a somewhat minimal segmentation density at 20 segments per wavelength.

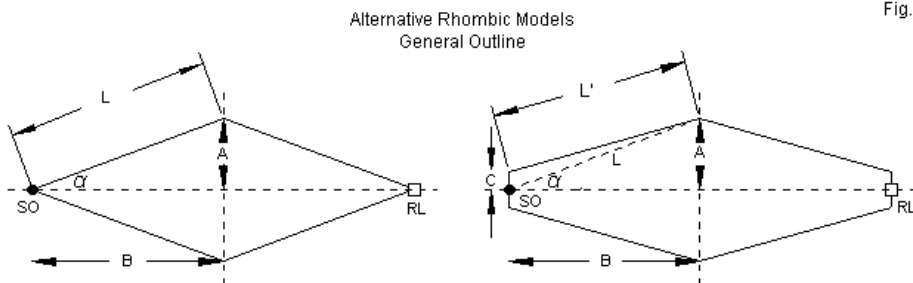


Fig. 2

Fig. 2 shows the pointed-end configuration used for the sample model. L is the leg length and is the square root of the sum of the squares of dimensions A and B . One advantage of this model is that it replicates angle α accurately. However, it does require the use of split sources and loads. An alternative configuration that we shall have to use shortly is on the right. The model places a single source and a single load on short end wires that create a blunt-end rhombic. The dashed line shows the virtual leg that has length L . However, the actual leg length is $L' + C$. As well, the wire labeled L' has a shallower angle relative to the junction with C than given by α . If we make dimensions A and B the same as for the configuration on the left, then we have slightly distorted the rhombic shape. The degree of distortion is a function of 2 factors: the length of C and the leg length L . If C is very short and L is very long, then the distortion will be small relative to the pointed-end model.

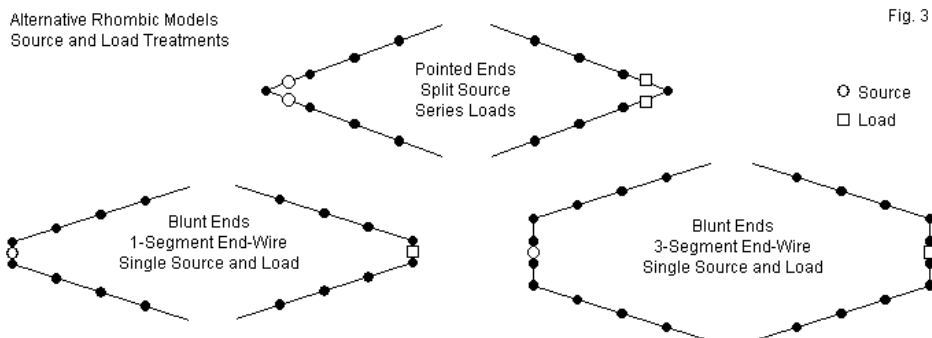


Fig. 3 illustrates the source and load treatments that accompany the two general configurations. Assume that all segments or distances between dots on the sketch have the same length. The pointed-end model places source excitation on the left-most segments of each of the two wires forming the feedpoint end of the rhombic. These sources are in series, and the net impedance of the source is the simple sum of the resistive and reactive components of each source. If we increase the segmentation density of the model, then the sources move closer to the actual tip of the rhombic. A similar condition applies to the series loads placed on the right-most segments of each wire approaching the termination end of the rhombic. The net resistive load is the sum of the two resistances, but if we increase segmentation density, the loads move closer to the actual tip of the rhombic.

The lower sections of the sketch show alternative methods of placing sources and loads at the furthest extremes of the rhombic. The method on the left uses a single segment wire for the source and another for the load. If we carefully size the 1-segment wires so that their length just about equals the length of each segment, NEC should yield accurate results, although it is preferable to have equal-length segments in a line on each side of the source segment. The lower right sketch shows a 3-segment wire at each end of the rhombic that achieves this goal. However, even with careful sizing of the wire length to equalize segment lengths throughout the model, the 3-segment wires increase the distortion of the rhombic shape relative to either the pointed-end or the 1-segment blunt-end versions.

Physical Dimensions of the Test Rhombic with 4-WL Legs						Table 1
Pointed End 4-Wire Version: All Segmentation Densities						
	A	B	C	L	L'	L'+C
	1.6588	3.6398	0	4	4	4
Blunt-End 6-Wire Design with Source and Resistor on 1-Segment End Wires						
Seg/WL	A	B	C	L	L'	L'+C
20	1.6588	3.6398	0.025	4	3.9897	4.0147
40	1.6588	3.6398	0.013	4	3.9946	4.0076
80	1.6588	3.6398	0.007	4	3.9971	4.0041
Blunt-End 6-Wire Design with Source and Resistor on 3-Segment End Wires						
Seg/WL	A	B	C	L	L'	L'+C
20	1.6588	3.6398	0.07	4	3.9715	4.0415
40	1.6588	3.6398	0.04	4	3.9836	4.0236
80	1.6588	3.6398	0.02	4	3.9918	4.0118
Notes:	Seg/WL = Models segments per wavelength of wire.					
	See Fig. 5-8 for explanation of dimension designations.					

The amount of distortion in the rhombic shape is not large, even with a 3-segment wire at each end. **Table 1** provides information on the dimensions of a test rhombic using 4-wavelength legs and an alpha angle of 24.5°, the angle needed to optimize for maximum gain in the original pointed-end model. The table shows the dimensions for all three versions, including the changing value of C as the segments in the main legs (L') grow shorter with increasing segmentation density. The worst case of distortion occurs with a segmentation density of 20 segments per wavelength while using a pair of 3-segment end wires. For 20 segments per wavelength, the end wires have individual lengths of

0.14 wavelength (or $C = 0.07$ wavelength). The distortion amounts to adding about 4% to each leg wire overall, although the angular portion of the wire is under 4 wavelengths. Nonetheless, the combination of configuration, source, and load changes can affect the modeling outputs.

Varying Segmentation Density in 4-Wavelength-Leg Rhombic Beams 1 Wavelength above Average Ground										
Pointed-End 4-Wire Design with Split Sources and Series Terminating Resistors at the Sharp Ends										
Seg/WL	Tot Segs	El Ang	Gn dBi	FB dB	HBW deg	F/SL dB	Feed R	Feed X	SWR 850	
20	320	13	17.39	45.04	13.3	8.75	871	28	1.04	
40	640	13	17.38	29.42	13.4	8.75	871	-104	1.13	
80	1280	13	17.37	25.48	13.4	8.75	856	-177	1.23	
Blunt-End 6-Wire Design with Single Source and Terminating Resistor on 1-Segment End Wires										
Seg/WL	Tot Segs	El Ang	Gn dBi	FB dB	HBW deg	F/SL dB	Feed R	Feed X	SWR 925	
20	322	13	17.38	32.00	13.4	8.78	924	-41	1.05	
40	642	13	17.37	26.71	13.4	8.82	900	-124	1.15	
80	1282	13	17.35	24.23	13.4	8.82	885	-174	1.22	
Blunt-End 6-Wire Design with Single Source and Terminating Resistor on 3-Segment End Wires										
Seg/WL	Tot Segs	El Ang	Gn dBi	FB dB	HBW deg	F/SL dB	Feed R	Feed X	SWR 975	
20	326	13	17.42	32.46	13.2	8.46	970	-29	1.03	
40	646	13	17.47	28.37	13.4	8.71	934	-92	1.11	
80	1286	13	17.48	24.00	13.4	8.83	908	-148	1.19	
Notes:	Seg/WL = Segments per wavelength in model									
	Tot Segs = Total number of segments in model									
	El Ang = Elevation angle in degrees									
	Gn dBi = Maximum gain in dBi									
	FB dB = 180-degree front-to-back ratio in dB									
	HBW deg = Horizontal half-power beamwidth in degrees									
	F/SL dB = Front-to-sidelobe ratio in dB									
	Feed R = Feedpoint resistance in Ohms									
	Feed X = Feedpoint reactance in Ohms									
	SWR nnn = SWR referenced to value of terminating resistor in Ohms									Table 2

Table 2 provides the results of running all models under identical environmental conditions by placing each rhombic 1 wavelength over average ground at the test frequency. We need to scan the table in several different ways. First, if we compare the 3 models regardless of segmentation, we note that the terminating resistor increases value as we add the blunt end wires and increase their length. The terminating resistor was set with a segmentation of 20 segments per wavelength and remains unchanged as we increase the segmentation density for each model. The SWR reference impedance is also the resistance of the termination. For each model, as we increase the segmentation density, the feedpoint reactance grows more capacitive, and the feedpoint resistance decreases. The change in reactance is more radical than the decrease in resistance. However, reducing the terminating resistance in each model for a

better match with the feedpoint impedance for a given segmentation density will also reduce the magnitude of the reactance.

Second, we can scan each model's table for other trends occasioned by increasing the number of segments per wire. The most dramatic case is the 180° front-to-back ratio, which is also a measure of the relative size of the lobe projecting directly rearward along the rhombic centerline. In all cases, it decreases as we increase the segmentation density, leveling off in the 24-25-dB region for all three models with 80 segments per wavelength. The beamwidth is stable for all models. So too is the front-to-sidelobe ratio, although the 3-segment end-wire model shows the greatest internal variation with changes in segmentation density.

With respect to the reported forward gain, the pointed-end and 1-segment blunt-end models show the closest coincidence in two respects. First, the gain levels closely match at all levels of segmentation, as do most of the other data related to radiation patterns. Second, both models show a slowly decreasing gain value as the segmentation density increases. In contrast, the blunt-end model using 3 segments in each cross wire shows an initially higher gain value, and that value continues to increase with the segmentation density.

The relatively close values that we find in **Table 2** with respect to the performance of the pointed-end and blunt-end arrays, when each uses an optimized terminating resistor, can hide some differences. To show one of the differences, I varied the value of the terminating resistor across a wide set of values. The data in **Table 3** selects 3 values that surround the final value and suffices to reveal the critical differences in model performance.

The data columns related to the radiation patterns reveal a consistent set of curves. The gain shows almost no change, with a slight numerical increase as the value of the terminating resistor increases. The front-to-side ratio also increases with the value of the terminating resistor. The front-to-back ratio peaks at mid-range, a characteristic of rhombics as the terminating resistor approaches its optimal value. In these respects, the two models are fully consistent. Since the terminating resistor values are not too far apart, even the feedpoint resistance values are not distant from each other.

Single Wire Rhombic Performance Trends					Table 3
with Varying Terminating Resistances					
4-Wavelength Legs; 1 Wavelength above Average Ground					
Pointed-End 4-Wire Model: 20 Segments/WL					
Optimum R 850 Ohms					
R Load	Gn dBi	FB dB	F/SL dB	Feed R	Feed X
700	17.39	23.57	8.63	795	-9
900	17.39	31.99	8.78	894	41
1100	17.42	20.22	8.91	980	115
Blunt-End 6-Wire Model: 20 Segments/WL, 1-Segment End-Wire					
Optimum R 925 Ohms					
R Load	Gn dBi	FB dB	F/SL dB	Feed R	Feed X
700	17.38	22.71	8.65	807	-11
900	17.38	36.23	8.77	912	-38
1100	17.40	21.29	8.86	1004	-64
R Load = Terminating resistor value in Ohms					
Gn dBi = Maximum gain in dBi					
FB dB = 180-degree front-to-back ratio in dB					
F/SL dB = Front-to-sidelobe ratio in dB					
Feed R = Feepoint resistance in Ohms					
Feed X = Feedpoint reactance in Ohms					

The key difference between the progression of values lies in the reactance column. The pointed-end model shows a reactance that becomes more inductive as the value of the terminating resistor increases. In contrast, the blunt-end model, even though it uses only 1 segment on the short end wire, shows a reactance that becomes more capacitive as the value of the terminating resistor increases. Older literature from the 1940s suggests that the rhombic builder should use a set of perhaps 3 to 4 resistors in series rather than a single terminating resistor. The goal is to reduce the capacitance across the total termination by creating several capacitors in series. If the models reflect reality (a major presumption in the absence of a physical test rhombic), then the reactance columns might be natural. The pointed-end model already uses 2 resistors in series, and they extend from a position on one side wire to a position on the other. In contrast, the one-segment blunt-end model uses a single resistive load on a very short wire.

With respect to physical reality, much of the variation among models falls below the level of practical measurement in HF arrays, and almost all lies outside operational concerns. However, internal to a series of interrelated modeling tasks, the data in **Table 2** and in **Table 3** are important. Some models cannot use the pointed-end geometry and so must use some form of the blunt-end model. The data at hand strongly suggests that if we wish to compare the results of the new models with past models, the 1-segment end-wire blunt model yields results that are most consistent with the pointed-end models. Since our goal is to detect and appreciate general trends in rhombic performance, consistency is a virtue, if not an absolute necessity.

Multi-Wire Rhombics

Many references on rhombic design recommend the use of multiple side wires to improve performance. The wires come together at each end of the rhombic to form a single source and a single terminating resistor. However, at the midline from which we measure the tilt angle or ϕ , the wires are vertically separated by a space that runs from a few feet at lower frequencies to a few inches in the upper HF range. Some literature warns about ensuring that the center wire of the set--the one that is level with respect to ground--is not shorter than the outer wires. However, the warning is misplaced, since the actual length difference is a small part of 1%. The key caution to use in creating a multi-wire rhombic is to ensure that all wires place equal tension on the connecting points. Although some 5-wire rhombics have existed, the most common configuration uses 3 wires.

The multi-wire rhombic has enjoyed many claims of advantages over the single wire rhombic. Some have reported quieter operation, suggesting that the 3-wire array has weaker sidelobes. As well, the 3-wire array shows more forward gain than its 1-wire counterpart with the same leg length. In some places, we find claims that the 3-wire array shows a better SWR curve over an extended frequency span due to interaction among the wires that compensates for reactance. It also provides a better match for a 600-Ohm terminating resistor and common 600-Ohm transmission line. To evaluate the foundation of some of these claims, we must figure out how to model a 3-wire rhombic in a relatively reliable manner.

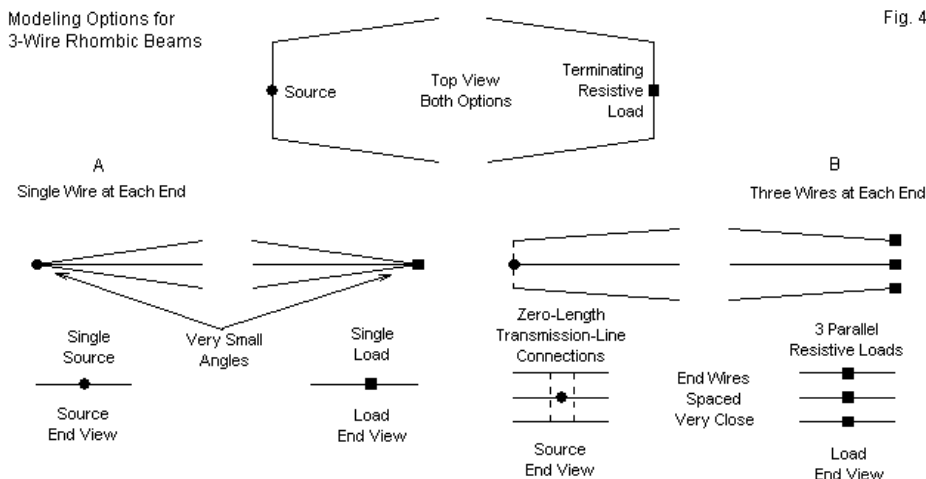


Fig. 4 shows two alternative methods of modeling the 3-wire rhombic. The top view would be the same for both models. It only indicates that we must use a blunt-end technique for the model. Given the discussion of blunt-end vs. pointed-end models in the previous section, we shall use a 1-segment end wire to form the blunt ends.

When we turn to end treatments in the lower portion of the figure, we can see more clearly our options. The simplest option (A) uses a single end wire at the source and load ends of the rhombic. The three side wires come together at each end of these wires. The source and the load are effectively centered within each end wire. The configuration presents two challenges to NEC as a calculating instrument. First, the three side wires approach the junction at very shallow angles, allowing for significant inter-penetration in the segments that form the junction. Second, NEC prefers a single segment on each side of a source segment prior to any division of the current.

The alternative to the single end wire is the use of separate end wires for each side wire (B). We may place these wires very close together so long as we allow spaces that are several times the wire radius. We may model the separate end wires using a spacing of 0.001 wavelength to achieve a simulation of a single wire. At the load end of the array, we may use separate terminating resistors on

each line. The value for a 3-wire rhombic is simply 3 times the desired equivalent single terminating resistor, since the loads are in parallel. Since the loads do not have a physical dimension, they do not affect the wire spacing.

The source wires call for slightly different treatment, although we might use 3 sources and calculate their parallel value. A simpler procedure is to create a transmission line between each outer wire and the center wire. Since lines have no physical dimensions due to the wire geometry, we can assign them any desired length. Because we wish to simulate a parallel connection, we can assign a length of $1\text{e-}10$ m or similar. The line's characteristic impedance can be virtually any value, since almost nothing happens over a near-zero line length. Using an impedance of about 600 Ohms will satisfy the situation. Of course, we place a single source on the center end wire, since transmission lines are in parallel with any source on the same segment.

One way to evaluate the alternative modeling techniques is to track what happens if we vary the value of the terminating resistor. As a test case, we can create 3-wire rhombics with 4-wavelength legs. **Table 4** provides the comparison. Since the two types of models call for different optimized terminating resistors, the resistor ranges differ. As well, they differ from the ranges used in **Table 3**, which compared pointed-end and blunt-end models of 1-wire rhombics with 4-wavelength legs. The data in that earlier table will also be important to the evaluation of 3-wire models. The 3-wire models use 1-segment end wires, so the 1-segment blunt-end model of the single wire rhombic is the appropriate comparator. All models will be 1 wavelength above average ground and use 0.16" diameter lossless wire.

Three-Wire Rhombic Performance Trends					Table 4
with Varying Terminating Resistances					
4-Wavelength Legs; 1 Wavelength above Average Ground					
Single End Wires: 20 Segments/WL. Optimum R 700 Ohms					
R Load	Gn dBi	FB dB	F/SL dB	Feed R	Feed X
500	19.14	21.57	8.26	627	118
700	19.15	26.27	8.41	702	119
900	19.17	19.51	8.52	763	120
Triple End Wires: 20 Segments/WL; Optimum R 600 Ohms					
R Load	Gn dBi	FB dB	F/SL dB	Feed R	Feed X
400	18.73	20.57	8.30	525	-67
600	18.74	30.17	8.48	599	-79
800	18.77	19.31	8.60	656	-96
R Load = Terminating resistor value in Ohms					
Gn dBi = Maximum gain in dBi					
FB dB = 180-degree front-to-back ratio in dB					
F/SL dB = Front-to-sidelobe ratio in dB					
Feed R = Feepoint resistance in Ohms					
Feed X = Feedpoint reactance in Ohms					

The use of a single end wire with 3 side wires joining at very small angles yields rather optimistic gain estimates compared to the 3-end-wire version of the model. In addition, the reactance undergoes virtually no change as we vary the value of the terminating resistor by 400 Ohms. Both of these data columns are at odds with the results for a 1-wire blunt-end rhombic model. In contrast, the 3-wire model that uses 3 end wires shows a more modest gain. As well, the pattern of capacitive reactance parallels the pattern shown in **Table 3** for the blunt-end 1-wire rhombic. Finally, the triple end-wire model shows an optimized terminating resistor value of about 600 Ohms, a value that corresponds well with actual practice.

A second relevant test of the modeling options is to compare them by varying the spacing between side wires at the midline point. As a sample, I ran the models for both options at 3 spacing increments: 0.0125 wavelength (narrow), 0.025 wavelength (medium), and 0.05 wavelength (wide). Wide spacing is 4 times narrow spacing. The total distance at the midline between the top and bottom wires is twice the spacing increment. The end-wire spacing for the triple end-wire model does not change. The results of these tests appear in **Table 5**.

Three-Wire Performance of Rhombics with 4-WL Legs with Varying Midline Separation Distances							Table 5
All Models 1 WL Above Average Ground: 13-Degree Elevation Angle 1-Segment End Wires 0.04-WL Long Single End Wire Models with Single Sources and Loads							
Mid Sp	Gn dBi	FB dB	BW deg	F/SL dB	Feed R	Feed X	SWR 700
0.013	19.15	26.27	13.2	8.41	702	119	1.18
0.025	19.27	24.22	13.2	8.42	672	123	1.20
0.050	19.40	22.36	13.2	8.44	638	127	1.24
Triple End Wire Models with Zero-Length Transmission Lines to Source and Paralleled Terminating Resistors, 1 Resistor Per Line							
Mid Sp	Gn dBi	FB dB	BW deg	F/SL dB	Feed R	Feed X	SWR 600
0.013	18.74	30.17	13.2	8.48	599	-79	1.14
0.025	18.88	30.51	13.2	8.43	600	-52	1.09
0.050	19.01	29.74	13.2	8.40	593	-42	1.07
Mis Sp = Midline maximum wire spacing in wavelengths							
Gn dBi = Maximum gain in dBi							
FB dB = 180-degree front-to-back ratio in dB							
BW deg = Half-power beamwidth in degrees							
F/SL dB = Front-to-sidelobe ratio in dB							
Feed R = Feepoint resistance in Ohms							
Feed X = Feedpoint reactance in Ohms							
SWR nnn = nnn-Ohm SWR (= terminating resistance)							

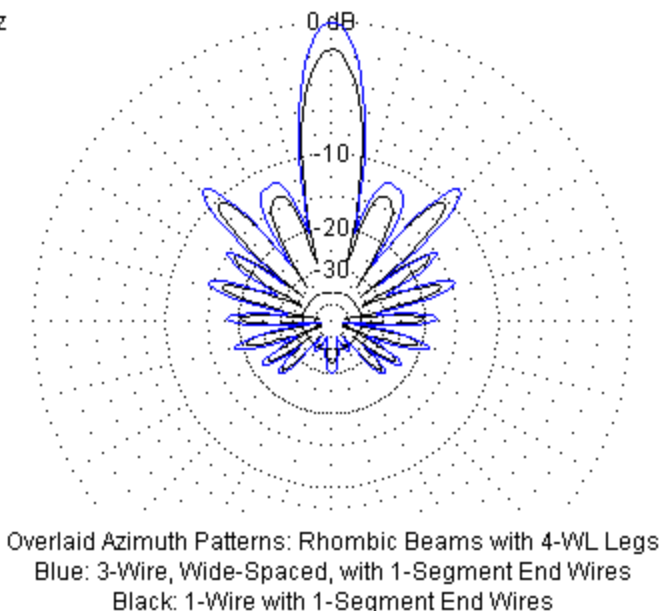
The weakness of the model using single end wires shows up in the table. The key datum is the feedpoint resistance, especially as we compare it with the corresponding datum for the triple end-wire model. As we increase the wire spacing for the triple end-wire model, the reactance undergoes some change, but the resistance remains essentially constant. In contrast, the single end wire model shows only a small change of reactance, but a large change of resistance. As we increase the angle of the side wires as they approach their junction at the end wires, the resistive component moves closer to the 600-Ohm value of the triple end-wire model. The resistance change suggests that widening the angle at the junction reduces any calculation aberrations produced by wire inter-penetration.

Option B, the triple end-wire model provides results that are thus superior to those of option A in at least 2 ways. First, they are consistent with the results for the blunt-end 1-wire rhombic model. Second, the results are internally consistent

relative to widening the midline spacing between wires. Although the reported gain is lower for the triple end-wire model, it nevertheless shows an increase with respect to increasing wire spacing. Moreover, it shows a useful gain over a 1-wire rhombic. For wide 3-wire rhombic midline spacing, the gain improvement can be up to about 1.6 dB, as shown in **Fig. 5**. The gain advantage is slightly less for narrower midline wire spacing.

3.5 MHz

Fig. 5



Note that the 3-wire rhombic not only magnifies the main forward lobe. As well, it enlarges virtually every other lobes in the radiation pattern proportionally, and without changing either the angle or the general shape of each lobe. Especially interesting in the pattern are the two innermost forward sidelobes. From the shapes, we can tell that they are in fact pairs of overlapping lobes. Both the 1-wire and the 3-wire models use an alpha angle of 24.5° to maximize gain. The lobe structure might change slightly with other values of alpha. For example, if we widen the angle further, the combined innermost sidelobes on each side of the present main lobe will eventually become stronger than the central lobe, resulting in a 3-lobe forward pattern.

To assure ourselves that we have fairly represented the advantages of the 3-wire rhombic over its 1-wire counterpart, we can perform one further test. We can increase the segmentation density of the triple end wire model and compare the progression with the one that we examined in the case of the blunt-end 1-wire rhombic. The comparison appears in **Table 6**. For both antennas, the steps use 20, 40, and 80 segments per wavelength, and the length of the end wire is reduced to maintain length parity with the adjacent segments of the side wires.

Varying Segmentation Density in 4-Wavelength-Leg Rhombic Beams 1 Wavelength above Average Ground										
Blunt-End Single-Wire Design with Single Source and Terminating Resistor on 1-Segment End Wires										
Seg/WL	Tot Segs	EI Ang	Gn dBi	FB dB	HBW deg	F/SL dB	Feed R	Feed X	SWR 925	
20	322	13	17.38	32.00	13.4	8.78	924	-41	1.05	
40	642	13	17.37	26.71	13.4	8.82	900	-124	1.15	
80	1282	13	17.35	24.23	13.4	8.82	885	-174	1.22	
Triple-Wire Design with 3 End Wires, TL to Source, and Parallel Resistors; Midline Spacing 0.025 WL										
Seg/WL	Tot Segs	EI Ang	Gn dBi	FB dB	HBW deg	F/SL dB	Feed R	Feed X	SWR 600	
20	966	13	18.88	30.51	13.2	8.43	600	-52	1.09	
40	1926	13	18.87	25.29	13.2	8.47	574	-106	1.20	
80	3846	13	18.85	22.92	13.2	8.48	558	-136	1.28	
Notes:	Seg/WL = Segments per wavelength in model									
	Tot Segs = Total number of segments in model									
	EI Ang = Elevation angle in degrees									
	Gn dBi = Maximum gain in dBi									
	FB dB = 180-degree front-to-back ratio in dB									
	HBW deg = Horizontal half-power beamwidth in degrees									
	F/SL dB = Front-to-sidelobe ratio in dB									
	Feed R = Feepoint resistance in Ohms									
	Feed X = Feedpoint reactance in Ohms									
	SWR nnn = SWR referenced to value of terminating resistor in Ohms									
	Table 6									

The 1-wire and 3-wire rhombics show quite precise parallels in the progression of values in each data column, indicating that the models are appropriate comparators. The only small divergence occurs in the reactance data, as the 1-wire rhombic model has a 133-Ohm total range, while the 3-wire model varies by only 84 Ohms. In both cases, the capacitive reactance increases as the end-wires become shorter. (However, even at the shortest length with the highest segmentation density, the modeled end wires are long compared to typical physical structures until we reach the high end of the upper HF range.)

The claims for 3-wire rhombics with which we began this section of notes find only partial confirmation in the models used to evaluate them. Using 3 wires does raise forward gain by an average of 1.5 dB for a 4-wavelength leg rhombic. The exact gain advantage depends on the wire spacing at the midline. As well, the

optimum value for the terminating resistor drops from a value between 800 and 900 Ohms down to 600 Ohms. In both cases, the models reflect both calculations and practical experience with rhombics. However, reports of quieter operation--presumably meaning freedom from what Bruce called "static" in 1931--do not find confirmation in any property of the models. For a given leg length and value of α , the 3-wire rhombics produce patterns that are congruent in almost every detail with those produced by 1-wire rhombics. If 3-wire rhombics are in fact quieter than their 1-wire counterparts, the reasons must lie outside the realm of properties that NEC models can reveal.

Among the claims associated with 3-wire rhombics is a flatter SWR curve over an extended frequency range. Over the intervening decades since the appearance of the original literature on rhombic design, accounts have undergone truncation, especially after the heyday of rhombics had passed into the history of radio communications. My suspicion is that the claim of a flatter extended-frequency SWR applies only to the use of 600-Ohm transmission lines, likely occasioned by early difficulties in constructing mechanically stable wider lines with a higher characteristic impedance. If we match the line impedance to the terminating resistor, then extended-frequency SWR curves show no significant differences. For example, **Fig. 6** provides SWR curves for the 1-wire blunt-end model and for the narrow-spaced 3-wire rhombic, with each using the terminating resistor as the SWR reference impedance.

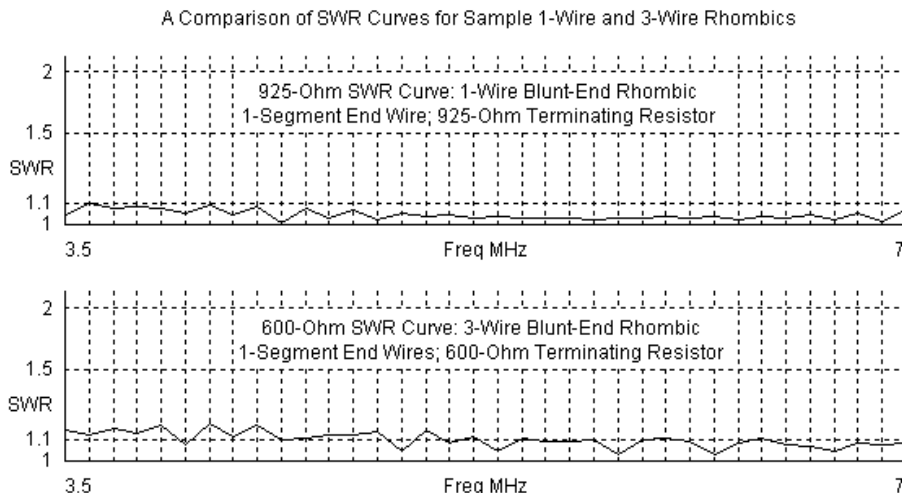


Fig. 6

The curves use a 0.1-MHz increment, which is sufficient to pick up at least some of the peak values that might occur. However, the peak SWR is 1.2:1 or less for both antennas, suggesting that there is no significant difference between them. The slightly higher values in the 3-wire curve result from the fact that the similar reactive components in both antennas represent a higher percentage of the resistive component in the more complex array. In the end, reactance compensation during final design and construction, when combined with the selection of the correct feedline impedance, will do more for the flatness of the SWR curve than the presence of 3 wires.

(In fact, one account of single-wire rhombics suggested in one paragraph the use of 600-Ohm transmission line to the feedpoint and in another suggested that the terminating load might be placed conveniently near ground level by the use of another transmission line. If the termination line had a characteristic impedance of 800 Ohms, then line length would make no difference to performance, since it would match the presumed impedance of the terminating load and the antenna when viewed as a transmission line over ground. The account reflected common practice at the time of writing, and common practice is often the source of unnoticed inconsistencies.)

In the end, a 3-wire rhombic appears to have no calculable properties other than those associated with the simulation of a very large diameter wire through the use of multiple conductors. Cage antenna elements and multiple-conductor dipole and quad loop elements are fairly common practices to increase the effective diameter of an element without resorting to excessively heavy single large elements. The rhombic 3-conductor side wires function in much the same way, although their tapered arrangement makes the determination of a single effective diameter a somewhat uncertain calculation. The use of multiple side wires is optional unless one requires either the small gain advantage or the use of 600-Ohm lines and an equal value of terminating resistor.

Our small side-trip into 3-wire rhombics has had two goals. The first was to find an effective technique for modeling the antenna, a technique that would produce results that are fully consistent with both good NEC modeling practices and reports emerging from relevant 1-wire rhombic models. "Option B," the triple end-wire model accomplished this goal. The second goal was to understand within the limits of what models can tell us whether a 3-wire rhombic might have advantages over a 1-wire version of the same rhombic. Although we focused on a single mid-size rhombic (with 4-wavelength legs) designed to optimize gain, the results are suggestive for the entire range of possible rhombic sizes.

Conclusion

Our case study has illustrated one way in which an antenna with a relatively simple initial geometry can grow into a fairly complex model. The goal in all of the modeling exercises was to produce models that met as closely as possible all of the limits inherent in NEC (in this case, NEC-4). Key to the decisions as to which of alternative models best met these requirements were two factors. One was the internal consistency of results as tested by examining short progressions of variations in model designs and segmentation. The other factor was the reasonableness of the outcomes when compared to actual field practices in the construction of commercial rhombics.

One may well ask why we should be so finicky with the selection of a model geometry. At various places, I have noted that the models are suited only for developing general trends in rhombic performance and not for specific guidance in building a rhombic. Let's look at the trends in these brief notes and extrapolate them to a larger project, perhaps one involving a systematic exploration of rhombics of many leg sizes ranging from perhaps 2 to 11 wavelengths. The trends include not just the common concerns for forward gain and front-to-back

ratio. They encompass as well trends in the value of the terminating impedance, the feedpoint resistance and reactance (at both the design frequency and over a usable passband), and the nature of the forward sidelobes. Geometrically, rhombic concerns do not cease with the selection of the leg length, but also include the angles of the wires and the effects of those angles on the resultant radiation pattern.

Fig. 5 overlaid patterns for single-wire and 3-wire rhombics in a direct comparison of radiation patterns. If we are to make such comparisons with any assurance that the comparison is valid, then the model on which each pattern is based must be consistent to the highest feasible level with the other model. Otherwise, we would have good reason to distrust the comparison--and the data that led up to it. One way to avoid rational distrust of model comparisons is to spend the required time to validate the models with respect to each other. These exercises have shown an example of the process.

In some cases, modelers appear to be content if they can achieve **a** model of the antenna they may be studying. In other cases--like this one--it is important to find **the** model for the geometry involved.

114. Modeling Folded Monopoles

The folded monopole is an interesting variation on the standard linear monopole. Essentially, the folded monopole is one-half of a folded dipole. As such it retains two important properties. First, the act of folding results in an increase in the feedpoint resistance relative to the linear or open-ended monopole. The exact ratio of impedance transformation depends on the relative diameters of the fed and the "other" wire. The transformation ratio answers to the same equation that we have often seen for the folded dipole. Although the ratio of wire diameters provides the key variable in the equation, the spacing between the wires plays a significant role in two ways. The terms of the ratio itself are each ratios of diameter to spacing. For reference, the following equation appears in many texts, where R is the ratio of impedance compared to the open-ended linear antenna, s is the center-to-center spacing of the wires, and d_1 and d_2 are the 2 diameters, with d_1 representing the fed wire.

$$R = \left(1 + \frac{\log \frac{2s}{d_1}}{\log \frac{2s}{d_2}} \right)^2$$

As well, the wires must be close enough to each other to ensure that the pair forms a transmission line and not a simple wide-spaced half loop. The fact that the folded monopole is itself a transmission line comprises the second major property of the folded monopole.

If the folded monopole is shorter than a self-resonant length, that is, is shorter than an electrical quarter wavelength, then the transmission-line aspect of folded monopole behavior is a shorted transmission line. Alternatively expressed, the line is an inductive reactance up to about 50 degrees electrical length, depending upon the diameters and spacing of the wires in the folded monopole. The characteristic impedance of the line is mostly a function of the folded monopole physical properties. For a two-wire monopole, the key elements that set the characteristic impedance are the center-to-center element spacing and the diameter of the elements. For a given construction (that is, for a given element diameter, spacing, and total height), the characteristic impedance does not change with frequency (if we ignore the effects of a real or lossy ground for the moment). The inductive reactance becomes a function of the folded monopole

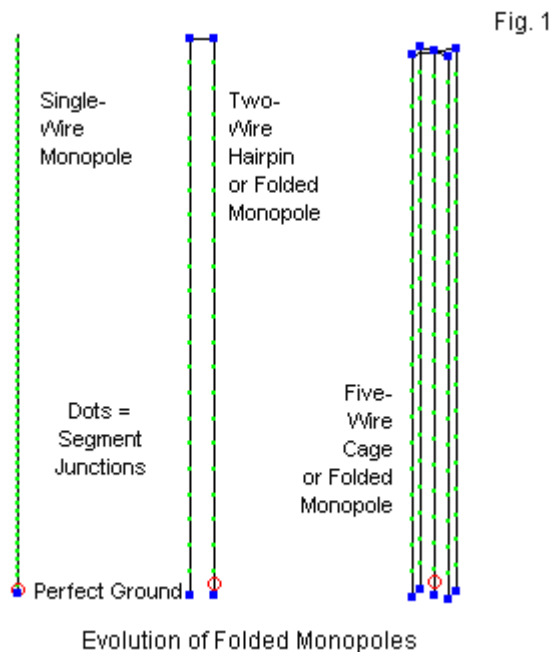
height measured in terms of a wavelength. The inductive reactance is then a tangent function of the electrical length translated into degrees or radians. We then may calculate the equivalent inductance by using the standard relationship among reactance, inductance, and frequency. However, the source impedance of the folded monopole, being a function of both radiation and transmission-line characteristics, will not be the same as the inductive reactance of a shorted transmission having the same length.

Many antenna designers for the MF and lower HF ranges prefer the folded monopole to the linear monopole, especially when the overall height must be shorter than a resonant length. Since the transmission-line aspect of the antenna's behavior always yields an inductive reactance for such lengths, tuning networks may use inherently high-Q capacitors exclusively and avoid low-Q inductors. The effort to design such antennas leads to modeling attempts in NEC or MININEC. The seemingly simple antenna should yield equally simple models. Unfortunately, all too often the simple models prove to be quite inadequate. In these notes, I want to review a number of places in which the modeling may go astray.

For uniformity through the exercise, I shall use some constants. The modeling frequency will be 3.5 MHz. The lossless wire will be 0.1" in diameter, although we shall also use a 1" wire under certain specified conditions. To simplify ground radial aspects of the model--which might create some ungainly models--and to avoid the variable of the ground losses, I shall place the model on perfect ground. This ground type will satisfactorily reveal most of the modeling dangers that we may encounter. I shall also use two different programs and cores. One core is NEC-4, which performs better than NEC-2, but still not perfectly. I shall contrast the NEC-4 results with MININEC outputs from Antenna Model, perhaps the most corrected version of MININEC 3.13 available.

Fig. 1 shows the initial evolution of the models that we shall examine in detail. The linear resonant monopole will become the standard against which we may compare the other models. Next, we shall turn to the two-wire or "hairpin" folded monopole. Finally, we shall examine a simple 5-wire cage folded monopole. In all cases, we shall designate a prime or fed wire. In the case of the cage, we shall use the center wire to simplify feeding. We shall later briefly note how to feed the outer wires in parallel. For reasons that we shall explain as we move along, the linear monopole uses more segments for essentially the same height as the outlines of the folded monopoles. The brief reason is that folded monopole

models using the higher segment density would not show the space between wires very well.



Both linear and folded monopoles show about the same gain and the same pattern shape, as revealed in **Fig. 2**. There is one very minor exception to this statement. A two-wire folded monopole will show a very slight difference between the gain broadside to the pair of wires than in line with the wires. Gain on the fed side will always be numerically but not operationally higher than gain in the direction of the unfed wire. The exact differential varies with the wire spacing, but generally is less than 0.1 dB for all practical spacing and wire-diameter values.

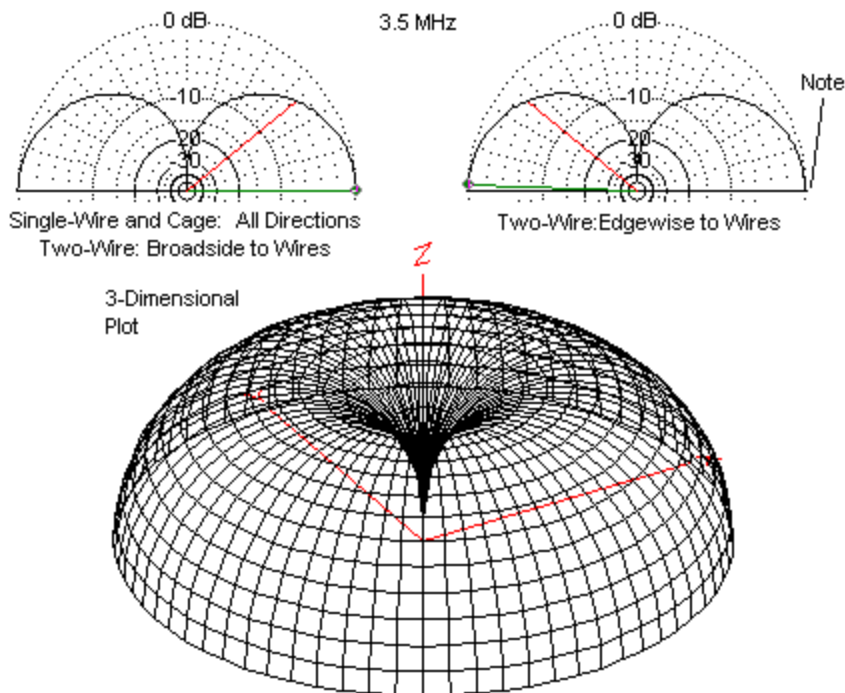


Fig. 2 Typical Plots for All Monopoles over Perfect Ground

Let's model the linear monopole over perfect ground in both NEC-4 and MININEC as a baseline data set for future reference. **Table 1** shows the results of supplying the models with 69 segments, with the feedpoint or source on the lowest segment.

Table 1. Model Reports: Single Wire Monopole 69 Segments at 3.5 MHz
Wire Diameter 0.1", Lossless Wire; Perfect Ground

	NEC-4 (EZNEC)	MININEC (Antenna Model)
Height in feet	68.4	68.4
Max. Gain in dBi	5.15	5.15
Feedpoint Impedance		
R +/- jX Ω	36.0 - j0.6	36.0 - j0.6
AGT	1.000	0.9998
AGT dBi	0.00	0.00

The table shows that both cores provide the same output reports, just as we might expect for this modest frequency and well-segmented model. Each segment is about 1' long. Both models show an ideal or nearly ideal Average Gain Test (AGT) score. Antenna Model actually provides the raw calculated number, which over perfect ground is twice the value shown. I have adjusted the number to coincide with the EZNEC or free-space value. My reason is simple. 10 times the common log of the free-space AGT score provides the adjustment factor necessary to correct the gain report when the AGT score is not ideal. The AGT dBi entry provides the calculated correction factor, which is 0.0 for this simple model.

We are now ready to create a model of a two-wire folded monopole. **Fig. 3** will provide some guidance.

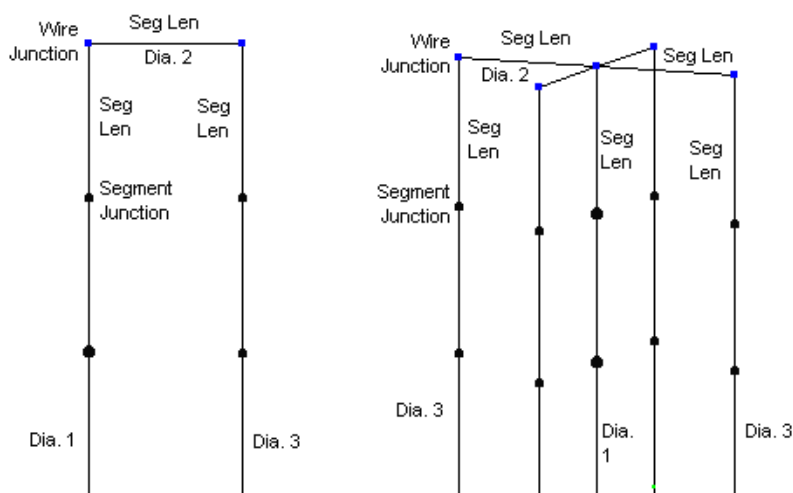


Fig. 3

Basic Modeling Requirements for the Monopole Wires

Good modeling practice dictates that we adhere to certain guidelines when constructing the wires of a model. In NEC, keeping the segment length more than twice the diameter or 4 times the wire radius ensures the most accurate current calculations. We can reduce that ratio in NEC-2 by invoking the EK command, and NEC-4 generally is accurate with a 2:1 segment-length-to-diameter ratio. Antenna Model recommends that the segment length be at least 1.25 times the wire diameter for best accuracy with its modified MININEC core. The use of 1' segment lengths with 0.1" diameter wire ensures that we shall not have problems in this department.

Second, adjacent segments should have similar lengths, especially in NEC and especially in high-current regions of the antenna assembly. The two-wire portion of the figure shows a spacing (and 1-segment end wire) that is 1' long, matching the segment length of the long wires. The resulting folded monopole will have 139 segments, not very high for today's fast computers. Some programs, like EZNEC, provide for a length-tapering feature to reduce the segment count while keeping the segment length at one or both ends of the wire at a selected minimum length (in this case 1'). The NEC GC command achieves the same goal but uses a different length-tapering algorithm. We may bypass these steps by

creating a 139-segment model both in EZNEC and in Antenna Model. The results appear in **Table 2**.

Table 2. Model Reports: Two-Wire Monopole 69 Segments at 3.5 MHz;
Wire Separation: 1', Wire Diameter 0.1", Lossless Wire; Perfect Ground

	NEC-4 (EZNEC)	MININEC (Antenna Model)
Height in feet	67.25	67.25
Max. Gain in dBi	5.15 (5.17/5.13)	5.15 (5.17/5.13)
Feedpoint Impedance		
R +/- jX Ω	143.5 + j0.12	143.5 - j0.7
AGT	1.000	0.9998
AGT dBi	0.00	0.00
Calculated Impedance (Ω)	144	

Once more, the output reports from the two programs are almost identical. Both programs can handle the folded monopole composed of a single wire diameter throughout with all of the other modeling guidelines in order. The height of the resonant folded monopole is shorter than the height of the linear monopole because, with respect to its radiation behavior, the double wire acts like a single fatter wire. The gain entry shows a sample of the in-line gain differential, while the main part of that entry shows the broadside value.

The resistive component of the source impedance is 143.5 Ohms. The fact that the wires have the same diameter with a constant spacing between them yields the familiar 4:1 impedance transformation ratio. 4 times 36 Ohms (for the linear monopole) is 144 Ohms. So far, all is simple and well.

Let's now create a cage-type folded monopole with the center wire fed, using the right side of **Fig. 3** as a guide. The outer wires that return to ground use the same segmentation as the single return wire of the model that we have just reviewed. The end wires are each 1' long to preserve the identity of segment lengths throughout the model. Since we shall be reducing the overall antenna height, the total segment count for the model is 319. **Table 3** shows the results.

Table 3. Model Reports: Five-Wire Monopole 69 Segments at 3.5 MHz;
Wire Separation: 1', Wire Diameter 0.1", Lossless Wire; Perfect Ground

	NEC-4 (EZNEC)	MININEC (Antenna Model)
Height in feet	63.0	63.0
Max. Gain in dBi	5.05	5.11
Feedpoint Impedance		
$R \pm jX \Omega$	1659 + j227.4	1679 + j175.8
AGT	0.988	0.9996
AGT dBi	-0.05	0.00
Adjusted Gain	5.10	5.11

The models show several interesting facts about modeling cage-type folded monopoles. Starting with the impedance, we notice a very great increase in the resistive component. (The reactive component did not go to zero using height increments of 0.1', so the table shows the lowest value attained.) The cage monopole is essentially a form of coaxial transmission line structure. Ideally, the wire diameter values used to calculate the impedance transformation would use the center wire value and the effective diameter of the ring of cage wires. For these cases, the transformation equation will not work. If we feed the center wire, then $2S/d2$ is 1 and its log is zero, leading to a calculational error or to an indefinitely large value for the ratio, depending on whether you are using a computer or a scratch pad. Likewise, if we feed the outer wires in parallel, then $2S/d1$ becomes 1 and its log is zero. This partial result leads to a ratio of 1.0 for all cases. However, we cannot be certain that the value of $d2$ is in fact 2' for this example, since the structure has more open area than closed area, and the cage wires are thin. The reported values from the model are sufficiently high to establish that we have a thin fed wire and a very fat "other" or return wire, just the conditions that yield a very large transformation value by standard calculations. The other significant fact to note is the AGT of the NEC-4 output report. 0.988 is not an ideal value and requires a correction of 0.05 dB to the gain report. As the table suggests, when the calculated adjustment factor is negative, we increase the raw report by the absolute value of the adjustment factor. Had the calculated adjustment factor been positive, we would have subtracted it from the raw gain report. The MININEC AGT score shows no need for adjustment, and the raw gain report is very close to the adjusted NEC-4 number.

NEC-4 appears to drift somewhat off an ideal AGT value due to the proximity of 4 wires to the fed wire, as well as the current division at the top of the model. A single return-wire did not produce this consequence. NEC-2 is even further distant from an ideal AGT score, yielding a value of 0.928 for the same model. Hence, its gain report would be 0.32-dB low. Some scales of model adequacy as measured by the AGT score use limits of 1.05 and 0.95 as marking the ends of truly reliable models. I tend in most of my work to use even tighter limits. The NEC-2 AGT value lies well outside even fairly loose limiting values.

Although the Average Gain Test is a necessary, but not a sufficient, condition of model adequacy, it is an important test for all models. Modelers should routinely apply the test, since it may minimally require correction of the gain reports. If one is conducting systematic modeling exercises designed to show performance trends, then the AGT is essential lest one misread the trends.

If we are searching for general properties of a particular type of antenna, we may alter the model to overcome some of the limitations that we might encounter initially. **Fig. 1** showed two-wire and five-wire folded monopoles that used fewer segments per unit of antenna height. However, each return wire used a wider spacing from the center fed wire. Let's explore this avenue of modeling to see what emerges. First, we may increase the spacing from the center wire to 3' and still have an effective folded monopole at 3.5 MHz. The end wires will use a single segment. To keep all segments roughly the same length, we shall reduce the total number of segments in the 2-wire monopole to 22. The overall height will be 66.3', in keeping with the increase in the "fat wire" effect of placing the wires 3' apart. **Table 4** shows the results from the new model using each program.

Table 4. Model Reports: Two-Wire Monopole 22 Segments at 3.5 MHz;
Wire Separation: 3', Wire Diameter 0.1", Lossless Wire; Perfect Ground

	NEC-4 (EZNEC)	MININEC (Antenna Model)
Height in feet	66.3	66.3
Max. Gain in dBi	5.15 (5.19/5.09)	5.15
Feedpoint Impedance		
$R \pm jX \Omega$	143.2 - j0.33	143.3 + j0.5
AGT	1.000	0.9988
AGT dBi	0.00	0.00
Calculated Impedance (Ω)	144	

Increasing the spacing yields a two-wire NEC-4 model that is almost identical in performance to the more narrowly spaced two-wire model. The AGT is ideal and the impedance a virtually the same at 4 times the linear monopole value (within less than 1 Ohm). Interestingly, the MININEC results in Antenna Model show a nearly ideal AGT value and a very close impedance coincidence to the NEC-4 model. The gain remains on target (using the value broadside to the plane of the 2 wires).

We have enough data to let us try a five-wire model in each system using the wider spacing and the reduced overall segmentation. The five-wire model will be shorter than the two-wire model, so the vertical wires will use 21 segments each. **Table 5** provides the output reports.

Table 5. Model Reports: Five-Wire Monopole 21 Segments at 3.5 MHz;
Wire Separation: 3', Wire Diameter 0.1", Lossless Wire; Perfect Ground

	NEC-4 (EZNEC)	MININEC (Antenna Model)
Height in feet	63.0	63.0
Max. Gain in dBi	5.09	5.12
Feedpoint Impedance		
R +/- jX Ω	1568 + j231.4	1237 + j252.3
AGT	0.999	0.9988
AGT dBi	0.00	0.00

Both models provide excellent AGT values. As well, the difference between the gain values has decreased to merely 0.03 dB. However, we see a considerable difference in the reported impedance values. It is likely that some, if not all, of the difference stems from the fact that with a high impedance, very small differences between models will result in outsized changes of some calculated results. We normally think of such changes as modifications that we might make to the geometric structure. However, in this case, the difference is most likely a product of the difference in the calculation methods.

Most folded monopole systems consist of one fat element (often a tower structure) and one or more thin wires. Without changing anything else, we may explore what happens when we increase the diameter of the fed wire to 1", that is, increase the diameter by a factor of 10. 1" is well below the effective diameter of most towers, but the differential with the return wire should be enough to

reveal any calculation difficulties that might be a core function. If we apply the fed-wire diameter increase to the two-wire folded monopole, we obtain the results in **Table 6**. Note that we did not change the overall antenna height relative to the previous two-wire model.

Table 6. Model Reports: Two-Wire Monopole 22 Segments at 3.5 MHz;
Wire Separation: 3', Wire Diameter 0.1", Lossless Wire; Perfect Ground
Fed Wire Increased to 1" Diameter

	NEC-4 (EZNEC)	MININEC (Antenna Model)
Height in feet	66.3	66.3
Max. Gain in dBi	5.27	5.15
Feedpoint Impedance		
R +/- jX Ω	100.7 + j1.5	97.8 + j1.9
AGT	1.029	0.9985
AGT dBi	0.12	0.00
Adjusted Gain	5.15	5.15
Calculated Impedance (Ω)	98.0	

The MININEC version of the model shows one advantage of its system: it is less sensitive than NEC to junctions of wires having dissimilar diameters, whether those junctions are linear or angular. The AGT value is very close to the ideal and requires no gain report change. Both the gain and the impedance reports are closer to the calculated value than is the NEC report, although the difference is small.

NEC-4 shows an AGT score that is off the mark by a noticeable amount. Hence, the raw gain report is about 0.12-dB too high, but after correction, it returns to the expected value. (NEC-2 under the same conditions produced an AGT score of 1.137, a wholly unreliable score for a model. The correction factor requires a raw gain reduction of 0.56 dB. The result might be in the ballpark for expectations, but we likely could not trust the impedance reports.) NEC-4's raw impedance report is fairly close to the MININEC report. However, trying to adjust it with the AGT multiplier carries it further from the MININEC value. In effect, we are now modeling in a region where NEC (-2 and -4) does not produce the most accurate results due to the junctions of wires with different diameters.

The impedance reports are less than 4 times the impedance of the (36-Ohm) linear monopole because the fed wire is considerable larger in diameter than the

return wire. As the fed wire increases in diameter for a constant-diameter return wire, the transformation ratio will continue to decrease, but it can never descend below a 1:1 ratio. A folded monopole (or a folded dipole) cannot be an impedance down-converter.

When we apply the same fed-wire diameter increase to the five-wire model, we obtain interesting results. Once more, we retain the same overall antenna height that we used in the previous five-wire model with its uniform wire diameter. **Table 7** shows the model reports.

Table 7. Model Reports: Five-Wire Monopole 21 Segments at 3.5 MHz;
Wire Separation: 3', Wire Diameter 0.1", Lossless Wire; Perfect Ground
Fed Wire Increased to 1" Diameter

	NEC-4 (EZNEC)	MININEC (Antenna Model)
Height in feet	61.6	61.6
Max. Gain in dBi	5.52	5.10
Feedpoint Impedance		
$R \pm jX \Omega$	770.3 + j1.5	686.3 - j57.4
AGT	1.100	0.9995
AGT dBi	0.41	0.00
Adjusted Gain	5.11	5.10

The NEC-4 model shows near resonance almost accidentally. However, the most important aspect of the report is the further departure from an ideal AGT score and the requirement for a sizable correction factor to the raw gain report. (NEC-2 produced an AGT score of 1.177 for the same model, indicating a required correction of 0.71 dB to the raw gain report.) In contrast, the MININEC model--as provided by Antenna Model--remains close to ideal in its AGT score. The raw gain report is also very close to the NEC-4 corrected value and well-suited to the shorter overall height of the model, relative to the 68.4' linear monopole. (Hence, the slightly higher two-wire gain reports remain an anomaly in the overall model progression.)

Simple models of folded monopoles tend to ignore the remaining structure of a tower or mast that has been converted to folded monopole use. We may easily test whether or not we are well or poorly advised to ignore such upper-end

lengths of structure beyond the limits of the folded-monopole proper. For these initial tests, we may add an extension to the 1" fed or center wire of both folded monopoles that we have just tested without an extension. Let's add 10' of 1" diameter wire to the top of the structure and use about 5 segments. Because the extension is a low-current region of the antenna, the exact segmentation will make only small differences to the source impedance report and almost none to the gain and AGT reports. The height of the antenna up to the extension is the same as in the previous two-wire and five-wire folded monopoles. See **Fig. 4**. Our goal is to see if the mast extension makes a difference, and if there is a difference, we expect it to appear most prominently in the source impedance report.

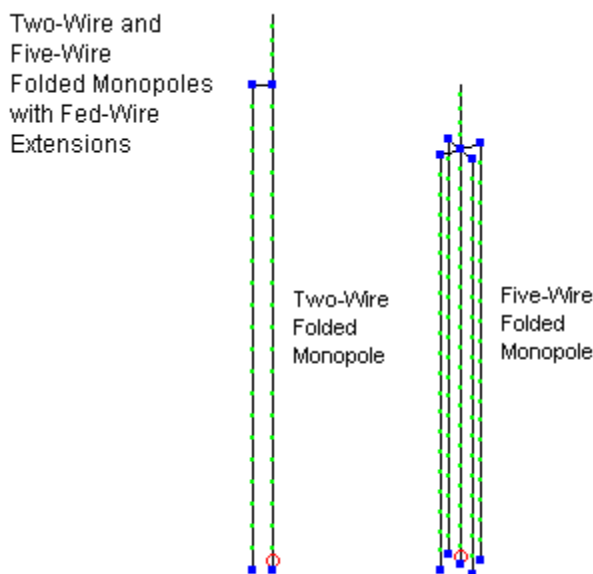


Fig. 4

If we run both models using EZNEC/4 and Antenna Model, we obtain the results in **Table 8**. In this case, we may pass over the AGT issues and focus on the source impedance. Compared to the values shown in **Table 6**, the new values clearly show that the extension raises the resistive component of the impedance and adds a very significant inductive reactance to the overall impedance.

Table 8. Model Reports: Two-Wire Monopole 22 Segments at 3.5 MHz;
Wire Separation: 3', Wire Diameter 0.1", Lossless Wire; Perfect Ground
Fed Wire Increased to 1" Diameter; Extended 10'

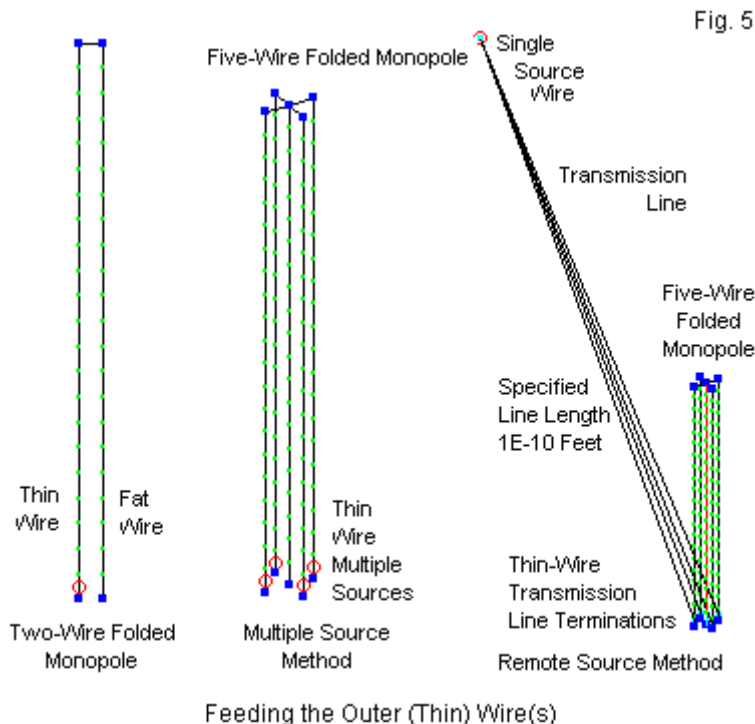
	NEC-4 (EZNEC)	MININEC (Antenna Model)
Height in feet	66.3 + 10.0	66.3 + 10.0
Max. Gain in dBi	5.42	5.29
Feedpoint Impedance		
R +/- jX Ω	133.5 + j129.7	132.1 + j127.5
AGT	1.042	0.9987
AGT dBi	0.18	0.00
Adjusted Gain	5.24	5.29

The five-wire version of the folded monopole shows the same general pattern of impedance. Compare **Table 9** to **Table 7**. The inductive reactance has grown significantly--faster than in the two-wire model.

Table 9. Model Reports: Five-Wire Monopole 21 Segments at 3.5 MHz;
Wire Separation: 3', Wire Diameter 0.1", Lossless Wire; Perfect Ground
Fed Wire Increased to 1" Diameter; Extended 10'

	NEC-4 (EZNEC)	MININEC (Antenna Model)
Height in feet	61.6 +10.0	61.6 +10.0
Max. Gain in dBi	5.57	5.16
Feedpoint Impedance		
R +/- jX Ω	593.0 + j291.2	583.3 + j239.6
AGT	1.099	1.0001
AGT dBi	0.41	0.00
Adjusted Gain	5.16	5.16

Although feeding the center wire/fat wire of the various folded monopole models has served well to reveal some features of modeling, it does not reflect what AM BC and amateur applications may encounter in practice. Normally, we would feed the thinner wire, while leaving the central tower or fat wire grounded. The two-wire monopole requires only a small adjustment to correct this situation, but the five-wire models will need a different strategy. **Fig. 5** shows our options.



The two-wire model only requires that we move the source from the fat wire to the thin wire. We shall use the same model whose results appear in **Table 6**: a 66.3' folded monopole. This time we shall place the source on the lowest point of the 0.1" thin wire and leave the 1" fat wire as a return to perfect ground. The results of this model revision appear in **Table 10**.

Table 10. Model Reports: Two-Wire Monopole 22 Segments at 3.5 MHz; Wire Separation: 3', Wire Diameters 1.0" and 0.1", Lossless Wire; Perfect Ground Thin Wire Fed.

	NEC-4 (EZNEC)	MININEC (Antenna Model)
Height in feet	66.3	66.3
Max. Gain in dBi	4.96	5.15
Feedpoint Impedance R +/- jX Ω	221.5 + j9.0	232.5 + j8.8
AGT	0.958	0.9993
AGT dBi	-0.19	0.00
Adjusted Gain	5.15	5.15
Calculated Impedance (Ω)	232.0	

We do not lose the deficiencies of NEC by moving the source point. The AGT value shows that we need to adjust the gain report by 0.19 dB to obtain the expected value of about 5.15 dBi. However, note that the AGT value is now less than an ideal 1.0 rather than being greater than 1.0. The Antenna Model version of the revised model shows an admirable AGT value and gain value. Finally, note the increase in the source resistance that results from using a thin fed wire and a fat return wire (relative to the reverse situation shown in **Table 6**). Once more, the MININEC core reports an impedance that is closer to the calculated value.

The five-wire monopole presents us with a different challenge. We might be tempted to end all 4 outer thin wires above ground by a foot and then connect all of them around the center wire. A short wire to ground from one corner would become the source wire. This procedure might seem to reflect the actual physical structure of a folded cage-type monopole, but it creates a number of modeling error sources. The segment lengths in the model are 3' long, so the series of connecting wires and the source wire introduces aberrant segment lengths. As well, the source segment and the adjacent segments would not have equal lengths, a desirable situation especially in NEC for the most accurate calculations. Moreover, the segment junctions of the outer wires would no longer parallel the segment junctions of the center wire, an undesirable condition in NEC for highest accuracy. Finally, the current division among the outer wires would not be equal, resulting in possible pattern and impedance errors

A more secure method to retain whatever accuracy the model has would be to use 4 sources, one on each outer thin wire. This technique is equally applicable to NEC and to MININEC. To arrive at a net single-source impedance value, we need only divide one of the source impedance reports by 4, taking the resistive and the reactive components separately. If we use the model whose result appear in **Table 7** as our starting point, we need only replace the single source on the center 1" wire with 4 sources, one on each of the outer thin wires. We shall leave the modeled antenna height at 61.3'. The results of our efforts appear in the top portion of **Table 11**.

Table 11. Model Reports: Five-Wire Monopole 21 Segments at 3.5 MHz;
Wire Separation: 3', Wire Diameter: Center: 1.0" Outer: 0.1"; Lossless Wire
Perfect Ground; Thin Wires Fed

Parallel Sources	NEC-4 (EZNEC)	MININEC (Antenna Model)
Height in feet	61.6	61.6
Max. Gain in dBi	4.98	5.10
Feedpoint Impedance		
R +/- jX Ω /4	211.6 - j92.0	214.3 - j94.0
Net R +/- jX Ω	52.9 - j23.0	53.6 - j23.5
AGT	0.973	0.9994
AGT dBi	-0.12	0.00
Adjusted Gain	5.10	5.10
Remote Single Source	NEC-4 (EZNEC)	
Height in feet	61.6	
Max. Gain in dBi	4.98	
Feedpoint Impedance		
R +/- jX Ω	52.9 - j23.0	
AGT	0.973	
AGT dBi	-0.12	
Adjusted Gain	5.10	

Because we are now feeding the outer conductor, the effective diameter of which is greater than 1", the net impedance is considerably lower than the value found in **Table 7**, the model the feeds the inner and effectively thinner conductor of this concentric model. However, do not be fooled by the deceptively attractive resistive value. An actual tower situation will place a much larger diameter center

conductor into the model. As a useful but imperfect guide, BC engineers conventionally use the following diameters as 1-wire substitutes for antenna towers. For a triangular tower, use a wire with a radius of 0.37 times the face dimension. For a rectangular tower, use a wire with a radius that is 0.56 times the face dimension. You can adjust the spacing of the wires from the central tower and their diameter (and even their number) to arrive at a desired impedance, since the value (over perfect ground) will not go below 36 Ohms in an adequate model.

The parallel-source method of feeding the cage folded monopole is convenient for initial modeling, but it will not suit models to which we wish to add matching components or loads. We may use in NEC an alternative technique that arrives at the same source impedance value, but uses only a single source. The right portion of **Fig. 5** shows the essential elements of the technique. We terminate a transmission line at each of the former source segments. The other set of terminations appear on a single segment wire that is a considerable geometric distance from the antenna. The distance is sufficient to prevent the wire from interacting significantly with the main antenna wires. In the present case, the wire happens to be about 140' from the antenna. As well the wire is very short (0.3' in this case) and may be very thin, although I retained the 0.1" diameter used with other wires. The 4 transmission lines that terminate on this new wire are in parallel with each other and in parallel with a source that we place on the wire. The physical position of the new wire only prevents wire interactions, but does not itself determine the length of the transmission lines. We may set these lines to the shortest length feasible. I used 1E-10 feet in EZNEC, but you may use simply the shortest length allowed by your particular core. Because the line is not a physical line and plays no role in the matrix calculations, line routing is unimportant. As well, because the line is so short, its characteristic impedance is unimportant. I used 200 Ohms, which roughly corresponds to the impedance of the individual former source segments. The transmission-line technique places all 4 outer-wire segments in parallel. The single source on the remote wire records the parallel source value. The lower portion of **Table 11** shows that we obtain the same source impedance that we derived from the parallel source technique.

The alternative transmission-line feeding system has an important advantage. We may extend the remote wire structure and incorporate loading/matching impedances. Essentially, we use a matrix of very short and thin wires to replicate the structure of a network, adding components to the series and/or parallel legs

as needed to make up the actual network. (NEC2GO has a built-in method for creating source point networks.)

However, the method also carries a caution. NEC-4 shows a usable but less than ideal AGT score. As we have seen, NEC-2 AGT values are much worse when we have junctions of wires with different diameters. The networks that we add can only be as accurate as the initial source impedance values prior to adding the new components, and NEC-2 source impedance values may be inaccurate.

A folded monopole also tends to imply a buried radial system in the MF and lower HF regions of the spectrum. We have not looked at the effects of adding such a system or how best to model such a system. However, experience has taught that none of the alternative modeling systems that we might use will adequately substitute for a NEC-4 set of below-ground radials. (There are copious notes on this situation with respect to standard monopoles in *Ground-Plane Notes*, available from *antenneX*.) The folded monopole requires careful treatment as we approach ground level to ensure that we do not violate good modeling procedures while developing a common ground point for all necessary wires.

Those who build and install wire cages for AM BC antennas tend to call them "skirts," although the general informal name is often associated with an alternative use for the cage. Between the cage base and ground, installers may place tuning elements and thus detune the tower relative to a given frequency. The technique has application to cellular and other UHF antenna towers that fall within the quite large near-field radius of an existing AM BC antenna, where unwanted interactions might distort the certified pattern for the AM antenna system. It may also apply to the antennas of different stations whose antennas lie within the near-field of each other. In most cases, skirt assemblies have standard sizes (at least with respect to outside diameter). Installers have developed a considerable number of techniques for bringing the overall tuned filtering frequency to the desired point. If you model a commercial assembly, note the presence of periodic spacers and shorting rings. These assemblies serve both mechanical and electrical purposes. Hence, the shorting ring belongs in the model.

Some engineers who employ cages on towers to convert the monopole into the alternative transmitting assembly also prefer the term "skirt," since the assembly (as noted above) does not answer to standard equations for folded

dipoles/monopoles. See, for example, the NAB 1997 paper by Rackley, Cox, Moser, and King ("An Efficiency Comparison: AM/Medium-Wave Series-Fed vs. Skirt-Fed Radiators"). Other engineers retain the term "folded monopole" or use the expression "folded isopole." Whatever the preferred label, the cage-style folded monopole retains its incomplete shielding by the cage and hence leaves an impedance that one may best approximate by appropriate models, subject to field testing and adjustment.

For those interested in ferreting out the effects of a relatively open but surrounding skirt, modeling may provide more data than just the anticipated feedpoint impedance. With respect to 2-wire folded or hairpin monopoles, Kuecken's method of separating transmission line from radiation currents (see pp. 224 ff of his *Antennas and Transmission Lines*) has proven effective for the analysis of both folded monopole and folded dipole models that use 2 wires. NEC and MININEC both provide a record of relative current levels along the wires of a caged or skirted antenna, and investigators might well use the data to develop the relative roles of transmission-line and radiation currents with these antennas.

As incomplete as this treatment may be, it still provides some guidance on the initial modeling of both two-wire and cage-type folded monopoles. With due attention to AGT values and correctives, as well as to the reasonableness of reported output values from the calculating core in use, we may successfully model folded monopoles using either NEC or MININEC. However, as always, hasty or careless modeling leads to relatively useless results. The rule of GIGO strictly applies to antenna modeling.

115. Single, Bifilar, and Quadrifilar Helices

Every so often, someone asks me if I have a sample file for a bifilar or a quadrifilar helix. Such helices are subject to numerous variations in mounting, connections, and feeding. Hence, rather than simply show a sample file, it may be useful to examine at least two ways in which we can create these antenna structures. In the following notes, we shall look at a version in which every segment appears as a separate wire and at a version that uses some of the "summary" or "global" geometry structure commands available in NEC-2 and NEC-4.

All helices within these notes will use a single set of specifications. The helix turns will have a radius of 1 meter. The turns will be separated by 1 meter, and we shall use 3 turns, for a total helix length of 3 meters. Throughout, there will be 20 segments per turn to simulate within reasonable boundaries a continuously nearly circular structure. The wire diameter will be 1 mm (0.001 m), which gives us a wire radius of 0.5 mm (0.0005 m). The importance of giving both the diameter and the radius will become apparent as we proceed through the methods that we shall explore.

A Review of Single-Helix Models using GH

In episodes 62 and 63 of this series, we explored in some depth the use of the GH command to form a helix. In those episodes, we noted that the GH command was a later addition to NEC-2 and may differ according to the version you might be using. To form a single helix having the requisite specifications in the version of the command used by NEC-Win Pro, we can employ the help screen shown in **Fig. 1**.

Generate Helix - NEC2

Tag: Spacing between Turns:

Segments: Total Length of the Helix:

Wire Radius:

Radius in X at Z = 0: Radius in X at Z = Total Length:

Radius in Y at Z = 0: Radius in Y at Z = Total Length:

Structure will be a helix if X at Z = 0 equals X at Z = Total Length and Total Length is greater than zero.

Fig. 1

Several items are worth reviewing. The NEC-2 GH command requests a user specification of the spacing between turns and the total helix length, from which it calculates the number of turns. The helix uses a single wire radius throughout. The basic helix begins at $Z=0$ and progresses upward, with the first radius point along the X-axis. The basic helix orientation is right-handed. To create a left-handed helix, we would make the total length entry negative. The resulting model, carried only as far as the GE line plus a frequency entry, looks like the following lines:

```
CM single helix-nec-2
CE
GH 1 60 1 3 1 1 1 1 .0005
GE
FR 0 1 0 0 299.7925 1
EN
```

In NEC-4, the GH command changes its form, and the help screen in GNEC for our current structure appears in **Fig. 2**.

In NEC-4, we specify the number of turns (with fractional turns possible) and the total length of the helix; the command then calculates the space required for each turn. NEC-2 had offered us separate radii for the X- and the Y-axes, but NEC-4 employs a uniform radius. In part, this change results from the desire to give the user a choice between log and Archimedes spirals. Our simple structure uses the uniformly spaced Archimedes spiral. Like the NEC-2 helix, the NEC-4 version begins at $Z=0$ with the first radius point along the X-axis. However, to form a left-hand helix in NEC-4 requires that we use a negative numbers for the number of turns. The resulting NEC-4 model of the basic single helix appears in the following lines:

```
CM single helix-nec-4
CE
GH 1 60 3 3 1 1 .0005 .0005 1
GE
FR 0 1 0 0 299.7925 1
EN
```

In both cases, we entered the total number of turns in the helix, allowing the command to distribute them among the individual turns. **Fig. 3** shows the conventionalized outline of the helix that we created with the 2 versions of the GH command. The sketch includes segment markers to allow counting. More significantly, the sketch provides the reason why I chose the specifications for the sample model: they provide a very open structure so that we can hope to see the details of more complex helical arrangements.

A GH-Generated Single Helix

Radius = 1m

No. Turns = 3

Turn Spacing = 1 m

Total Length = 3m

Wire Diameter = 0.001m

Wire Radius = 0.0005 m

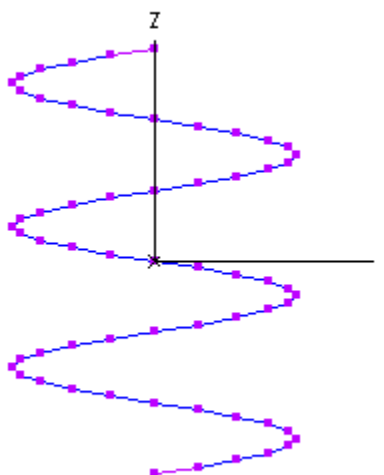


Fig. 3

A few reminders may be in order here. Foremost is one that even some experienced modelers forget. Even though the model structure shown in the sample model files has no excitation or output request, we can still run the model and obtain an output report. The first lines of this report appear in **Table 1**.

Table 1. Single GM-based helix

- - - STRUCTURE SPECIFICATION - - -

extract from NEC output report

WIRE NO.	X1	Y1	Z1	X2	Y2	Z2	RADIUS	NO. OF SEG.	FIRST SEG.	LAST SEG.	TAG NO.	
1	THIS WIRE IS AN ARCHIMEDES SPIRAL OR HELIX							60	1	60	1	
SPIRAL DATA: TURNS=		3.0000	LENGTH=		3.0000E+00	H.RAD=	1.0000E+00	1.0000E+00	W.RAD=	5.0000E-04		
TOTAL LENGTH OF WIRE IN THE SPIRAL = 1.90103E+01												
TOTAL SEGMENTS USED= 60 NO. SEG. IN A SYMMETRIC CELL= 60 SYMMETRY FLAG= 0												

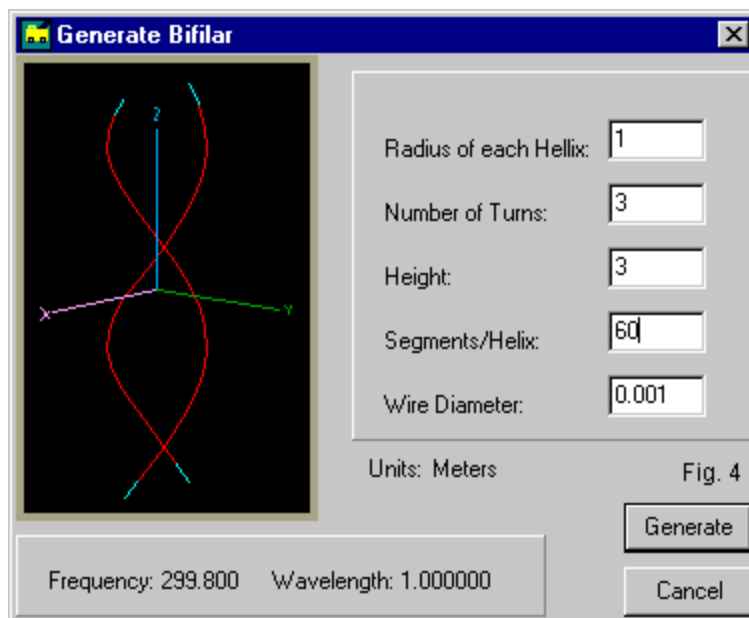
The output report is very useful for checking the correctness of our geometry entries. The lines replicate the instructions that we thought we gave the command (and sometimes, we do transpose numbers, mis-strike a key, etc.). As well, the NEC-4 GH command yields the total wire length in the helix, a useful piece of data for someone planning to build what he or she models.

The GH command is not the only way to form a single helix. For example, EZNEC provides a helix-formation facility that will produce a segment-by-segment models. Its version of the single helix in our example will have 60 wires.

If we wish to alter the position of either of our two sample models, we may employ the GM command. However, since this exercise will never get around to adding a source or an output request to the structural entries, we can leave the basic position alone. Besides, we shall have another use for the GM command. While we can employ as many GM commands as we need--so long as we use them in the correct order--minimizing other uses of them will make our fundamental use clearer.

A Bifilar Helix

There are several ways to form a bifilar helix. We shall give primary attention to two techniques. The first uses a program that creates geometry structures called NEC-Win Synth. Among the program's preset shapes is a bifilar helix. All that we need to do is to enter the critical data about the helix, namely our specifications from the beginning of these notes. **Fig. 4** shows the specification screen.



The data are the same that we used to generate a single helix. Although the program offers the option of using the wire diameter or the wire radius, it happens to be set in the diameter mode. That fact explains why I gave both values in the beginning. Since the helix values are by now quite familiar, we can see what our creation looks like in **Fig. 5**.

Radius = 1 m
No. Turns = 3
Turn Spacing = 1 m
Total Length = 3 m
Wire Diameter = 0.001 m
Wire Radius = 0.0005 m

A Bifilar Helix Generated
by NEC-Win Synth

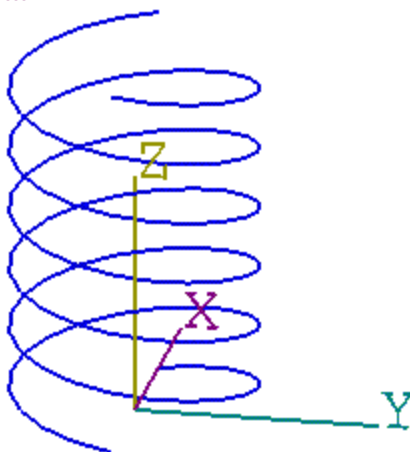


Fig. 5

The screen is part of the Synth program, which places the origin of the axes at the base of the created structure. Note that like the single helix, one of our double-helix starting points is along the X-axis. The program produces a wire-by-wire model in its own format, but you may save the structure file in the standard .NEC format for use in either NEC-2 or NEC-4. The model is incomplete as it emerges from Synth. It contains only the geometry structure and a frequency specification. You must add all other desired elements from within NEC-2 or NEC-4. The geometry section alone will contain 120 GW entries, as suggested by the following partial replication of the model:

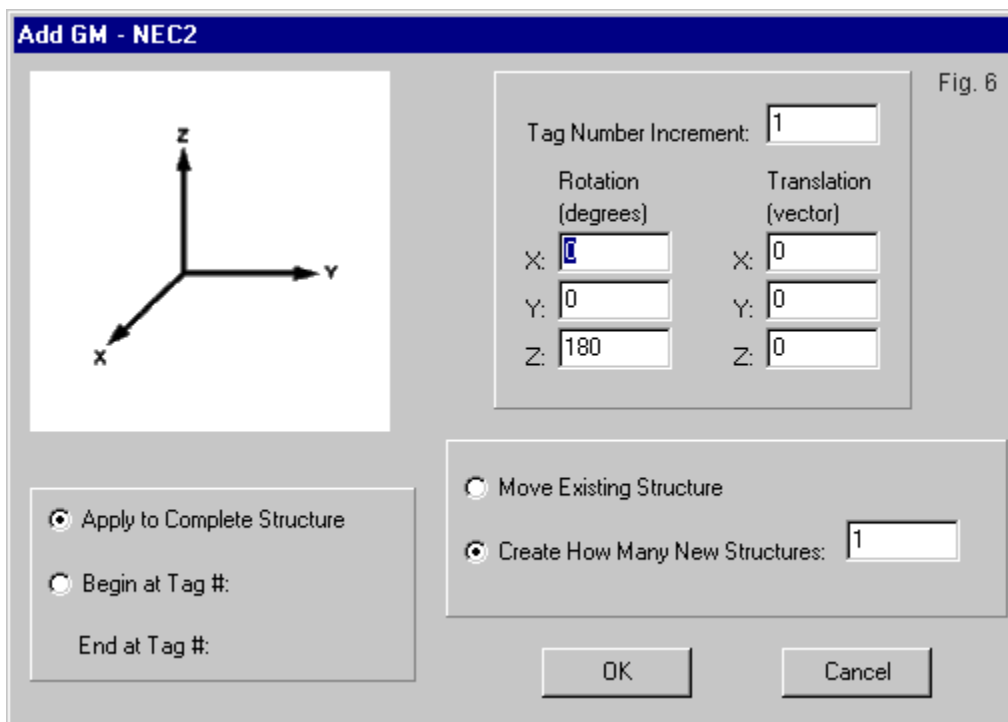
```

CM Bifilar helix from NEC-Win Synth 1.0
CE
GW 1 1 1.00000 0.00000 0.00000 0.95106 0.30902 0.05000 0.00050
GW 2 1 0.95106 0.30902 0.05000 0.80902 0.58779 0.10000 0.00050
GW 3 1 0.80902 0.58779 0.10000 0.58779 0.80902 0.15000 0.00050
GW 4 1 0.58779 0.80902 0.15000 0.30902 0.95106 0.20000 0.00050
GW 5 1 0.30902 0.95106 0.20000 0.00000 1.00000 0.25000 0.00050
GW 6 1 0.00000 1.00000 0.25000 -0.30902 0.95106 0.30000 0.00050
GW 7 1 -0.30902 0.95106 0.30000 -0.58779 0.80902 0.35000 0.00050
GW 8 1 -0.58779 0.80902 0.35000 -0.80902 0.58779 0.40000 0.00050
GW 9 1 -0.80902 0.58779 0.40000 -0.95106 0.30902 0.45000 0.00050
GW 10 1 -0.95106 0.30902 0.45000 -1.00000 0.00000 0.50000 0.00050
GW 11 1 -1.00000 0.00000 0.50000 -0.95106 -0.30902 0.55000 0.00050
GW 12 1 -0.95106 -0.30902 0.55000 -0.80902 -0.58779 0.60000 0.00050
GW 13 1 -0.80902 -0.58779 0.60000 -0.58779 -0.80902 0.65000 0.00050
GW 14 1 -0.58779 -0.80902 0.65000 -0.30902 -0.95106 0.70000 0.00050
GW 15 1 -0.30902 -0.95106 0.70000 0.00000 -1.00000 0.75000 0.00050
GW 16 1 0.00000 -1.00000 0.75000 0.30902 -0.95106 0.80000 0.00050
GW 17 1 0.30902 -0.95106 0.80000 0.58779 -0.80902 0.85000 0.00050
GW 18 1 0.58779 -0.80902 0.85000 0.80902 -0.58779 0.90000 0.00050
GW 19 1 0.80902 -0.58779 0.90000 0.95106 -0.30902 0.95000 0.00050
---
GW 110 1 0.95106 -0.30902 2.45000 1.00000 0.00000 2.50000 0.00050
GW 111 1 1.00000 0.00000 2.50000 0.95106 0.30902 2.55000 0.00050
GW 112 1 0.95106 0.30902 2.55000 0.80902 0.58778 2.60000 0.00050
GW 113 1 0.80902 0.58778 2.60000 0.58779 0.80902 2.65000 0.00050
GW 114 1 0.58779 0.80902 2.65000 0.30902 0.95106 2.70000 0.00050
GW 115 1 0.30902 0.95106 2.70000 0.00000 1.00000 2.75000 0.00050
GW 116 1 0.00000 1.00000 2.75000 -0.30902 0.95106 2.80000 0.00050
GW 117 1 -0.30902 0.95106 2.80000 -0.58778 0.80902 2.85000 0.00050
GW 118 1 -0.58778 0.80902 2.85000 -0.80902 0.58779 2.90000 0.00050
GW 119 1 -0.80902 0.58779 2.90000 -0.95106 0.30902 2.95000 0.00050
GW 120 1 -0.95106 0.30902 2.95000 -1.00000 0.00000 3.00000 0.00050
GS 0 0 1.000000
GE
FR 0 1 0 0 299.7925 1
EN

```

You may arrive at a virtually identical model in EZNEC with only a few steps. The first would be to create a single helix to the desired specifications. The program will produce a 60-wire structure in the Wires table. Next, you may copy the wires just produced and then rotate them 180 degrees in either a clockwise or counterclockwise around the Z axis. There are also functions for moving and rotating all 120-wires of the structure so that it ends up where and how you want it in the model.

An alternative procedure that uses up much less model-file space uses the commands within NEC. Essentially, if we begin with the NEC-2 helix shown earlier, we need only use the GM command to rotate the helix by 180 degrees while replicating it once. The NEC-2 GM help screen appears in **Fig. 6**.



The total NEC-2 model (so far) is somewhat shorter than the Synth or EZNEC models.

CM Bifilar helix-nec-2

CE

GH 1 60 1 3 1 1 1 1 .0005

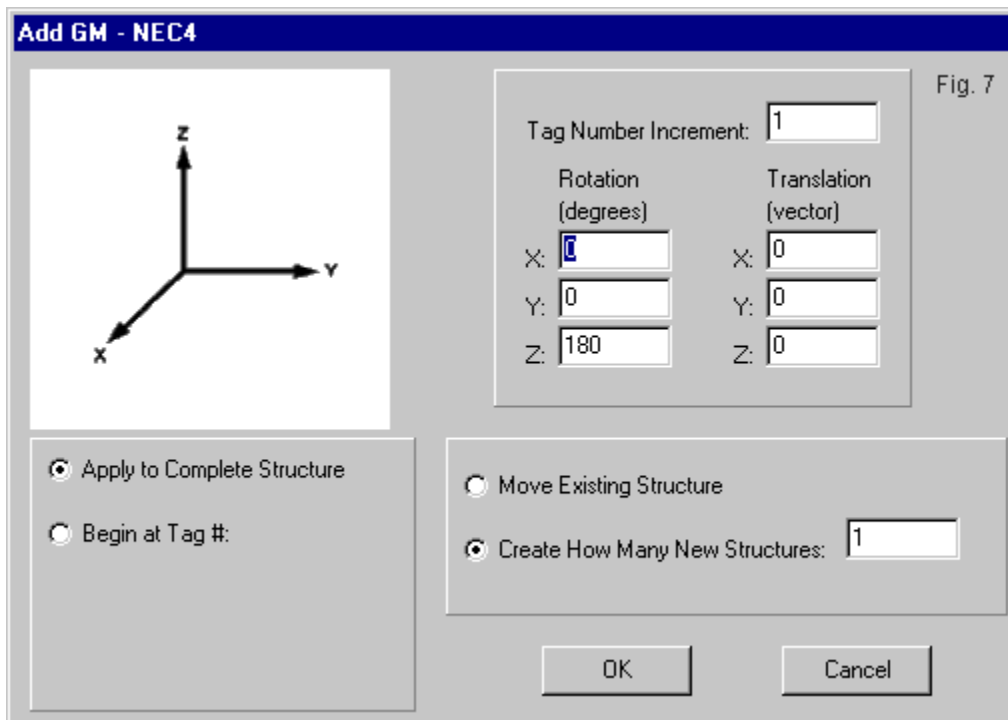
GM 1 1 0 0 180 0 0 0

GE

FR 0 1 0 0 299.7925 1

EN

The GM portion of the process when using NEC-4 looks almost exactly like the NEC-2 version, as suggested by the GM help screen for that core in **Fig. 7**.



For our present needs, which only require us to replicate the entire original structure--with the half-twist--the screens of NEC-2 and NEC-4 are alike. However, had we wished to manipulate partial structures, NEC-2 would have allowed us to specify only complete tags. NEC-4 allows specification of start and stop tag and segment numbers. The difference lies in what does not appear in the lower left corner of each help screen. Had we used the start-stop option, the following NEC-4 model would not have a GM line that looks so much like the corresponding NEC-2 line.

```

CM Bifilar helix-nec-4
CE
GH 1 60 3 3 1 1 .0005 .0005 1
GM 1 1 0 0 180 0 0 0
GE
FR 0 1 0 0 299.7925 1
EN

```

The results of using GM on the initial GH line in either NEC-2 or NEC-4 produces a bifilar helix with the appearance of **Fig. 8**.

A Bifilar Helix Generated by GH & GM
 Radius = 1m
 No. Turns = 3
 Turn Spacing = 1 m
 Total Length = 3m
 Wire Diameter = 0.001m
 Wire Radius = 0.0005 m

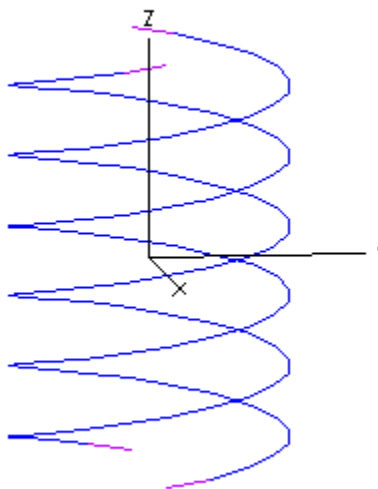


Fig. 8

Although I have tipped the axes in a slightly different manner than I did in **Fig. 5**, the GH-GM combination produces a bifilar helix with the same structure and orientation as the one that emerged from NEC-Win Synth. Since I have omitted the segment markers, the verification that all is well requires that we run the partial model and check the data in the NEC output file. **Table 2** gives us the opening lines.

Table 2. GM-based bifilar helix

-- STRUCTURE SPECIFICATION --

extract from NEC output report

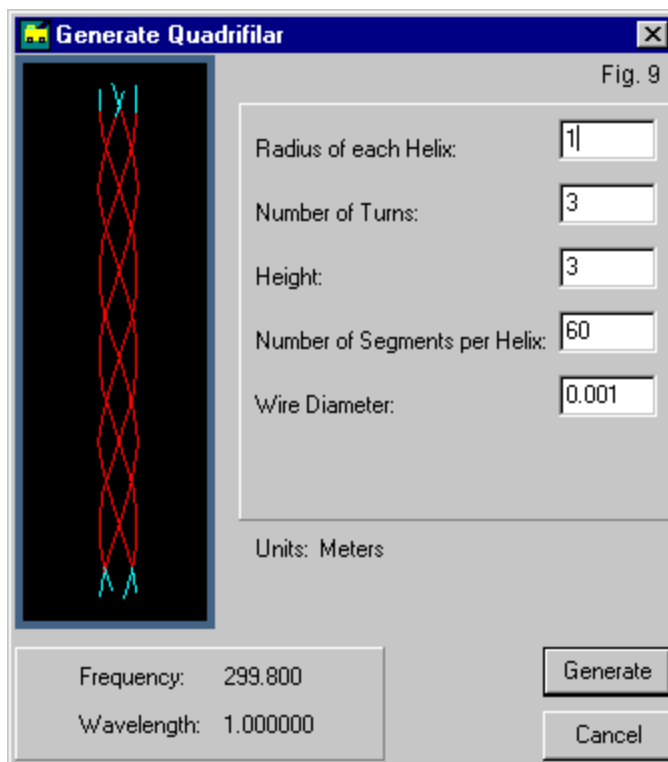
WIRE NO.	X1	Y1	Z1	X2	Y2	Z2	RADIUS	NO. OF SEC.	FIRST SEC.	LAST SEC.	TAG NO.
1	THIS WIRE IS AN ARCHIMEDES SPIRAL OR HELIX										
	SPIRAL DATA: TURNS=		3.00000	LENGTH=		3.0000E+00	H.RAD=	1.0000E+00	1.0000E+00	W.RAD=	5.0000E-04
	TOTAL LENGTH OF WIRE IN THE SPIRAL = 1.90103E+01										
	THE STRUCTURE HAS BEEN MOVED, GM COMMAND DATA IS -										
1	1	0.00000	0.00000	180.00000	0.00000	0.00000	0.00000	0	1	0	60
TOTAL SEGMENTS USED= 120 NO. SEG. IN A SYMMETRIC CELL= 120 SYMMETRY FLAG= 0											

The bottom line of this section of the report tells us that we have a 120-segment structure, just as planned, while the antenna sketch from the program tells us that we have opposing helices. The output report goes on to provide data on each segment within the 2-tag model, allowing us to correlate the two helices point by point. However, the NEC output report lists the coordinates at the center of each segment. In the programs used here, you would have to look at the antenna view facilities to identify the coordinates at each end of each segment, just in case you later wished to connect another wire to the structure, even at the top or the bottom.

Note that none of the techniques that we have examined joins any of the helix ends. If you wish to create a connection, you will have to add a wire having the correct end coordinates.

A Quadrifilar Helix

We can easily create a quadrifilar helical structure using either of the techniques shown so far. The quadrifilar helix consists of 4 identical single helices separated by 90 degrees. In NEC-Win Synth, the process is as simple as selecting the correct pre-set shape from the list and then entering the vital specifications. Fig. 9 shows the specifications screen for the quadrifilar helix.



Compare the data entries for **Fig. 9** with those for **Fig. 4**. Nothing has changed except the output. As shown in **Fig. 10**, the structure now has 4 helices as requested. Like the bifilar structure, the top is open, so you will have to add crossing (usually non-touching) wires to close the upper end.

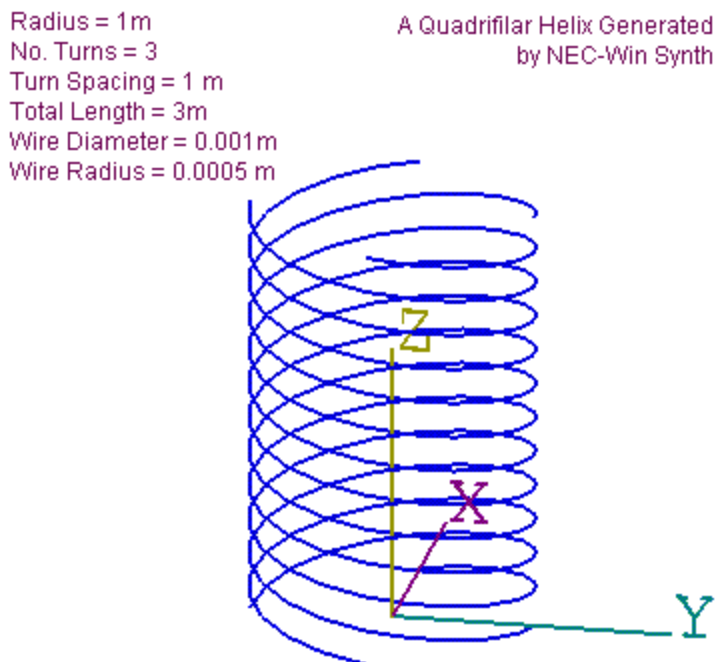


Fig. 10

Since we now have 4 inter-laced helices, the spacing between adjacent turns has shrunk accordingly. However, the individual helices are all identical to the original single helix with which we began.

The Synth version (or an EZNEC version) of the quadrifilar helix with the initial specifications will have 240 wire entries, even before adding any connecting wires. The following lines sample the beginning and the ending of the geometry section of the model.

CM Quadrifilar helix from NEC-Win Synth 1.0

CE

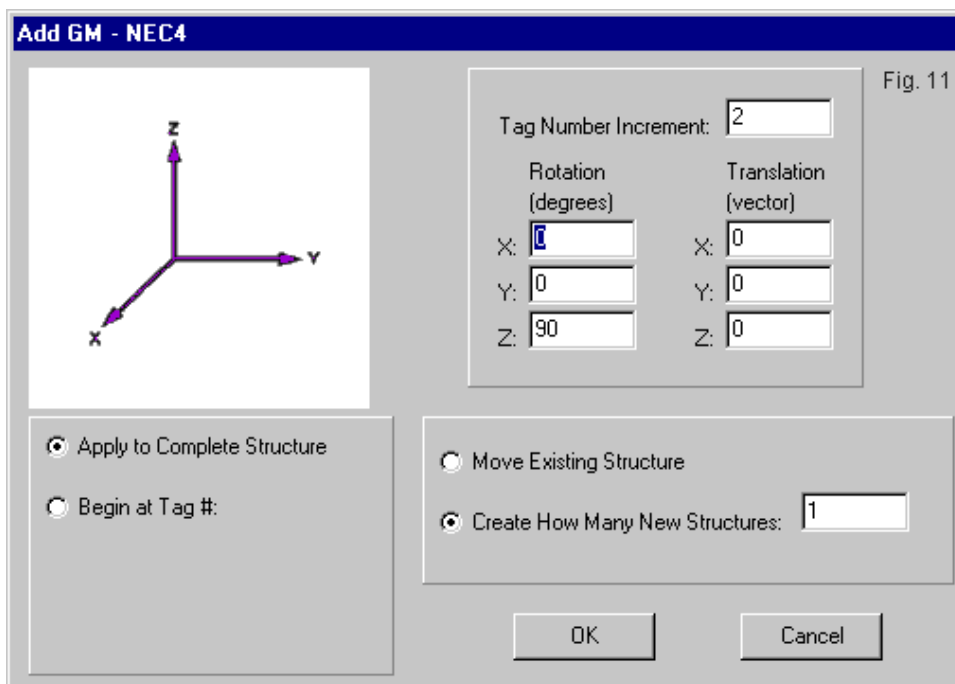
```
GW 1 1 1.00000 0.00000 0.00000 0.95106 0.30902 0.05000 0.00050
GW 2 1 0.95106 0.30902 0.05000 0.80902 0.58779 0.10000 0.00050
GW 3 1 0.80902 0.58779 0.10000 0.58779 0.80902 0.15000 0.00050
GW 4 1 0.58779 0.80902 0.15000 0.30902 0.95106 0.20000 0.00050
GW 5 1 0.30902 0.95106 0.20000 0.00000 1.00000 0.25000 0.00050
GW 6 1 0.00000 1.00000 0.25000 -0.30902 0.95106 0.30000 0.00050
```

```

GW 7 1 -0.30902 0.95106 0.30000 -0.58779 0.80902 0.35000 0.00050
GW 8 1 -0.58779 0.80902 0.35000 -0.80902 0.58779 0.40000 0.00050
GW 9 1 -0.80902 0.58779 0.40000 -0.95106 0.30902 0.45000 0.00050
GW 10 1 -0.95106 0.30902 0.45000 -1.00000 0.00000 0.50000 0.00050
GW 11 1 -1.00000 0.00000 0.50000 -0.95106 -0.30902 0.55000 0.00050
GW 12 1 -0.95106 -0.30902 0.55000 -0.80902 -0.58779 0.60000 0.00050
GW 13 1 -0.80902 -0.58779 0.60000 -0.58779 -0.80902 0.65000 0.00050
GW 14 1 -0.58779 -0.80902 0.65000 -0.30902 -0.95106 0.70000 0.00050
GW 15 1 -0.30902 -0.95106 0.70000 0.00000 -1.00000 0.75000 0.00050
GW 16 1 0.00000 -1.00000 0.75000 0.30902 -0.95106 0.80000 0.00050
GW 17 1 0.30902 -0.95106 0.80000 0.58779 -0.80902 0.85000 0.00050
GW 18 1 0.58779 -0.80902 0.85000 0.80902 -0.58779 0.90000 0.00050
GW 19 1 0.80902 -0.58779 0.90000 0.95106 -0.30902 0.95000 0.00050
---
GW 229 1 0.58779 0.80902 2.40000 0.30902 0.95106 2.45000 0.00050
GW 230 1 0.30902 0.95106 2.45000 0.00000 1.00000 2.50000 0.00050
GW 231 1 0.00000 1.00000 2.50000 -0.30902 0.95106 2.55000 0.00050
GW 232 1 -0.30902 0.95106 2.55000 -0.58778 0.80902 2.60000 0.00050
GW 233 1 -0.58778 0.80902 2.60000 -0.80902 0.58779 2.65000 0.00050
GW 234 1 -0.80902 0.58779 2.65000 -0.95106 0.30902 2.70000 0.00050
GW 235 1 -0.95106 0.30902 2.70000 -1.00000 0.00000 2.75000 0.00050
GW 236 1 -1.00000 0.00000 2.75000 -0.95106 -0.30902 2.80000 0.00050
GW 237 1 -0.95106 -0.30902 2.80000 -0.80902 -0.58778 2.85000 0.00050
GW 238 1 -0.80902 -0.58778 2.85000 -0.58779 -0.80902 2.90000 0.00050
GW 239 1 -0.58779 -0.80902 2.90000 -0.30902 -0.95106 2.95000 0.00050
GW 240 1 -0.30902 -0.95106 2.95000 0.00000 -1.00000 3.00000 0.00050
GS 0 0 1.000000
GE
FR 0 1 0 0 299.7925 1
EN

```

To create a quadrifilar helix using the NEC command set only requires that we add one more line to our bifilar model. It is another GM line. Since the GM lines are so similar between NEC-2 and NEC-4 in this application, a single sample will suffice for both cores. **Fig. 11** shows the required replication and manipulation.



The new GM command operates on the entire existing structure, which includes tags 1 and 2. We increment the tag numbers by 2 so that the new helices will bear the numbers 3 and 4. We replicate the entire structure once and give the new helices a 90-degree rotation. Now we have the quadrifilar helix, as shown in the following model lines. The lines show the NEC-4 version, which differs from the NEC-2 version only in the GH entry.

```
CM Quadrifilar helix-nec-4
CE
GH 1 60 3 3 1 1 .0005 .0005 1
GM 1 1 0 0 180 0 0 0
GM 2 1 0 0 90 0 0 0
GE
FR 0 1 0 0 299.7925 1
EN
```

We could have created the same structure with only one GM line, as shown in the following variant model. The GM line creates 3 replicas of the original helix spaced at 90-degree intervals around the Z-axis.

```
CM Quadrifilar helix-nec-4
CE
GH 1 60 3 3 1 1 .0005 .0005 1
GM 1 3 0 0 90 0 0 0
GE
FR 0 1 0 0 299.7925 1
EN
```

In either case, we can again use the NEC output file as one verification that our work is correct. **Table 3** shows the initial lines of the output file for the double-GM version of the model.

Table 3. GM-based quadrifilar helix - - - STRUCTURE SPECIFICATION - - - extract from NEC output report

WIRE NO.	X1	Y1	Z1	X2	Y2	Z2	RADIUS	NO. OF SEG.	FIRST SEG.	LAST SEG.	TAG NO.
1	THIS WIRE IS AN ARCHIMEDES SPIRAL OR HELIX							60	1	60	1
	SPIRAL DATA: TURNS= 3.0000 LENGTH= 3.0000E+00 H.RAD= 1.0000E+00 1.0000E+00 W.RAD= 5.0000E-04 5.0000E-04										
	TOTAL LENGTH OF WIRE IN THE SPIRAL = 1.90103E+01										
	THE STRUCTURE HAS BEEN MOVED, GM COMMAND DATA IS -										
1	1	0.00000	0.00000	180.00000	0.00000	0.00000	0	1	0	60	
	THE STRUCTURE HAS BEEN MOVED, GM COMMAND DATA IS -										
2	1	0.00000	0.00000	90.00000	0.00000	0.00000	0	1	0	120	
TOTAL SEGMENTS USED= 240 NO. SEG. IN A SYMMETRIC CELL= 240 SYMMETRY FLAG= 0											

Regardless of whether we use 1 or 2 GM lines to produce the quadrifilar helix, the result will have the appearance of **Fig. 12**. You may compare this helix to the quadrifilar helix in **Fig. 10** and to the other helical structures shown earlier.

A Quadrifilar Helix Generated by GH & GM

Radius = 1 m

No. Turns = 3

Turn Spacing = 1 m

Total Length = 3m

Wire Diameter = 0.001 m

Wire Radius = 0.0005 m

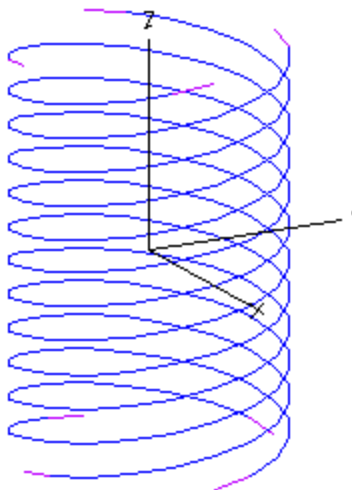


Fig. 12

The basic bifilar and quadrifilar structures are straightforward to produce, using either segment-by-segment techniques that yield many wires or using the GH and GM commands for a compact model file.

Which Model Should I Use?

In terms of producing a compact helix model file, nothing exceeds the GH-GM method of fashioning a bifilar or a quadrifilar helical assembly. However, the diminutive file size (which has no bearing on the comparative speed of the core run or on the size of the output file) comes at a cost. Except for the initial junction of the helices with the X-Y plane, the coordinate values for all junctions are unknown and require supplemental aids to discover. As noted, the antenna view function of NEC-Win Pro, GNEC and some other programs allows one to find any segment and learn its end-1 and end-2 coordinates.

In contrast, the seemingly very large geometry structure portions of files produced by NEC-Win Synth, EZNEC, and possibly other programs that create segment-by-segment helix models have the advantage of being quite transparent. By inspection, one can find any desired junction between

segments/wires and use that junction for any other desired wire connection. Most evidently, this facility applies to the free ends at the top of the multiple helix, where cross connections are common. However, the ease of finding connections also applies when bridging lower sections of a helix for a feed system.

Since each wire of a multiple helix is independent in the segment-by-segment construct, connections to ground often become simpler. Many initial experiments with multiple helices employ a perfect ground as an initial surface. However, advanced models may employ wire grids having either simple or complex geometries. The grid may offer connection junctions that do not align precisely with the lowest segments of the helices. In most cases, with a segment-by-segment model, one can simply alter the lowest coordinates to coincide with a wire ground junction without unduly distorting the overall shape of the bifilar or quadrifilar structure.

In the end, the decisions as to which type of bifilar or quadrifilar model to adopt rests with the uses to which one puts the basic structure and the role it plays in the total model. Because the roles and uses are so numerous and varied, these notes have confined themselves to a single topic: forming the multiple helix with assurance that it is correct. The samples provided in this episode may serve as a guide to the production of multiple helices less amenable to graphical clarity and more adept at fulfilling useful communication functions.

116. Insulation Revisited

In episode 50, we examined some of the basic factors in using the NEC-4 IS or Insulated Sheath command. 33 episodes later (in 83), we looked at a very partial workaround for implementing insulated sheaths in NEC-2 without rewriting the program to import the IS command. Another 33 episodes have gone by, and so we may revisit the IS command.

In our initial look at the command, we made an assumption, namely, that for virtually all cases of insulated antenna wires, the conductivity of the insulation would be less than 1E5 S/m. The assumption rested on general expectations of common modern wire insulation materials, but had no solid foundation in calculations. Indeed, unless one has a considerable reference library, finding the conductivity of wire insulation turns out to be much more difficult than finding its relative permittivity. In the original episode, the graphs and charts used a constant conductivity of 1E-10 S/m to simplify charting the properties of insulation and arriving at reasonable graphs of insulated-wire antennas, including their velocity factor relative to a bare wire antenna.

We should re-visit insulated wires to see if the assumptions in our original episode stand the test of calculation. In fact, differences between the way various programs implement the potential for insulating wires forces the issue upon us.

Some Basics of Insulated Sheaths

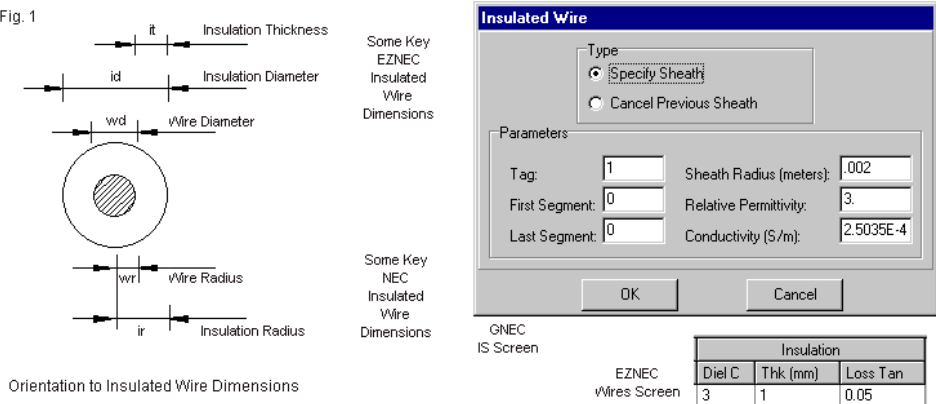
NEC-4's IS command assumes that the insulation extends from the surface of the wire to a user-designated outer limit, with no space between the wire and the insulation. Hence, the command is limited to common wire fabrication and does not extend to uses where we might suspend a bare wire within a tubular shell. The command itself is almost deceptively simple.

IS	I1	ITAG	ITAGF	ITAGT	EPSR	SIG	RADI	Mnemonics
	I1	I2	I3	I4	F1	F2	F3	Entry Labels
IS	0	1	0	0	3.	2.50E-4	.002	Sample Entry

As with all NEC entries, we have a series of integer (I1-I4) and a series of floating decimal (F1-F3) entries. I1 merely signals that new data will appear. (A -1 would cancel previous IS data.) I2 specifies the affected tag. I3 and I4 specify the first and last segments to which the data will apply. A pair of zeroes indicates that the data applies to all segments. We have only 3 floating decimal entries. The first is the relative permittivity of the insulation. The second specifies the conductivity of

the insulation. The last entry provides the radius of the outer limit of the insulation, where the inner limit is automatically the radius of the wire beneath the insulation. F3 must use a number higher than the radius specified in the GW line referenced by the Tag number in entry I2. In the sample command, the data applies to all segments of Tag 1. The relative permittivity is 3.0, with a conductivity of 2.5E-4 S/m. The sheath radius is 2 mm, which is valid for the wire of Tag 1, which has a 1-mm radius. In more common terms, the wire diameter is 2 mm, the sheath thickness is 1 mm, and the total insulated wire diameter is 4 mm. Essentially, the IS command sets up a second medium for a limited space around the wire, and the conductivity and relative permittivity values that we insert employ the same parameters we apply to ground media.

Some implementations of NEC use the IS command exclusively, while others--such as EZNEC--employ an entry system that differs in detail but not in calculation from the IS command. The differences involve shifting from one way of thinking about insulation to another, so let's compare the two entry systems. GNEC, as one example of an implementation using the IS command, provides a help screen that reflects the structure of the command. In contrast, EZNEC attaches insulation to the wire-entry screen. **Fig. 1** shows the two entry screens along with some sketchy guidance to the dimensional differences between the two. Both help screens show the same parameters and values.



The relative permittivity entries for the two insulations are the same, and the pencil-and-paper transformation of thickness to sheath radius is trivial (for this example, where the wire radius is 1 mm). The key is in the entries that are not

the same in the two systems. The IS command requires a value of conductivity, and hitherto, we have simply assumed a very low value. The EZNEC entry requires a value called the "loss tangent," and only some modelers know where to find that. Probably, only a few know how to go from one to the other and back again. Let's see how to perform the required calculation.

Relative permittivity (ϵ_r) is, of course a form of short hand for the value of permittivity (ϵ).

$$\epsilon = \epsilon_0 \epsilon_r$$

Epsilon₀ is the value of permittivity in a vacuum, namely 8.854E-12 F/m. Since the value is a constant, many computerized calculation system omit this term from user view, and NEC is one of those systems. So the relative permittivity of any material of concern is simply the comparative permittivity relative to a vacuum. Hence, we need only tabulate fairly simple numbers, ranging from 1 upward. We can often find lists of relative permittivity values in handbooks.

A few handbooks, such as *Reference Data for Engineers*, Table 9, pp. 4-20 to 4-23, will also list another value, the dissipation factor. The following entries sample the list, which covers 4 pages of materials and values.

Sample "Characteristics of Insulating Materials"

Material	Relative Permittivity			Dissipation Factor		
	10E3 Hz	10E6 Hz	10E8 Hz	10E3 Hz	10E6 Hz	10E8
Hz						
Polycarbonate	3.02	2.96	-----	0.0021	0.010	-----
Polyethylene	2.26	2.26	2.26	<0.0002	<0.0002	0.0002
Teflon (PTFE)	2.1	2.1	2.1	<0.0005	<0.0003	<0.0002
PVC (100%)	3.10	2.88	2.85	0.0185	0.0160	0.0081

The values may vary somewhat over the range of frequencies, but normally quite slowly. For 30 MHz, taking the mean values between 10E6 Hz and 10E8 Hz (1 and 100 MHz) will normally be as close to correct in the HF range as the data itself will allow.

The dissipation factor of an insulating material is the ratio of energy dissipated to energy stored in a dielectric. The value derived is the tangent of the loss angle (a function of the two factors having a 90-degree phase difference). In alternative terms and thanks to Roy Lewallen for the way of expressing it, the loss tangent is

the ratio of the imaginary to real parts of the complex permittivity, which in turn is a function of the real permittivity (dielectric constant), frequency, and conductivity. Immediately, we should see that the conductivity will vary with both the relative permittivity and the frequency for any loss tangent value. In fact, we may convert a listed loss tangent value to a value of conductivity in a straightforward equation:

$$C = 2 \pi \epsilon_0 \epsilon_r F \tan \delta$$

C is the conductivity in S/m, ϵ_0 is the permittivity of a vacuum, ϵ_r is the relative permittivity of the insulating material at hand, F is the frequency in Hz, and $\tan \delta$ is the listed loss tangent or dissipation factor. You may sometimes find a listing for a power factor: for values less than 0.1, you may treat the power factor, the dissipation factor, and the loss tangent as the same. In fact, all reasonable loss tangent values will be considerably less than 0.1.

The conversion equation includes several constants: 2, π , and ϵ_0 . If you wish to create a small spreadsheet to calculate back and forth between conductivity and loss tangent, you may combine the constants:

$$2 \pi \epsilon_0 = 5.5631 \times 10^{-11}$$

This simplification reduces the conversion process to a shorter equation:

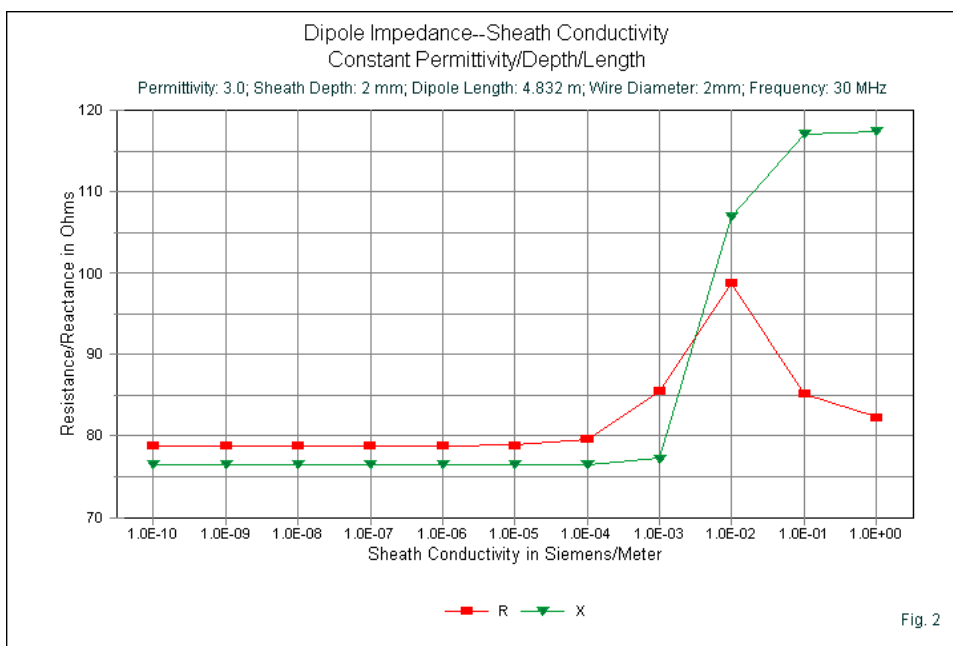
$$C = 5.5631 \times 10^{-11} \epsilon_r F \tan \delta$$

Let's create a 30-MHz dipole using the values shown in **Fig. 1** for the relative permittivity and for the EZNEC loss tangent. The result of conversion yields the conductivity value shown in the GNEC IS screen. This value of conductivity is very much less than the value assumed in episode 50 (1×10^{-10} S/m). So our next concern is whether there are any practical consequences of the higher conductivity values calculated by converting from the loss tangent to conductivity at the frequency of operation. My scan of the plastic material in my reference shows very low values of loss tangent (0.0002 is perhaps the most common value). Nonetheless, we should see what emerges from a systematic scan of values.

The Results from Using a Constant Conductivity and a Loss Tangent

In episode 50, we ran through some exercises exploring various insulation thicknesses (0.5 mm, 1.0 mm, and 2.0 mm) around a 2-mm diameter bare

copper wire dipole resonated at 30 MHz. In all cases, we used a constant value for conductivity. The constant rested on an initial exercise using some thick insulation with a constant value of relative permittivity and a variable conductivity. The initial results showed the changes in the antenna's feedpoint resistance and reactance without changing its length. The length originated from resonating the wire when bare. **Fig. 2** shows the results of that initial exercise, using free-space models.



The assigned relative permittivity is fairly high for plastics (although PVC may be as high as 3.5), and the insulation thickness is as great as the wire diameter. Even under these conditions, the feedpoint resistance remains stable until the conductivity increases above $1\text{E-}4$ S/m. The reactance remains stable until we pass $1\text{E-}3$ S/m. The calculated conductivity value in the sample in **Fig. 1** appears to be on the resistance borderline but below the threshold for reactance variation. Hence, a preliminary estimate would suggest that we might find a few Ohms of feedpoint resistance variation, but the resonant length of the insulated dipole

should not differ significantly from the modeled length using the very low conductance value of episode 50.

Table 1 provides the values derived under the conditions of episode 50. They provide us with a touchstone for some further work and with a reference for some original results.

Sample Dipole with Permittivity as a Variable and a Constant Conductivity (1E-10 S/m)								Table 1		
Dipole: 30 MHz, 2mm (0.002 m or 0.07874") diameter copper conductor										
TH=0.5 mm; Radius=1.5 mm								0.5 mm	1.0 mm	2.0 mm
Perm	1	1.25	1.5	1.75	2	2.25	2.5	2.75	3	
Res FQ	30.00	29.80	29.69	29.60	29.53	29.48	29.44	29.41	29.39	
DP Length	2.416	2.400	2.391	2.383	2.378	2.374	2.371	2.368	2.366	
Wire VF	1	0.9934	0.9897	0.9863	0.9843	0.9826	0.9814	0.9801	0.9793	
Zres	72.54	71.67	71.24	70.79	70.55	70.36	70.22	70.05	69.96	
TH=1.0 mm; Radius=2.0 mm										
Perm	1	1.25	1.5	1.75	2	2.25	2.5	2.75	3	
Res FQ	30.00	29.69	29.47	29.31	29.20	29.13	29.05	28.98	28.93	
DP Length	2.416	2.391	2.373	2.360	2.351	2.345	2.339	2.333	2.330	
Wire VF	1	0.9897	0.9822	0.9768	0.9731	0.9706	0.9681	0.9656	0.9644	
Zres	72.54	71.26	70.31	69.62	69.17	68.92	68.61	68.26	68.14	
TH=2.0 mm; Radius=3.0 mm										
Perm	1	1.25	1.5	1.75	2	2.25	2.5	2.75	3	
Res FQ	30.00	29.50	29.17	28.91	28.74	28.60	28.49	28.39	28.30	
DP Length	2.416	2.375	2.348	2.328	2.313	2.302	2.292	2.284	2.278	
Wire VF	1	0.9830	0.9719	0.9636	0.9574	0.9528	0.9487	0.9454	0.9429	
Zres	72.54	70.41	69.05	68.03	67.28	66.75	66.24	65.83	65.55	

This table (and others to come) require some background. In all cases, I varied the relative permittivity in increments of 0.25 between values of 1.0 and 3.0. The Res FQ entry shows the resonant frequency of the antenna at its original length under varying insulation conditions. The bare wire length was 4.832 m. However, for convenience, the following line marked DP Length uses the half-length of the dipole (based on modeling from -Y to +Y through the coordinate system origin). The DP length entry is for 30 MHz and produces resonance (within less than +/- j0.5 Ohms reactance). By comparison with the bare-wire length, we can arrive at a Wire VF or velocity factor for the specific insulation condition. The bottom line in each series lists the 30-MHz resonant feedpoint resistance (Zres) of the shortened antenna.

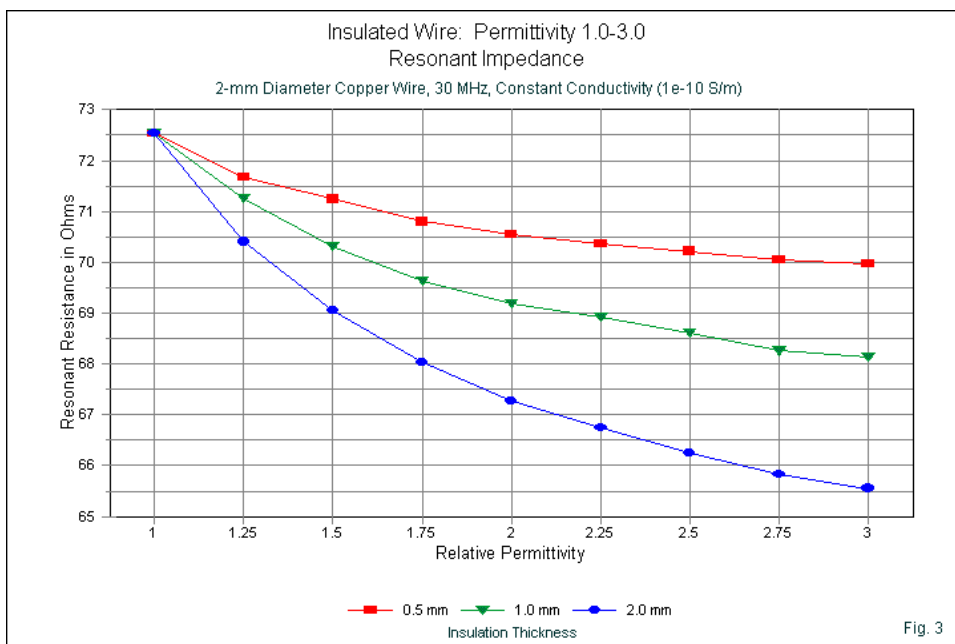
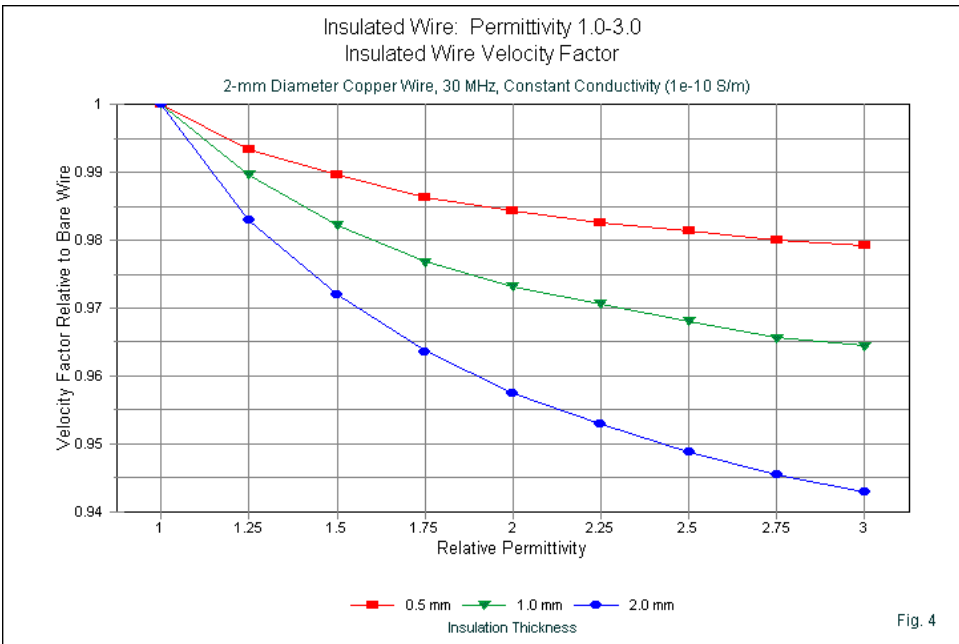


Fig. 3 shows the change of resonant feedpoint resistance under the insulation conditions listed in **Table 1**. **Fig. 4** shows the velocity factor of the insulated and resonated dipoles relative to a bare-wire dipole using the same basic starting wire diameter. Note that the curves are congruent between the two graphs, indicating the orderliness of the progressions. See episode 50 for other graphed results from the exercise.



Remember that the initial exercise used a constant conductivity ($1\text{E-}10\text{ S/m}$). Let's return to that exercise, but this time allow the conductivity to be variable, based on a selected loss tangent value. I have chosen a value of 0.0005, since this value is close to but somewhat higher than the most common value listed for plastic insulating materials. **Table 2** records the results of going through the same set of exercises, but this time calculating the value of conductivity for each case. As the table shows, conductivity rises with each increase in relative permittivity.

Sample Dipole with Both Conductivity and Permittivity as Variables									Table 2
Dipole: 30 MHz, 2mm (0.002 m or 0.07874") diameter copper conductor, loss tangent 0.0005									
TH=0.5 mm; Radius=1.5 mm									
Perm	1	1.25	1.5	1.75	2	2.25	2.5	2.75	3
Conductivity	8.34E-07	1.04E-06	1.25E-06	1.46E-06	1.67E-06	1.88E-06	2.09E-06	2.29E-06	2.50E-06
Res FQ	30.00	29.80	29.70	29.60	29.55	29.50	29.45	29.40	29.37
DP Length	2.416	2.400	2.390	2.383	2.377	2.374	2.371	2.368	2.366
Wire VF	1	0.9934	0.9892	0.9863	0.9839	0.9826	0.9814	0.9801	0.9793
Zres	72.57	71.68	71.17	70.81	70.46	70.37	70.27	70.06	69.97
TH=1.0 mm; Radius=2.0 mm									
Perm	1	1.25	1.5	1.75	2	2.25	2.5	2.75	3
Conductivity	8.34E-07	1.04E-06	1.25E-06	1.46E-06	1.67E-06	1.88E-06	2.09E-06	2.29E-06	2.50E-06
Res FQ	30.00	29.68	29.47	29.32	29.21	29.12	29.04	28.98	28.93
DP Length	2.416	2.390	2.373	2.361	2.352	2.344	2.338	2.333	2.329
Wire VF	1	0.9892	0.9822	0.9772	0.9735	0.9702	0.9677	0.9656	0.9640
Zres	72.57	71.20	70.33	69.73	69.28	68.85	68.53	68.27	69.07
TH=2.0 mm; Radius=3.0 mm									
Perm	1	1.25	1.5	1.75	2	2.25	2.5	2.75	3
Conductivity	8.34E-07	1.04E-06	1.25E-06	1.46E-06	1.67E-06	1.88E-06	2.09E-06	2.29E-06	2.50E-06
Res FQ	30.00	29.50	29.17	28.92	28.74	28.59	28.48	28.39	28.30
DP Length	2.416	2.375	2.348	2.328	2.313	2.301	2.292	2.284	2.278
Wire VF	1	0.9830	0.9719	0.9636	0.9574	0.9524	0.9487	0.9454	0.9429
Zres	72.59	70.45	69.09	69.06	67.31	66.69	66.26	65.85	65.57

Although the values of conductivity change relative to the single value used for **Table 1**, none of the other values change. (There is a very slight change in the Zres or resonant impedance line that we shall address in more detail shortly.) The values are virtually identical between tables. In the period between generating these table (several years), versions of the software have changed, as have the computers and CPUs. As well, the basic compilers for the Fortran code have also changed. Each of these changes can result in a change in the final decimal digit for any entry. Hence, between the two tables, we may for all practical modeling purposes say that no change occurs, despite the differences in the values of conductivity.

This result is consistent with the exercise shown in **Fig. 2**, even though the figure uses a thick insulation with a relative permittivity that is high for the range of plastics commonly used for wire insulation. The impedance values recorded in that table remain almost constant until the conductivity is significantly higher than the values that appear in **Table 2**. If the loss tangent is among the common values, then at 30 MHz, the presumption of a very low conductivity value does not harm the accuracy of the resulting models. In addition, the velocity factor graph (**Fig. 4**) remains usable as a general guide to dipole length shortening as a function of wire insulation of common sorts.

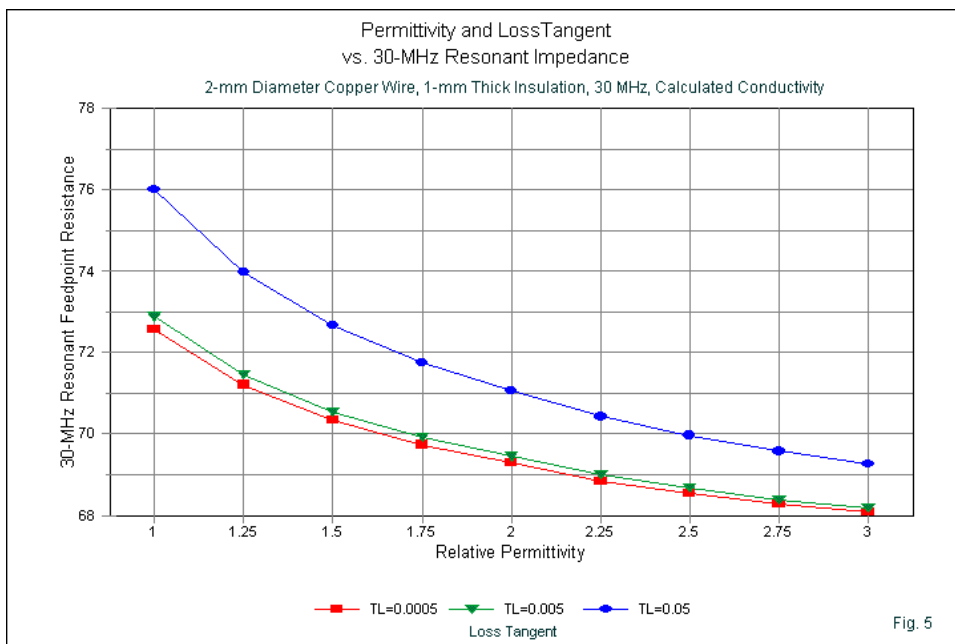
Even though a loss tangent of 0.0005 may be common, there are instances in which the value may be higher. In fact, EZNEC provides a loss-tangent value of 0.05 for PVC. This value is 2 orders of magnitude higher than the value used for **Table 2**. Therefore, we likely should perform at least one more exercise. Let's retain our 2-mm diameter copper wire dipole at 30 MHz. As well, let's select the middle case from **Table 2**, the situation in which we use 1-mm thick insulation. However, let's change the basis of comparison. Let's explore loss-tangent values of 0.0005, 0.005, and 0.05 in order to see what changes may occur in the data that we accumulate in these free-space models. For each model at each level of relative permittivity, we arrive at a new value of conductivity, as shown in **Table 3**.

Effects of Higher Loss-Tangent Values: Permittivity and Conductivity as Variables									Table 3
Dipole: 30 MHz, 2mm (0.002 m or 0.07874") diameter copper conductor									
Insulation: 1-mm thick (insulation radius 2.0 mm)									
Loss tangent = 0.0005									
Perm	1	1.25	1.5	1.75	2	2.25	2.5	2.75	3
Conductivity	8.34E-07	1.04E-06	1.25E-06	1.46E-06	1.67E-06	1.88E-06	2.09E-06	2.29E-06	2.50E-06
Res FQ	30.00	29.68	29.47	29.32	29.21	29.12	29.04	28.98	28.93
DP Length	2.416	2.390	2.373	2.361	2.352	2.344	2.338	2.333	2.329
Wire VF	1	0.9892	0.9822	0.9772	0.9735	0.9702	0.9677	0.9656	0.9640
Zres	72.57	71.20	70.33	69.73	69.28	68.85	68.53	68.27	68.07
Loss tangent = 0.005									
Perm	1	1.25	1.5	1.75	2	2.25	2.5	2.75	3
Conductivity	8.34E-06	1.04E-05	1.25E-05	1.46E-05	1.67E-05	1.88E-05	2.09E-05	2.29E-05	2.50E-05
Res FQ	30.00	29.68	29.47	29.32	29.21	29.12	29.04	28.98	28.93
DP Length	2.416	2.390	2.373	2.361	2.352	2.344	2.338	2.333	2.329
Wire VF	1	0.9892	0.9822	0.9772	0.9735	0.9702	0.9677	0.9656	0.9640
Zres	72.89	71.46	70.55	69.91	69.44	68.99	68.66	68.39	68.18
Loss tangent = 0.05									
Perm	1	1.25	1.5	1.75	2	2.25	2.5	2.75	3
Conductivity	8.34E-05	1.04E-04	1.25E-04	1.46E-04	1.67E-04	1.88E-04	2.09E-04	2.29E-04	2.50E-04
Res FQ	30.00	29.68	29.47	29.32	29.21	29.12	29.04	28.98	28.93
DP Length	2.416	2.390	2.373	2.361	2.352	2.344	2.338	2.333	2.329
Wire VF	1	0.9892	0.9822	0.9772	0.9735	0.9702	0.9677	0.9656	0.9640
Zres	76.02	73.99	72.67	71.75	71.06	70.43	69.96	69.57	69.26

Perhaps the first noticeable trait of the tabulated values is that a 10-fold increase in the loss tangent produces an exactly equivalent increase in the value of conductivity. Hence, the highest value of conductivity is about 2.5E-4 S/m. Nevertheless, almost nothing else changes. The self-resonant frequencies for the 4.832-m wire when insulated are the same, regardless of the conductivity. These frequencies would be determined largely by the feedpoint reactance, which does not change significantly until the conductivity reaches about 1E-3 S/m. Likewise,

the required half-element length for resonance at 30 MHz does not change over the range of loss-tangent values scanned in the table. As a consequence, the insulated-wire velocity-factor graph (**Fig. 4**) remains usable for the entire set of loss-tangent values covered by the exercise.

One factor does change: the feedpoint resistance at the 30-MHz resonant wire length. In fact, it shows a systematic rise as we increase the value of loss tangent, as shown in **Fig. 5**.



The amount of change is systematic but still quite small between loss-tangent values of 0.0005 and 0.005. This value range corresponds at 30 MHz to a range center of $1.6\text{E-}6$ S/m and $1.6\text{E-}5$ S/m. Both of these midpoint conductivity values fall well below the expected resistance upward swing vs. conductivity. The loss-tangent value of 0.05 produces a more noticeable change that averages about 1.5 Ohms relative to the 2 lower curves. The associated mid-point conductivity is about $1.6\text{E-}4$ S/m. Reference to **Fig. 2** shows that the resistance curve has entered its area of noticeable climb in this region.

The higher feedpoint resistance value is largely a function of the decreasing resistivity of the insulation under the specified conditions. Indeed, the mid-point value of resistivity is close to 6000 Ohms/m, a value that gives the insulation semi-conductor status. Small amounts of current may flow and equally may be dissipated as heat. With lower values of conductivity, the insulation is largely RF transparent. Dissipation appears to reach a peak at a conductivity of about $1\text{E-}2$ S/m (100 Ohms/m). Once the insulation is more conductive, it becomes a part of the radiating wire itself, and the overall feedpoint resistance begins to decline.

Conclusion

I have conducted these exercises at 30 MHz, the upper limit of the HF range. We find most uses of insulated antenna elements at HF. Since the value of conductivity will rise and fall with the frequency, the 30-MHz case represents a worst-case analysis. However, it is wise to remember that insulation of the proportions used in these exercises will increase the insulation conductivity by a factor of 10 if we increase the frequency to 300 MHz.

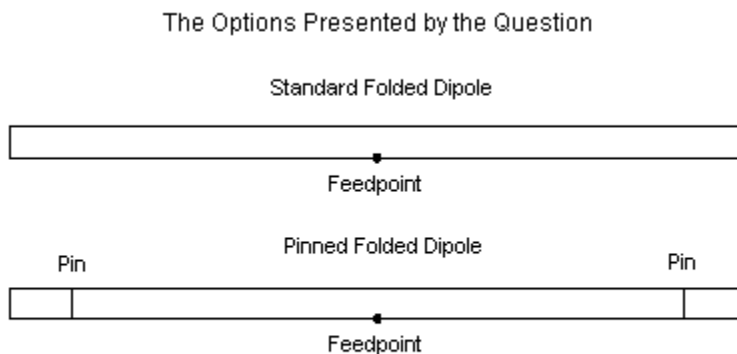
I sometimes receive questions about the effects of enamel (or its current replacement coating) on wire. In general, the enamel coating is too thin for its effect to appear when comparing it to bare wire of the same diameter. I have also received questions about anodized aluminum elements, and the same general answer applies. Forcing the emergence of aluminum oxide for a few molecules of depth into the aluminum has little effect on the element's performance compared to a bare element that has received a fresh polishing. However, both situations require special care with respect to ensuring good electrical contact at junctions.

Most plastic coating used to insulate wires have a relative permittivity between 2 and 3, with loss tangents in the HF region of less than 0.001. The exercises have shown that in this range, nothing critical changes with respect to the value of loss tangent or a calculated conductivity value. Hence, one might safely use a generalized loss tangent of about 0.0005 or some very low value of conductivity (depending upon the software) and still wind up with a model that is accurate enough to serve as a basis for antenna building. In the HF region, construction and environmental variables will generally override any slight differences one might see in modeling tables.

117. Modeling and the Logic of Question Resolution

Many beginning modelers quickly grow adept at arranging wires into the antenna geometry needed to create successful models. However, unless they are used to multi-step problem solving, these same modelers fail to realize that NEC and MININEC are useful for more than just stringing together wires into antenna forms and then requesting the usual output data. Modeling software is capable of resolving questions, although sometimes, the questions require multiple stages of modeling on the road to relatively final answers. Therefore, it might be useful to look at the logic of problem resolution as it applies to antenna modeling.

Because this episode is for the newer modeler, let's look at a fairly straightforward question as a vehicle to demonstrate multi-step modeling. During the past two decades, some antenna builders have proposed an alternative structure for the common folded dipole antenna, especially when we construct the antenna from common forms of insulated transmission lines. **Fig. 1** shows both the standard construction method and the "pinned" alternative.



Note: Both folded dipoles constructed from parallel transmission lines having a known velocity factor.

Fig. 1

The pre-modeling-era reasoning behind the pinned version of the antenna runs something like the following: the insulated (vinyl-covered) transmission line has a velocity factor. For highest efficiency or radiation effectiveness, the transmission line portion of the folded dipole requires a termination at the length determined by

multiplying the line's velocity factor as a transmission line times $1/2$ wavelength. Those favoring shorting the line or placing pins through the line from one conductor to the other claimed noticeable performance improvements, while other folded dipole builders found no detectable difference. Although the issue has largely disappeared from sight in recent years, perhaps it may serve as an example of how we may use a few antenna models to resolve it. Modeling is, after all, less strenuous than erecting folded dipoles and working out all that would go into range measurements sensitive enough to detect any differences in performance--or to record reliably an absence of difference.

Step 1: Setting Up the Test Situation

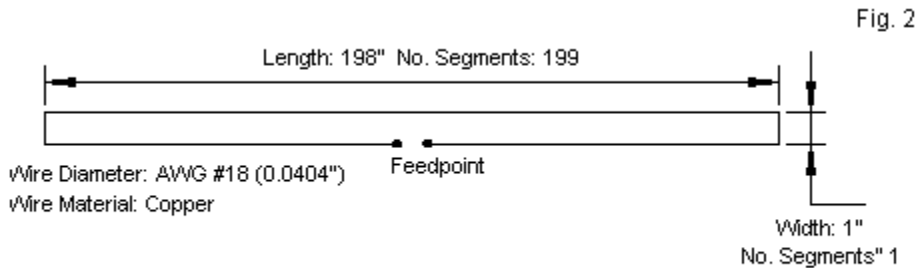
The first step is to set up a workable modeling experimental situation. For this step, we shall want to model a bare-wire folded dipole to ensure that the most basic parts of the work are usable throughout the exercise. We shall also need to have this bare-wire folded-dipole model on hand for comparisons with the versions yet to emerge.

a. We need to set up the basic modeling environment to yield fair comparisons among our models. For the present question, free-space is quite adequate. Any ground influences would apply equally to all versions of the folded dipole. Hence, we might as well eliminate ground effects entirely.

b. We need to choose a reasonable wire size. AWG #18 copper wire is a fair choice in this case because parallel transmission lines often use the 0.0404"-diameter material beneath the vinyl. As well, the wire will ensure a high segment-length-to-wire-diameter ratio once we establish the remainder of the basic antenna specifications.

c. We need to set a test frequency. I have selected 28.5 MHz. (Outside the realm of typical amateur radio installations, one might as easily have rounded this number to 30 MHz.) A folded dipole for this frequency will be about 200" long. However, since we eventually will be using a simulation of insulated transmission line, the wire separation will have to be fairly small. I selected 1" to ensure that the thin wires are not too close together for high accuracy. This decision sets the length of the segments on the end wires. Ideally, the segments in any model should all have the same length. For the anticipated antenna length, we would require close to 200 segments along each long wire in the folded dipole. At a total of about 400 segments, the model is large enough to be reliable but small

enough for rapid runs on the current generation of computers. **Fig. 2** shows the dimensions of the final model.



Step 1: Setting Up a Basic Bare-Wire Folded Dipole

Within the specified limits, the folded dipole produced the following free-space results:

Length: 198" Gain: 2.10 dBi Beamwidth: 78.2 deg. Impedance: 289.1 + j2.8 Ohms

The model for this antenna used EZNEC software in this case, although any version of NEC or MININEC would do equally well. The model wires appear in **Fig. 3**.

Wires

The Bare-Wire Folded Dipole Model Wires

Fig. 3

☐ Coord Entry Mode ☐ Preserve Connections Frequency: 28.5 MHz ☐ Show Wire Insulation

Wires										
No.	End 1				End 2				Diameter (in)	Segs
	X (in)	Y (in)	Z (in)	Conn	X (in)	Y (in)	Z (in)	Conn		
1	0	-99	0	W4E1	0	99	0	W2E1	#18	199
2	0	99	0	W1E2	0	99	1	W3E1	#18	1
3	0	99	1	W2E2	0	-99	1	W4E2	#18	199
4	0	-99	0	W1E1	0	-99	1	W3E2	#18	1
*										

This initial step is not an end in itself. Moreover, we should not merely accept and record the data. Instead we should spend a moment understanding it. A single-wire dipole when resonant will have a feedpoint impedance in free space that is between 70 and 72 Ohms. The folded dipole uses equal-diameter wires throughout, giving it a step-up ratio of 4:1 relative to the single-wire dipole impedance. If we subtract a tiny bit of the impedance as due to the losses in having twice the length of copper wire, then the reported impedance easily falls

wholly within the standard range. If we doubt this fact, we can easily back up one step and model a resonant dipole made from AWG #18 copper wire.

We might also expect a single wire resonant dipole made from AWG #18 wire to have a gain between 2.12 and 2.14 dBi. The folded dipole shows a tiny reduction--obviously too small to be operationally significant. The reduction is a natural consequence of the fact that a resonant folded dipole will be slightly shorter than a resonant single-wire dipole. As we shorten an antenna element, regardless of the feedpoint impedance, the gain will slowly decrease--again, insignificantly so, but noticeably from a numerical perspective.

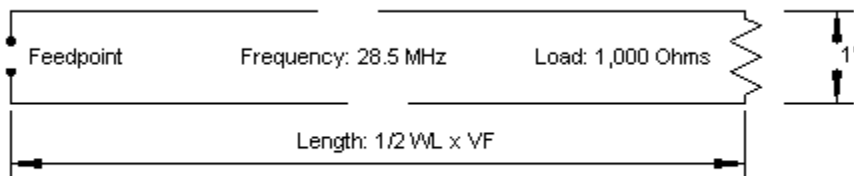
Now that we have a bare-wire folded dipole, we can begin the process of modeling a folded dipole from insulated parallel transmission line in which the wires are also 1" apart.

Step 2: Simulating Insulated Transmission Line

The bare-wire transmission line that forms the equally bare-wire folded dipole has the same form, that is, a 1" separation between two AWG #18 copper wires. Using common equations or a utility program, we discover that the line has an impedance of about 468 Ohms. However, this fact is only loosely applicable to our project.

More significantly, we shall set up a half-wavelength section of this line, modeling in the form of **Fig. 4**. A true half-wavelength at 28.5 MHz is about 207.1". However, the copper losses shorten the line to 206.2" to obtain a test source impedance with virtually no reactance.

Fig. 4



Setting Up a Transmission Line for Insulation

Note that we have used a load impedance of 1000 Ohms resistive. The aim is to adjust the line length until we obtain a resistive impedance at the source end of the line. The length that we used yielded $992.1 + j0.7$ Ohms. The difference in the resistive component goes to wire losses.

The importance of the initial transmission-line test is to develop an insulated transmission line with a velocity factor (VF) that is more distant from 1.0. We may be arbitrary here, but still within the realm of possibility. Let's select a VF of 0.80. Now the task is to create insulated wires that will yield a nearly resonant source impedance with a line length that is 0.8 times the original length. 165" will be close enough for the shortened line length. Within EZNEC, we would select a permittivity of 2.505, with an insulation thickness of 0.185". We may leave the loss tangent at zero, since for all practical purposes--as shown in the preceding episode of this series--the resulting wire conductivity will not play a significant role in the results.

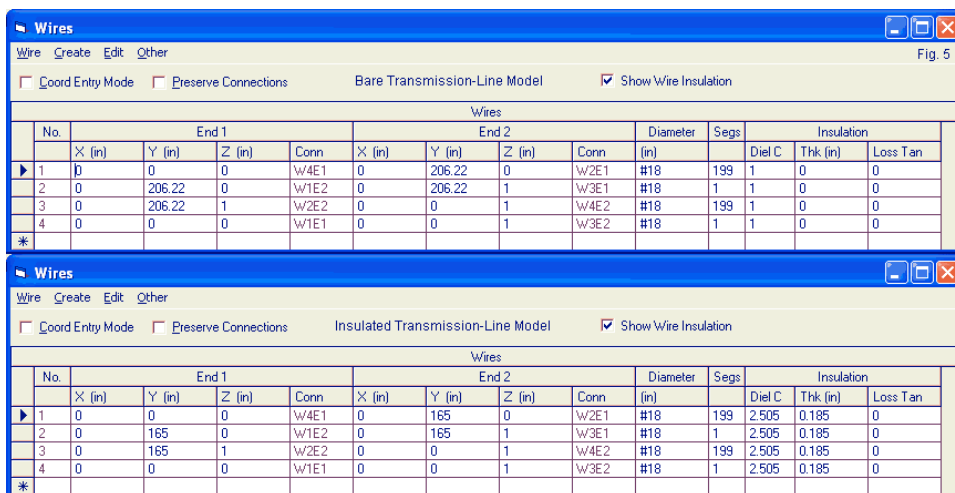


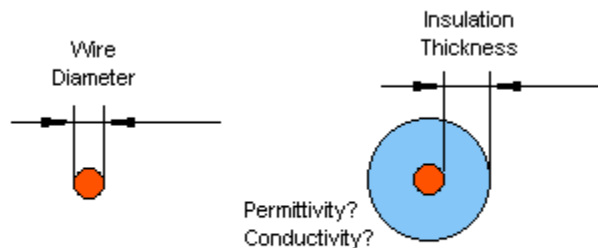
Fig. 5 compares the wire tables for the two transmission lines. (We might have left the end wires bare, but the results would not significantly change.) With the specified insulation and the given line length, the source impedance is $989.8 + j0.1$ Ohms. One reason for the slight difference between the bare-wire and the insulated-wire impedances is the fact that insulation between the wires does have a small but definite effect on the characteristic impedance of the line.

Wires													
No.	End 1				End 2				Diameter (in)	Segs	Insulation		
	X (in)	Y (in)	Z (in)	Conn	X (in)	Y (in)	Z (in)	Conn			Diel C	Thk (in)	Loss Tan
1	0	0	0	w/4E1	0	206.22	0	w/2E1	#18	199	1	0	0
2	0	206.22	0	w/1E2	0	206.22	1	w/3E1	#18	1	1	0	0
3	0	206.22	1	w/2E2	0	0	1	w/4E2	#18	199	1	0	0
4	0	0	0	w/1E1	0	0	1	w/3E2	#18	1	1	0	0

Wires													
No.	End 1				End 2				Diameter (in)	Segs	Insulation		
	X (in)	Y (in)	Z (in)	Conn	X (in)	Y (in)	Z (in)	Conn			Diel C	Thk (in)	Loss Tan
1	0	0	0	w/4E1	0	165	0	w/2E1	#18	199	2.505	0.185	0
2	0	165	0	w/1E2	0	165	1	w/3E1	#18	1	2.505	0.185	0
3	0	165	1	w/2E2	0	0	1	w/4E2	#18	199	2.505	0.185	0
4	0	0	0	w/1E1	0	0	1	w/3E2	#18	1	2.505	0.185	0

The EZNEC method of implementing wire insulation is a substitute for the NEC-4 IS command. Numerous other NEC packages have implemented wire insulation in a variety of ways. Essentially, we need to know only a few pieces of information, as indicated in **Fig. 6**.

Fig. 6



The Parameters of Modeled Wire Insulation

EZNEC requests the thickness of the insulation. The thickness creates a radius for the outer surface once we adjust that value for the radius (or diameter) of the copper wire at the center. The IS command itself requires the entry of the insulated sheath outer radius, which cannot be smaller than the radius of the center wire. Both raw NEC-4 and EZNEC require a value for the relative permittivity (dielectric constant) of the insulating material. The IS command also requires a value of conductivity for the insulating material. An entry of $1e-10$ will do for most excellent insulators. However, if we were using a specific insulating material, we likely would not find a conductivity value in reference books. Instead, we would find a value for the loss tangent, which--as shown last time--translates into a conductivity value. The following lines show just the wires and the IS commands of the EZNEC model saved in NEC format.

CM transmission line: covered

```
GW 1,199,0.,0.,0.,0.,4.191,0.,5.119E-4
GW 2,1,0.,4.191,0.,0.,4.191,.0254,5.119E-4
GW 3,199,0.,4.191,.0254,0.,0.,.0254,5.119E-4
GW 4,1,0.,0.,0.,0.,0.,.0254,5.119E-4
```

```
GE 0
IS 0, 1 ,0,0,2.505,0.,5.2109E-3
IS 0, 2 ,0,0,2.505,0.,5.2109E-3
IS 0, 3 ,0,0,2.505,0.,5.2109E-3
IS 0, 4 ,0,0,2.505,0.,5.2109E-3
```

EN

The IS lines specify the wire to which we apply the insulation. The following two zeroes indicate that we apply it to the entire wire, even though we might have selected only some of the segments. The next value is the relative permittivity, followed by the conductivity (which is zero, due to our selection of the zero loss tangent in the EZNEC model). The final value is the outer radius of the insulation in meters. In this translation from the EZNEC file, the wire radii also appear in meters. We might have used some other unit of measure for the wires in the geometry section and converted them to meters with the GS card. However, all ensuing control commands that involve a physical dimension, including the IS command, must use meters as the unit of physical measure.

This entire exercise has aimed at producing an insulated transmission line with a velocity factor of 0.80. The shape of the insulation does not resemble the "dumb-bell" shape typically shown by cross sections of vinyl-coated lines. For this project, that difference is not a matter of concern. We only need and have achieved a transmission line with the required velocity factor. Since the two parallel wires are the same diameter, the step-up ratio will still be 4.

Step 3: An Unpinned Insulated Folded Dipole

The next step is to create a model of a folded dipole that uses the insulated transmission-line wire that we just produced. We may begin with the bare wire and use the insulation values that went into the transmission line. However, we shall not change the length of the folded dipole initially. With the insulation in place, we obtain the following free-space performance values.

Length: 198" Gain: 2.10 dBi Beamwidth: 78.2 deg. Impedance: $419.8 + j271.5$ Ohms

The folded dipole is too long. Therefore, we may gradually reduce its length until we obtain a resonant feedpoint. When we stop, the free-space performance and length are as follows:

Length: 185.5" Gain: 2.06 dBi Beamwidth: 79.4 deg. Impedance: $262.5 + j0.3$ Ohms

The very slight gain reduction is solely a function of having shortened the antenna. The shorter antenna also yields a slightly lower feedpoint impedance at resonance, relative to the bare-wire version. Here we may repeat the bare-wire folded-dipole data as a reference for the very small changes.

Length: 198" Gain: 2.10 dBi Beamwidth: 78.2 deg. Impedance: $289.1 + j2.8$ Ohms

The insulated but unpinned folded dipole is shorter than the bare-wire version, but not by 20%. Rather the ratio of the bare-to-insulated wire lengths is 0.937, which gives us the velocity factor of the insulated wire in antenna service (in contrast to its value in transmission-line service). We have long known that wire insulation has a velocity factor in antenna service, even for single-wire elements. The value depends on the insulation thickness and the relative permittivity of the insulation. Insulated antenna-wire velocity factors tend to range from about 0.92 to 0.98. When we apply insulation to a folded dipole we obtain the same result.

Step 4: A Pinned Insulated Folded Dipole

The final step in our exploration of the idea of pinning a folded dipole at the length indicated by the transmission-line velocity factor is to create the pinned version of the antenna model. We have already learned that 80% of a half-wavelength at 28.5 MHz is just about 165". Therefore, we shall create two interior cross wires that are 82.5" from the antenna center. To implement these cross wires, we shall have to add 6 new wires to the overall model. **Fig. 7** compares the two insulated folded dipole models.

Wires													
Wire Create Edit Other													
Unpinned Version													
Show Wire Insulation													
Wires													
No.	End 1				End 2				Diameter	Segs	Insulation		
	X (in)	Y (in)	Z (in)	Conn	X (in)	Y (in)	Z (in)	Conn	(in)		Diel C	Thk (in)	Loss Tan
1	0	0	0	W4E1	0	185.5	0	W2E1	#18	199	2.505	0.185	0
2	0	185.5	0	W1E2	0	185.5	1	W3E1	#18	1	2.505	0.185	0
3	0	185.5	1	W2E2	0	0	1	W4E2	#18	199	2.505	0.185	0
4	0	0	0	W1E1	0	0	1	W3E2	#18	1	2.505	0.185	0
*													

Wires													
Wire Create Edit Other													
Pinned Version													
Show Wire Insulation													
Wires													
No.	End 1				End 2				Diameter	Segs	Insulation		
	X (in)	Y (in)	Z (in)	Conn	X (in)	Y (in)	Z (in)	Conn	(in)		Diel C	Thk (in)	Loss Tan
1	0	-82.5	0	W4E1	0	82.5	0	W2E1	#18	175	2.505	0.185	0
2	0	82.5	0	W8E2	0	82.5	1	W3E1	#18	1	2.505	0.185	0
3	0	82.5	1	W9E2	0	-82.5	1	W4E2	#18	175	2.505	0.185	0
4	0	-82.5	0	W5E2	0	-82.5	1	W6E2	#18	1	2.505	0.185	0
5	0	-92.4	0	W7E1	0	-82.5	0	W1E1	#18	10	2.505	0.185	0
6	0	-92.4	1	W7E2	0	-82.5	1	W3E2	#18	10	2.505	0.185	0
7	0	-92.4	0	W5E1	0	-92.4	1	W6E1	#18	1	2.505	0.185	0
8	0	92.4	0	W10E1	0	82.5	0	W1E2	#18	10	2.505	0.185	0
9	0	92.4	1	W10E2	0	82.5	1	W2E2	#18	10	2.505	0.185	0
10	0	92.4	0	W8E1	0	92.4	1	W9E1	#18	1	2.505	0.185	0
*													

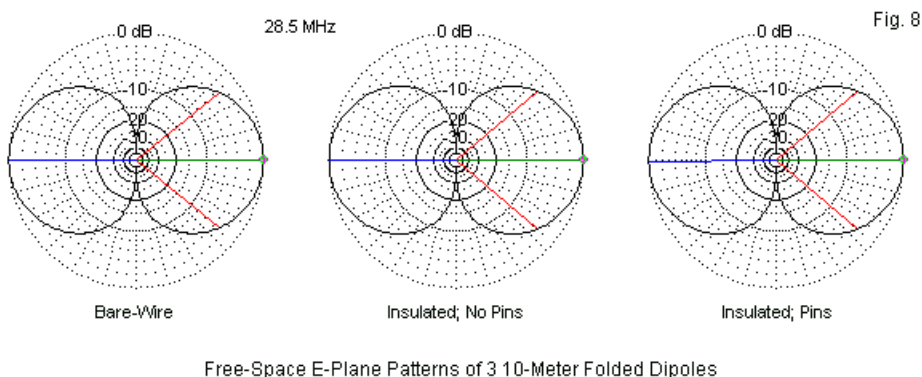
Whereas the unpinned folded dipole required a length of 185.5" for resonance, the pinned version is slightly shorter: 184.8". With this length adjustment, the pinned insulated folded dipole provides the following free-space performance numbers.

Length: 184.8" Gain: 2.05 dBi Beamwidth: 79.6 deg. Impedance: 258.0 + j2.8 Ohms

The initial model for the pinned folded dipole used the unpinned length but showed a j17.4-Ohm reactance at the feedpoint. We obtained the resonant length by shortening the outer ends in small increments until satisfied with the result. Had we moved the pins (interior cross wires), we might have made very large changes in position without significantly changing the feedpoint impedance by any significant amount. Feedpoint resonance is largely a function of the longest dimension of the folded dipole, not the pin position.

The further shortening of the antenna reduces the gain by a tiny amount and equally reduces the resistive component of the feedpoint impedance. The bare-wire folded dipole showed 289 Ohms, while the unpinned insulated version

showed 262.5 Ohms. The pinned folded dipole is down to 258 Ohms. All three values are equally usable, but the trend is worth noting. In operation, we would find not detectable difference among the 3 folded dipoles. **Fig. 8** shows the patterns, which display no visible differences in pattern shape or half-power beamwidth values.



Conclusion of the Problem

We began with an open question: when using insulated transmission line to create a folded dipole, does pinning or shorting the antenna at the places indicated by the transmission-line's velocity factor change the folded dipole's performance? While the use of insulated transmission line for the antenna does exhibit an antenna velocity factor, pinning in accord with the transmission-line velocity factor does not change the antenna performance in any detectable way (other than the very tiny numerical differences shown by the models).

It is likely that the idea of pinning a folded dipole arose when some radio amateurs realized that a folded dipole exhibited both transmission-line and radiation currents along its overall length. However, the existence of transmission line currents does not mean that the antenna requires transmission line treatment. If we were to separate the currents, following Kuecken's method developed for analysis of folded monopoles, we would discover that the transmission-line current remains constant along the wire and is 90 degrees out of phase with the radiation current. See "[Unfolding the Story of the Folded Dipole](#)" for further information on this aspect of folded dipoles. See Kuecken's *Antennas and Transmission lines*, page 225, for his analysis of the current along

a folded monopole or dipole. (To perform the analysis, we would have to revise the order and direction of some wires in the model, but not change the overall geometry. The required addition and subtraction of values on each wire require that we account for the phase angle as well as the magnitude of the current.)

In the end, the idea of pinning a folded dipole according to the transmission-line velocity factor rests on a misunderstanding of what occurs along the wires of the antenna. If we pin the folded dipole, we shorten the folded portion of the antenna. However, the wires extending outward form an extension that lengthens the antenna. The extensions are roughly equivalent to a single fat wire created by two thinner wires in parallel, with a common termination. There are numerous applications for using short folded dipoles or monopoles with short or long extensions. The gamma and T matches are cases in point, but well outside the scope of these notes.

Conclusion to the Episode

The exercise in analyzing the pinned insulated folded dipole was, of course, a pretext and a sample in this episode. Our efforts were designed to show the newer modeler that antenna modeling software has more applications than just the adjustment of wire geometries to analyze or perfect an antenna design. Sometimes, we can use the software to resolve sundry claims made about various types of antennas.

However, the resolution of open questions (which unfortunately turn into exercises in disputation all too often) may not be a one-step process. There are some questions that we can answer just by modifying antenna geometry. For example, we can find the patterns of maximum gain and resonant feedpoint impedance for simple dipoles (and for other types of antennas) simply by adjusting the height of the antenna above ground and then readjusting the length until the antenna is resonant. The present case does not fall into this simple category.

Our problem required us to pass through several steps in order to reach a resolution. The steps involved two different kinds of models, even though they were related to each other. More complex questions may involve more complex collections of models. The key is to develop an orderly process of steps required to set up as many bases as are necessary to combine into the final resolution. The logic of problem solution is a pre-requisite to advanced modeling exercises--even with entry-level modeling software.

Some problems do not allow us to set up separate bases that we then combine in essentially a parallel combination. Occasionally, we may have to invoke long series of reiterations as we change the values of multiple variables. However, that kind of process is for some future episode in this series.

Volume 6 to follow soon.

Other Publications

We hope you've enjoyed this 5th in a series of volumes of the **Antenna Modeling Notes**. Volume 6 of this series is soon to follow. Together with existing volumes 1, 2, 3 and 4 of this series, you'll find many other very fine books and publications by the author L.B. Cebik, W4RNL and other fine authors in the **antenneX Online Magazine BookShelf** at the web site shown below.

***A Publication by
antenneX Online Magazine***

<http://www.antennex.com/>

POB 271229

Corpus Christi, Texas 78427-1229

USA

August 2009

Copyright © 2009 by **antenneX Online Magazine**. All rights reserved. No part of this book may be reproduced or transmitted in any form, by any means (electronic, photocopying, recording, or otherwise) without the prior written permission of the publisher.

ISBN: 1-877992-55-0

Other Publications